UNIVERSITY OF PARDUBICE

FACULTY OF CHEMICAL TECHNOLOGY

Department of Analytical chemistry

Comprehensive analysis of glycosphingolipids in biological samples using HPLC/MS

Dissertation

Author: Mgr. Karel Hořejší

Supervisor: Prof. Ing. Michal Holčapek, Ph.D.

Pardubice 2024

Author´s Declaration:

I hereby declare:

This dissertatiton entitled "Comprehensive analysis of glycosphingolipids in biological samples using HPLC/MS" was prepared separately. All the literary sources and the information I used in the thesis are listed in the bibliography.

I got familiar with the fact that the rights and obligations arising from the Act No. 121/2000 Coll., Copyright Act, apply to my thesis, especially with the fact that the University of Pardubice has the right to enter into a license agreement for use of this thesis as a school work pursuant to § 60, Section 1 of the Copyright Act, and the fact that should this thesis be used by me or should a license be granted for the use to another entity, the University of Pardubice is authorized to claim a reasonable contribution from me to cover the costs incurred during making of the thesis, according to the circumstances up to the actual amount thereof.

I am aware that my thesis will be accessible to the public in the University Library and via the Digital Library of the University of Pardubice in agreement with the article 47b of the Act No. 111/1998 Coll., on Higher Education Institutions, and on the Amendment and Supplement to some other Acts (the Higher Education Act), as subsequently amended, and with the University Pardubice's directive no. 7/2019.

In Pardubice,

Mgr. Karel Hořejší

Acknowledgments

This work was supported by the following grants:

- the Czech Science Foundation (Projects No. 18-12204S and 21-20238S)
- the Czech Health Research Council (Grant No. NU21-03-00499)
- the Swedish Cancer Foundation (Grant No. 20 0759 PjF 01 H to S.T.)

I would greatly like to thank my supervisor prof. Michal Holčapek for the great opportunity to study the Ph.D. program in his research group with extremely friendly environment, valuable advice, and professional guidance during the entire period of my studies. I would also like to thank my colleagues and co-authors, namely Robert Jirásko, David Kahoun, Denise Wolrab, Michaela Chocholoušková, Zuzana Vaňková, Denisa Kolářová, Susann Teneberg, and Chunsheng Jin for leading, support, and friendship. Last but not least, special attention goes to Bohuslav Melichar and Ondřej Strouhal (also co-authors) for providing most of the samples, and Maria Blomquist for providing some specific carbohydrate-binding antibodies. Special acknowledgment belongs to my beloved family for their patience, support, and understanding.

ANNOTATION

Lipids are biomolecules found in all living organisms, where they have several vital functions. Lipids are the subject of lipidomics, a subgroup of metabolomics, which represents one of the so-called "omics" disciplines that also includes genomics, proteomics, and glycomics. Dysregulation of lipid metabolism can reflect the onset of various diseases including cancer, therefore, lipidomic analysis can provide valuable information about ongoing pathophysiological processes in humans.

The theoretical part provides an extensive overview of glycosphingolipids, including their biosynthesis, structure complexity, classification, nomenclature, and various biological functions in association with pathophysiological conditions as a hallmark of a variety of diseases, for example, cancer. Special attention is also paid to the sample preparation and key analytical methods for their identifications and quantitation. Qualitative and quantitative approaches are discussed as well, along with their advantages and limitations.

The experimental part deals with the development, optimization, and application of analytical methods for the analysis of especially glycosphingolipids in biological samples, such as human plasma/serum and tissues using chromatographic techniques coupled to mass spectrometry. Special attention is devoted to in-depth structural characterization and qualitative glycosphingolipids profiling using a lipid class separation approach (HILIC). Correspondingly, glycosphingolipid profiling is used to expand the database of lipids that are routinely analyzed, and for the mutual comparison of healthy volunteers and cancer patients. Therefore, the analysis of glycosphingolipids has the potential to facilitate the discovery of novel biomarkers for the early detection of various diseases.

KEYWORDS

lipidomics, glycosphingolipids, plasma, pancreatic tissue, extraction, purification, structural characterization, tandem mass spectrometry, hydrophilic interaction liquid chromatography

ANOTACE

Lipidy jsou biomolekuly, které se vyskytují ve všech živých organismech, kde plní několik životně důležitých funkcí. Lipidy jsou předmětem zkoumání vědního oboru zvaného lipidomika patřící do podskupiny metabolomiky, jež představuje jednu z omických disciplín, mezi které patří také genomika, proteomika a glykomika. Dysregulace metabolismu lipidů může odrážet nástup a rozvoj různých onemocnění včetně rakoviny, lipidomická analýza tedy může poskytnout cenné informace o probíhajících patofyziologických procesech u lidí.

Teoretická část práce poskytuje rozsáhlý přehled o glykosfingolipidech, jejich biosyntéze, strukturní složitosti, klasifikaci, názvosloví a nejrůznějších biologických funkcí ve spojení s patofyziologickými stavy, které jsou charakteristickým znakem různých onemocnění zahrnující i rakovinu. Zvláštní pozornost je také věnována přípravě vzorků a klíčovým analytickým metodám umožňující jejich identifikaci a kvantifikaci. Rovněž jsou zde diskutovány kvalitativní a kvantitativní přístupy spolu s jejich výhodami a omezeními.

Experimentální část se zabývá vývojem, optimalizací a aplikací analytických metod pro analýzu zejména glykosfingolipidů v biologických vzorcích jako je lidská plasma/sérum a tkáně, a to za použití chromatografických technik ve spojení s hmotnostní spektrometrií. Zvláštní pozornost je dedikována důkladné strukturní charakterizaci a profilování glykosfingolipidů za použití přístupu separace lipidových tříd (HILIC). V souladu s tím je profilování glykosfingolipidů použito k rozšíření databáze běžně analyzovaných lipidů a ke vzájemnému porovnání rozdílů mezi profily lipidů zzdravých dobrovolníků a pacientů s rakovinou. Lipidomická analýza glykosfingolipidů má tudíž potenciál umožnit a usnadnit objev nových biomarkerů pro včasnou detekci různých onemocnění včetně rakoviny.

KLÍČOVÁ SLOVA

lipidomika, glykosfingolipidy, plasma, pankreatické tkáně, extrakce, přečištění, strukturní charakterizace, tandemová hmotnostní spektrometrie, hydrofilní interakční kapalinová chromatografie

TABLE OF CONTENTS

LIST OF FIGURES

LIST OF TABLES

ABBREVIATIONS

^{13}C-TrEnDi	trimethylation enhancement using ^{13}C-diazomethane
2D-LC	two dimensional liquid chromatography
3-KSph	3-ketosphinganine
3-KSR	3-ketosphinganine reductase
ACE	acetone
AFADESI	air-flow assisted desorption electrospray ionization
Ag-HPLC	silver ion chromatography
AIMS	ambient ionization mass spectrometry
A-GSL	acidic glycosphingolipids
AMPP	N-(4-aminomethylphenyl)pyridinium
APCI	atmospheric pressure chemical ionization
API	atmospheric pressure ionization
API-MS	atmospheric pressure ionization mass spectrometry
APPI	atmospheric pressure photoionization
BIRD	blackbody infrared radiative dissociation
BuOH	butanol
CCS	collision cross-section
CE	cholesteryl ester(s)
Cer	ceramide
CerS1-S6	ceramide synthase S1 to S6
CERT	ceramide transfer protein
Cer-1-P kinase	ceramide-1-phosphate kinase (also CerK)
Cer-1-P	ceramide-1-phosphate
CGalT	ceramide galactosyltransferase
CGase	ceramide glycanase
CGlcT	ceramide glucosyltransferase
CGN	cis-Golgi network
CI	chemical ionization
CID	collision-induced dissociation
CID-MS^3	triple-stage collision-induced dissociation
CMAH	cytidine monophosphate N-acetylneuraminic acid hydroxylase
CMP-Neu5Ac	cytidine monophosphate N-acetylneuraminic acid

CMP-Neu5Gc	cytidine monophosphate N-glycolylneuraminic acid
CoA	coenzyme A
CRF	charge-remote fragmentation
DG	diacyglycerol(s)
DCM	dichloromethane
DDA	data dependent acquisition
DES1	dihydroceramide desaturase 1
DES2	dihydroceramide desaturase 1
DESI	desorption electrospray ionization
DESI-MS	desorption electrospray ionization mass spectrometry
dHCer	dihydroceramide
dHSph	dihydrosphingosine
DIA	data independent acquisition
DIL	differential isotope labelling
DIMS	differential ion mobility spectrometry
DI-MS	direct infusion mass spectrometry
DIPE	diisopropylether
DMA	differential mobility analyzer
DMABA-NHS	4-(dimethylamino)benzoic acid N-hydroxysuccinimide ester
DMEN	N,N-dimethylethylendiamine
DMPI	3-(N,N-dimethylamino)propyl isothiocyanate
DMS	differential mobility spectrometry
DMSO	dimethylsulfoxide
DTIMS	drift time ion mobility spectrometry
d6-DMBNHS	d6-S,S-dimethylthiobutanoylhydroxysuccinimide
EC	external calibration
ECD	electron capture dissociation
EDD	electron detachment dissociation
EDTA	ethylendiamintetraacetic acid
EGCase	endoglycoceramidase
EI	electron ionization
EID	electron-induced dissociation
EIEIO	electron impact excitation of ions from organics
ER	endoplasmatic reticulum

ESI	electrospray ionization
ESI-MS	electrospray ionization mass spectrometry
ETD	electron transfer dissociation
EtOH	ethanol
FA	fatty acyls/acids
FAIMS	field asymmetric ion mobility spectrometry
FAPP2	four-phosphate adaptor protein 2
FFA	free fatty acids
FIA	flow injection analysis
FID	flame ionization detector
FMOC-Cl	9-fluorenylmethoxyl carbonyl chloride
FT-ICR	Fourier transform ion cyclotron resonance
Fuc	fucose
FUT1/2	α1,2-fucosyltransferase
FUT3	α1,3/4-fucosyltransferase
GA	Golgi apparatus
Gal	galactose
GALC	galactosylceramidase
GalNAcT	N-acetylgalactosaminyl transferase
Ga2Cer	galabiosylceramide(s)
Gb3Cer	globotriaosylceramide(s)
Gb4Cer	globotetraosylceramide(s)
Gb5Cer	globopentaosylceramide(s)
GC-MS	gas chromatography–mass spectrometry
GCS	glucosylceramide synthase
GLCC	glucosylceramidase
GalCer	galactosylceramide(s)
GalT	galactosyltransferase
GalSph	galactosylsphingosine
GlcSph	glucosylsphingosine
GEM	glycosphingolipids-enriched microdomains
GL	glycerolipids
Glc	glucose
GlcCer	glucosylceramide(s)

GM3	monosialodihexosylganglioside(s)
GP	glycerophospholipids
GSL	glycosphingolipids
GTA	α1,3-N-acetylgalactosaminyl transferase
GTB	α1,3-D-galactosyltransferase
GTF	glycosyltrasferase
HCA	hierarchical cluster analysis
HCD	higher-energy collisional dissociation
HILIC	hydrophilic interaction liquid chromatography
HPTLC	high-performance thin-layer chromatography
HRMS	high-resolution mass spectrometry
IC	internal calibration
ICR	ion cyclotron resonance
IM	ion mobility
iPrOH	isopropylalcohol
IRMPD	infrared multiphoton dissociation
IS(s)	internal standard(s)
IUPAC	International Union of Pure and Applied Chemists
IVR	intramolecular vibrational redistribution
LacβSph	lactoside receptor
LacCer	lactosylceramide
LAESI	laser ablation electrospray ionization
LC-MS	liquid chromatography–mass spectrometry
LC/ESI-MS^2	liquid chromatography–electrospray ionization tandem mass spectrometry
LDI	laser desorption ionization
$Le^{a/b/x/y}$	Lewis a, b, x, or y epitope
LILY	lipidome isotope labelling of yeast
LLE	liquid-liquid extraction
LLOQ	lower limit of quantitation
LPC	lysophosphatidylcholines
LRMS	low-resolution mass spectrometry
LSD	lysosomal storage disorder
LTP	low-temperature plasma

MAD	metastable atom-activated dissociation
MG	monoacylglycerol(s)
MALDI	matrix-assisted laser desorption ionization
MALDI-MS	matrix-assisted laser desorption ionization mass spectrometry
MALDI-TIMS	matrix-assisted laser desorption ionization coupled to trapped ion mobility spectrometry
MALDI-TOF/(TOF)	matrix-assisted laser desorption ionization coupled to time-of-flight analyzer(s)
MDR	multi-drug resistance
MDMS-SL	multidimensional MS-based shotgun lipidomics
MeCN	acetonitrile
MeOH	methanol
MRM	multiple reaction monitoring
MS	mass spectrometry
MS^2 or MS/MS	tandem mass spectrometry
MS^n	multistage collisional dissociation
MSI	mass spectrometry imaging
MTBE	methyl tert-butyl ether
MUFA	mono unsaturated fatty acyls
m/z	mass-to-charge ratio
Nano-ESI	nano electrospray ionization
NCE	normalized collision energy
NDA	naphtalene-2,3-dicarboxyaldehyde
Neu5Ac	N-acetylneuraminic acid
Neu5Gc	N-glycolylneuraminic acid
N-GSL	neutral glycosphingolipids
NIST	the National Institute of Standards and Technology
nLc4Cer	neolactotetraosylceramide(s)
nLc6Cer	neolactohexaosylceramide(s)
NPLC	normal-phase liquid chromatography
OMS	overtone ion mobility spectrometry
OPLS-DA	orthogonal projections to latent structures discriminant analysis
OzID	ozone-induced dissociation

OzID-MS	ozone-induced dissociation mass spectrometry
PAEA	2-(2-pyridilamino)-ethylamine
PanIN	Pancreatic Intraepithelial Neoplasia
PB	Paterno-Büchi reaction
PC	phosphatidylcholines
PCA	principal component analysis
PDAC	pancreatic ductal adenocarcinoma
PGC	porous graphitized carbon
PK	polyketides
PLS-DA	partial least-square regression discriminant analysis
PPM	protein precipitation method
PQD	pulse Q dissociation
PR	prenols
PUFA	poly unsaturated fatty acyls
QA/QC	quality assurance/quality control
QqQ	triple quadrupole
QTOF	quadrupole time-of-flight
RDD	radical-directed dissociation
rEGCase II	recombinant endoglycoceramidase II
RIC	reconstructed ion current
RM(s)	reference material(s)
RPLC	reversed-phase liquid chromatography
RSD	relative standard deviation
SA	sialic acid(s)
SALSA	sialic acid linkage specific alkylamidation
SAT 1–3	sialic acid transferase 1–3
SGalCer	sulfogalactosyl ceramide(s)
SID	surface-induced dissociation
SIL	stable isotope labelling
SIL IS(s)	stable isotopically-labelled internal standard(s)
SIMS	secondary ion mass spectrometry
SL	saccharolipids
SLacCer	sulfolactosyl ceramide(s)
$SLe^{a/b/x/y}$	sialyl Lewis a, b, x, or y epitope

SLIM	structures for lossless ion manipulation
SM	sphingomyelin
SM4	monohexosylsulfatide(s), SHexCer
SM3	dihexosylsulfatide(s), $SHex_2Cer$
SNFG	symbol nomenclature for glycans
SP	sphingolipids
SPB	sphingoid base
SPE	solid-phase extraction
Sph	sphingosine
SphK	sphingosine kinase
Sph-1-P	sphingosine-1-phosphate
Sph-1-P kinase	sphingosine-1-phosphate kinase
SRM	standard reference material
SSEA-4	stage-specific embryonic antigen 3 (Gb5Cer)
S-Gb5Cer	sialyl globopentaosyl ceramide(s)
S-nLc4Cer	sialyl neolactotetraosyl ceramide(s)
S2-nLc4Cer	disialyl neolactotetraosyl ceramide(s)
S2-Gb5Cer	disialyl globopentaosyl ceramide(s)
ST	sterols
TAA	tumor-associated antigen
TG	triacylglycerol(s)
TGN	trans-Golgi network
TIMS	trapped ion mobility spectrometry
TLC	thin-layer chromatography
TMSD	timethylsilyldiazomethane
TWIMS	traveling wave ion mobility spectrometry
TWIMS-QTOF	traveling wave ion mobility coupled to quadrupole time-of-flight
UDP-Gal	uridine diphosphate galactose
UDP-GalNAc	uridine diphosphate N-acetylgalactose
UDP-Glc	uridine diphosphate glucose
UDP-GlcNAc	uridine diphosphate N-acetylglucose
(U)HPLC	(ultra)high-performance liquid chromatography
UHPSFC	ultrahigh-performance supercritical fluid chromatography

UHPSFC-MS	ultrahigh-performance supercritical fluid chromatography–mass spectrometry
ULOQ	upper limit of quantitation
UVPD	ultraviolet photodissociation

INTRODUCTION

Lipidomics is a relatively young scientific field, which belongs to the so-called "omics" disciplines, undergoing tremendous development in recent years that attracts major attention throughout the scientific field. Lipidomics deals with the study and analysis of the lipidome, *i.e.*, the total lipid composition of a cell, a tissue, an organ, or an organism, that is very variable and complex. The major goal of lipidomics is to precisely identify and quantify lipid species on a molecular level in order to understand the functions of lipids in living systems (*e.g.*, metabolic pathways) due to their importance in metabolism and various (patho)physiological changes associated with the onset of distinct diseases.

Generally, lipids are naturally occurring substances of both plant and animal origin that are usually water-insoluble, but highly soluble in organic solvents. Lipids represent the fundamental structural component of cell membranes, serve as a storage of energy and also have many other key biological functions. Lipids are a heterogeneous group of hydrophobic or amphipathic compounds with relatively low molecular weight and are characterized by the presence of alkyl chains of various lengths (commonly with an even number of carbon atoms) or isoprene units in a linear or cyclic arrangement. Lipid molecules may also be modified with various functional groups or covalently linked to other polar molecules, such as glycerol, carbohydrates, phosphate residues, *etc.*, which emphasize their amphipathic nature.

Lipids are an integral part of our life and play an important role in the development and progression of many diseases including cancer. In the case of cancer, when abnormal multiplication of cells occurs, a large amount of building material is needed for further development and growth of the tumor. This building material is mostly represented by lipids, which are obtained by cells from their surrounding environment. The differentiation between a healthy and tumor cell is therefore based on an assumption that both normal and tumor cell differ from each other in the lipidome composition. It is assumed that these changes can also manifest in the composition of body fluids, such as blood, plasma, serum, or urine.

Although the analysis of lipids is an extraordinarily challenging task due to their structural diversity, knowledge of the composition and metabolism of the lipids is highly important since alterations in lipid metabolism may be associated with a number of serious diseases including various types of cancer. A comprehensive analysis of lipids can lead to a better understanding of the progression of the diseases or to the revelation of disease-associated biomarkers. This would allow detection of the given disease at an early stage and thus increase the chance of saving many human lives.

1 THEORETICAL PART

Lipidomics is a research field using the principles and techniques of analytical chemistry to study the total lipid composition of cells, commonly known as the lipidome, in order to monitor their metabolic pathways and understand lipid metabolism. Lipidomics is enormously growing research area with a large number of papers published annually [1], as depicted via the statistics from Web of Science for topics 'lipidomics' and 'mass spectrometry' with 4576 papers published in the last 21 years **(Fig. 1).**

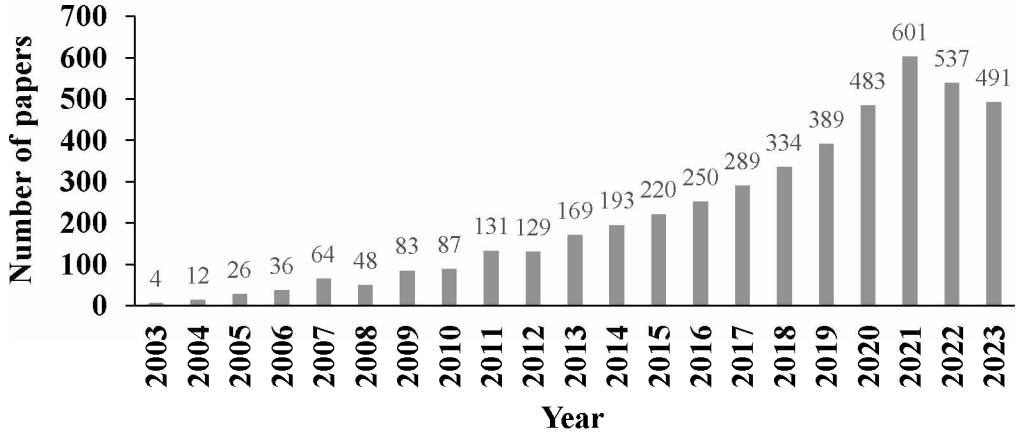

Fig. 1: Number of papers published in lipidomics in the last 20 years (as of January, 2024).

Lipids are naturally occurring compounds of both plant and animal origin that play many key roles in our lives [2]. The consortium of Lipid Metabolites and Pathways Strategy (LIPID MAPS, https://www.lipidmaps.org/) defines lipids as small biomolecules of either hydrophobic or amphipathic nature that originate by carbanion-based condensation of thioesters and/or carbocation-based condensation of isoprene units. In 2005, LIPID MAPS introduced the Lipid Classification System dividing lipids into 8 categories, which has been widely accepted. The lipid categories are fatty acids/acyls (FA), glycerolipids (GL), glycerophospholipids (GP), sphingolipids (SP), sterols (ST), prenols (PR), saccharolipids (SL), and polyketides (PK). Each lipid category has its own and often extensive subclassification hierarchy (**Table 1**) [3,4].

In this thesis, we will further deal practically only with sphingolipids, especially a huge subgroup of glycosphingolipids, which represent the majority of the sphingolipids category, and are the pivotal part of this doctoral thesis.

Table 1: Lipid categories with their general structure and subclassification hierarchy [3,4].

Category	Structure	Major representatives
FA	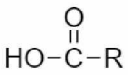	**R** = alkyl chain (with varying numbers of double bonds): 0: saturated fatty acids 1: monounsaturated fatty acids (MUFA) 2: polyunsaturated fatty acids (PUFA)
GL	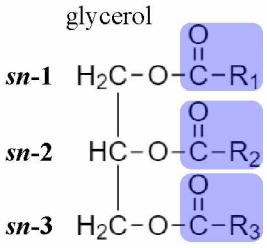	**Number of esterified fatty acids:** 1: MG = monoacylglycerols 2: DG = diacylglycerols 3: TG = triacylglycerols
GP	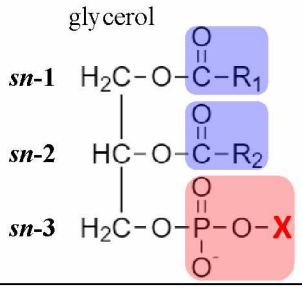	**X** = H: PA = phosphatidic acid Serine: PS = Phosphatidylserines Glycerol: PG = Phosphatidylglycerols Inositol: PI = Phosphatidylinositols Choline: PC = Phosphatidylcholines Ethanolamine: PE = Phosphatidylethanolamines
SP	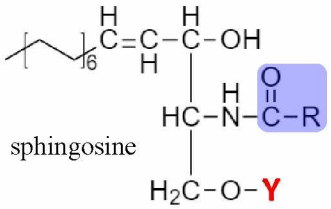	**Y** = H: Ceramide (Cer) Phosphocholine: Sphingomyelin (SM) Glycan: Glycosphingolipids (GSL) More detail description in the Chapter 1.1
ST	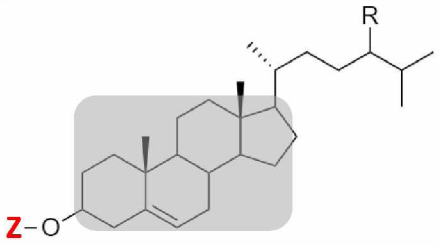	**Z** = H: cholesterol FA: cholesterol esters (CE) Glycan: steryl glycosides Among others: secosteroids, bile acids, estrogens, androgens, progestogens
PR	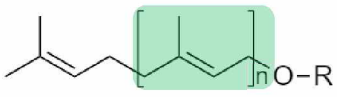 core structure (length may vary)	**R can be:** H, glycan, (pyro)phosphoglycan, *etc.* *E.g.*, isoprenoids, polyprenols, (hydro)quinones
PK	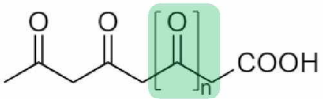 general precursor	*E.g.*, **Aflatoxin B1** from *A. parasiticus*
SL	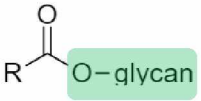	*E.g.*, **Kdo$_2$-Lipid A** from *E.coli*

1.1 Glycosphingolipids (GSL)

The discovery of glycosphingolipids (GSL), an important class of sphingolipids, can be attributed to Johann Ludwig Wilhelm Thudichum, who studied chemical composition of the brain, and isolated several compounds called cerebrosides from the brain in 1884 [5,6].

GSL comprise a vast group of remarkably heterogeneous biomolecules that are found in essentially all eukaryotes, as well as some prokaryotes and viruses. GSL are ubiquitous membrane components, which are almost exclusively located on the outer leaflet of cell plasma membranes and in intracellular organelles, facing the extracellular matrix [7,8]. The distribution of GSL across the plasma membrane is not uniform, but they rather cluster into small (*i.e.*, 10–50 nm) GSL-enriched microdomains (GEM) called lipid rafts, each consisting of hundreds of lipid molecules together with a few proteins (**Fig. 2**) [5,9]. Cholesterol (30–40 mol%), sphingomyelins, and glycosylphosphatidylinositol(GPI)-anchored proteins are dominant, whereas GSL are present in variable amounts [10].

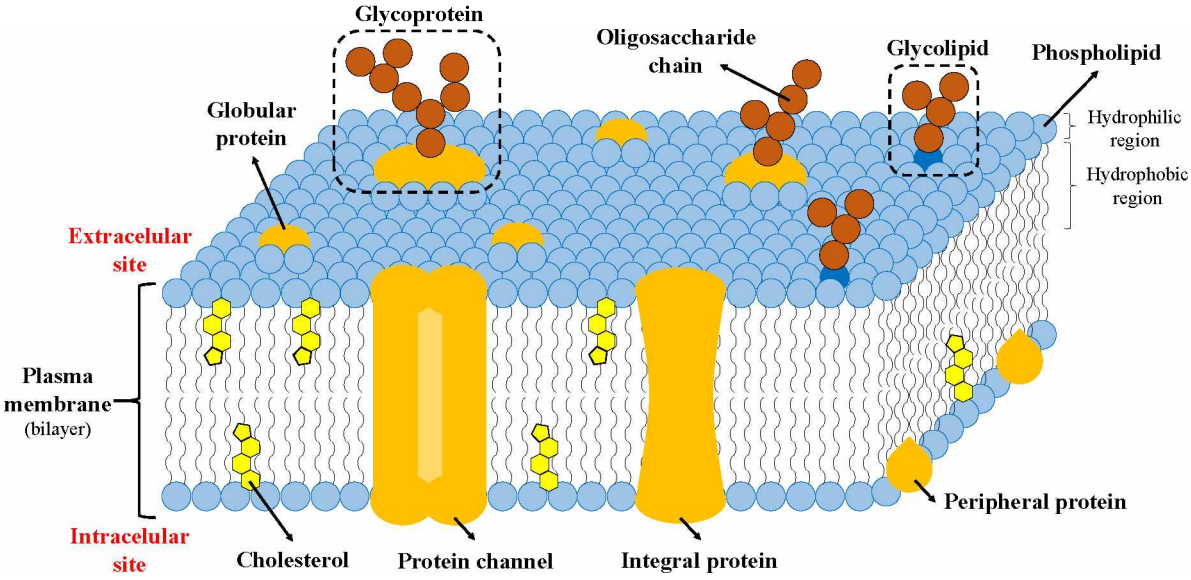

Fig. 2: Cross-section and structure of the cell plasma membrane (modified from [11]).

GSL are also found in plasma/serum, where they either circulate freely and/or are bound to protein complexes [12]. GSL as many of the other lipids are amphiphilic molecules composed of two distinct parts. The hydrophobic region consist of ceramide backbone anchored into the plasma membrane, while the hydrophilic region composed of glycan moiety glycosidically linked to a ceramide backbone faces the extracellular environment [2].

1.1.1 GSL biosynthesis

Biosynthesis of GSL occurs in a stepwise fashion initiated with the addition of fatty acyl-CoAs of different chain length to a sphingoid base (*i.e.*, sphinganine in *de novo* pathway or sphingosine in the salvage pathway) catalyzed by enzymes ceramide synthases (CerS) to yield either dihydroceramide or ceramide, depending on the substrate [13].

Briefly, the *de novo* biosynthesis of the most common ceramide (Cer) 18:1;O2/16:0 (34:1;O2, **Fig. 3**), is initiated in the endoplasmic reticulum (ER) by the rate-limiting condensation of L-serine and acyl-CoA catalyzed by serine palmitoyltransferase (SPT). Then, the resulting dehydrosphingosine 18:0;O is reduced to dihydrosphingosine 18:0;O2 (*i.e.*, conversion of 3-keto-sphinganine to D-erythro-sphinganine) by 3-ketosphinganine reductase (3-KSR). Subsequently, the CerS catalyzes the conjunction of C16:0-CoA and transforms dihydrosphingosine to dihydroceramide 18:0;O2/16:0 (*i.e.*, N-acylsphinganine). In mammals, there are at least six CerS isoforms (namely CerS1–CerS6), which are cell-type specifically expressed, and catalyze the same reaction. Nevertheless, each isoform exhibits specific preferences for fatty acyl-CoAs of different chain length (see **Table 2**) [13,14].

Table 2: Ceramide synthases (CerS) fatty acyl chain-length specificity [14,15].

Name	CerS1	CerS2	CerS3	CerS4	CerS5	CerS6
Specificity	C18-C20	C20–C26	C18–C32	C18–C20	C16	C14-C18

Finally, the carbon–carbon double bond is introduced by dihydroceramide desaturases (*i.e.*, DES1, DES2) to yield Cer 18:1;O2/16:0 (34:1;O2, *i.e.*, N-acylsphingosine) [14].

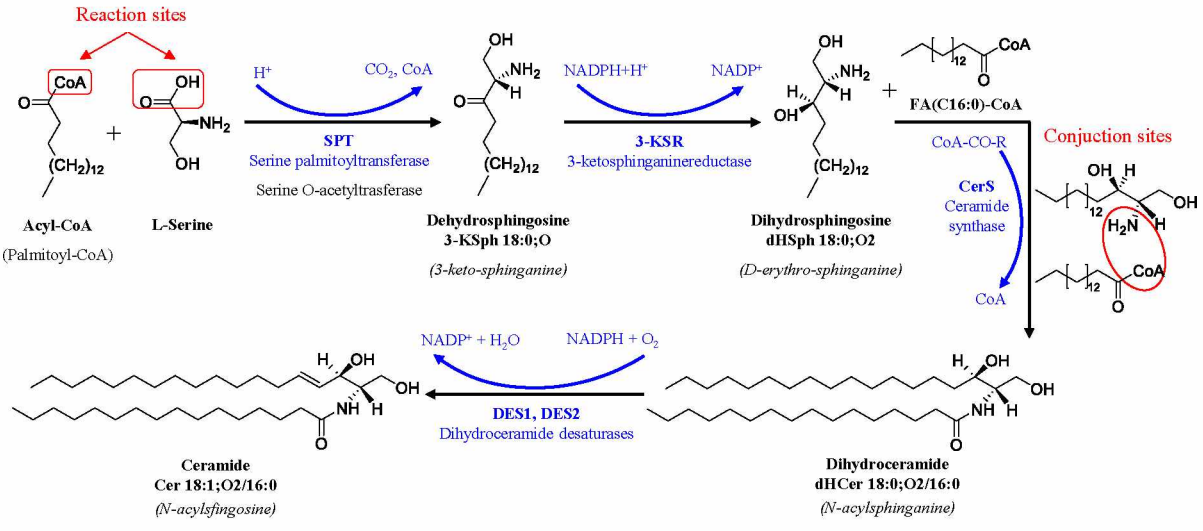

Fig. 3: De novo biosynthesis of ceramide 34:1;O2 (adopted and modified from [16]).

Ceramide is the key precursor in the synthesis of various (glyco)sphingolipids that are synthesized by stepwise addition of carbohydrate units first to the Cer and then to the growing glycan structure. The first sugar unit glycosidically linked to the 1-hydroxyl of Cer is typically β1→1 linked glucose (Glc) or galactose (Gal) producing either glucosylceramide (GlcCer) or galactosylceramide (GalCer) [5,7]. Alternatively, Cer can be converted to additional bioactive sphingolipids, such as sphingosine (Sph), sphingosine-1-phosphate (Sph1P), ceramide-1-phosphate (Cer-1-P), or sphingomyelin (SM) (**Fig. 4**) [16].

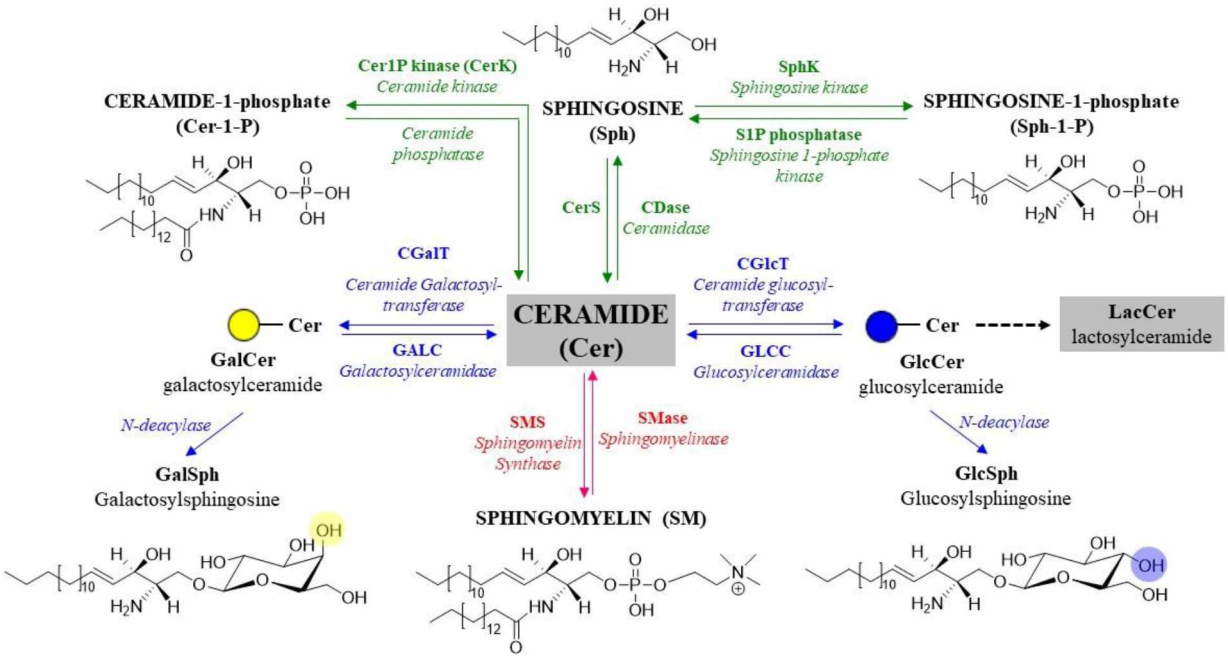

Fig. 4: Biosynthetic pathways of ceramide and formation of simple GSL (modified from [16]).

GalCer and GlcCer are synthesized in the ER and the Golgi apparatus (GA), respectively. However, the GlcCer production is dependent on the transport of Cer from the ER to the GA through one of two major pathways (**Fig. 5**). On the one hand, Cer can be transported from the ER to the *trans*-Golgi network (TGN) via ceramide-transfer protein (CERT), the pathway primarily used for the synthesis of SMs. On the other hand, Cer can be transported from the ER to the *cis*-Golgi network (CGN), most likely via vesicular trafficking [17–20]. Alternatively, GlcCer can be transferred from the CGN to TGN by lipid-transfer protein called four-phosphate adaptor protein 2 (FAPP2) followed by translocation to the luminal membrane leaflet of the GA [21–23] mediated most probably by the multidrug resistant P-glycoprotein to participate in the synthesis of neutral GSL [24]. The luminal-oriented GSL then reach plasma membrane via transport vesicles and therefore are mainly located on the extracellular side of plasma membrane [25].

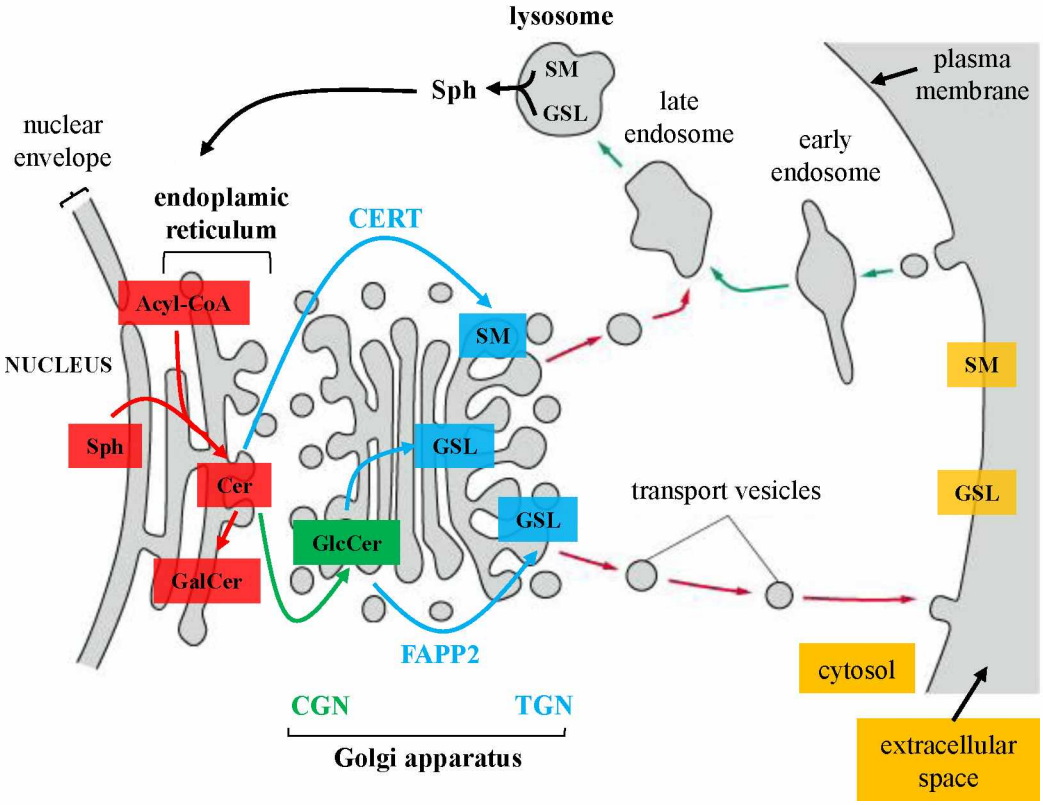

Fig. 5: Biosynthetic routes of GSL in the cell (adopted and modified from [19] and https://www.zoology.ubc.ca/~berger/B200sample/, accessed on December 7, 2022).

GlcCer and GalCer are the precursors of majority GSL generated in the GA by various glycosyltransferases (GTFs), enzymes that transfer a specific carbohydrate from the relevant nucleotide donor to a specific position on the Cer or non-reducing end of a growing glycan. In GSL synthesis, the uridine diphosphate glucose/galactose/N-acetylglucose/N-acetylgalactose (*i.e.*, UDP-Glc, UDP-Gal, UDP-GlcNAc, UDP-GalNAc) serve as nucleotide donors [26,27]. Prior to subsequent elongation by a series of GTFs to form complex GSL, GlcCer and GalCer must first be translocated from the cytosolic to the luminal leaflet of the GA membranes [28].

For example, GalCer can be sialylated by β-galactoside α-2,3-sialyltransferase (ST3Gal) to produce the most simple ganglioside GM4 (expressed mainly in brain and erythrocytes) [29], or sulfated by galactose-3-O-sulfotransferase (Gal3ST), which adds an $-OSO_3^-$ group to the C3 of Gal to produce monohexosylsulfatides (SHexCer) [26].

On the contrary, GlcCer can be galactosylated by β-1,4-galactosyltransferase (β4GalT) to form lactosylceramide (LacCer) representing a key metabolic branch point for the formation of different GSL series [26]. Furthermore, the elongation or formation of branched glycan structures in GSL is the result of the ordered action of specific GTFs (see **Fig. 6**) [27].

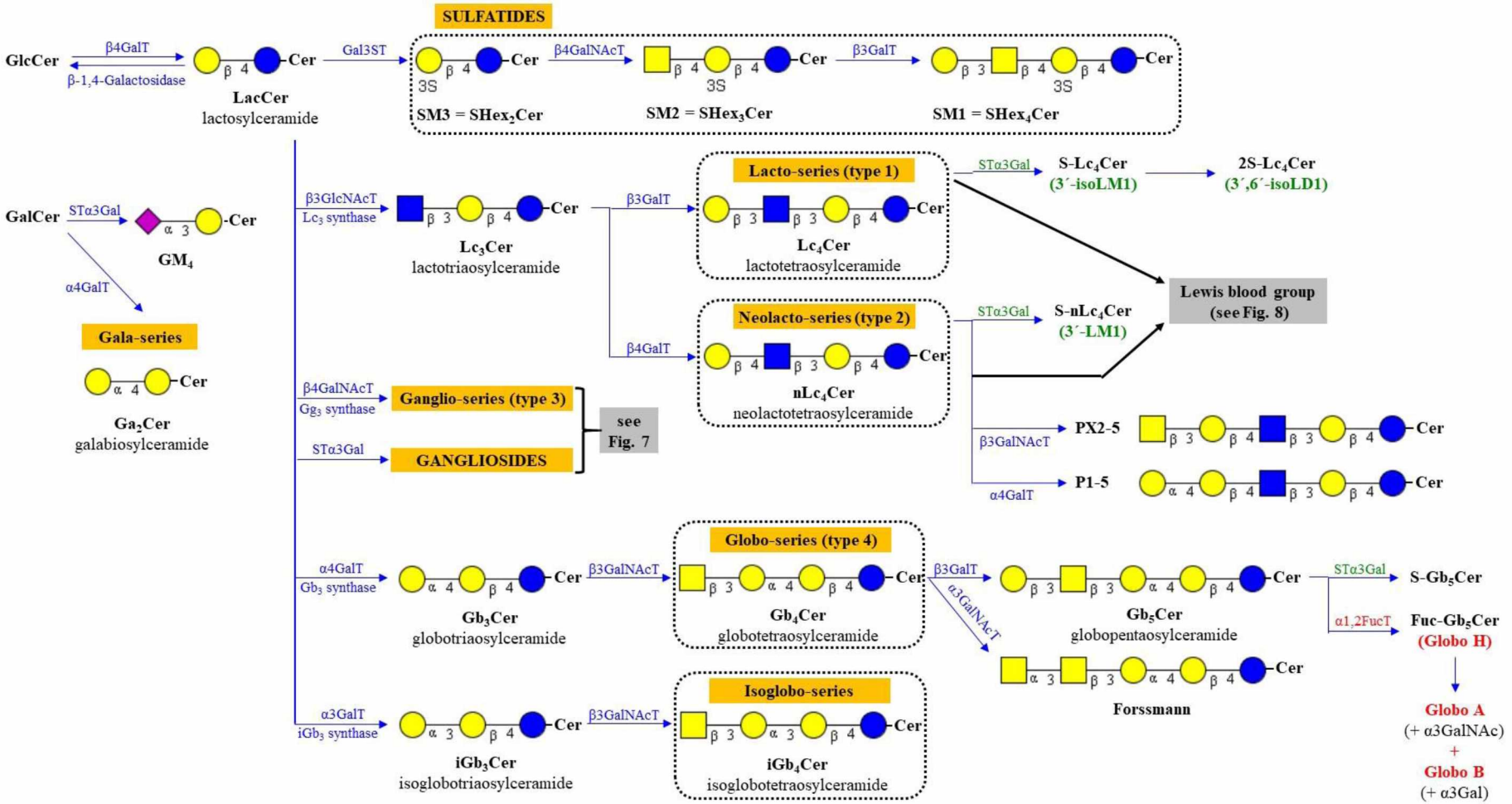

Fig. 6: Major biosynthetic pathways of complex GSL with corresponding enzymes (combined and modified from [16,30–33]).

Newly synthesized GSL and SM are then transported from the TGN to the cell surface in membrane-bound transport carriers [20,28]. GSL can be then rebuilt by glycosidases [34] or transported to endo-lysosomal district (*i.e.*, endosomes, lysosomes) with acidic pH required for enzymatic degradation by glycohydrolases to yield glycans and Cer. Cer is subsequently degraded by three isoforms of ceramidases classified based on their optimal pH as neutral (plasma membrane), acidic (lysosome), and alkaline (ER/GA) [35]. The resulting catabolism products of Cer (*i.e.*, Sph and FA) can be reverted to the ER and used for the synthesis of GSL (*i.e.*, salvage pathway), **Fig. 5.** The Sph is exclusively of catabolic origin derived from sphingolipids degradation[36].

Although GSL are expressed in a cell-specific manner that is principally determined by the intracellular distribution of the enzymes required for their biosynthesis (**Figs. 6 and 7**), most of these enzymes have rather poor specificity for their respective substrates. Therefore, in some cases, multiple enzymes can compete for the same GSL precursor leading to a great structural diversity. Gangliosides, a sialic acid-containing GSL, are synthesized across all cells with levels varying according to cell type and developmental stage. The synthesis begins with the transfer of sialic acid residues to LacCer with further elongation by sialyltransferases (SATs) and GTFs [37]. The synthesis of gangliosides in the brain where they predominate is thus a typical example of how competing pathways can lead to glycan diversity (**Fig. 7**) [5].

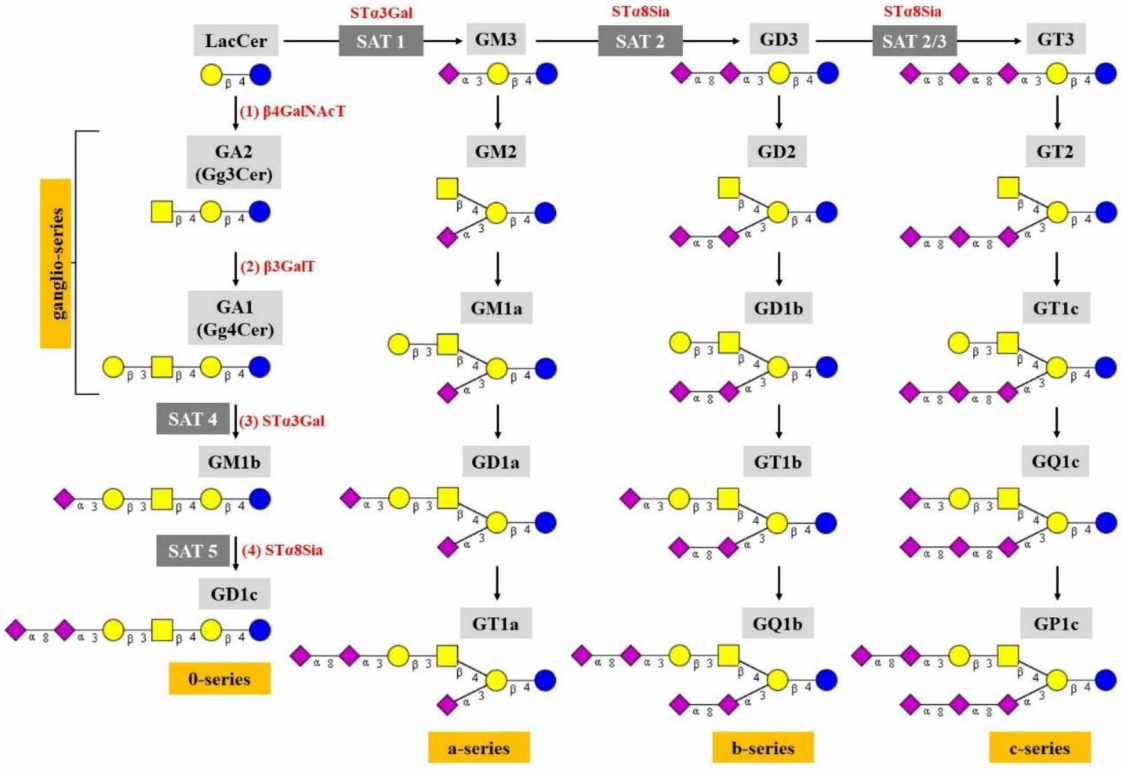

Fig. 7: Biosynthesis pathway of gangliosides (modified from [30,38]).

In this case, the competition between SATs transferring sialic acid residues to a nascent oligosaccharide chain and N-acetylgalactosaminyltransferase (GalNAcT) catalyzing the transfer of N-acetylgalactosamine to a-, b-, and c-series gangliosides (*i.e.*, converting GM3 into GM2, GD3 into GD2, or GT3 into GT2) at a key branch point determines the relative expression levels of the final GSL product. Similarly, further elongation of GM2, GD2 or GT3 with Gal to yield GM1, GD1b or GT1c, respectively, is accomplished by the same galactosyltransferase (GalT) [5].

Both N-acetylneuraminic (Neu5Ac) and N-glycolylneuraminic (Neu5Gc) acids are the two most common sialic acid residues mammalian cells. However, the sialic acids of human gangliosides are exclusively in the form of Neu5Ac and its O-acetylated derivatives due to a dysfunction of the enzyme cytidine monophosphate N-acetylneuraminic acid hydroxylase (CMAH) that converts cytidine monophosphate Neu5Ac (CMP-Neu5Ac) to cytidine monophosphate Neu5Gc (CMP-Neu5Gc) [5].

Although the enzymes catalyzing the initial steps in GSL biosynthesis are specific for GSL, outer sugars, such as outermost sialic acid or fucose are sometimes added by GTFs that also act on glycoproteins, resulting in terminal structures being shared by GSL and glycoproteins. One example is the blood group ABO(H) and Lewis system [5] (**Fig. 8**).

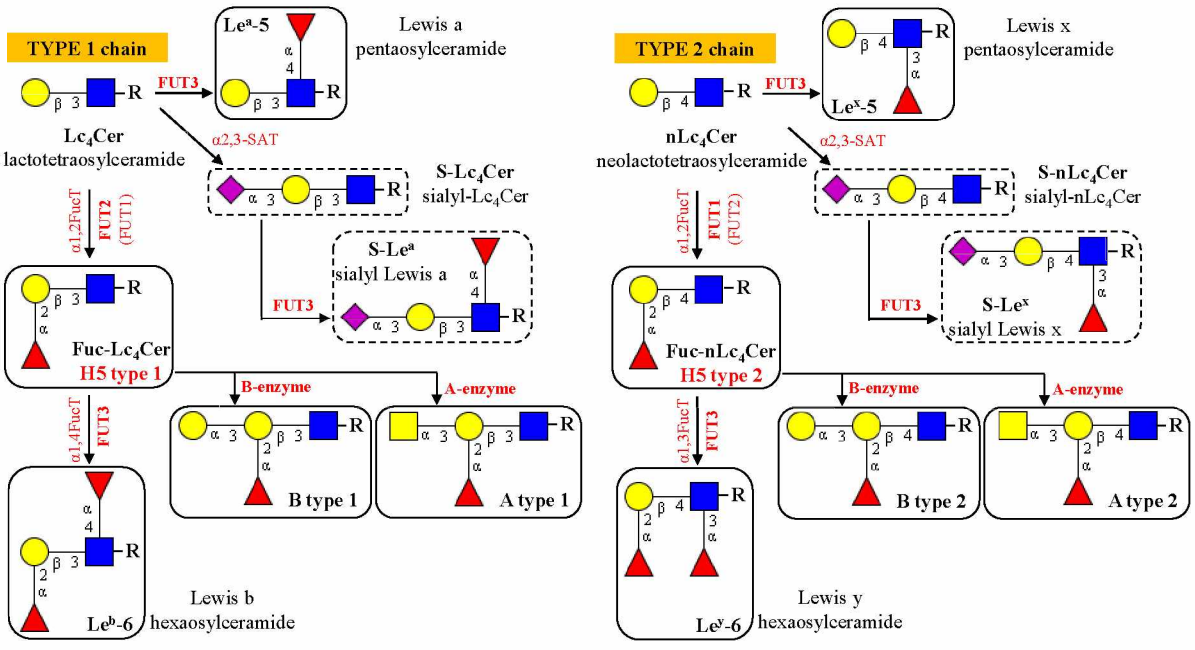

Fig. 8: Biosynthesis of blood group ABO(H) and Lewis GSL (modified from [39,40]).

ABH and Lewis blood group antigens are carbohydrate antigens expressed on GSL (~10%) and glycoproteins (~90%) [41,42]. They are synthesized by a variety of GTFs, mainly

FUTs. The majority of N-FUTs are located in the GA, while O-FUTs are located in the ER [43]. ABH antigens are mainly present on the red blood cell (*i.e.*, erythrocytes) membranes. The H type GSL, a biosynthetic precursor to A and B type GSL, is synthesized by the α1,2-fucosyltransferases (*i.e.*, FUT1 and FUT2), which add a terminal Fuc to Galβ1-3/4GlcNAc residue. H type GSL can then serve as a substrate for A- or B-transferase, which by adding α1,3-linked GalNAc or Gal to the same subterminal Gal produce A or B type GSL, respectively. Moreover, the synthesis of type 2 chain GSL requires the FUT1 that preferentially recognizes Galβ1-4GlcNAc residue, while type 1 chain GSL requires FUT2 that favors Galβ1-3GlcNAc residue (**Fig. 8**) [40,42].

Except for red blood cells, ABH antigens are also widely distributed in many tissues as thoroughly described by Ravn *et al.* [44], and in soluble form in body fluids and secretions. Specifically, expression of ABH antigens on type 2 chain GSL or Galβ1-4GlcNAc residue primarily occurs on human red blood cells and platelets, whereas they are a relatively minor component of epithelial cells. In contrast, ABH antigens on type 1 chain GSL are typical of gastrointestinal and genitourinary epithelial cells together with fluids and secretions [40,42].

Correspondingly, the synthesis of Lewis blood group GSL is dependent on the action of FUT2 and α1,3/4-fucosyltransferase (*i.e.*,FUT3) [41,45] with tissue-restricted expression (*i.e.*, strong expression in fluids, gastrointestinal, genitourinary, and respiratory tissues) [46]. FUT3 competes with FUT2 and A-/B-transferases (*i.e.*, GTA, GTB). Nonetheless, the type of precursor that FUT3 uses determines the type of Lewis antigen produced. On the one hand, Lewis a (Le^a) GSL is synthesized by FUT3 adding an α1-4Fuc to the subterminal GlcNAc of the type 1 chain. On the other hand, Lewis b (Le^b) GSL firstly requires the synthesis of H type 1 by FUT2, which is further processed by FUT3. Owing to the synthesis of H type 1 GSL, the synthesis of type 1 ABH-related GSL usually occurs as well. Direct conversion of Le^a to Le^b GSL is not possible due to steric hindrance of the α1-4Fuc. In addition, when the type 1 precursor is missing, FUT3 can use the type 2 precursors to generate Lewis x (Le^x) and Lewis y (Le^y) antigens, which commonly occurs in gastrointestinal tissues. It is thus evident that FUT3 can act on both type 1 and 2 chains [40]. There are also other FUTs with α1,3-activity (*i.e.*, FUT3–7 and FUTs 9–11) and α1,4-activity (*i.e.*, FUT3 and FUT5) [43]. Unlike ABH antigens, Lewis antigens, such as Le^a and Le^b are not synthesized in erythrocytes, but are taken up from plasma glycolipids and/or glycoproteins, and then can be incorporated into the red blood cell membrane. The fucosylation is a terminal modification, therefore, the presence of Fuc stops further chain elongation and branching as well [47,48]. Major enzymes involved in ABH and Lewis blood group determinants are summarized in **Table 3**.

Table 3: Major enzymes involved in the synthesis of ABH and Lewis type GSL [49,50].

Enzyme		Synthesized GSL
FUT 1 = α1,2-fucosyltransferase		H type 2
FUT 2 = α1,2-fucosyltransferase	Secretor factor	H type 1
FUT 3 = α1,3/4-fucosyltransferase	Lewis factor	Le^a, Le^b, Le^x, Le^y
GTA = α1,3-N-acetylgalactosaminyltransferase	ABO system	A type 1/2
GTB = α1,3-galactosyltransferase		B type 1/2

1.1.2 GSL structure and complexity

The majority of sphingoid-based lipids including GSL can be illustrated with a general structure composed of three building blocks (**Fig. 9**).

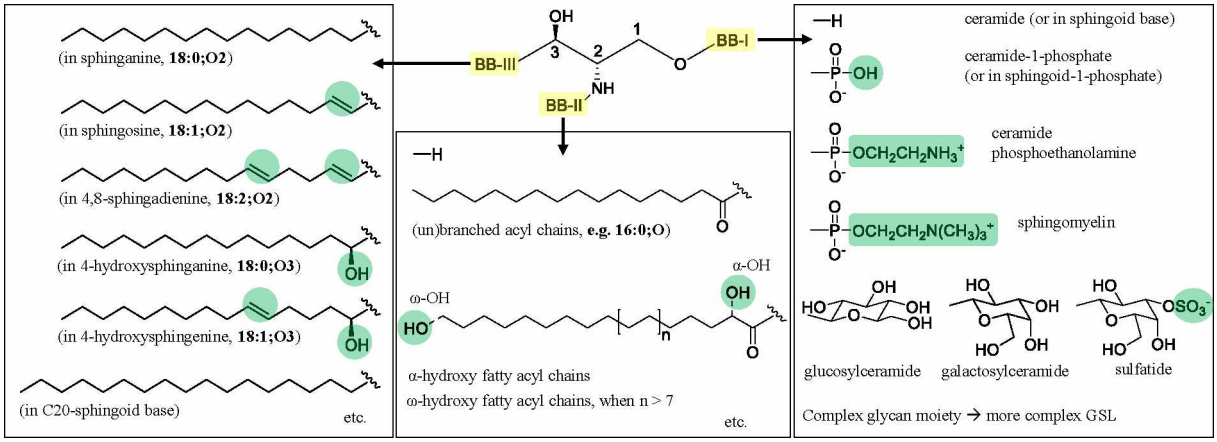

Fig. 9: General structure of (glyco)sphingolipids according to building block approach [2].

Building block I represents various head groups (*e.g.*, glucose, galactose, sulfated galactose, and other more complex glycoconjugates) linked at the C1 position of a sphingoid base to a 1-hydroxyl group. This part is primarily responsible for the hydrophilic properties of GSL molecules and allows head group classification of GSL (see **Figs. 6–8**).

According to the LIPID MAPS Structure Database, the composition of monosaccharide units may range from 1 to 20 units with the most frequently occurring residues summarized in **Table 4**, while the other residues are found less often. Only a limited subset of disaccharide combinations is found in vertebrates, including, for instance, Glc always linked to Gal, Fuc as a terminal unit, frequent repetition of Gal–GlcNAc residue, and unique chaining of sialic acid species, such as N-acetylneuraminic and N-glycolylneuraminic acid (*i.e.*, NeuAc and NeuGc). In addition, the anomeric nature of the glycosidic bond (*i.e.*, α- or β-linkage) together with the branching of the glycan chain contributes to the GSL heterogeneity [19].

Table 4: Abundance of the most frequently occurring monosaccharide units in GSL.

Residue	Glc	Gal	GlcNAc	GalNAc	Fuc	NeuAc
Symbol						
Abundance	~14%	~40%	~20%	~8%	~10%	~5%

Although Gal is the most common residue in GSL, only a few GSL are derived from GalCer compared to GlcCer, which makes up the majority of structurally diverse GSL [16].

Building blocks II and III represent a ceramide backbone composed of amide-linked FA at C2-position and C3-linked aliphatic chain to a sphingoid base via carbon–carbon bond. The backbone can vary in length of FA chains (usually C14–C30), degrees of unsaturation (*i.e.*, the number and positions of double bonds), potential branching, and the presence of α-hydroxyl group. Additionally, amide-linked FA can sometimes also have α- or ω- hydroxyl group [2,7]. The predominant sphingoid bases found in most mammalian cells are 18:0;O2, 18:1;O2, and 18:0;O3 [51,52] together with minor 18:2;O2 (*e.g.*, plasma [53]) and 18:1;O3 (*e.g.*, skin ceramides [54,55]). This is in accordance with the preference of mammalian SPT for saturated FA(C16)-CoAs [56] combined with the abundance of palmitoyl-CoA [51,52]. Nevertheless, other sphingoid bases (*i.e.*, C14–C26) have been also reported [57–59].

FAs are one of the major constituents of ceramides and information about their structure and cellular levels are also pivotal to fully understand many (patho)physiological properties of lipids. A simplified synthesis of FAs in mammals is depicted in **Fig. 10**. FAs of the n-7 and n-9 families, along with saturated FAs, are produced by the cellular machinery (**Fig. 10A**). Conversely, FAs of n-3 and n-6 families **(Fig. 10B)** are absent in mammals, thus, they can only be synthesized from their respective precursors obtained from dietary sources [60].

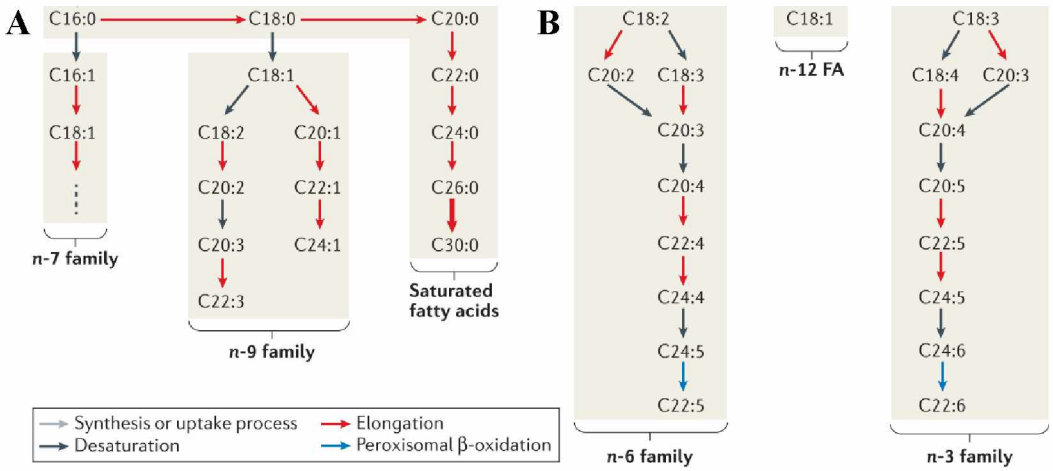

Fig. 10: Simplified synthesis of fatty acids in mammalian cells (modified from [60]).

The high degree of structural variations derived from the heterogeneous elongation of glycan chains covalently linked to the diverse ceramide backbones that can be assembled into countless combinations gives rise to an astonishing number of structurally distinct molecular species. The remarkable structural diversity of mammalian GSL, including >60 different sphingoid bases [7,61,62] and >300 distinct glycan chains [63], has been characterized and addressed on a number of omics websites (**Table 5**). Recently, considerably higher structural complexity of the glycosphingolipidome than previously anticipated was revealed together with additional cell- and tissue-specific structural heterogeneities found in both ceramide and glycan moieties. Most recently, the structures of major GSL glycans discovered in nature have been surveyed and listed by Guo [64]. Accordingly, it is likely that the >3000 unique GSL listed in the Lipid MAPS database are underestimated, as many GSL remain undetected or uncharacterized. It should be stressed that multiple evidence suggest that the ceramide backbone can affect the function of the glycan moiety, highlighting the importance of analyzing GSL in their native form to understand their biological functions [65].

Table 5: List of common omics-based websites.

Name	Website
LIPID MAPS	https://www.lipidmaps.org/
SphinGOMAP	http://www.sphingomap.org/
The Japanese Lipid Bank	https://lipidbank.jp/
Glycoforum	https://www.glycoforum.gr.jp/
The Consortium for Functional Glycomics	http://www.functionalglycomics.org/
The Complex Carbohydrate Research Center	https://ccrc.uga.edu/

1.1.3 Classification and nomenclature

GSL are classified based on their charges into neutral, acidic, and basic. Neutral GSL (N-GSL) include cerebrosides (1 sugar) and globosides (≥ 2 sugars), while acidic GSL (A-GSL) are subdivided into sialic acid-containing GSL called gangliosides and sulfated GSL called sulfatides with sulfate group at C3 hydroxyl of Gal. In contrast, basic GSL are rare [8].

Besides, the majority of GSL molecules are also classified based on their core structure called "series" (**Table 6**). The major series in vertebrates are ganglio, globo, and neolacto series, whereas in invertebrates the mollu and arthro series with mannose dominate [5,8].

Table 6: Classification of GSL according to their oligosaccharide core and their localization.

GSL series		Predominant occurrence	Core structure IV III II I
Ganglio	**Gg**	brain	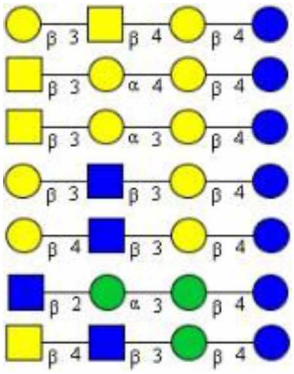
Globo	**Gb**	erythrocytes	
Isoglobo	**iGb**		
Lacto	**Lc**	secretory organs	
Neolacto	**nLc**	hematopoietic cells	
Mollu	**Mu**	invertebrates	
Arthro	**At**	invertebrates	

Generally, there is a need for a comprehensive and standardized nomenclature for lipids that are routinely analyzed by mass spectrometry-based methods. A uniform nomenclature is crucial for the unambiguous interpretation of lipidomic data and further progress of this evolving omics discipline. Adopting such a unified naming convention would facilitate automated data acquisition and import into databases with only minimal data processing [66]. As a result, the International Lipidomics Society (ILS, https://lipidomicssociety.org/) and the Lipidomic Standards Initiative (LSI, https://lipidomics-standards-initiative.org/) have recently been established in close collaboration with LIPID MAPS [67,68] to develop unified guidelines for the interpretation of lipidomic data across the lipidomic community.

Researchers need to know certain information about the levels of structural resolution of individual lipid species obtained by mass spectrometric analysis along with additional data to explain the shorthand annotation. These data should at least include the measured *m/z* values of the intact lipid species, characteristic adduct ions and fragment ions used for identification together with retention time if chromatography is applied [66].

There are many ways of naming and depicting GSL. Commonly, it is recommended to use the International Union of Pure and Applied Chemists (IUPAC) nomenclature [69], which is also followed by LIPID MAPS consortium. The LIPID MAPS annotation of GSL [4] in addition to updated versions published by Liebisch *et al.* [66,70] is followed throughout this work. GSL are annotated by (sub)class shorthand notation, followed by a space and number of C-atoms:DBE;O-atoms of the sphingoid base and N-linked fatty acyl residue mutually separated by a slash (*e.g.*, LacCer 18:1;O2/16:0). If the composition of the ceramide is not known, then the composition of the ceramide backbone is given in abbreviated form as the sum number of C-atoms:DBE;O-atoms (*e.g.*, LacCer 34:1;O2) (**Fig. 11**).

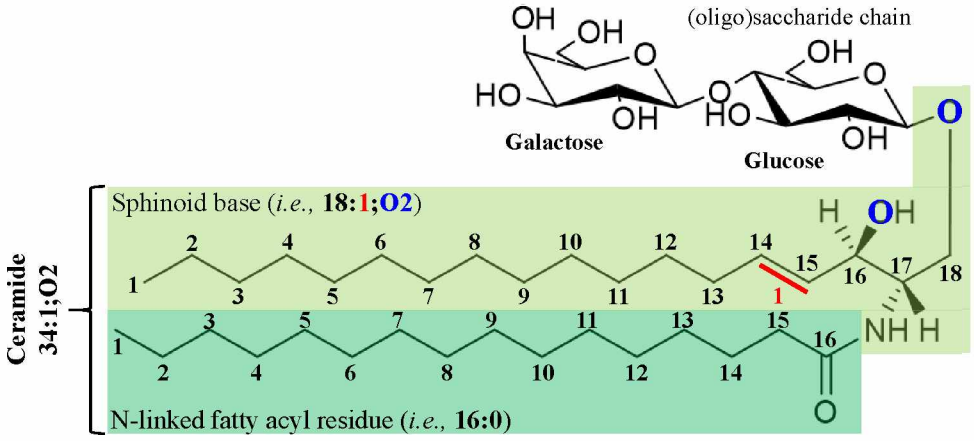

Fig. 11: Example of shorthand annotation of lactosylceramide (LacCer 18:1;O2/16:0).

Moreover, complex GSL are more easily understood from the explicit structure obtained from drawing software (*e.g.*, ChemDraw) or using glycan symbols (*e.g.*, GlycoWorkbench). Symbols for graphical representations of glycans used in this work follow the Symbol Nomenclature for Glycans (SNFG) [71,72] that have been widely adopted and anchored by the Consortium for Functional Glycomics and the Kyoto Encyclopedia of Genes and Genomes (http://www.functionalglycomics.org/fg/, http://www.genome.jp/kegg/glycan/) .

The nomenclature for gangliosides is too complex for daily use. Thus, gangliosides are usually referred by specific shorthand notation, where the first letter "G" refers to ganglioside, the following letter correspond to the number of sialic acids (*i.e.*, A, asialo-; M, monosialo-; D, disialo-; T, trisialo-; Q, tetrasialo, *etc.*), and the last numeral is calculated as 5–n, where 'n' refers to a number of monosaccharide units. The number of sialic acid (SA) residues linked to the internal Gal classify the gangliosides into 0- (no SA), a- (one SA), b- (two SA), or c-series (three SA) (see **Fig. 7**). It should also be noted that all sialylated GSL are well known as gangliosides regardless of whether they are based on the ganglio-series core structure [73].

1.1.4 Biological functions

GSL are bioactive effectors with many intriguing and versatile roles in cell physiology and pathophysiology. Their functions are largely governed by the glycan head group. In addition to being major constituents of cell plasma membranes, they also play a role in the organization of membrane microdomains (**Fig. 12A**), provide a rigid barrier for the separation

of cellular organelles, and are essential for the development of multicellular organisms. GSL also serve as energy storage necessary to ensure many biological processes [2,19].

GSL are unique molecules preferentially expressed on the cell surface, making them readily accessible. GSL functions generally fall into two major categories. The first one is modulating activities of receptors residing on the same plasma membrane (*i.e.*, cis-regulation) **(Fig. 12B–C)**. The second one is regulation of cell–cell interactions through binding with external molecules of extracellular matrix, soluble ligands or membrane receptors (*i.e.*, trans-regulation) (**Fig. 12D**) [74]. Both extra- and intra-cellular signaling processes and their interconnections are regulated by GEMs, cluster platforms moving in the fluid bilayer of the membrane [75].

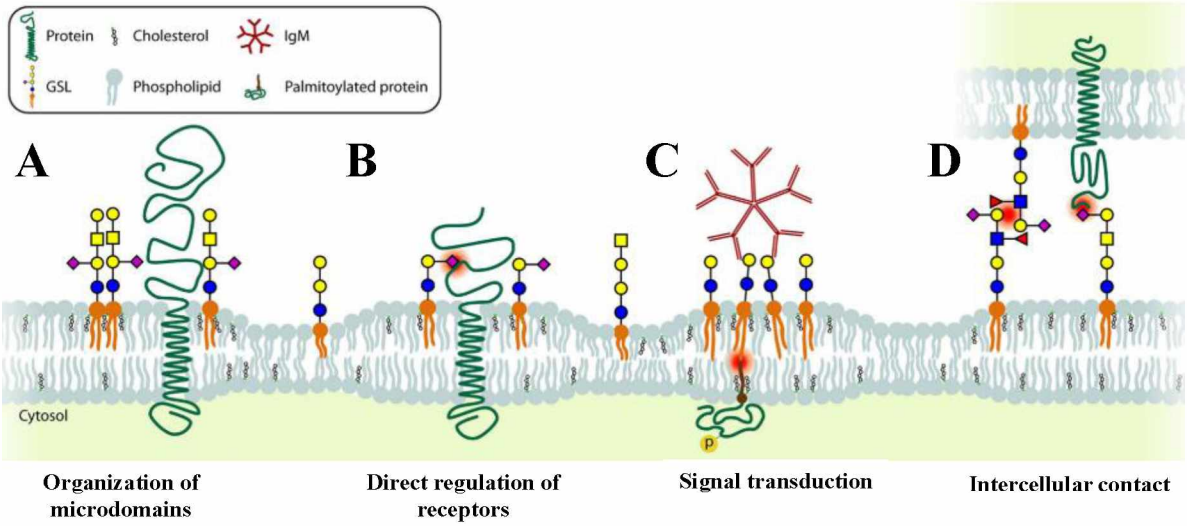

Fig. 12: Illustration of various GSL functions (adopted and modified from [76]).

As a result, GSL play a vital role as key transmembrane receptors via protein-protein, carbohydrate-carbohydrate, or protein-carbohydrate interactions. Specifically, GSL may serve as binding ligands or adhesion receptors for various proteins (*e.g.*, antibodies, lectins) [77], cellular molecules (*e.g.*, hormones), microbes (*e.g.*, bacteria and viruses) [78,79], and microbial products (*e.g.*, bacterial toxins) [80,81]. Glycan-binding proteins called lectins are classified into three major groups, namely selectins, siglecs, and galectins. Lectins are widely used in immunology due to their ability to recognize and bind specific glycans. The functions and binding properties of lectins are summarized in **Table 7** [82]. GSL act as modulators of signal transduction and messengers in cell signaling [83–88].

Table 7: Functions and properties of lectins [89–91].

Lectins	Bind to glycans with	Function
Selectins	NeuAc and Fuc	Major mediators of cell–cell adhesion and migration
Siglecs	NeuAc	Regulate cell adhesion, cell signaling, *etc.*
Galectins	β1,3- or β1,4-linked Gal to GlcNAc	Regulate cell growth, differentiation and adhesion Induce T-cells apoptosis → immunosuppression

It should be noted that GSL may not always be fully accessible. Glycan chains can also be hidden in a tangle of membrane (glyco)proteins or masked by sialylated glycoconjugates located in close proximity to GSL, which lead to reduced accessibility [92]. Furthermore, a few studies support the idea that GSL affect the cell cycle [93] and cell growth via inhibition or promotion of growth factor receptors, such as tyrosine kinase [94–96]. Studies have also reported the involvement of GSL in apoptosis [97–99] similar to cell-induced production of elevated levels of Cers in pathways leading to cell death [100]. Namely, increased levels of Sph, Cer, and dHCer, intermediates in GSL biosynthesis, are often linked with induction of cell cycle arrest and/or cell death, whereas increased levels of Sph-1-P, Cer-1-P, GlcCer, and LacCer are associated with increased cell survival and proliferation [101].

Gangliosides are found in almost all tissues, especially in membranes of the central and peripheral nervous system (make up to 6% of total lipids), where they form multi-layered membrane insulation called myelin that envelops nerve axons and allow rapid nerve conduction. They are predominantly found in the brain (>50% of the total glycoconjugates), where more than 90% of mammalian brain gangliosides is represented by GM1, GD1a, GD1b, and GT1b [102]. Gangliosides and other GSL have been shown to have crucial regulatory roles during embryogenesis and differentiation [103] resulting in several expressed GSL identified as stage-specific embryonic antigens (SSEA, see **Table 8**) [104].

Table 8: Stage-specific embryonic antigens (SSEA).

SSEA	SSEA-1	SSEA-2	SSEA-3	SSEA-4
GSL structure	Le^x	unknown	Gb5Cer	S-Gb5Cer

Next, normal extraneural-human tissues mainly express ”simple” gangliosides from 0- and a-series, while “complex” gangliosides from b- and c-series are primarily synthesized in developing tissues, during embryogenesis, and mainly restricted to the nervous system of healthy adults [102]. Moreover, ganglioside-associated suppression of the activity of several

immune cells is well documented in several studies, *e.g.,* downregulation of T- and B-lymphocytes activity and/or natural killer cell cytotoxicity [105–107]. Furthermore, GM3 and GD3 gangliosides were found to constitute ~65% of the total amount of gangliosides in the epidermis and dermis, with GD3 content increasing with age [108]. Similarly, SM4 sulfatides and their precursors GalCer are predominantly expressed GSL of oligodendrocytes and Schwann cells in central and peripheral nervous system [16,109]. GlcCer, constituting about 4% of the total epidermal lipid mass, together with Cers with long ω-hydroxy fatty acyl chains (C30–C36), are essential components of the skin that have key roles in normal functioning, such as a protective barrier against foreign substances and maintaining water impermeability [110,111]. The current knowledge on GSL indicates that they have membrane-organizing functions, while certain GSL species interact with specific proteins and/or lipids [112]. In addition, GSL expression is tightly regulated during development and differentiation, however, when GSL metabolism is dysregulated, specific GSL are expressed under certain pathophysiological conditions. Indeed, dysregulation of GSL metabolism has been found to play an important role in various diseases including cancer.

1.1.5 Association of GSL with disease

Lipidomics has tremendous potential to improve our understanding of pathophysiological conditions. Numerous perturbations of lipid metabolism have been identified as key factors in the onset and progression of a diverse array of conditions. Several lipids have already been proposed as diagnostic or prognostic markers, however, none of these have been translated into clinical trials principally because of the lack of large population-based studies [113].

Glycosylation represents the major post-translational modifications of biomolecules in eukaryotic cells that take place in the GA and ER via catalyzed action of GTFs, whose expression and function are tightly regulated in each cell, resulting in the formation of two major types of O-linked and/or N-linked glycoconjugates. Glycans are commonly covalently attached to proteins (*i.e.,* glycoproteins, proteoglycans, GPI-linked proteins), lipids (*i.e.,* glycolipids,), or other organic compounds [114,115]. Over the past decades, altered cell-surface glycosylation has been observed in many pathophysiological processes, leading to a large number of human diseases including cancer. Altered glycan structures are also often accompanied by the expression of tumor associated antigens (TAAs) that help cancer cells evade the immune system. These alterations in GSL profiles are mainly attributed to the gene expression dysregulation of glycosyltransferases [75].

GSL and diseases

Impacts of the simplest GSL, GlcCer and GalCer, on health and disease have been reviewed in detail by Reza *et al.* [116] with other more complex GSL described below. GSL have been shown to be implicated in the pathogenesis of various diseases, such as glycosphingolipidoses (reviewed in **Table 9**), autoimmune diseases (reviewed in **Table 10**), infectious diseases (reviewed in **Table 11**), diabetes, and cardiovascular diseases [117].

Glycosphingolipidoses, also termed lysosomal storage disorders, are the most common subgroup of inborn metabolic disorders caused by mutations in GSL catabolizing enzymes, defective transport molecules or dysfunctional accessory proteins. This leads to the blockage of specific GSL degradation pathways in lysosomes followed by their accumulation (**Fig. 13**). Glycosphingolipidoses represent a group of severe diseases manifested by a progressive neurodegenerative course accompanied by neuronal apoptosis (*i.e.,* neuropathy) with a relatively high collective frequency of 1:18,000. GSL are abundantly expressed in the nervous system, mainly gangliosides. Brain is frequently affected by the storage, *e.g.,* GM1-, GM2-, and GM3-gangliosidoses (**Table 9**) [102,118–121].

Table 9: Overview of (glyco)sphingolipidoses [118–120,122–125].

Disease		Defected enzyme	Accumulated lipids
GM1-gangliosidosis		GM1-β-galactosidase	GM1, GA1,
GM2-gangliosidosis:	Tay-Sachs disease	β-hexosaminidase A	GM2
	Sandhoff disease	β-hexosaminidase A,B	GM2, GA2, Gb4Cer
GM3-gangliosidosis:	Sialidosis	sialidase	GM3
Gaucher disease		GlcCer-β-glucosidase	GlcCer, GlcSph
Krabbe disease		GalCer-β-galactosidase	GalCer, GalSph
Fabry disease		α-galactosidase A	Gb3Cer, Ga2Cer
Farber disease		acid ceramidase	Cer
Metachromatic leukodystrophy		arylsulfatase A	SHexCer
Niemann-Pick type A and B		acid sphingomyelinase	SM

Another problem associated with the excessive storage of GSL is their susceptibility to N-acylsphingosine deacylase (acid ceramidase), a lysosomal enzyme allowing the cleavage of the N-linked fatty acyl from ceramide backbone, ultimately leading to the formation of lyso-glycosphingolipids species (*i.e.,* lyso-GSL), whose fate is also determined by the existence of other non-lysosomal catabolic activities [121].

Thus, most efforts aiming to fight these diseases have focused on enzyme replacement or substrate reduction therapies with the ultimate objective to balance the rates of synthesis with the impaired degradation, thus preventing accumulation of GSL. For example, intravenous enzyme replacement has been successful in treating Fabry and Gaucher disease [118].

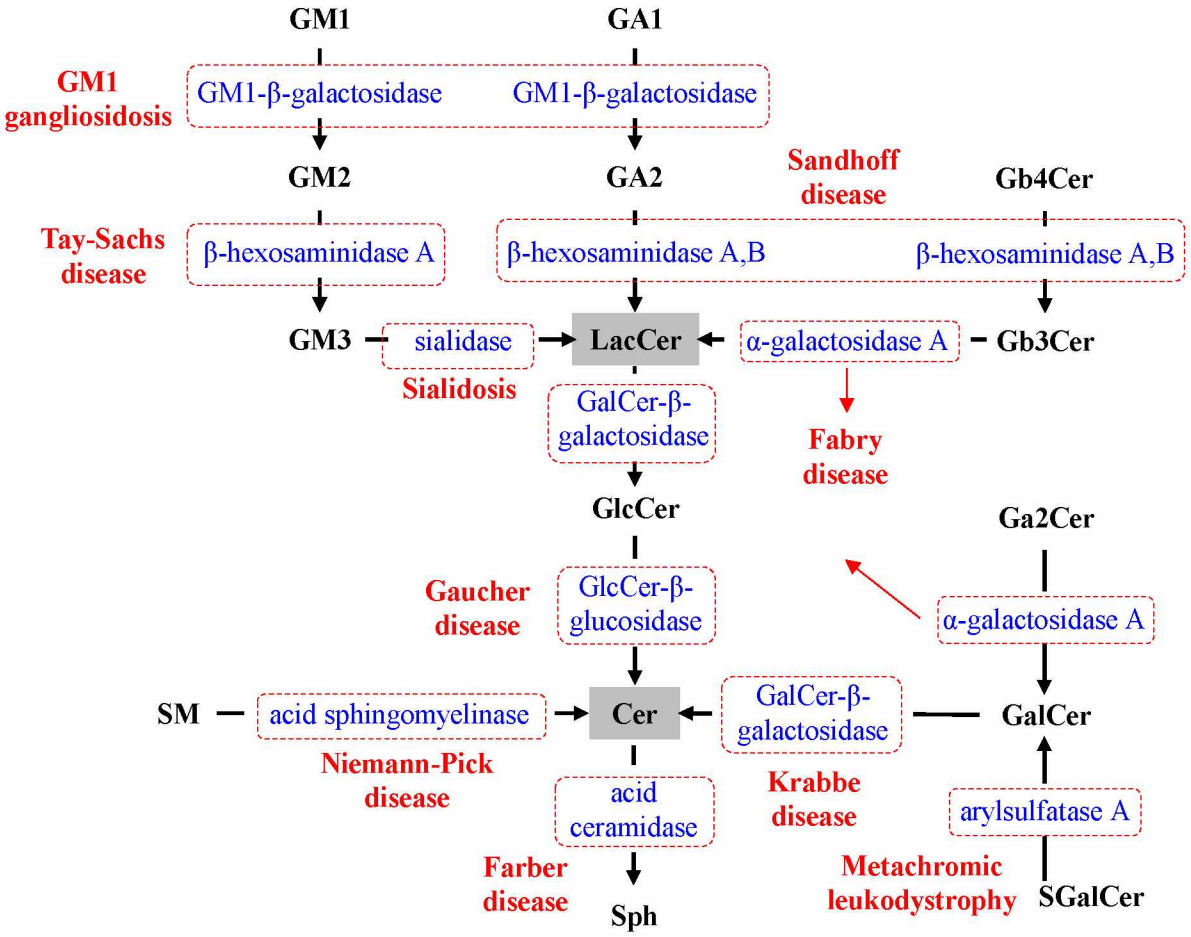

Fig. 13: GSL catabolism and mutual connection of lysosomal storage disorders [118,119].

GSL may also act as antigens for circulating antibodies in various autoimmune diseases in humans, affecting the nervous system. Several anti-ganglioside antibodies are expressed in a wide range of peripheral neuropathies including Guillain-Barré syndrome, Miller-Fisher syndrome, multifocal motor neuropathy, chronic idiopathic ataxic neuropathy, and acute motor axonal neuropathy (**Table 10**) [126–128].

Table 10: Selection of autoimmune diseases (peripheral neuropathies).

Autoimmune disease	Antibody produced against
Guillain-Barré syndrome	GM1a, GM1b, GM2, GD1a, GQ1b, SGalCer, S-nLc4Cer
Miller-Fisher syndrome	GT1a, GQ1b
Multifocal motor neuropathy	GA1, GM1a, GD1b
Acute motor axonal neuropathy	GM1, GD1a
Chronic ataxic neuropathy	GD1b, GD2, GD3, GT1b, GQ1b

Although the role of anti-GSL antibodies in the pathogenesis of those neuropathies is not fully understood, they are probably caused by mechanisms involving selective damage to motor neurons or sensory neurons [129], disturbances of ion channels function [130], and inhibitions of remyelination resulting in degeneration of axons (**Fig. 14**) [131,132].

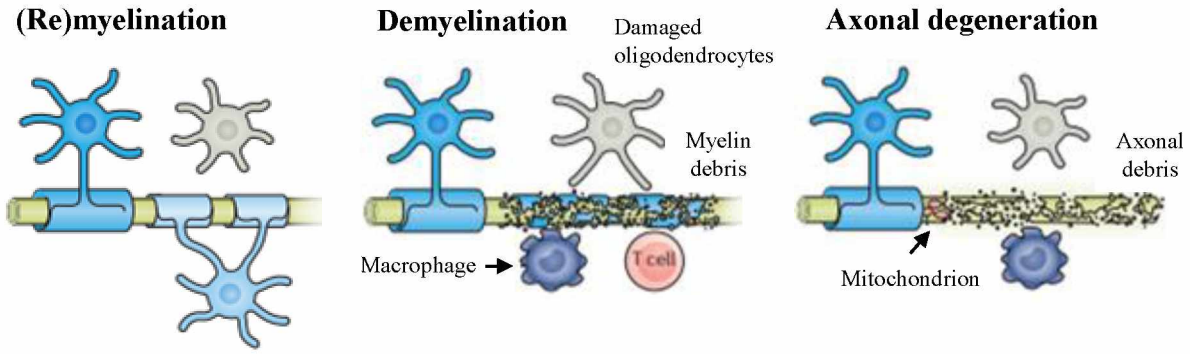

Fig. 14: Inhibition of remyelination in neuropathies (modified from [133]).

GSLs also function as binding sites or receptors for viruses, bacteria, and their toxins (**Table 11**). One of the well-studied examples is cholera toxin (from *Vibrio cholerae*) expressing a sialidase that removes terminal Neu5Ac from GSL of the intestinal epithelia cells and heat-labile enterotoxin LT-I (from *Escherichia coli*). These toxins consist of an A-subunit (catalytic activity) and pentameric B-subunit (binding activity) with a high binding affinity for GM1 ganglioside, resulting in massive secretory diarrhea [134–138]. Heat-labile enterotoxins of type LT-IIa, LT-IIb, and LT-IIc were also found to bind other gangliosides including sialylated nLc-GSL [139]. Moreover, globoside has been reported as binding ligand of Shiga toxins produced by *E. coli* [140–142]. Sialic acid-binding lectins from *Helicobacter pyroli* recognize complex gangliosides and cause gastric ulcers and infect the gastric lining [143,144]. Among others, LacCer has been reported as an adhesion receptor for *H. pyroli* [145]. Roche *et al.* [146] described the binding of *H. pyroli*-produced vacuolating cytotoxin to

GlcCer, GalCer, Ga2Cer, LacCer, and Gb3Cer. The binding ability to short-glycan GSL leads to a tight membrane attachment that may simplify the incorporation of the toxin into the cell. Interestingly, bacteria, viruses, and toxins can also be inactivated after binding with GSL provided exogenously in the diet to prevent the translocation of microorganisms into the internal environment [147].

Table 11: Selection of infectious diseases linked with gastrointestinal tract.

Disease	Pathogen	GSL involved	Reference
Cholera	*V. cholerae* (cholera toxin)	GM1	[135,136]
Severe diarrhea	*E. coli* (heat-labile enterotoxins)	GM1, GM2, GM3, GD1, GT1, S-nLc4, S-nLc6, S-nLc8	[138,139]
	E. coli (Shiga toxins)	Gb3Cer	[142]
Gastritis and gastric ulcers	*H. pyroli* (vacuolating cytotoxin)	S-nLc6, S-nLc8, S-dimeric-Le^x	[144]
		Glc-/Gal-Cer, Ga2Cer, Gb3Cer	[146]
		LacCer	[145,146]

GSL and cancer

It is well-known that GSL impact cancer cell energy metabolism. Accelerated uptake of nutrients is essential for the production of new biomass to sustain increased cell proliferation. A large number of clinical studies have repeatedly reported altered glycosylation patterns as a common feature of carcinogenesis. The dysregulation of glycosyltransferases, such as fucosyltransferases (FUTs) [148] and sialyltransferases (SATs), [149] that are involved in the modification and termination of GSL, have been reported. Thus, aberrant glycosylation with associated enzymes and the shift from type 1 (Lc-series) to type 2 (nLc-series) GSL are now widely accepted as one of the hallmarks of tumor initiation and progression [150].

Altered GSL patterns observed in tumors initially depend on an enzyme called glucosylceramide synthase (GCS), which is responsible for the formation of the simplest GSL, GlcCer. Upregulation of GCS has been shown to lead to a depletion of Cer pools, which would otherwise exhibit cytotoxicity, by conversion into GlcCer. Many agents, such as physical stress (*e.g.*, heat shock, ionizing radiation), anticancer drugs (*e.g.*, cisplatin), cytokines, or hormones, can trigger cell cycle arrest and apoptosis by increasing intracellular ceramide levels via exogenous delivery, stimulation of *de novo* synthesis, or inhibition of ceramide metabolism for the biosynthesis of complex sphingolipids. Cer is known to play an important role in the regulation of cell fate by being directly involved in the regulation of

mechanisms controlling growth arrest. Therefore, Cer has emerged as a critical mediator of blockage of specific survival signaling pathways that are typically triggered by kinases or growth factors. Consequently, cytotoxic drug-induced accumulation of Cer can target tumor cells apoptosis and become an attractive chemotherapeutic strategy. However, the cytotoxicity can be significantly suppressed by elevated GCS activity caused by cancer cells aiming to escape apoptosis. Thus Cer, GlcCer, and GCS are key players in cancer [104,151–156].

Dysregulated glycosylation is also closely associated with the development of multidrug resistance (MDR) in cancer chemotherapy through the establishment of an apoptosis-resistant phenotype. Resistance to drugs can be either mediated by already existing factors in tumor cells or acquired during therapy (*e.g.,* novel mutations or adaptive responses) [156].

Simple GSL can be further modified by various GTFs including SATs (sialylation) and FUTs (fucosylation). For instance, ganglioside-enriched profiles have been associated with apoptosis-resistant behavior, along with markedly up-regulated sialidase-3 in some types of cancer [156]. Moreover, healthy human tissues exclusively contain NeuAc, however, NeuGc is expressed in certain tumors and human fetal tissues, hence, it is referred to as an oncofetal antigen [92]. Additionally, sialylation of the type 2 chain takes place extensively compared to the type 1 chain resulting in the production of terminally α2,3-sialylated structures [157].

Remarkable alterations in GSL expression can particularly be observed in human brain tumors. Glioblastoma multiforme, the most malignant brain tumor, is characterized by the accumulation of GM3 and GD3 gangliosides together with increased levels of newly synthesized globo- and lacto-series GSL, while brain-typical complex gangliosides are completely absent [158]. Furthermore, b-series gangliosides, specifically GD2 and GD3, have been reported to enhance the malignant properties of cancer cells in various cancers. For example, GD3 ganglioside has been identified as a melanoma-specific antigen resulting in a high amount of GD3 in melanoma cells compared to levels of GD3 expressed in melanocytes, a normal counterpart of melanoma cell, suggesting that GD3 might play an important role in the transformation of melanocytes into melanomas [159]. On the other hand, a-series gangliosides, such as GM1, GM2, and GM3, often suppress malignant properties of various cancer cells. This implies that GD3 synthase represents a key enzyme determining the cell phenotypes based on the ganglioside expression patterns (**Fig. 15**) [77].

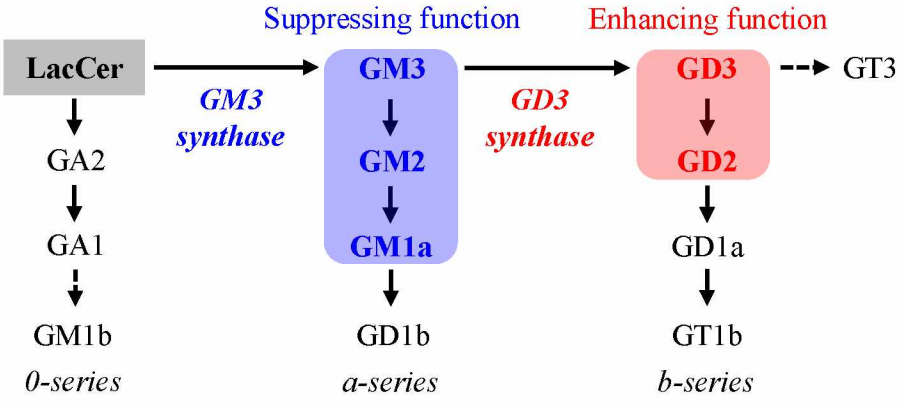

Fig. 15: Distinct roles of various gangliosides in cancers (modified from [77]).

Fucosylation, one of the most important glycan modifications in cancer, was first reported by Hakomori's group [157,160]. It has also been reported that FUTs are elevated in various malignancies. Both FUT1 and FUT2 have been shown to have a pivotal role in cancer cell progression [161,162]. Similarly, the upregulation of FUT4 [163], FUT5 [164], FUT6 [165], and FUT7 [166] promotes proliferation of cancer cells and obstructs their apoptosis [167], highlighting the importance of impaired fucosylation during malignant transformation.

Fucosylation contributes to the expression of ABH and Lewis antigens in cancer cells, and these antigens may represent potential biomarkers in cancer diagnosis. ABH antigens are typically absent from glyco-lipids/proteins of tumor tissues despite being found in the adjacent normal tissues. In many cases, the loss of ABH antigens from tumor cells, especially A and/or B antigens, arises from reduced or vanished activity of A- and/or B-transferases. This results in the accumulation of H, Le^a, Le^x, their sialyl derivates (*i.e.*, S-Le^a or S-Le^x), and also Le^b and Le^y, which is in line with the increased fucosylation. Furthermore, both SLe^a and SLe^x have been associated with an increased ability to develop metastases and poor survival of the patients[168]. In the very rare Bombay phenotype, mutations in both FUT1 and FUT2 result in individuals lacking all ABH antigens. Consequently, knowledge of the distribution of these antigens in normal tissues is of importance for the evaluation of tumor-associated alterations [40,168]. The mechanisms underlying the tumor-specific glycosylation changes are not yet fully understood and should be investigated in more detail [169].

Dysregulation of GSL in various cancers has previously been review by Zhuo *et al.* [170], Hakomori [171], Hakomori and Zhang [172], and Russo *et al.* [155]. However, more comprehensive overview of the GSL involved in the pathogenesis of a variety of cancers is summarized in **Table 12**.

Table 12: List of upregulated (↑) and/or downregulated (↓) GSL for various types of cancer.

Dysregulated GSL		Cancer type [reference]
SULFATIDES	SHexCer (SM4)	Kidney cancer ↑ [173–175] ↓ [173,176,177], colon cancer ↑↓ [178], ovarian cancer ↑ [179]
	$SHex_2Cer$ (SM3)	Kidney cancer ↑ [173,175,176,180], liver cancer ↑ [181,182]
	6-HSO_3-GSL	Colon cancer [183]
GANGLIOSIDES	GM1	Colorectal cancer ↓ [184], lung cancer ↑
	GM2	Melanoma ↑ [185–188], gastrointestinal cancer ↑ [189], lung cancer ↑ [190], breast cancer ↑ [191], pancreatic cancer ↑ [192]
	GM3(NeuAc) + de-Ac-GM3*	Melanoma ↑ [185,186,193], lung cancer ↑ [194], kidney cancer ↑ [174,195,196], leukemia ↑ [197] ↓ [149], bladder cancer ↓ [198], ovarian cancer ↓ [199], colorectal cancer ↓ [200], melanoma* ↑ [201,202]
	GM3(NeuGc)	Glioblastoma ↑ [203], breast cancer ↑ [204], lung cancer ↑ [205], colon cancer ↑ [206], multiple cancer types ↑ [207]
	GM4	No reference found
	GD1a	Prostate cancer ↑ [208], breast cancer ↑ [191], colon cancer ↓ [184]
	GD1b	Glioblastoma ↑ [209] ↓ [203], breast cancer [210]
	GD2 +9-O-Ac-GD2*	Melanoma ↑ [185,186,211,212], neuroblastoma ↑ [213–219], osteosarcoma ↑ [220], sarcoma ↑ [221], lung cancer ↑ [194,222], breast cancer ↑ [191,223–226], retinoblastoma ↑ [227]
	GD3 +9-O-Ac-GD3*	Melanoma ↑ [159,185,186,193,228–231], osteosarcoma ↑ [220], sarcoma ↑ [221], leukemia ↑ [232], breast cancer ↑ [191,204,223,224], glioma ↑ [233,234], glioblastoma ↑ [203], ovarian cancer ↑ [235], neuroblastoma ↑ [212], lung cancer* ↑ [236,237]
	GT1b	Glioblastoma ↓ [203]
	GT2	No reference found
	GT3	Breast cancer ↑ [224]
	S-Gb5Cer	Prostate cancer ↑ [238,239], breast cancer ↑ [240], glioblastoma ↑ [241]
	S2-Gb5Cer	Kidney ↑ [242–244], prostate cancer ↓ [245], liver cancer ↑ [246]
	S-Lc4Cer	Glioma ↑ [233,247], lung cancer ↑ [248]
	S2-Lc4Cer	Glioma ↑ [247]
	S-nLc4Cer	Prostate cancer ↑ [208]
N-GSL	GlcCer	Kidney cancer ↓ [249], leukemia ↓ [250]
	GalCer	Ovarian cancer ↑ [179]
	α-GalCer	Leukemia ↓ [251], lung cancer ↓ [252,253], melanoma ↓ [254,255], colorectal cancer ↓ [256,257]

… table continues

N-GSL	LacCer	Kidney cancer ↑ [196,249], prostate cancer ↑ [258], breast cancer ↑ [259]
	Lc3Cer	Leukemia ↑ [197], ovarian cancer ↑
	Lc4Cer	Human embryonal carcinoma ↑ [260]
	nLc4Cer	Leukemia ↑ [197], ovarian cancer ↑ [261]
	Gg3Cer	No reference found
	Gg4Cer	Prostate cancer ↑ [262,263], breast cancer ↓ [264]
	Gb3Cer	Burkitt´s lymphoma ↑ [265,266], breast cancer ↑ [267] ↓ [191], colon cancer ↑ [268–271], ovarian cancer ↑ [272], testicular cancer ↑ [273], gastrointestinal cancer ↑ [274,275], lung cancer ↑ [276]
	Gb4Cer	Gastrointestinal cancer ↑ [274], colorectal cancer ↑ [270,277]
	Gb5Cer	Lung cancer ↑ [278], testicular cancer ↑ [279], breast cancer ↑ [280,281], colorectal carcinoma ↑ [282]
	P1-5	Ovarian cancer ↑ [283], gastric cancer ↑ [284]
	PX2-5	No reference found
Fucosylated and fucosialylalted GSL	H5 (Fuc-(n)Lc4Cer)	Colon cancer ↑ [285,286]
	Globo H (Fuc-Gb5Cer)	Breast cancer ↑ [259,280,287], ovarian cancer ↑ [288], thyroid cancer ↑ [289]
	Le^a	No reference found
	Le^x	Colon cancer ↑ [157,172,286], bladder cancer ↑ [290], gastric cancer ↑ [172], breast cancer ↑ [157,172]
	Le^b	Colon cancer ↑ [285]
	Le^y	Colon cancer ↑ [285]
	Le^a-Le^a	Gastric and colon cancer ↑ [157,172]
	Le^x-Le^x	Gastric, colon and breast cancer ↑ [157,172]
	Le^y-Le^x	Lung, colon and pancreatic cancer ↑ [172]
	Fuc-LacCer	Breast cancer ↑ [259]
	Fuc-nLc4Cer	Breast cancer ↓ [191]
	Fuc-GM1	Lung cancer ↑ [291–295], liver cancer ↑ [246]
	SLe^a	Lung cancer ↑ [296,297], gastrointestinal cancer ↑ [298], pancreatic cancer ↑ [298], colon cancer ↑ [298–300], breast cancer ↑ [301], bladder cancer ↑ [302]
	SLe^x	Lung cancer ↑ [297], colon cancer ↑ [157,299,300] ↓ [286], breast cancer ↑ [301], liver cancer ↑ [303], bladder cancer ↑ [290,302], pancreatic cancer ↑ [172]
	SLe^b	Lung cancer ↑ [296]
	SLe^y	No reference found

Pancreatic cancer

Pancreatic cancer is one of the most frequent cause of cancer-related deaths worldwide despite the low lifetime risk of developing pancreatic cancer (~1.3% to age 70 years) [304]. Pancreatic ductal adenocarcinoma (PDAC) is an aggressive malignant epithelial neoplasm representing the most prevalent type of pancreatic cancer (accounts for >90% of cases). PDAC is also characterized by early distant metastases formation [304–307].

The global incidence of PDAC is higher in males compared to females (5.7 vs. 4.1 per 100,000 people) and varies among countries, with the highest incidence rates in Europe and North America [308]. It is also higher in developed countries than in developing countries [309]. The highest mortality rates belong to Europe and North America as well (7.2 and 6.5 per 100,000 people), with at least 90% of PDAC deaths reported in patients aged ≥ 55 years, indicating an increased onset of PDAC with increasing age [310]. Overall 1-year and 5-year survival is <20% and <10% [311,312]. In addition, the number of PDAC patients continues to increase globally with reported annual increase >1% [310]. These unfavorable facts rank PDAC as one of the most devastating cancer worldwide [313].

The development of PDAC is also strongly related to family history, genetic disorders (*e.g.,* hereditary pancreatitis), complications (*e.g.,* obesity, diabetes, chronic pancreatitis), and modifiable factors. All those factors have been reported to increase the risk of PDAC [310,314]. It has been reported that up to 10% of PDAC patients have an inherited genetic predisposition caused by specific mutations in multiple genes [315,316] and individuals with non-O blood groups have been associated with a higher risk of PDAC [317–319]. Life style habits, such as have been shown to increase the risk of PDAC, *e.g.,* tobacco smoking or heavy alcohol consumption [320–324]. Additionally, eating red meat containing carcinogens, such as NO_2^-, NO_3^-, or N-nitroso compounds [325], and the exposure to chemical substances (*e.g.,* chlorinated hydrocarbons) [326] have also been identified as risk factors of PDAC.

Unfortunately, the clinical manifestation of PDAC in the early stages is non-specific and usually without any symptoms. Therefore, even imaging of early-stage tumors by magnetic resonance imaging, computed tomography, positron emission tomography, or endoscopic ultrasound is very difficult. The diagnosis of pancreatic cancer thus relies on imaging methods and invasive procedures, such as tissue biopsies used for the final confirmation [327].

The pathogenesis of PDAC is a multi-stage mutation from normal pancreatic tissue followed by the formation of microscopic precursor lesions, such as pancreatic intraepithelial neoplasia (PanIN), that can eventually progress into invasive PDAC (**Fig. 16**) [304,313,328].

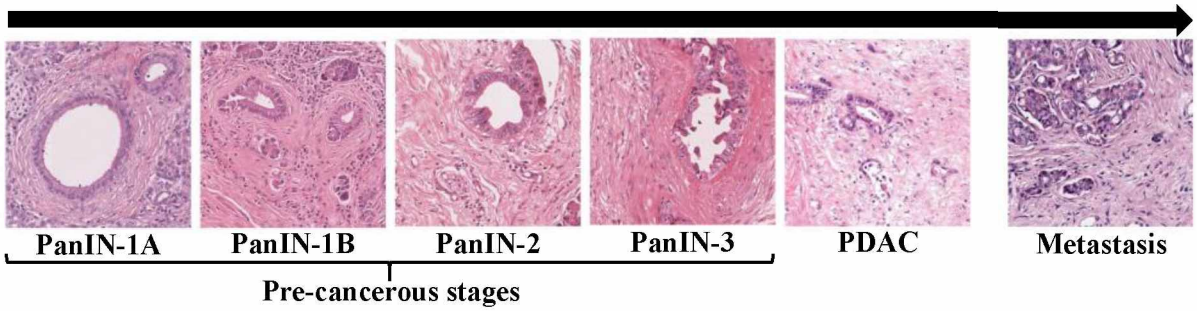

Fig. 16: Histological development and progression of PDAC (adopted from [313]).

Roughly 60–70% of PDAC cases are located in the head of the pancreas and are usually diagnosed earlier than tumors arising from the body and tail, which are characterized by a worse prognosis [327,329]. Additionally, only about 2% of PDAC patients are diagnosed at the pre-cancerous stage (*i.e.*, T0), or at an early stage (*i.e.*, T1 and T2) [310,328]. Conversely, most of them (80–90%) are diagnosed at the locally advanced (*i.e.*, T3) or metastatic (*i.e.*, T4) stage, when the surgery is no longer an option (**Fig. 17**) [305,306,330].

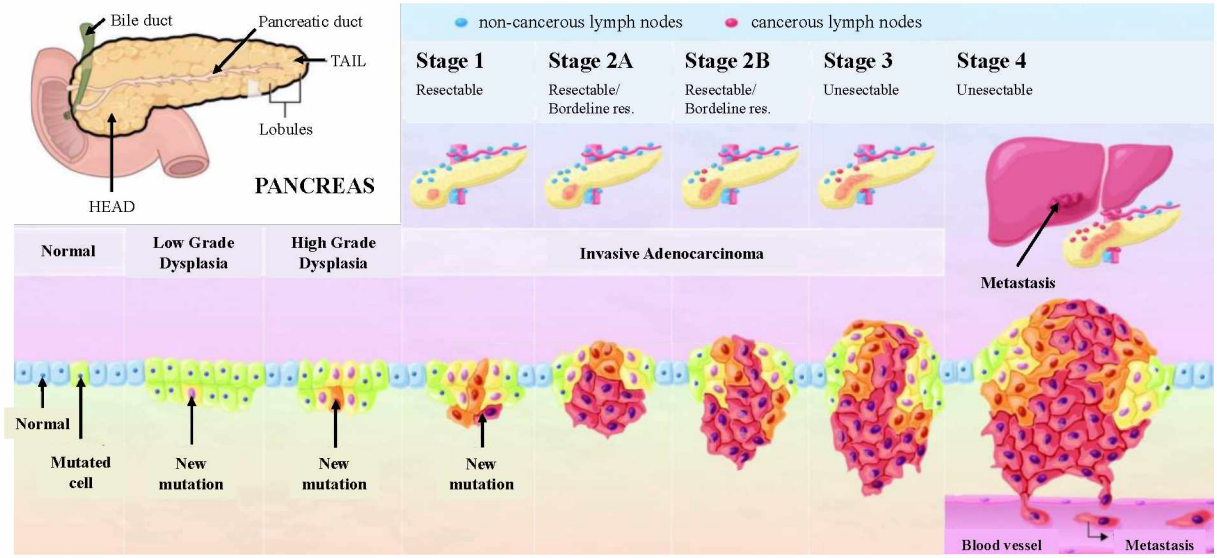

Fig. 17: Pancreatic cancer staging (adopted from [313] and *https://immunoviainc.com/*, accessed on January 11, 2023).

The tumor, node, and metastasis (TNM) system (**Tables 13 and 14**) is a widely adopted and universal staging system for solid tumors primarily intended for cancer surveillance, deciding eligibility for clinical trials, and guiding treatment and prognosis. The tumor size prognosis of PDAC is however not reliable due to unpredictable behavior compared to other solid tumors. Moreover, TNM system does not take into account the resection status [331].

Table 13: T-staging system for solid tumors modified from [331].

T-stage (tumor size)						
T0[a]	**T1a**	**T1b**	**T1c**	**T2**	**T3**	**T4**[b]
---	≤ 0.5 cm	0.5–1 cm	1–2 cm	2–4 cm	> 4 cm	---
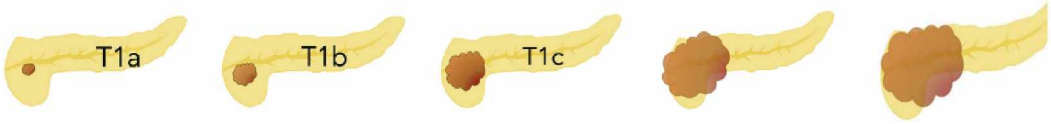						

[a]no tumor lesions, [b]tumor penentrates deep into the peritoneum or affect other organs

Table 14: N-staging system for solid tumors modified from [331] and M-category.

N-stage			**M-stage**	
N0 0 lymph nodes	**N1** 1–3 lymph nodes	**N2** ≥ 4 lymph nodes	**M0**	**M1**
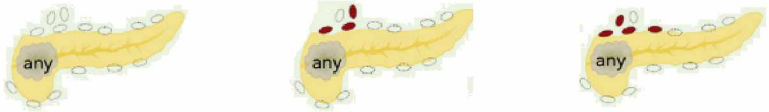			No distant metastases	Distant metastases

Another hallmark of PDAC is its extremely poor survival rate caused mostly due to the lack of reliable and effective diagnostic methods, a tendency to metastasize at an early stage, and high degree of resistance or tolerance against virtually any kind of available therapeutic options (*i.e.*, chemotherapy, radiotherapy, molecularly targeted therapy, and immunotherapy). Moreover, these traditional methods do not exhibit any significant improvements [332–334], which renders the development of novel treatment strategies one of the superior challenges in current oncological research. As a result, the effectiveness of PDAC treatment is primarily determined by the stage at the time of diagnosis and the possibility of resection (**Table 14**).

Table 15: Surgical resectability of PDAC tumors related to the tumor stage [304].

% of patients	**Tumour stage**	**Surgical resection**
10–20	T0, T1, (T2)	resectable
30–40	T2	borderline resectable pancreatic cancer
	T3	locally advanced unresectable pancreatic cancer
50–60	T4	unresectable (metastases)

Gemcitabine, capecitabine, paclitaxel, or 5-fluorouracil are commonly used chemotherapeutic medicaments together with FOLFIRINOX, a polychemotherapy regiment composed of folinic acid (FOL), 5-fluorouracil (F), irinotecan (IRIN), and oxaliplatin (OX)

that is used for treatment of advanced and metastatic pancreatic cancer. Unluckily, these protocols are accompanied with relatively high toxicity and a number of side effects, thus complete surgical resection remains the only curative therapy [307,335]. Consequently, there is an urgent need for (1) the discovery of new and highly specific biomarkers enabling non-invasive early diagnosis, such as those from plasma/serum, and/or (2) the development of new therapeutic strategies to overcome treatment resistance in order to improve the overall prognosis of PDAC representing a global public health issue that needs to be addressed [310].

The use of diagnostic biomarkers for the early detection of cancer is crucial for successful therapy, however, their development and implementation are challenging and slow. To improve the ability to detect pancreatic cancer at a curable stage, it is critically important to find accurate and reliable biomarkers or more effectual routes of treatment [336].

The most widely used biomarker of pancreatic cancer, carbohydrate antigen 19-9 (*i.e.*, CA 19-9 or SLe^a-5), remains the only diagnostic biomarker approved by the U.S. Food and Drug Administration (FDA) in the clinical use for pancreatic cancer. However, it is recognized as a poor screening tool due to insufficient sensitivity, selectivity, and high risk of both false positive and false negative diagnoses [336–339]. It has been shown that CA 19-9 is not increased in approximately 25–35% of patients at the cut-off value of 37 U/mL [340]. In the two meta-analyses, CA 19-9 had a median sensitivity and specificity of 78% and 83% (~3000 patients, meta-analysis A [339]) and 79% and 82% (~2000 patients, meta-analysis B [341]). Moreover, CA 19-9 levels can be elevated even in individuals with benign conditions (~20%) and may therefore be difficult to distinguish from cancer patients [341,342]. Additionally, individuals with a negative Lewis blood type (~5%) do not elevate CA 19-9 levels due to mutation in FUT3 gene as well [343]. Despite the limitation of the CA 19-9 test for the early diagnosis, CA 19-9 assays are applicable for monitoring of PDAC progression, recurrence, and/or therapy response. Extremely high levels of CA 19-9 are also indicative of metastatic disease [339,344]. We should also mention the work of Wolrab *et al.* [345], who developed a method for the early diagnosis of pancreatic cancer based on the lipidomic analysis of human serum. Remarkably, the method outperformed commonly used CA 19-9 assays in terms of sensitivity and specificity (>90%), and provided comparable results to commonly employed imaging methods. Moreover, Zhang *et al.* [346] analyzed the expression profiles of glycosylation-related genes, in particular genes encoding GTFs. The obtained results suggest that O-glycosylation have more dominant role compared to N-glycosylation in pancreatic cancer. Last but not least, Abd-El Halim *et al.* [347] studied an expression profiles of 169 GTFs and identified a combination of 19 GTFs allowing to discriminate PDAC

patients with different clinical outcomes. This glycol-signature could further contribute to guide the clinical decision by predicting patient outcomes. Ultimately, a combination of several biomarkers could provide better performance than any individual marker, therefore, their combined use could not only improve diagnostic accuracy, but also shed light on molecular differences between tumors [340].

(Immuno)therapies

Tumours often actively shed high levels of specific GSL from the cell surface resulting in their accumulation in the tumor microenvironment, impairing the killing capacity of the immune system [76]. Consequently, GSL may serve as tumor-associated antigens (TAAs) and eventually be used as target molecules in therapies [171].

The principal approaches to fight against cancer are chemotherapy and radiotherapy, the efficacy of which depends on their ability to increase ceramide levels in tumor cells, leading to ceramide-mediated apoptosis. Though, drug resistance still remains a considerable problem that can severely limit the effectiveness of therapies [152,156]. There are also several types of (immuno)therapies, including glycosyltransferases inhibitors (*e.g.,* glycomimetic drugs), glycan-based vaccines, monoclonal antibodies (mAbs), immune system modulators, and immune effector-cell therapy [91,348].

Notably, immunotherapy is a highly promising and rapidly evolving field representing a much more targeted approach using the immune system to treat cancer. Immunotherapy promises higher specificity while eliciting fewer side effects compared to traditional therapies like chemotherapy or radiotherapy [92]. However, the genetic instability of tumor cells should be taken into consideration, as tumor cells are able to rapidly adapt to changes in their environment. There are two major commonly applied approaches in clinical studies targeting GSL: passive and active immunotherapy [349]. On the one hand, passive immunotherapy is short-lived (*i.e.,* requires repeated application) and is induced by supplying high amounts of effector molecules (*i.e.,* tumor-specific antibodies or effector cells) to induce tumor antigen-specific response. On the other hand, active immunotherapy is long-lasting and vaccine-induced. The response can be further enhanced by unspecific stimulators, such as cytokines [172,350,351].

The most common available immunotherapeutics are mAbs or immune checkpoint molecules [348]. For instance, GD3 ganglioside is considered a melanoma-specific antigen [352] and has been used as a target of mAbs therapy and/or immune cell-mediated therapy for

malignant melanomas [353,354]. The mAbs provide limited duration since tumor cells may escape immune surveillance by downregulating the targeted antigen. In contrast, pAbs targeting several epitopes could strongly reduce evasive potential, and may eventually prevent tumor escape. Transplantation of embryonic stem cells or any other allogeneic stem cells has shown the potential for the treatment of various human diseases through cell replacement therapy despite the possible immunological rejection of cells or their derivatives after transplantation, which is the major concern limiting their use in therapies [355].

A more extensive overview of the role of GSL in immunology is given in several reviews [356,357]. It is also predicted that glycan-based immunotherapies will be flourishing in the foreseeable future since the list of targets of commercially approved substances is limited and, moreover, these are almost exclusively protein molecules [348]. There have been numerous papers published on candidate biomarkers although this research is difficult and time-consuming. The major assumption for the establishment of biomarkers in clinical practice is to proceed three steps with the sufficient number of samples, *i.e.*, discovery, qualification, and verification. However, the vast majority of biomarker research does not advance the last step (verification) despite the reportedly excellent performance [358].

The major issues are the absence of the large number of case-control studies covering all risk groups and the inconsistent reporting of statistics making comparisons difficult. Once a biomarker test is developed, it should be first used to monitor high-risk patients followed by confirmatory tests, such as imaging, endoscopy, *etc.* Then, if the test shows a good performance, it could be used more broadly (*e.g.*, in low-risk populations).

1.2 Sample pre-treatment and processing

1.2.1 Sample collection, storage and handling

Sample collection and storage are the first and one of the most critical steps how maintain the integrity of the sample. These pre-analytical steps should be performed thoroughly to ensure the reproducibility of the data, as up to 50% of laboratory errors can originate from this pre-analytical processing [359]. Various pre-analytical factors affecting the stability of plasma, serum, and urine samples were deeply reviewed by Stevens *et al.* [360].

Briefly, fresh biological samples should be used, but most biological samples are collected in hospitals and analyzed elsewhere rendering the storage of samples prior to analysis inevitable. Consequently, samples must be processed as quickly as possible and

further kept either in cold or rapidly flash-frozen in liquid nitrogen and stored at -80 °C [361]. Lipids with unsaturated double bonds are specifically prone to variable chemical reactions, such as oxidation, peroxidation, enzymatic activity, and hydrolysis in the presence of water. A crucial matter is mainly the high susceptibility of FAs to degradation via peroxidation and their behavior related to temperature. The stability of lipids in human plasma and serum with respect to temperatures were previously examined [362,363] pointing out that biases may arise even when samples are stored at -80 °C, especially when stored for months, years, or decades. Specifically, non-polar lipids have been shown to be prone to change over time, while Cer and SM were relatively stable [362,363]. Furthermore, Kronenberg *et al.* demonstrated compositional changes in samples that had been stored for 24 months at -80 °C and that had undergone 1–3 freeze-thaw cycles, while, no difference was found between freeze-thaw cycles [364]. On the contrary, GSL are considered to be more resistant since their ceramide backbones are generally more saturated [361]. In addition, it has also been shown that certain biological matrices can be safely stored for years at -80 °C [365]. Next, ethylenediaminetetraacetic acid (EDTA) was found to be the preferred anticoagulant for blood samples [366]. It is also highly advisable to aliquot samples to avoid freeze-thaw cycles and fill the vials completely to minimize contact with oxygen that could potentially stimulate the lipid degradation [367,368].

Blood-derived samples, *i.e.*, serum (**Fig. 18A**) and plasma (**Fig. 18B**) that can be obtained after clotting and/or centrifugation, are most commonly used samples in clinical studies since they can be easily obtained in a less invasive procedure and are considered to represent overall metabolic behavior. Other biofluids including urine, saliva, or cerebrospinal fluid are not commonly used because the lipid content is comparably lower [359,369].

As a consequence, proper storage conditions and handling protocols are key factors minimizing analytical errors and variability in samples. Nonetheless, there is still little information about specific storage conditions and handling protocols.

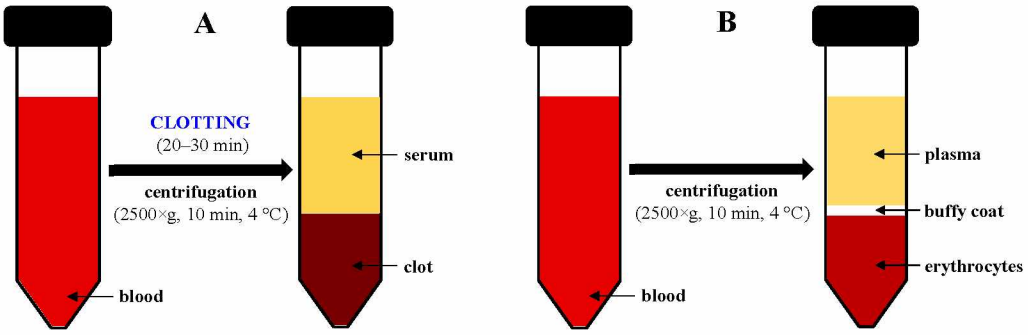

Fig. 18: Preparation of plasma and serum form blood samples (modified from [360]).

1.2.2 Homogenization

In order to ensure the homogeneity of the sample, the homogenization is usually necessary. The type of homogenization differs depending on the biological sample used. The homogenization of biofluids is not necessarily required, but it is crucial for solid samples, where the disintegration of complex and rigid cell walls is essential to access intracellular environment to facilitate the solvent penetration and extraction of lipids [361,370]. Several mechanical, chemical, and biological methods are used, including vortexing, centrifugation, ultrasonication, manual grinding, bead milling, or high-speed and high-pressure homogenizer [371]. Currently, the biggest gap in sample homogenization is the processing of solid samples, which require an additional step (*e.g.,* slicing into smaller pieces, lyophilization), thus, is more labor-intensive and complex compared to biofluids that can be immediately aliquoted and frozen upon collection [372]. Major disadvantages and obstacles facing sample storage and homogenization were pointed out elsewhere [371,373,374].

1.2.3 Extraction and purification

Regardless of the analytical approach, the next crucial step for successful lipid profiling is their efficient extraction from highly complex biological matrices using an appropriate organic solvent mixtures along with the removal of interfering substances (*e.g.,* salts, proteins, nucleic acids, sugars, and other small biomolecules) [361]. Generally, less abundant and more complex GSL are co-present with phospholipids and other substances with which they compete for ionization in. Consequently, these molecules must be removed during sample preparation [65]. In particular, the removal of phospholipids is important to reduce matrix effects and increase the ionization efficiency of GSL [361]. Thus, the extraction and purification (if necessary) are first critical steps toward their isolation and enrichment [375].

Due to the uniqueness of each sample, various extraction methods have been developed to isolate and enrich GSL from complex matrices [65]. Nonetheless, uniform extraction of GSL is challenging due to their structural complexity and heterogeneity, as well as different chemical stability and coverage of a wide range of polarities. Since GSL present the contradictory properties of being both hydrophilic and hydrophobic, they are rather amphiphilic than “lipid-like” biomolecules. These specific physicochemical properties must be taken into account during their isolation and purification [372]. Moreover, their abundance within the biological samples significantly varies. Therefore, it is crucial that the polarity of

the solvent systems allows the simultaneous solubilisation of relatively hydrophobic GSL (*e.g.,* cerebrosides), relatively hydrophilic GSL (*e.g.,* globosides, complex GSL), and highly polar GSL (*e.g.,* gangliosides and sulfatides) [376].

To date, no single extraction method is able to recover all lipid subclasses and species uniformly with a high recovery as reported by Reis *et al.*[375], thus relying on a single extraction method may fail to detect these molecules [65,375]. However, the recoveries of the major lipid subclasses are similar, and structural similarities do permit the use of many analogous techniques to extract a wide range of lipid subclasses [377]. The following subsections describe common extraction methods used in lipidomics.

Liquid-liquid extraction (LLE)

The most predominant extraction method used in lipidomics is liquid-liquid extraction (LLE). The extraction from biological samples is typically accomplished by the use of two-phase LLE based on the partitioning of hydrophobic lipids to an organic layer, while hydrophilic and/or ionic lipids and unwanted molecules (*e.g.,* salts, proteins, nucleic acids, polar metabolites, and cellular debris) are partitioned to an interphase and aqueous layer. A variety of organic solvent mixtures is used for LLE extraction. The solvent mixtures typically consist of polar and less polar or non-polar solvent. The polar solvent disrupts the electrostatic forces and/or hydrogen-bonding network between proteins and lipids, while the other one mediates the diffusion and mass transfer of lipids across the cell wall. Therefore, the solvent polarity substantially influences the diffusion of lipids across the cell wall [371].

Specifically, the chloroform/methanol-based extraction systems introduced more than a half of century ago by Folch [378] and Bligh-Dyer [379] (**Fig. 19A**), generally regarded as "the gold standard", are routinely applied. In these protocols, lipids are partitioned into the lower chloroform phase of the binary solvent system. Polar solvent, such as (*e.g.,* MeOH, EtOH or iPrOH) are used to increase the solubility of the lipids in the organic phase [65,371]. These biphasic systems are able to recover wide range of lipids, however, sialylated and sulfated GSL or neutral GSL with at least four glycan residues mostly partition to the methanol-rich layer. On the contrary, neutral GSL with less than four glycan residues and other less polar lipids remain rather in the chloroform-rich layer. Thus, these methods do not provide effective recovery of the amphiphilic and highly polar GSL, as they generally require more aqueous portion [65,377]. The major drawback, besides the use of harmful chloroform, is the collection of the bottom layer, in which a glass pipette or a needle must penetrate the

voluminous layer of insoluble residues at the interface of two phases. As a result, even a minute amount of these insoluble residues accidentally taken together with the chloroform layer can contaminate the lipid extract and eventually clog the HPLC tubing system, the chromatography column, or the electrospray interface of the mass spectrometer. These protocols usually require an additional micro-filtering step prior to analysis [372,380].

Over the years, several modifications and alternative strategies to these original protocols have been developed and evaluated to improve the extraction process along with overcoming the above-mentioned shortcomings. One of them is the method described by Matysh *et al.* [380] (**Fig. 19B**), which utilizes methyl tert-butyl ether (MTBE) and which was specifically developed for shotgun lipidomics of samples with excessive amounts of biological matrices. The MTBE method is generally similar to Folch and Bligh-Dyer protocols and provides comparable or better recoveries of lipid species [380]. However, Teo *et al.* [369] reported that MTBE method was able to extract only 10% of major polar lipids (*e.g.*, glycolipids). Additionally, MTBE method greatly simplifies sample handling making the method faster and extracts cleaner since lipids are recovered into an easily accessible upper phase while non-extractable residues resides at the bottom of the extraction vial. Additionally, MTBE is nontoxic, non-carcinogenic, non-corrosive and chemically stable, which reduces the environmental and health burdens [370,380].

Furthermore, single-phase butanol-methanol (BUME) extraction system firstly described by Löfgren *et al.* [381,382] and further modified by Alshehry *et al.* [383] (**Fig. 19C**) has been reported to provide a similar yield of lipids compared to traditional Folch and Bligh-Dyer methods. It should be also mentioned that Wong *et al.* [384] investigated the comparison of monophasic and biphasic extraction methods, which resulted in Alshehry's single-phase method being able to extract more GPs and their lyso-derivatives compared to conventional biphasic extraction methods. Despite the good feasibility of single-phase extraction reducing picking up non-extractable residues, as well as the adaptability to capture a wide range of lipids of interests, the monophasic nature of the extraction does not allow the removal of polar and ionic impurities, leading to an increased risk of matrix effects and ion suppression.

Interestingly, Vale *et al.* [385] used a three-phase solvent system with two organic layers and one aqueous layer at the bottom for successful extraction of GLs, GPs, and SLs. Last but not least, non-polar lipids, such as free and esterified FAs, cholesterol, CEs, TGs, and DGs, are commonly extracted with non-polar solvents, such as hexane, toluene, hexane-iPrOH [371].

Nonetheless, the use of alternative solvents do not exhibit significant differences in the recovery compared to the traditional protocols, but they rather minimize chlorinated solvents, such as carcinogenic and environmentally unfavorable chloroform [375,380,381,386,387]. In addition, spontaneous decomposition of chloroform yielding phosgene ($COCl_2$) and hydrochloric acid (HCl) may cause chemical modification of labile lipid species [388].

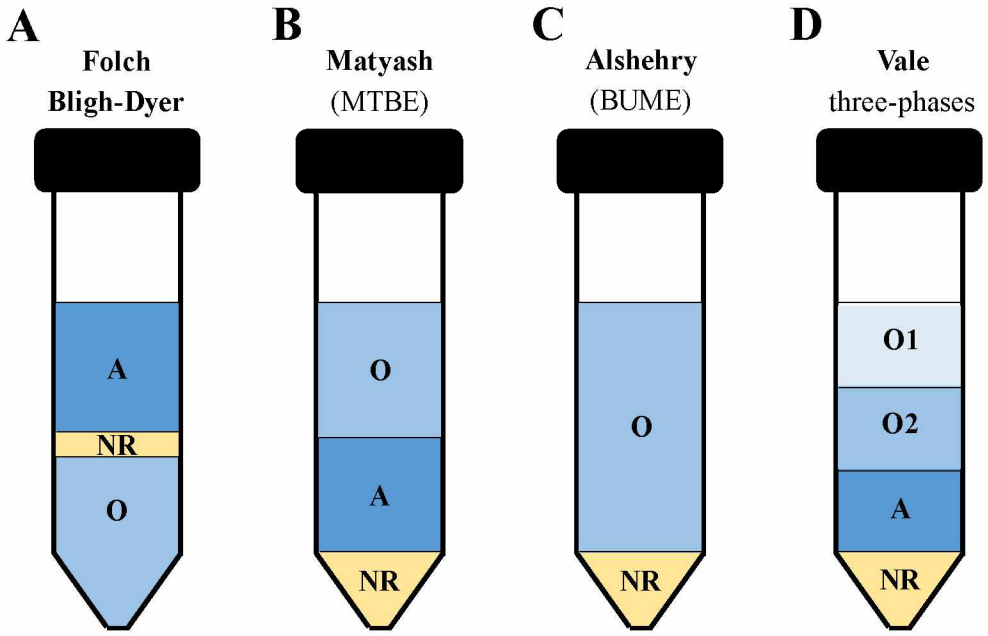

Fig. 19: Schematic illustration of phase separation in common LLE methods (modified from [384] and [385]). (A, aqueous phase; O, organic phase; NR, non-extractable residues)

Over the past years, monophasic extractions like the Alshehry method, also simply termed as protein precipitation methods, have gained popularity and have been applied to the simultaneous analysis of polar and non-polar lipids and other metabolites. The one-phase extraction methods are generally faster, cheaper and less complex compared to conventional two-phase partition systems, and eliminates the risk of losses during transfer between phases. The extraction is usually achieved through simultaneous protein precipitation with a variety of organic solvents including methanol (MeOH), ethanol (EtOH), acetonitrile (MeCN), acetone (ACE), isopropanol (iPrOH), 1-butanol (BuOH), as well as their mixtures [361,384,389,390].

Although one-phase extractions provide high recoveries (>90%) of a wide range of lipids with high reproducibility (RSD<20%), highly non-polar lipids are not efficiently extracted as they can stick to the proteins and be lost due to their precipitation in polar solvents [361,389]. Furthermore, Sarafian *et al.* [390] have compared 8 extraction protocols and found out that one-phase extraction using iPrOH is the most suitable method for lipid profiling, providing

similar results to those well-established biphasic methods. Additionally, one-phase extraction suffers from an inability to remove salts and other polar impurities, making it more prone to adverse matrix effects. Thus, the application of one-phase extractions should be limited to polar lipid classes or should be followed by a sample clean-up using liquid-liquid extraction (LLE) and/or solid-phase extraction (SPE) [361,372,389]. The brief summary of LLE methods used in lipidomic analysis is shown in **Table 16**.

Table 16: Overview of LLE methods used in lipidomic analysis

Method	Solvent system (v/v)	Phase separation (or reextraction)	Phases	Ref.
Folch (1957)	$CHCl_3$/MeOH (2:1)	+H_2O or salt 2:1:0.8	2	[378]
Bligh-Dyer (1959)	$CHCl_3$/MeOH (1:2)	+H_2O 1:2:0.8	2	[379]
Cham (1976)	BuOH/DIPE (2:3)	Separation induced by H_2O in sample	2	[391]
Hara-Radin (1978)	hexane/iPrOH (3:2)	~0.5M Na_2SO_4 (~ half of volume)	2	[392]
Retra (2008)	$CHCl_3$/MeOH (1:2)	H_2O + 0,5% 6M HCl 1:2:0.8	2	[393]
Matyash (2008)	MTBE/MeOH (10:3)	+H_2O 10:3:2.5	2	[380]
Hammad (2010)	iPrOH/EtOAc (3:17)	iPrOH/EtOAc/formic acid (3:17:1)	2	[366]
Löfgren (2012,2016)	BuOH/MeOH (3:1)	heptane:EtOAc:1% AA (3:1:4)	1 (2)	[381,382]
Lydic (2014)	$CHCl_3$/MeOH/H_2O (1:2:0.74)	$CHCl_3$/MeOH (1:2)	1	[394]
Lee (2014)	MeCN/iPrOH/H_2O (3:3:2) ACE/MeOH (3:7)	--------- ---------	1 1	[395]
Alshehry (2015)	BuOH/MeOH (1:1)	---------	1	[383]
Vale (2019)	hexane/MeOAC/MeCN/H_2O (4:4:3:4)	---------	3	[385]
Hořejší (2021)	EtOH/H_2O (5:1) + C18-SPE	---------	1	[396]

Several extraction protocols also utilize acidification to improve the solubility of anionic lipids in the organic phase. However, care must be taken to avoid hydrolysis under long exposure times to concentrated acids, especially at elevated temperatures, to minimize the generation of possible artifacts [370]. Unfortunately, lipid species with hydrophilic glycan chains (*e.g.*, gangliosides and sulfatides) or amphiphilic nature (*e.g.*, complex neutral GSL) are mostly partitioned into the aqueous phase and/or are lost to the interphase, limiting the scope of many studies. Consequently, comprehensive lipidomic studies aiming to analyze a wide range of lipids with various polarities typically require more specialized extraction protocols [397], which may otherwise increase sample preparation time, analysis time, or introduce additional experimental errors. Furthermore, such extraction may not be feasible from limited amounts of biological samples, such as tissues or cells.

Solid-phase extraction (SPE)

Solid-phase extraction (SPE) is well-grounded method for the isolation and purification of selected lipids and enrichment of minor lipid classes as well [371]. The most frequently used SPE columns (**Fig. 20**) include normal-phase (*e.g.*, silica, **Fig. 20A**), reversed-phase (*e.g.*, C8 and C18, **Fig. 20B**), and ion-exchange (*e.g.*, aminopropyl, **Fig. 20C**) columns. For instance, passing sample through C18 SPE column is the most convenient method removing interfering substances, such as salts and/or other water-soluble non-lipid contaminants [377]. It should be bear in mind that SPE has limitations, such as limited selectivity and/or sensitivity, and may adsorb matrix constituents as well, eventually leading to an increased matrix effects. SPE is also usually applied in combination with LLE as an additional clean-up step [361,369].

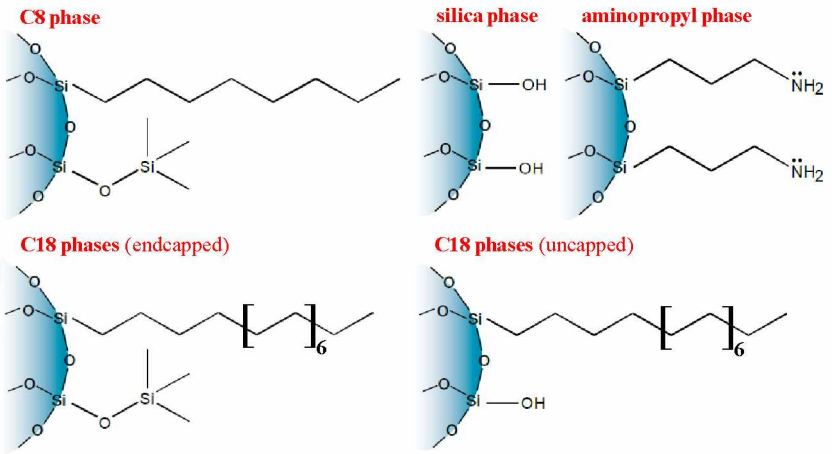

Fig. 20: The most common sorbents used in SPE extractions (modified from [398]).

Interestingly, ZrO_2/TiO_2-coated silica-based sorbents [399] have been reported to be useful for GSL isolation, with ZrO_2 appearing to be superior to TiO_2 particles as elution of SMs prior to GSL is not necessary in this case [400,401]. Furthermore, sulfobetaine-based zwitterionic sorbents and silica-based sorbents coated with TiO_2 or ZrO_2 particles (**Fig. 21**) have allowed selective extraction of GSL from phospholipids without the use of alkaline hydrolysis, using only the elution with 2,5-dihydroxybenzoic acid in MeOH. This method has shown to be useful for removal of especially alkali-resistant SMs and GPs possessing ether bonds [401,402]. More recently, Phree SPE columns (ZrO_2-based) may be used for selective removal of phospholipids [403]. Additionally, graphitized carbon sorbent can be applied for glycan purification and desalting using water as a wash solvent followed by sequential elution of neutral glycans with 25% CH_3CN and then acidic glycans with 25% CH_3CN containing 0.05 M trifluoroacetic acid [404].

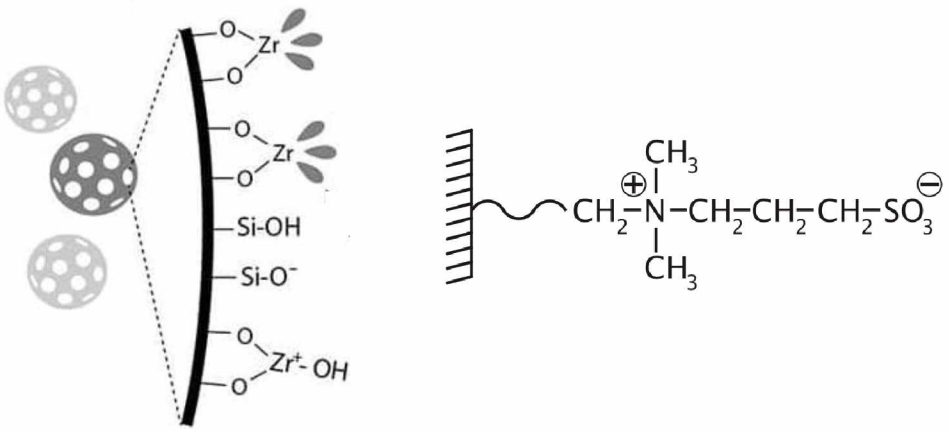

Fig. 21: Illustration of ZrO_2/TiO_2-coated silica [399,402] and sulfobetain zwitterionic sorbents [405].

There are also several other extraction methods that are not routinely used:

Solid-phase microextraction (SPME) using fused-silica fiber coated with an appropriate stationary phase may be used for the analysis of fatty acid methyl esters (FAME) and/or eicosanoides with either gas chromatography–mass spectrometry (GC-MS) or liquid chromatography–mass spectrometry (LC-MS). SPME allows highly efficient sample clean-up due to small volumes used, which is beneficial when the sample amount is limited or targeted compounds are low abundant [369]. Another method is supercritical fluid extraction (SFE). SFE is modern technique based on an increase in solvation power of a supercritical fluid above its critical values. The most popular supercritical fluid is CO_2 because it is non-toxic, easily removable and has relatively low critical parameters (*i.e.*, 32 °C and 7.4 MPa). SFE is more effective, in particular for hydrophobic lipids, compared to commonly applied LLE

methods. However, polar lipids may be extracted if modifiers, such as MeOH, EtOH, H_2O or other polar solvents are used to increase the polarity of the supercritical fluid [361,369]. Despite being not yet very popular in lipidomics with only a few studies published in dry blood spot [406,407], it is expected to be an ideal extraction method for modern clinical lipidomic studies. Next, ultrasonic-assisted extraction (UAE) applying ultrasonic energy to facilitate mass transfer between immiscible phases to improve extraction efficacy is usually combined with LLE method. The major advantages of the UAE are high reproducibility and time efficiency [408]. Then, microwave-assisted extraction (MAE) can be used for the analysis of FAs and FA esters as well, nevertheless, it is not generally applied in lipidomics due to potential degradation of thermally labile compounds [409]. Furthermore, Soxhlet extraction can be used in the case large amount of samples are available. Nevertheless, continuous heating can lead to oxidation and degradation of heat-labile compounds. A more detailed investigation comparing the efficiency of Soxhlet extraction using various extraction solvents for lipid analysis has been published by Ramluckan et al. [410]. Last but not least, relatively novel extraction approach called dispersive liquid-liquid microextraction (DLLME) can be used to enrich lipids from small volumes of aqueous samples. DLLME is based on ternary solvent system, where mixture of dispenser (*e.g.*, CH_3OH, CH_3CN or $(CH_3)_2CO$) and extraction solvent (*e.g.*, CH_2Cl_2, $CHCl_3$, CCl_4) is rapidly injected into the aqueous sample forming a cloudy solution of fine droplets. Then, the solution is centrifuged and sedimented solvent is collected and analyzed [411]. DLLME has several major advantages, such as (1) simple operation, (2) inexpensive extraction, (3) environmentally friendly character, and (4) rapid and efficient extraction with high recovery. Nonetheless, no lipidomic study has used this approach to date [412].

1.2.3 Enzymatic digestion

The preparation of intact glycans from GSL has received substantial attention, and the emphasis on their detailed structural analysis, including information on the glycan sequence and linkage positions, is of long-standing interest since many biological functions of GSL are determined by their glycan head group. Moreover, complex GSL generally require multistep fragmentation to achieve stepwise cleavage of glycosidic bonds and ceramide moieties [376,413]. Specific glycan-detaching enzymes that cleave the β-glycosidic linkage between the oligosaccharide chain and the ceramide moiety of various GSL have been discovered.

Specifically, endoglycoceramidase (EGCase) [414], ceramide glycanase (CGase) [415], and sphingolipids ceramide N-deacylase (SCDase) [416] have allowed the digestion (**Fig. 22**).

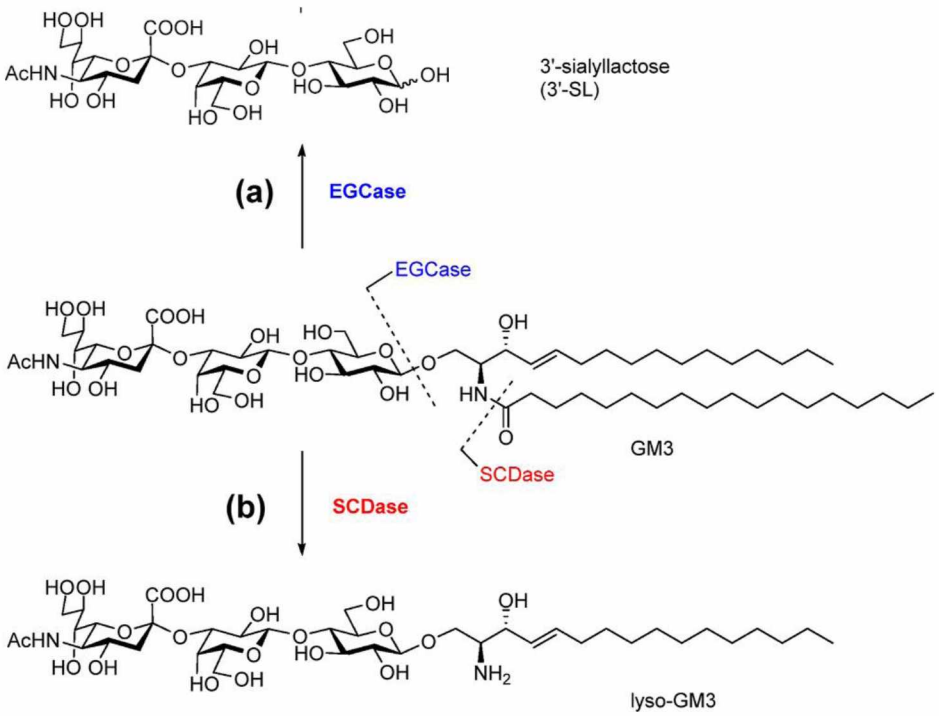

Fig. 22: Action of EGCase and SCDase on GSL (adopted and modified from [65,416]).

This platform for GSL head group profiling is preferred against harsh chemical methods based on ozonolysis [417] and Os-catalyzed peroxidate oxidation [418] followed by alkaline treatment, as these glycan-releasing methods cause various disruptions in the GSL structure. To permit the optimal enzymatic release of glycans from GSL, a reaction buffer containing detergent (*e.g.,* Triton X-100 or sodium cholate) is required. However, it has to be removed prior to subsequent isolation, purification and analysis of released glycans. Volatile buffers are preferred to avoid the inclusion of inorganic salts as well. It was also found that about 10% of organic solvents, such as dimethylsulfoxide, dimethylformamide, tetrahydrofuran, or ethyl acetate, can replace sodium cholate when using CGase and may be beneficial in inhibiting microbial growth during prolonged incubation time [413].

To date, three isoform species of EGCases are known to be derived from *Rhodoccocus* strains (*i.e.,* EGCase I, II, and III) [419]. The substrate specificities of known EGCases for various GSL (sub)classes are shown in **Table 17,** where the extent of hydrolysis (0–100%) is determined for ~1–2 mU of the enzyme applied to ~2nmol of GSL in similar conditions as a heat map. The blank areas correspond to those GSL, whose enzymatic hydrolysis was not investigated within the respective work.

Table 17: The extent of hydrolysis by EGCases for different GSL in various studies.

GSL	EGCase I					EGCase II				EGCase III
GA1										
GM1a										
GM2										
GM3										
GD1a										
GD1b										
GD3										
GT1b										
Fuc-GM1										
GlcCer										
GalCer										
Gala-series										
LacCer										
Gb_3Cer										
Gb_4Cer										
Gb_5Cer										
S-nLc_4Cer										
SHexCer										
Reference	[413]	[420]	[419]	[421]	[422]	[413]	[420]	[419]	[421]	[413]

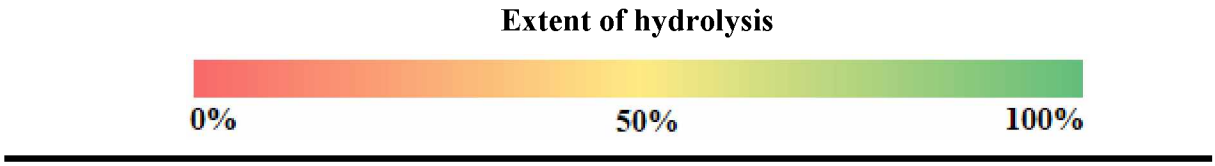

It can be inferred that EGCase I is able to effectively hydrolyze not only gangliosides, but also globo- and (neo)lacto-series GSL compared to EGCase II. Both EGCase I and II are not capable of hydrolysing sulfatides, GlcCer, GalCer and gala-series GSL. Moreover, globo-GSL are strongly resistant to hydrolysis by EGCase II compared to EGCase I. In contrast, EGCase III is the only enzyme allowing hydrolysis of gala-type GSL [419,421]. The ideal enzyme would have been the CGase from *Macrobdella decora*, which has a more universal hydrolytic activity toward GSL than the *Rhodococcus* endoglycoceramidase. However, the M. decora enzyme is no longer commercially available [423]. Thus, EGCase I is the best glycan-detaching enzyme for GSL to date and well-suited to a complex analysis of GSL [422]. Furthermore, it has also been shown that the extent of hydrolysis is largely dependent on the amount of enzyme used [419] and the incubation time [422].

It could also be feasible to employ a mixture of both EGCase I and II for complex glycan analysis [424]. Additionally, a type of anomeric linkage of the monosaccharide residue linked to Gal-GlcCer residue appears to affect susceptibility to the hydrolysis. Specifically, α-linked Gal to Gal-GlcCer residue of a globo-GSL can reduce substrate availability for EGCase II [419]. Han *et al.* [420] also showed that EGCase I and II possess several major structural differences in their substrate-binding cavities that could explain their different substrate specificities. Namely, EGCase I has an enlarged substrate-binding pocket that could accommodate more extended and/or branched oligosaccharides. Finally, the glycans released from the GSL are separated by Folch partitioning and enriched in the aqueous phase.

1.2.4 Alkaline hydrolysis

Since phospholipids are dominant lipids in cellular membranes, the mild alkaline hydrolysis using diluted sodium or potassium hydroxide in methanol is used to cleave ester linkages to eliminate major lipid classes, such as GPs, GLs, and sterol esters (**Fig. 23**), that are further removed by using silica-based column chromatography fractionation. On the contrary, core structure and glycosidic linkages between of GSL are under these mild alkaline condition quite stable [377,425,426]. As a result, this step efficiently removes major lipid contaminants significantly enhancing ionization and detection of GSL by LC-MS [65,427], which would otherwise be suppressed to a greater extent [370]. It should be bear in mind that O-acetylated derivatives are also alkali-labile and may be degraded as well, if they are present [377].

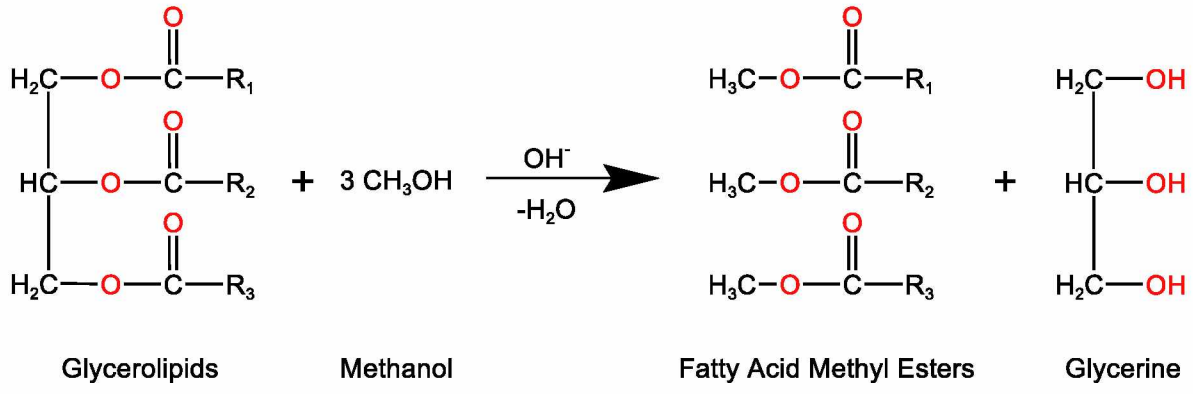

Fig. 23: Illustration of possible alkaline hydrolysis of glycerolipids.

1.2.5 Open column chromatography

The use of large amounts of starting material allows performance of multiple purification and sub-fractionation to isolate even a more complex GSL. Since the more complex GSL are generally very minor, there is a significant problem of contamination. Consequently, it is strongly recommended to remove highly abundant lipids, mainly alkali-labile phospholipids (see chapter 1.2.4 – alkaline hydrolysis) and other contaminants from glycolipids and alkali-stable phospholipids (*i.e.,* SMs) by, for instance, silica-based column chromatography [425]. The silica-based column chromatography is commonly carried out on silicagel 60 pre-soaked in appropriate solvent(s), then the sample is loaded onto the column, and finally purified and fractionated using various solvents with variable concentrations (*e.g.,* gradient elution) [425].

In addition, weak anion-exchange chromatography using diethylaminoethyl(DEAE)-linked matrices (**Fig. 24**) is convenient to separate A-GSL from N-GSL using a 5% (w/v) LiCl in methanol. The obtained fractions can be further purified by various methods, such as dialysis with 3 kDA molecular weight cut-off membrane, solvent partition, C8/C18-SPE, silica gel chromatography, or gel filtration chromatography on Sephadex G-50 gel [425,426].

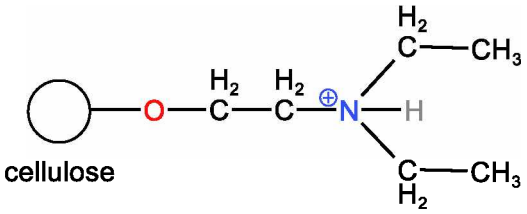

Fig. 24: Structure of DEAE-cellulose used as a weak anion-exchange sorbent.

1.3 Analysis of GSL and other lipids in biological samples

Following the lipid extraction, the next key step in the lipidomics workflow is the analysis of lipids present in the samples. Lipids can be analyzed by various analytical methods depending on what information is required, which include thin-layer chromatography (TLC), chromatogram binding assay (CBA), nuclear magnetic resonance (NMR) spectroscopy, gas chromatography or liquid chromatography coupled with mass spectrometry (*i.e.,* GC-MS or LC-MS). The most powerful tool for complete lipid profiling in current lipidomic analysis is the use of either matrix-assisted laser desorption ionization (MALDI) or atmospheric pressure ionization (API) mass spectrometry with or without separation method, such as (ultra)high-performance liquid chromatography, (U)HPLC [372].

1.3.1 Thin-layer chromatography (TLC)

TLC (regular particle size 10–50 μm) and its advanced version, high-performance TLC (*i.e.*, HPTLC, reduced particle size ~5 μm and ~0.2 mm thin layer), are very simple, rapid, and inexpensive methods that has been the cornerstone of biochemical detection and analysis of GSL for decades. Currently, it is still an indispensable and convenient method of modern analytical chemistry employed for the preparative isolation and detection of selected lipid (sub)classes or monitoring the purification process of GSL [428,429].

There are still several limitations that restrict the application of TLC. On the one hand, there is a risk of potential oxidation due to the exposure to atmospheric oxygen. On the other hand, the resolution and sensitivity is insufficient compared to HPLC methods. However, there are some methods able to separate GSL and other lipids according to the degree of unsaturation of FAs in ceramides, and even *cis* and *trans* isomers of FAs (*e.g.*, $AgNO_3$-impregnated TLC plate) [430,431] or distinguish different *sn*-isomers of DG, MG and phospholipids (*e.g.*, H_3BO_3-impregnated TLC plate) [432]. Regardless, TLC can provide valuable information on possible glycan structures, especially if compared to reference GSL [432]. The major advantages are (1) consumption of smaller amounts of solvents, (2) absence of "carry-over effect", (2) rapid semi-quantitative analysis (*i.e.*, staining with a dye that binds specifically to characteristic functional groups or residues, (3) simultaneous analysis of several samples despite the recent availability of "multiplexing" LC solutions, and (5) analysis of "suspicious" and overloaded samples that could contaminate an HPLC system [432].

TLC is usually performed in a one-dimensional (1D-TLC) or two-dimensional (2D-TLC) set up, where both resolution and sensitivity is significantly improved. Nonetheless, 2D-TLC has also serious drawbacks limiting its applications. First, only a single sample can be analyzed. Second, simultaneous application of various references is impossible making the spot assignment highly difficult. Consequently, multiple development in one dimension is often used as an alternative using the solvent system with high elution power followed by lower elution power [432]. The typical solvent systems are composed of either $CHCl_3$/MeOH/H_2O (60:35:8; v/v/v) for analysis of N-GSL or $CHCl_3$/MeOH/0.5% $CaCl_2$ in water (55:45:10; v/v/v), which is advantageous for the resolution of gangliosides [372,426]. More detailed inspection on the use of 1D- and 2D-TLC is described in the review published by Fuchs *et al* [432]. Co-migration of neutral and anionic GSL on TLC should be avoided to prevent poor resolution [65,433]. If needed, the resolution of TLC can be significantly

increased by the use of micro-TLC combined with a multidimensional separation technique and other methods [428]. The silica gel is the most popular and dominant stationary phase used for separations and is typically pre-coated on plastic-, aluminium- or glass-backed plates. The latter ones are preferred since the particles size and thickness of the layer provide better separation of GSL, and lower detection limits can be achieved [428,432].

Tiny quantities of GSL (pmol to nmol) can be chemically detected on TLC using various staining reagents of different specificity and sensitivity as well reviewed by Fuchs *et al.* [432]. The most commonly used staining reagents are orcinol, resorcinol, or anisaldehyde (**Fig. 25**). Briefly, the staining reagent is applied in a fine mist sprayer that moves in a zigzag pattern over the entire TLC surface. Finally, the plate is heated in an oven for color development [426]. Resorcinol is very specific reagent used to identify and/or quantify sialic-acid containing GSL (*e.g.*, gangliosides) appearing as blue-violet zones. This method was firstly established and reported several times by Svennerholm *et al.* [434–436]. The orcinol is nowadays not commonly used but can be used to detect monohexosylceramides [437].

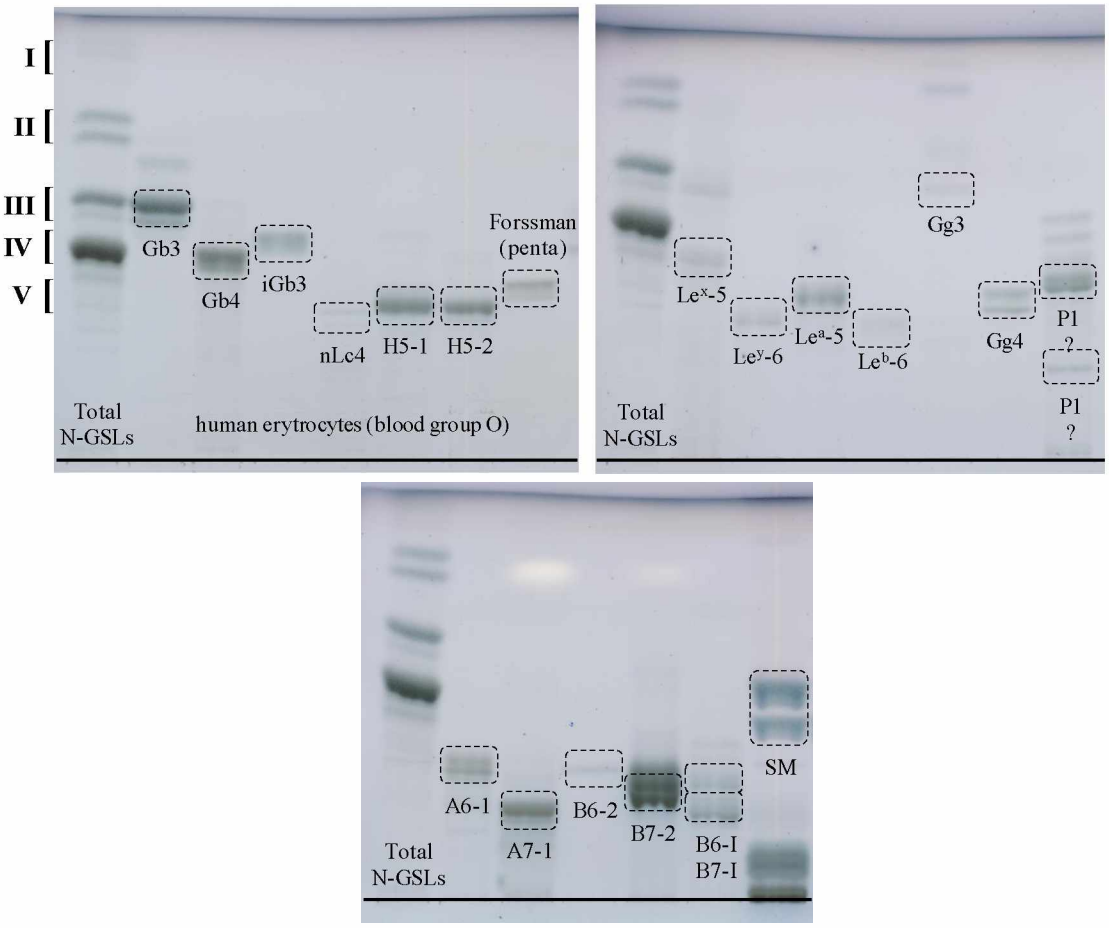

Fig. 25: Reference GSL separated on HPTLC plate using $CHCl_3$/MeOH/H_2O (60:35:8; v/v/v) mobile phase and stained with anisaldehyde reagent.

Nowadays, TLC is only seldomly used alone. Despite it is hard to hyphenate TLC with MS detection, TLC can be coupled to modern MS-based techniques, such as matrix-assisted laser desorption/ionization mass spectrometry (MALDI-MS) or desorption electrospray ionization mass spectrometry (DESI-MS), which provide a developmental advance in exploring the glycosphingolipidome of various biological samples [426,428]. In 2009, Stübiger *et al.* used HPTLC-MALDI-MS for the first time to monitor several lipid classes in human plasma samples [438] alongside Goto-Inoue *et al.*, who reported highly sensitive and semiquantitative TLC-blot-MALDI-MS method for imaging of detailed patterns of phospholipids in human brains. Paglia *et al.* introduced 2D-TLC hyphenated with DESI-MS for the analysis of several lipid categories in porcine brain, including cholesterol, FAs, GPs, and sphingolipids [439]. It is evident that coupling HPTLC or 2D-TLC with MALDI or DESI-MS opens new possibilities for the application of TLC in lipidomics.

1.3.2 Chromatogram binding assay (CBA)

Chromatogram binding assay (CBA) is an easy, rapid and sensitive overlay technique introduced by Magnani *et al.* [440], where GSL separated on TLC plate are directly detected *in situ* with specific carbohydrate-binding ligands, such as proteins (*e.g.*, antibodies or lectins), organisms (*e.g.*, bacteria or viruses), or their metabolites (*e.g.*, toxins), see **Fig. 26**.

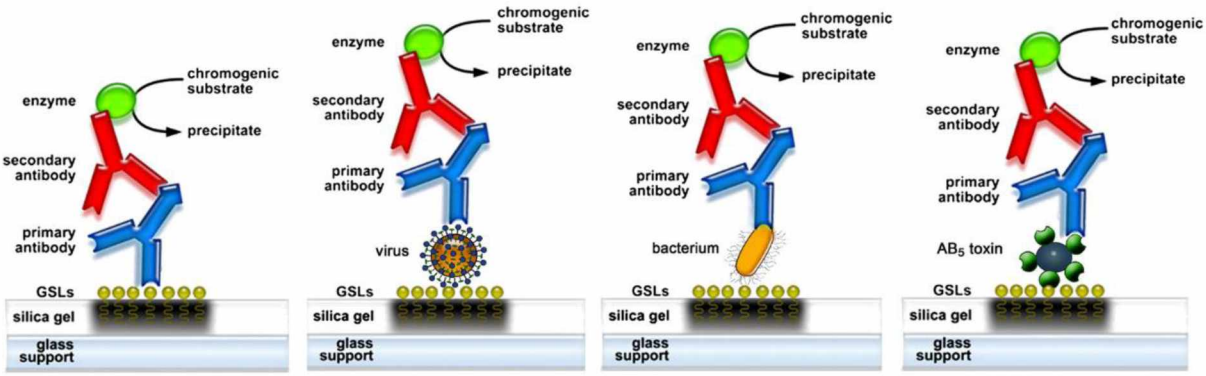

Fig. 26: Various TLC overlay assay schemes (adopted from [441]).

The CBA is similar to the enzyme-linked immunosorbent assay (ELISA) but uses a chromogenic substrate (*e.g.*, 5-bromo-4-chloro-3-indolylphosphate, BCIP) for staining (see **Fig. 27**). In order to avoid scratching off the silica gel from the plate during incubation and washing steps, a TLC plate is fixed with plastic prior to overlay assay [441].

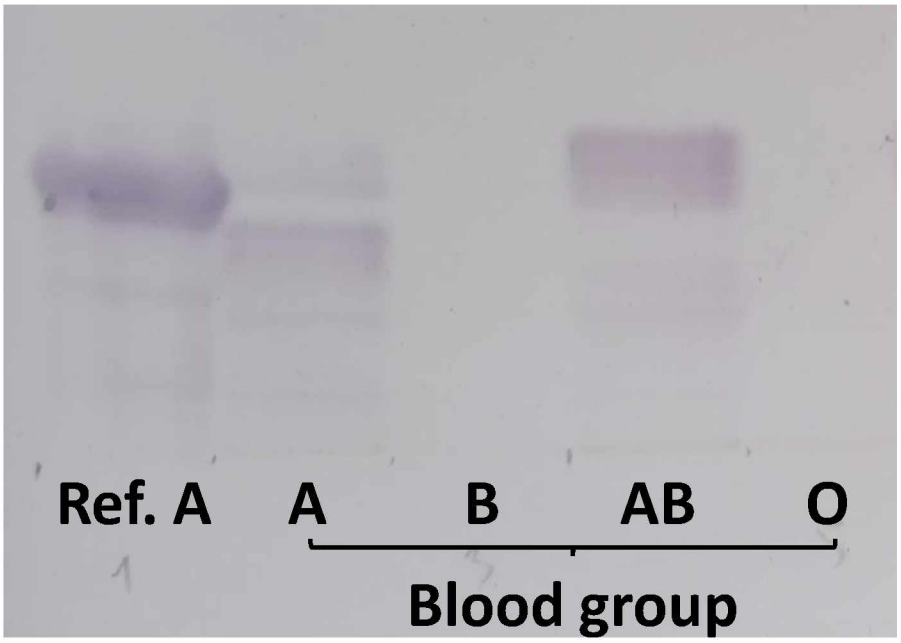

Fig. 27: BCPI staining of GSL isolated from plasma of various blood groups using anti-A antibody showing the presence of A-type GSL in blood group A and AB extracts.

The advantage of this strategy is that even crude lipid extract containing minor complex GSL can be detected and analyzed, avoiding laborious and time-consuming purification. Such a typical overlay assay used for the detection of GSL is well demonstrated in works of Barone *et al.* [442–444]. Although the use of specific anti-GSL antibodies allows specific detection of lipid-bound glycan epitopes, cross-reactivity of monoclonal antibodies (mAbs) with GSL has been reported. The cross-reactivity is mainly caused by antibodies reacting to different extents with the same glyco-epitope included in different glycoforms or glycoconjugates, which may pose difficulties in detecting particular GSL [355]. Meisen *et al.* also established multiple immunostaining combined with multicoloring [441]. Lectins are powerful tool for simple oligosaccharide analyses as well, although there are applicable to only a few glycan epitopes because often exhibit cross-reactivity as well as low affinity for specific oligosaccharides [169].

Alternatively, TLC overlay analysis using radioactive ^{125}I-labeled carbohydrate-binding proteins may be employed in combination with autoradiography for the detection of extremely small amounts of glycolipids without the use of expensive instrumentation [377]. Generally, the TLC plate with separated GSL is covered with an X-ray film, inserted into a light-tight autoradiograph cassette and left exposed for appropriate time. Then the X-ray film is developed [426], see **Fig. 28**.

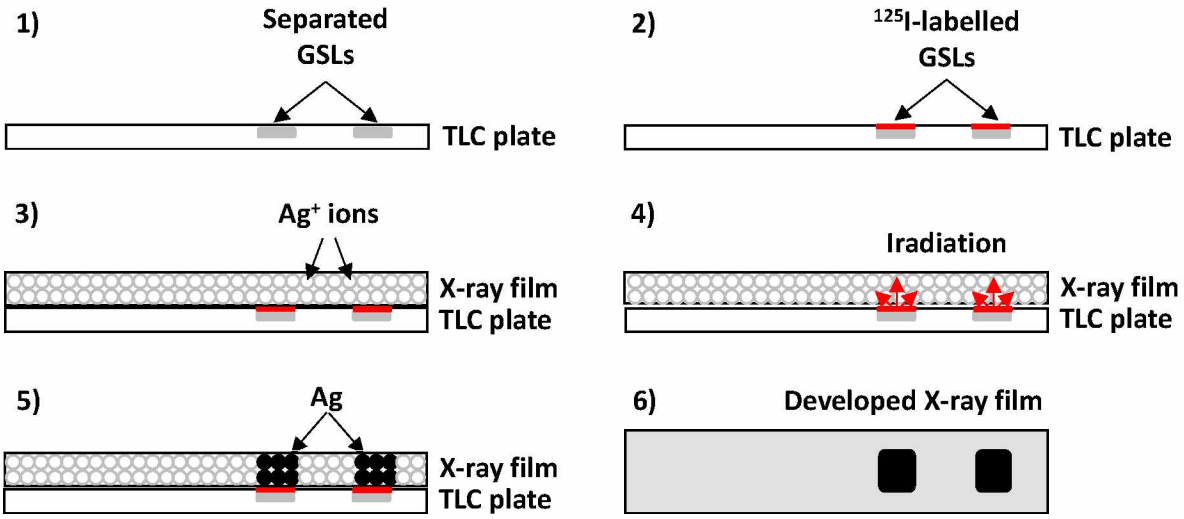

Fig. 28: Principle of autoradiography using radioactive iodine isotope ^{125}I.

By the introduction of immunohistochemical techniques and monoclonal antibodies targeting specific terminal carbohydrate epitopes, it is possible to detect and localize the spatial distribution of specific antigens (*e.g.*, histo-blood group antigens) together with related carbohydrate structures in tissues based on specific antibody–antigen binding. The major drawback of these techniques is that the methods relies on targeted antibodies and are time-consuming [44].

1.3.3 Nuclear magnetic resonance (NMR) spectroscopy

Nuclear magnetic resonance (NMR) spectroscopy, generally used as complementary method to LC-MS methods [445], is a non-destructive technique and powerful tool for the elucidation of molecular structures of purified non-polar and polar lipids (^{1}H-NMR and ^{13}C-NMR) and phospholipids (^{31}P-NMR) [446]. The method is able to locate the position(s) of the double bond(s), distinguish between stereoisomers (*i.e.*, cis/trans) and positional isomers within the glycan sequence (*e.g.*, α- or β-anomeric configurations) [432].

Nonetheless, NMR spectroscopy is much less sensitive compared to LC-MS methods and requires a large amount of highly pure material for the analysis (*e.g.*, 20–100 µg for ^{1}H-NMR and 0.5–1 mg for ^{13}C-NMR), which are the major drawbacks limiting the use of NMR [444,445,447]. In addition, the high complexity of NMR spectra for biological samples may pose a challenge for trace and/or multicomponent analysis [448].

Specifically, ^{31}P-NMR is used exclusively for phosphorus-containing lipids allowing selective qualitative and quantitative analysis of all phospholipid subclasses within a single spectrum based on head group differences. However, it is less effective in differentiating the FAs composition. ^{31}P-NMR spectra are typically acquired in the presence of a suitable detergent (*e.g.*, sodium cholate) to minimize phospholipids aggregation [432]. Key applications of NMR spectroscopy in the lipid analysis have been described elsewhere [449].

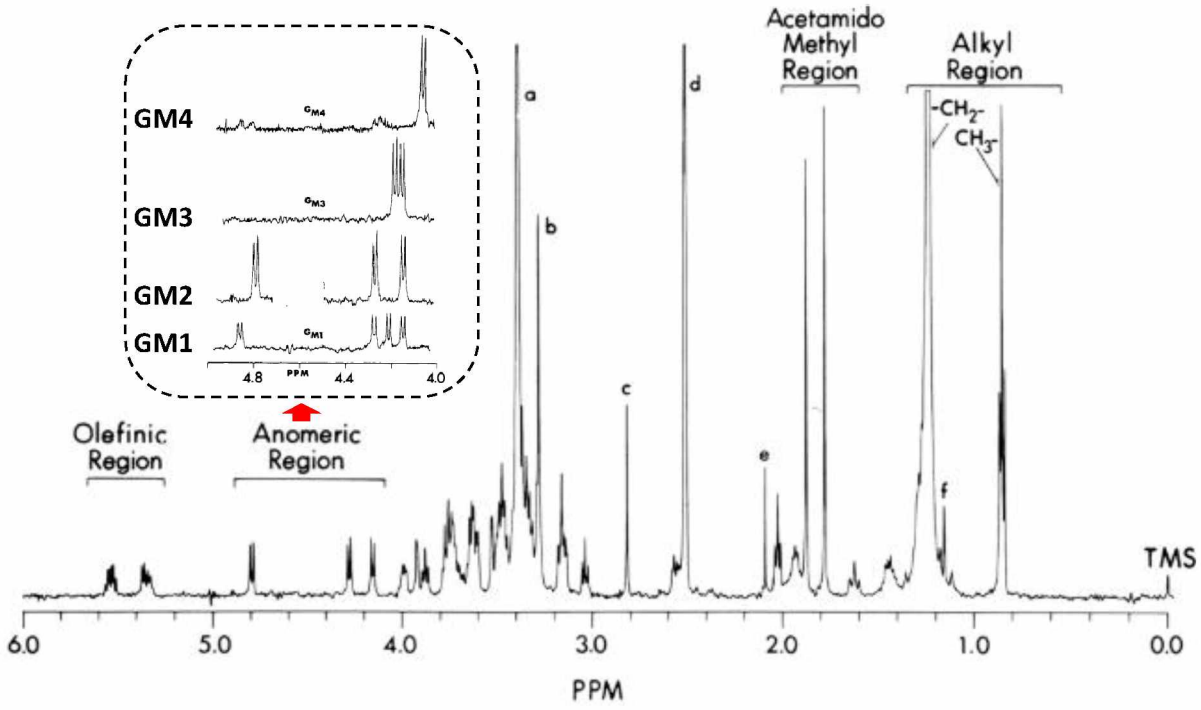

Fig. 29: ^{1}H-NMR spectrum of GM2 ganglioside obtained at 500 MHz with respective regions [447].

In addition, 2D-NMR, such as ^{1}H-^{15}N-NMR, has recently been used to differentiate between oligosaccharide isomers isolated from human milk [450].

1.3.4 Gas chromatography–mass spectrometry (GC-MS)

GC-MS is a technique used for the analysis of volatile and thermally stable analytes that are eluted from the chromatographic column according to their increasing boiling points followed by ionization using either electron ionization (EI) or chemical ionization (CI) [451]. Since most lipids are not volatile and some lipids are easily degraded under high temperature, GC is not widely used method in lipidomics because of the complexity of derivatization required for most lipids, which is a major drawback [452]. Consequently, pre-separation is absolutely necessary to analyze different lipid subclasses [453]. Nevertheless, GC-MS is

a convenient method regularly used for the profiling of fatty acids (FAs) in the form of fatty acid methyl esters (FAMEs), and other lipids after derivatization of polar moieties since it provides higher resolution ability compared to liquid chromatography (LC) [454]. For instance, Sánchez-Ávila *et al.* demonstrated the ability to separate *cis/trans* isomers of FAs using conventional GC-MS method [455] together with Hejazi *et al.*, who successfully differentiated *cis/trans* isomers of octadecatrienoic acid methyl ester (18:3) using GC-MS [456]. Furthermore, Martin *et al.* reported method for the separation of *cis/trans* oleic acid methyl esters (18:1) regioisomers using flame ionization detector (FID) coupled with GC [457]. Destaillats *et al.* presented GC-MS method able to identify MG regioisomers based on different MS fragments [458]. There are also few application on sterols [459]. GC-MS provide good reproducibility and allow comparison of MS spectra with libraries [460]. However, the majority of lipidomic studies are performed using liquid chromatography–mass spectrometry (LC-MS).

1.3.5 Liquid chromatography–mass spectrometry (LC-MS)

A) Liquid chromatography

LC and its advanced version (ultra)high-performance liquid chromatography ((U)HPLC) are the most widely used chromatographic techniques in lipidomics able to separate analytes as they migrate through a column based on distinct physical and chemical interactions with the stationary and mobile phases [369]. Over the last decade, UHPLC with sub-2-μm particles and high-operating pressures has increasingly replaced conventional HPLC systems, providing superior separation and higher resolution together with significant reduction of the analytical runtime [461].

There are several chromatographic modes used for the lipidomic analysis. Reversed-phase liquid chromatography (RPLC) provides an excellent separation of different molecular species within one lipid subclass based on the different fatty-acyl chains (*i.e.*, lipid species separation), eventually allowing the separation of isomeric and/or isobaric lipids [462,463]. The retention time increases with increasing number of carbon atoms and decreases with the increasing number of double bonds [370]. Normal-phase liquid chromatography (NPLC) separates different lipid subclasses based on their polar head groups (*i.e.*, lipid class separation) [464], however, it is poorly compatible with electrospray ionization due to extremely high nonpolar solvents used, thus is mainly applied for the (sub)class separation of nonpolar lipids [370]. A more recent approach using much less hydrophobic solvents is

hydrophilic interaction liquid chromatography (HILIC). HILIC separates lipids mainly according to their polar head groups based on electrostatic forces associated with the polarities of individual lipid species and, therefore, is the most preferred mode for quantitative analysis of polar lipid (sub)classes [465–467] and polar GSL, such as gangliosides [174]. The selectivity in HILIC is complementary to that of RPLC. As a consequence, both RPLC and HILIC modes may be utilized in combination to 2D-LC methods for separation of a wide range of lipids with polarities ranging from polar to non-polar [465,468]. An alternative and highly specialized normal-phase technique called silver-ion chromatography (Ag-HPLC) represents a unique mode of separation, where silver ions are embedded into the normal phase. The separation is based on interactions between electrons of silver ions and π-electrons of double bonds in the lipid molecule. Ag-HPLC can be applied for the separation of lipids with different numbers and positions of double bonds, cis/trans isomers, as well as regioisomers [469,470]. Another separation technique capable of separating regioisomers and enantiomers is chiral HPLC [471]. Another popular tool is the use of two-dimensional liquid chromatography (2D-LC), where two chromatographic modes with orthogonal separation selectivity can be coupled to provide higher peak capacities either in offline [465] or online [468] modes.

B) Mass spectrometry

Qualitative and quantitative information about lipids are usually achieved by coupling HPLC with mass spectrometry (MS), which is the most popular and very powerful detector in the lipidomic analysis [472]. Mass spectrometer is an instrument composed of three main parts: (1) ion source, (2) mass analyzer, and (3) detector [2]. The principle of MS is following: The molecules of interest are first introduced into the ion source through an inlet system followed by molecules vaporization and ionization. The resulting ions are then transmitted to the mass analyzer, where they are separated according to their mass-to-charge ratio (*m/z*) and subsequently detected. The detected signals are recorded and displayed as a mass spectrum, a plot of relative ion intensity (y-axis) dependent on *m/z* (x-axis) [2,472].

Ion source

Ion source aims to vaporize and ionize analytes present in the sample. Many ionization techniques have been developed for lipidomic analysis. The most applied ionization in combination with HPLC are atmospheric pressure ionization (API) techniques, including electrospray ionization (ESI), atmospheric pressure chemical ionization (APCI), and

atmospheric pressure photoionization (APPI), **Fig. 30** [473]. Ambient ionization techniques, such as matrix-assisted laser desorption/ionization (MALDI) is also frequently used [2].

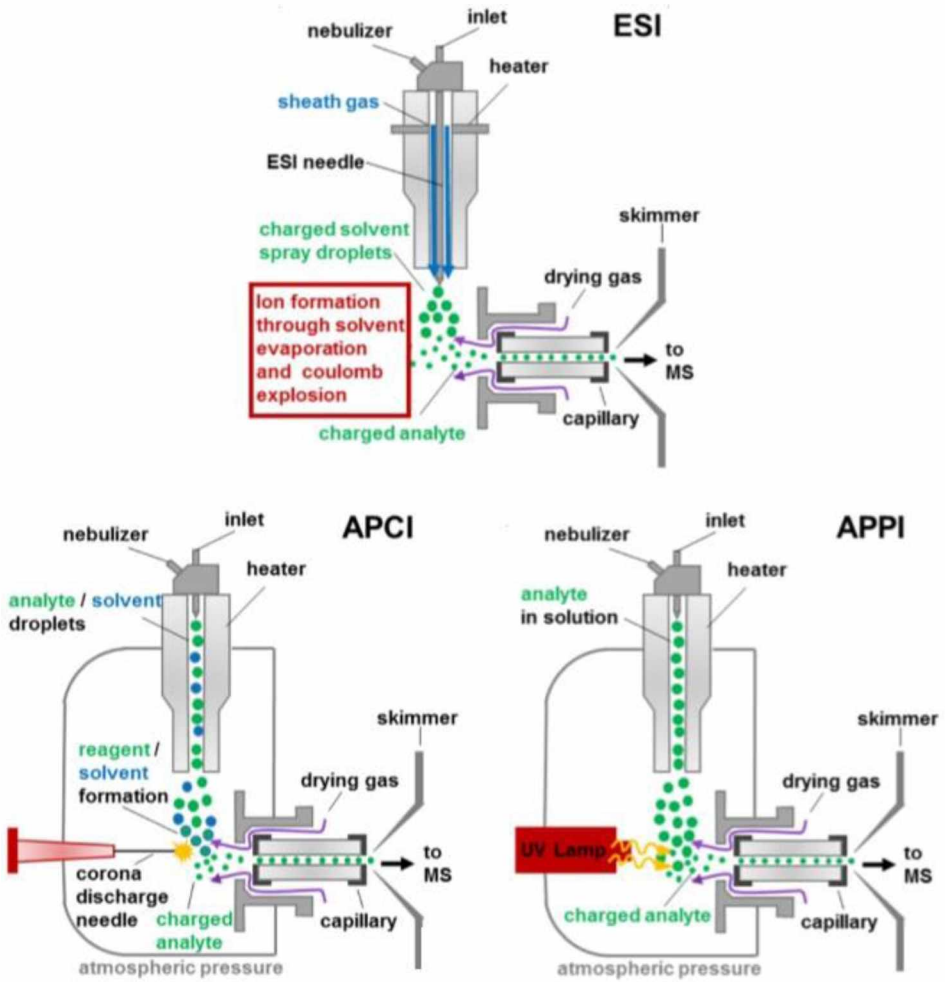

Fig. 30: Scheme of atmospheric pressure ionization interfaces (adopted from [473]).

The invention of ESI by John Fenn in 1984 has revolutionized the lipidomics since it has become the major ionization mode [474]. In ESI, a solution containing the analytes is first introduced into the ion source via an inlet port. The solution pass through the capillary that is maintained at high voltage and form the Taylor cone. A fine aerosol of small droplets is then produced with the aid of high temperature and stream of drying gas. Due to the high voltage, the aerosol particles can carry positive or negative charges [2,475]. As the solvent evaporates from charge droplets, their size decrease, which lead to an increased surface charge density. After the critical point is reached, the droplets become unstable and deforms due to strong electrostatic repulsion. At this point, the droplets undergo Coulomb fission, and the original droplets explodes creating many smaller and more stable droplets. This process is repeated until the stable ion of analyte is produced (**Fig. 31)** [2,472].

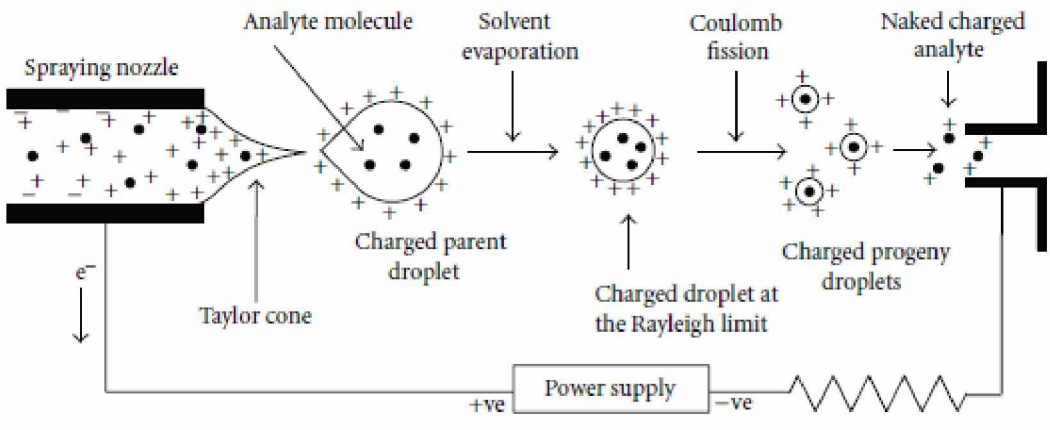

Fig. 31: Schematic illustration of electrospray ionization process (adopted from [475]).

ESI is perfectly suited for GSL analysis although the heavily glycosylated GSL may suffer from low ionization efficiency because of their hydrophilicity and low volatility, and care must be taken when ionizing GSL with labile structures (*i.e.*, containing sialic acids and/or fucose) that may be cleaved off and overlooked [65]. GSL ionized by ESI (typically 1–3 kV) may form several ions depending on the operational mode (*i.e.*, positive or negative mode) and composition of mobile phase and samples. These include, for example, $[M+H]^+$, $[M-H]^-$, $[M+Na]^+$, $[M+K]^+$, $[M+NH_4]^+$, $[M+halide]^-$, $[M+formate]^-$, and $[M+acetate]^-$ [2]. Furthermore, gangliosides may form multiply charged species $[M-xH]^{x-}$ due to the presence of sialic acids [476]. In addition, common background ions (Na^+, K^+) are the most commonly observed ions in the MS spectra due to their ubiquity and high affinity to GSL molecules, which may increase the ambiguity of molecular species assignment [380]. However, the addition of formic or acetic acid overwhelms those adducts and gives favor to protonated $[M+H]^+$ ions [65]. Additionally, the development of nano-electrospray ionization (nano-ESI) has greatly expanded the applicability of ESI due to signal enhancement, minimization of sample amount, and less susceptibility to salted samples. However, the stability of nano-ESI may vary as it is more prone to capillary clogging [370]. In contrast, APCI and APPI are less frequently used ionization techniques despite being less susceptible to the matrix effects as the ionization of analytes occurs in the gaseous phase. APCI has been applied as an alternative technique for the analysis of neutral sphingolipids [477], human skin ceramides [478], and sterols [479]. The applicability of ESI, APCI, and APPI in the lipidomic analysis is demonstrated in **Fig. 32**.

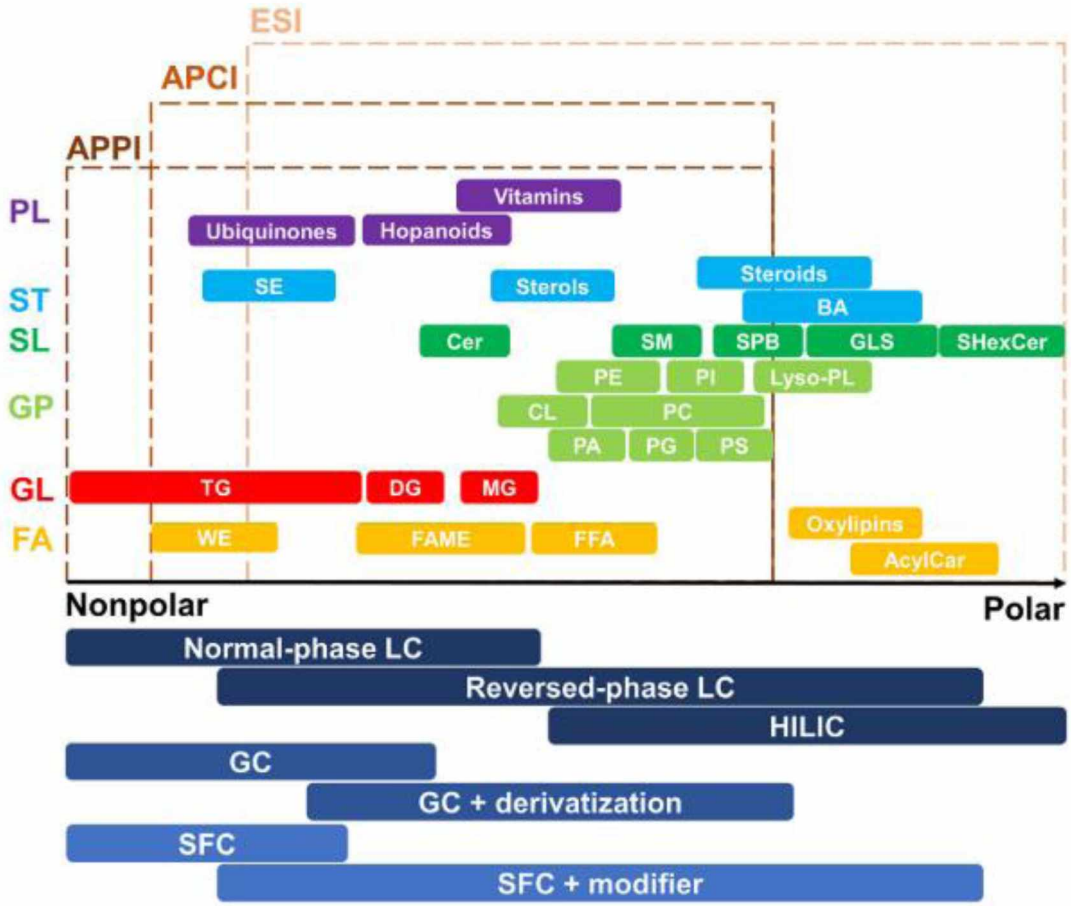

Fig. 32: Applicability of ESI, APCI, and APPI in lipidomics analysis (adopted from [480]).

Mass analyzer

Mass analyzer is a key component of the mass spectrometer that separates different type of ions of an ion beam based on their *m/z*. There are several types of mass analyzers, for example, magnetic (B) or electric (E) sector mass analyzer, quadrupole (Q), ion trap (IT), time-of-flight (TOF), orbitrap, and ion cyclotron resonance (ICR) mass analyzer. Some of these analyzers can also be combined in tandem arrangements, such as triple quadrupole (QqQ), quadrupole time-of-flight (QTOF), or tandem time-of-flight (TOF-TOF). Each mass analyzer separate ions based on different physical principles and most laboratories employ different mass analyzers for particular applications [481,482]. More detailed information about the construction and principles of individual mass analyzers can be read here [482]. In addition, mass analyzer can be categorized into three group based on their resolving power characterized by the full width at half maximum (FWHM), which is calculated as FWHM = $(m/z)/(\Delta m/z)$ and mass accuracy characterized by ppm, which is calculated as ppm = $10^6 \times [(m/z)_{theor} - (m/z)_{exp}]/(m/z)_{theor}$ (**Table 18**) [483].

Table 18: Characterization of three groups of mass analyzers adopted from [483].

Type of analyzer	Resolving power	Mass accuracy	Examples
Low-resolution (LRMS)	<10,000	>5 ppm	Q, QqQ, IT
High-resolution (HRMS)	10,000–100,000	<5 ppm	TOF, QTOF
Ultrahigh-resolution (UHRMS)	>100,000	<1 ppm	Orbitrap, FT-ICR

Detector

The purpose of the detector is to transform electric signal to graphical output (*i.e.*, mass spectrum). The simplest detector is a Faraday cup, where ions are neutralized and the resulting current is measured. However, modern detector use a variety of electron multipliers, where the energetic ions strike the conversion dynode leading to emission of secondary electrons. The emitted secondary electrons are accelerated and focused onto the subsequent dynodes resulting in an increasing number of electrons emitted. The output current is then converted to a voltage signal and finally translated to a mass spectrum [475].

1.3.6 Supercritical fluid chromatography–mass spectrometry (SFC-MS)

Supercritical fluid chromatography (SFC) is a separation technique similar to LC, but using supercritical fluid as the mobile phase for the separation of hydrophobic compounds. SFC has made a breakthrough in the early 2010s as more robust and reproducible instruments were commercialized, *e.g.*, hybrid SFC/UHPLC and ultrahigh-performance supercritical fluid chromatography (UHPSFC), followed by the development of columns with sub-2 μm particles [484,485]. Historical background and major developments along with the overview of application range of SFC compared to other technologies have been illustrated in the following review [484].

Carbon dioxide (CO_2) is by far the most widely used supercritical fluid because it is cheap, has low critical parameters (*i.e.*, T_C = 31 °C and p_C = 7.3 MPa), and fulfil several other health, safety, and environmental properties, such as low toxicity, non-flammability, non-corrosiveness, and miscibility with most organic solvents [486]. Moreover, due to the low viscosity and high diffusivity of the mobile phase, higher velocities can be used without significant loss of efficiency [484]. In order to maintain the mobile phase in the supercritical

state during the analysis, SFC instruments are equipped with a backpressure regulator, which has a key role for the reproducibility [484]. Although the solvation power of CO_2, a non-polar solvent, is not sufficient to elute more polar compounds, the addition of an organic modifier (*e.g.,* MeOH, EtOH, iPrOH, and MeCN) and/or additives (*e.g.,* organic acids, bases, buffers, and water) changes the polarity and the density of the mobile phase, and modifies or blocks the active sites on the stationary phase. Such flexibility significantly extends the application area of SFC allowing the fast, highly efficient, and simultaneous analysis of a diverse range of analytes with different physico-chemical properties. Nonetheless, organic modifiers also affect the critical parameters by shifting them to a higher values resulting in the fluid considered as a subcritical [484,486,487]. Additionally, SFC can also facilitate a move towards green chemistry via reduced usage of organic solvents [369]. Despite SFC is not directly compatible with ESI, the compatibility can be greatly improved with the addition of a make-up solvent after the column. [370].

Bamba and co-workers have played a key role in demonstrating the promising use of supercritical fluid chromatography–mass spectrometry (SFC-MS) in both targeted and non-targeted lipidomics with multiple applications reported in the last decade, including, for instance, phospholipid profiling in plasma [406,488]. They have further demonstrated the technological progress, such as improved sample injection system [489] or the on-line coupling with SFE [490]. An interesting recent development is the on-line coupling of SFE to SFC, where extracted analytes from the SFE cell are transferred via a trap column to the SFC column to re-focus the analyte band prior to elution [486]. Furthermore, Holčapek and co-workers employed ultrahigh-performance supercritical fluid chromatography mass spectrometry (UHPSFC-MS) for the analysis of human plasma and serum [491], as well as tumor tissue and erythrocytes of kidney cancer patients [492], where 30 lipid classes were separated within 6 min and quantified after systematic method optimization and validation. Recently, Yang *et al.* [493] reported a novel on-line 2D-SFC×RPLC method combined with a triple quadrupole MS for the analysis of plasma lipids of the breast cancer candidates, which was more than 4× faster than the reference RPLC×NPLC method.

Although SFC-MS is not expected to fully substitute other chromatographic methods, the growing number of bioanalytical applications, as well-reviewed by van de Velde *et al.* [484], support the major role of SFC-MS in lipidomics. SFC represents a promising alternative to improve lipid coverage, while further increasing the analysis throughput.

The summary of applicability of GC-, LC-, and SFC-based methods in metabolomics and lipidomics is illustrated in **Fig. 33**.

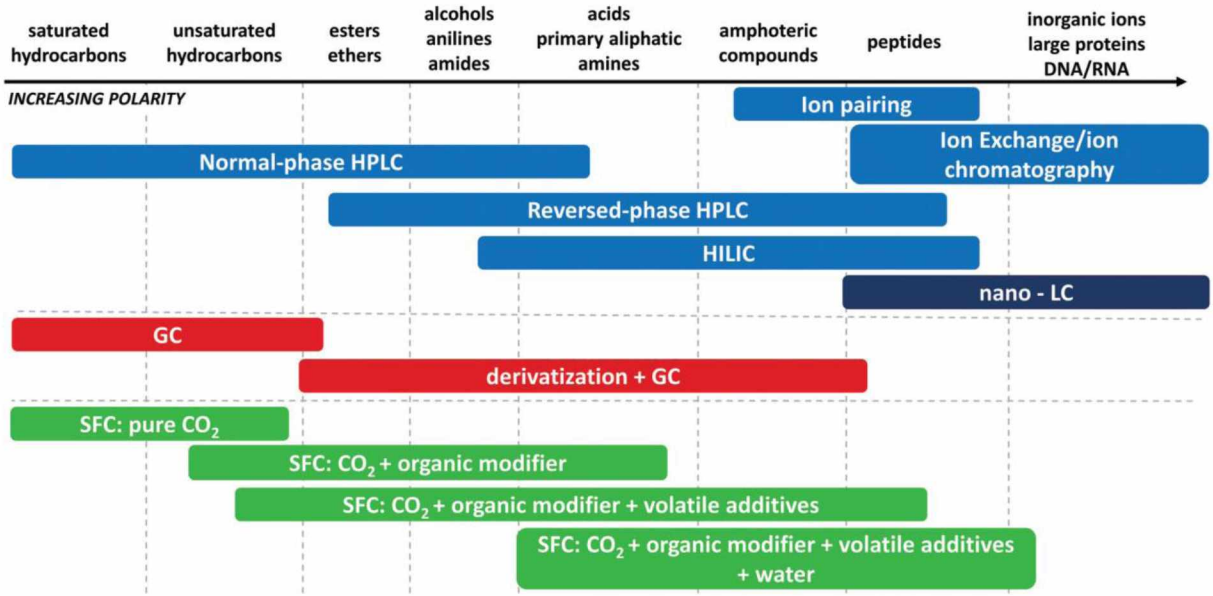

Fig. 33: Applicability of various chromatographic techniques (adopted from [494]).

1.3.7 Ion mobility (IM)

Ion mobility (IM) is an emerging gas-phase separation technique with the applicability in lipidomics and other omics approaches. The historical background and important milestones leading to conceptualization, design, and construction of IM technologies have been well-described and illustrated through the timeline in the work of May and McLean [495]. IM is an ultrafast, proficient, and highly reproducible separation technique, where ions driven by an electric field migrate through a drift tube filled with an inert gas (commonly termed buffer gas, *e.g.*, He or N_2) with different velocities correlated to their size and shape [495,496]. For many analytical applications, the ion mobilities are converted into the calculated collision cross-section (CCS) values, a unique physicochemical measure related to the conformational structure of ions (*i.e.*, size and shape), which is also highly reproducible across different instruments and laboratories. Generally, smaller and more compact ions travel to detector faster than larger and more extended ions [497–499].

While standalone IM is very powerful, interfacing with mass spectrometry has seen significant improvements and has flourished in the last two decades. IM nested in-between LC and MS gives an additional dimension of separation (*i.e.*, CCS values) together with retention time and *m/z*. As a consequence, IM provides a valuable complementary source of information leading to exceptional levels of selectivity (*i.e.*, separation power of isomers and isobars and more confident structural elucidation that helps in reducing the number of

misidentifications) and sensitivity (*i.e.,* significant reduction of chemical noise allowing analysis even low abundant ions and superior quality spectra acquisition) [495–497,500].

IM can be categorized into three groups based on the separation concept: (1) time-dispersive IM, (2) space-dispersive IM, and (3) trapping and selective release IM.

Time-dispersive IM

Time-dispersive IM is the most common type used in untargeted lipidomics as it allows the analysis of all ionized molecules in a sample in the same cycle. However, relatively low resolving power limits the detection of low abundant lipids and the isomer separation [495,499]. In time-dispersive IM, ions travel through the same drift path, but reach the detector at different times [499]. The most common time-dispersive IM technologies are drift tube ion mobility spectrometry (DTIMS) and traveling wave ion mobility spectrometry (TWIMS), which are typically coupled to QTOF analyzers [499], together with less used overtone ion mobility spectrometry (OMS) [496].

DTIMS consist of several closely-situated ring electrodes filled with an inert buffer gas with no directional flow so that the ions are driven only by the uniform electric field [495,499]. The resolving power of DTIMS can be increased by increasing the voltage drop (in V/cm) across the drift cell and decreasing temperature [496].

TWIMS has similar configuration as DTIMS. However, TWIMS utilizes an oscillating electric field creating voltage waves (*i.e.,* non-uniform electric field) that push the ions through the drift cell towards detector [495,496]. The major caveat of TWIMS is that each instrument must be calibrated using structurally similar calibrator with known mobility (*i.e.,* CCS value) prior to calculating CCS values of unknowns [496]. Two CCS calculation methods used for corrections were described in the following review [499]. In order to increase resolving power, new TWIMS-based systems, such as structures for lossless ion manipulation (SLIM), have been developed, in which drift paths are greatly increased to promote collisions with the buffer gas and improve ion separations [499].

Space-dispersive IM

Space-dispersive IM is mostly used for targeted approaches as only one ion can reach the detector at a time [497]. In space-dispersive IM, ions are transported by a buffer gas through different paths caused by alternating low and high electric fields strengths applied between two

electrodes that guide the ion with a particular mobility to the detector [499]. The space-dispersive separation is very selective and has high resolving power, so it is the most useful for isomer separation [495]. In this group, the major types are field asymmetric waveform ion mobility spectrometry (FAIMS), differential mobility spectrometry (DMS), and differential ion mobility spectrometry (DIMS), which are typically coupled to triple quadrupole (QqQ) or Orbitrap analyzers along with and differential mobility analyzer (DMA) [496,499].

FAIMS, DMS, and DIMS are extremely small IM technologies typically interfaced directly behind the ion source of the MS. All three platforms operate at atmospheric pressure and under the same mechanism differing only in the geometry of electrodes. The periodic waveform is applied to separate ions under a parallel buffer gas flow. These platforms utilize compensating voltage scans to transmit ions with various responses to change the mobility over a set period, thus, in this manner, functioning as mobility filters analogous to quadrupole analyzer. As a result unwanted chemical noise in MS spectra can be avoided increasing the signal-to-noise ratio for the ions of interest [496].

DMA operates in a similar fashion to DTIMS, however, DMA operates at ambient pressure, has a well-characterized unidirectional buffer gas flow, and scanned for the detection of the molecule of choice. DMA is commonly less used than FAIMS [497] and is primarily designed for measuring extremely large molecules not possible with other IM-based methods [496]. There is also less used transversal modulation ion mobility spectrometry (TMIMS) [495].

Trapping and selective release IM

Trapping and selective release is typically applied for targeted approaches. However, it can be used for untargeted approaches as well. In trapping and selective release IM devices the ions are trapped by an electric potential and subsequently selectively ejected by decreasing the electric potential in a stepwise manner so the bigger ions with smaller mobility (*i.e.*, larger CCS values) reach the detector first. The main representative is trapped ion mobility spectrometry (TIMS) [497,499].

TIMS operates in the static electric field as DTIMS. The TIMS mobility region is utilized to accumulate, trap, and elute ions of interest as a result of the interplay between gas flow and an opposing electric field [496]. The ions pass through the drift region towards MS parallel with the buffer gas flow. The electric field strength is slowly decreased to eject ions of specific mobilities. The small size of TIMS (ca 5–10 cm) is extremely advantageous in creating smaller instruments [496]. Moreover, TIMS is very selective device with higher resolving power than time-

dispersive instruments making it a great candidate for isomer separation [495]. In conventional TIMS-MS/MS analysis, the quadrupole selects only one *m/z* for fragmentation in each TIMS separation, while all other ions are not fragmented, losing about 90% of the acquisition efficiency. To improve this, parallel accumulation-serial fragmentation (PASEF), where quadrupole is set to isolate as many precursor as possible by changing the selected *m/z* for each ion that elutes from TIMS, was developed [499]. Another alternative is multi-pass cyclic TWIMS, which enhances resolution by performing several ion passes through the closed-loop drift cell included in the instrument or segmented quadrupole gas counterflow IM [495].

CCS values can be calculated in DTIMS, TWIMS and TIMS so, when CCS values are reported, ideally, they should be reported with both the type of drift gas (*e.g.*, CCS_{N2} in case of nitrogen is used) and instrumentation used (*e.g.*, $^{DT}CCS_{N2}$ or $^{TW}CCS_{N2}$ in case DTIMS or TWIMS are used) [501,502].

Moreover, Paglia *et al.* [503] provided a comparison of four main types of IM technologies, namely DTIMS, TWIMS, FAIMS, and TIMS, together with the use of TWIMS in lipidomics and metabolomics. The summary of separation principled of time-dispersive, space-dispersive, and trapping and selective release IM technologies is illustrated in **Fig. 34**.

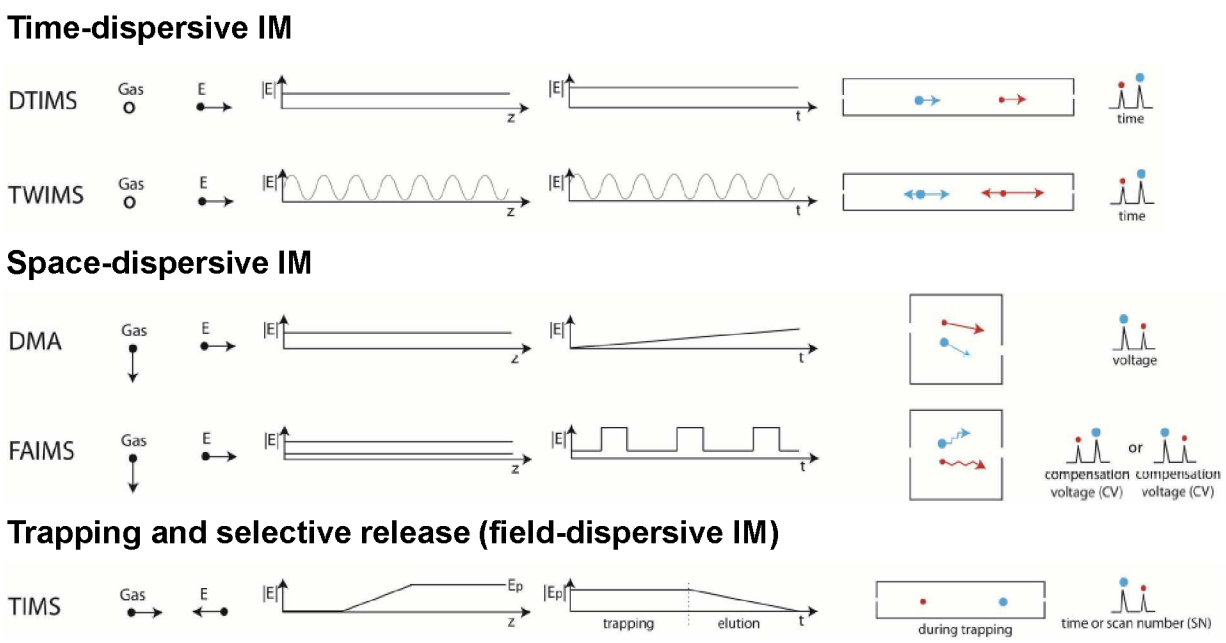

Fig. 34: Separation parameters and principles of various IM technologies (adopted from [501]).

IM is advantageous since it does not require special solvents or complicated sample preparation, can be used for high-throughput analyses, and allows the real-time analysis of

highly complex samples. Despite enormous progress in IM technologies, the separation of isomers still remains very challenging. Nonetheless, recent advances in chromatography and continual innovation of IM through novel instrumental developments pushed the popularity of IM forward by enhancing its sensitivity and selectivity, which in turn then aid in discovery of new and rare structures, deciphering of isomers and elucidating their roles in biological systems [496]. In addition, changing the experimental variables can lead to the ion mobility shift and eventually enhance the separation of lipid isomers as previously well-reviewed [497]. Briefly, these modifications include (a) complexation and adducts formation with metal ions, (b) introduction of buffer gas additives (*e.g.*, 1-propanol, 2-propanol, 1-butanol), and (c) changes in the pressure, temperature, and composition, polarity, of the buffer gas (*e.g.*, He, Ar, O_2, N_2, CO_2, or their mixtures) [497].

It should also be emphasized that IM can be operated as a mobility filter, decreasing the background noise along with increasing the signal-to-noise ratio of ions of interest in order to acquire cleaner and high quality spectra free of interferences [496,499]. This is of particular importance in situations, where background noise has high relative abundance compared to ions of interests, or contaminating ions are present (**Fig. 35**). Space-dispersive IM technologies are well-suited for this purpose. This capability has been a key feature in avoiding biases in trap-based analyzers, which require an automated gain control [496].

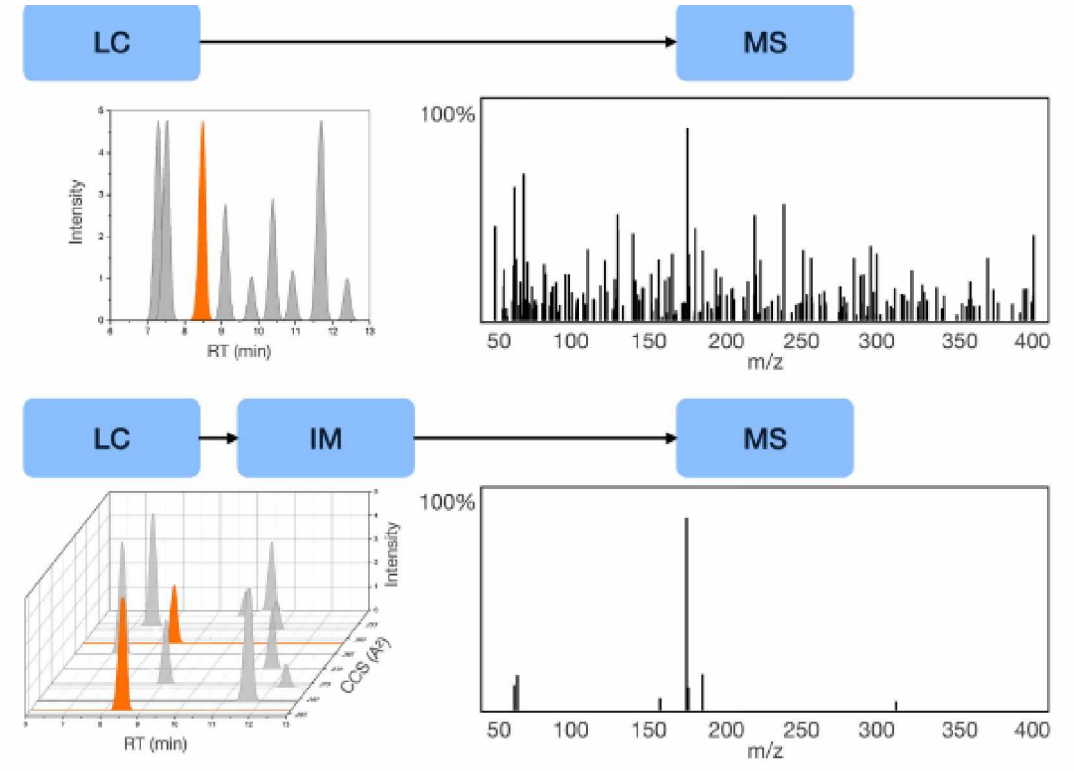

Fig. 35: Illustration of the filtering ability of ion mobility spectrometry (IM) (adopted from [499]).

To date, only a limited number of lipidomic studies utilizing IM technologies have successfully been applied for the separation of lipid isomers, however, the potential applications of this strategy are still being discovered [496]. Despite having a great potential for unambiguous characterization of various GSL isomers, the application of IM in GSL analysis remains very limited. More extended overview about IM approaches utilized for structural characterization of geometrical lipid isomers in combination with other pre-ionization (*e.g.*, C=C bond selective derivatization approaches) and post-ionization (*e.g.*, conventional CID-MS/MS or advanced MS/MS, such as OzID, electron- and photon-based fragmentations) strategies was provided in this review [497].

1.4 Overview of approaches used in lipidomics

There are three major approaches used in lipidomics including direct infusion MS analysis (DI-MS), liquid chromatography or supercritical fluid chromatography coupled to mass spectrometry (LC-MS or SFC-MS), and mass spectrometry imaging (MSI).

1.4.1 DI-MS

DI-MS also termed "shotgun" lipidomics is a technique when lipid extracts are directly introduced into the MS instrument without upfront separation and processed within few minutes in a high-throughput fashion [504]. DI-MS was firstly coined about three decades ago by Han and Gross, who also first utilized DI-MS for lipidomics [505]. DI-MS is primarily designed for targeted studies to detect unique intra-source fragments generated by specific lipid (sub)classes. The molecular characterization of lipid species thus relies either on the accurate *m/z* determination of precursor ions (*i.e.*, using a high-resolution mass spectrometry; HRMS) or on the detection of specific product ions or neutral losses in MS^n experiments (*i.e.*, using a low-resolution mass spectrometry; LRMS). Nevertheless, the HRMS instruments are preferred due to their ability to differentiate the isomeric and isobaric compounds [372,380,506]. Additionally, multi-dimensional MS-based shotgun lipidomics (MDMS-SL) allows the separation of many lipid (sub)classes through selective ionization of certain category of lipids in the ion source (*i.e.*, intra-source separation), even if the lipids are minor [504,507,508]. Although ESI and MALDI are by far the most widely used ion sources in DI-MS, few relatively novel soft ionization technologies, namely DESI [509], laser ablation electrospray ionization (LAESI) [510], and matrix-free laser desorption ionization (LDI)

[511], have been successfully applied for the direct analysis of lipids in biological samples without complex sample pretreatment.

The major advantage of shotgun analysis is reproducibility and relative high-throughput capability allowing rapid acquisition of full mass spectrum within seconds while providing similar or better sensitivity than LC-MS approaches, especially in coupling with nano-ESI [512]. On the contrary, the major drawbacks are possible carry-over effect and susceptibility to ion suppression due to the presence of other major lipids or polar compounds (*e.g.*, salts and/or polar metabolites). Taken together, this limit ionization capacities and, in the worst case scenario, may even completely suppress signals of minor and/or poorly ionizable lipids. Thus, thorough sample preparation is required to ensure the removal of these interfering compounds. Another limitation is limited discovery of novel or unexpected lipid species since only lipids with known MS/MS fragmentation patterns can be usually analyzed [369,370,383]. In addition, flow injection analysis (FIA), where sample is infused from a pump, has been proven as a simple alternative to DI-MS [513]. More detailed reviews on MS-based shotgun lipidomics can be read elsewhere [514,515].

1.4.2 LC-MS and SFC-MS

LC-MS and SFC-MS, respectively (U)HPLC-MS and UHPSCF are key and well-established conventional analytical methods in lipidomics. They are powerful tools allowing lipid subclass and/or molecular species separation before MS analysis as well as the analysis of very low abundant lipids. However, care must be taken as there are many structural isomers in the sample and, therefore, a single analysis may lead to misinterpretations. The most frequently used API technique is ESI, which is best suited for a wide range of lipids that can be analyzed either in positive or negative ion modes. APCI and APPI are valuable alternatives for less polar lipids, such as MG, DG, TG, and CE [372].

ESI-MS is by far the most frequently used analytical technique utilized successfully in large-scale lipidomic studies due to several significant advantages including high sensitivity, easy coupling with chromatography techniques, and structural details based on the use of tandem mass spectrometers with high mass accuracy [451]. Last but not least, interfacing LC with IM has shown a great potential for lipid isomers separation together with increased selectivity and sensitivity [497].

1.4.3 MSI

MSI has become a popular and powerful method perfectly designed for the analysis of solid samples with the ability to simultaneously display both spatial distribution and molecular level information. The most frequently used ionization technique employed in MSI is MALDI. However, many other less common ionization techniques, *e.g.,* DESI, LAESI, or secondary ion mass spectrometry (SIMS) with the ability to produce sub-micron spatial resolution by using a tiny probe size, have been applied [369,460].

In MALDI, the samples are first cryodissected into slices (~μm), placed on a target surface, co-crystallized and immobilized with a suitable matrix, and then irradiated by laser to produce ions (typically singly charged). MALDI is also more tolerant to salts and can even ionize heavily glycosylated GSL, but generally have lower ionization efficiency compared to ESI [65]. Common matrices used for GSL analysis include, for example, 2,5-dihydroxybenzoic acid, 1,5-diaminonaphtalene, 4-hydrazinobenzoic acid, 6-aza-2-thiothymine, 6,7-hydroxycoumarin (esculetin), and α-cyano-4-hydroxycinnamic acid [65,516]. Cheng *et al.* also demonstrated a selective ionization of sulfatides by using 9-aminoacridine [517]. MALDI matrices used in lipidomics were also well-reviewed by Leopold *et al.* [518]. Since MSI requires minimal sample preparation, potential analyte losses are reduced with the most critical step being the decomposition of the MALDI matrix, which should be highly homogeneous [370]. MALDI also has a few limitations. It can barely resolve isomers without prior separation and generally experiences high background noise and ion suppression effects due to the formation of matrix clusters that preclude the application of this technology in full lipid profiling in complicated biological samples [65,452].

MALDI coupled to time-of-flight analyzers (MALDI-TOF or MALDI-TOF/TOF) is the most widely used MSI technology applied for rapid *in situ* screening of biomolecules in biological samples (*e.g.,* a thin slice of a tissue, body fluid drop, or cultured cells) to map spatial distribution of individual lipid species. Specific *m/z* values of interest are then assigned different colors and plotted in 2D space using the associated imaging software to obtain a molecular image of the sample, which can directly visualize pathological changes, thus providing valuable information for the study of many biological processes [519–521]. Although MALDI-TOF/(TOF) generally provides high accuracy, a wide detection range, and good compatibility, these parameters can greatly vary depending on the selection of the instrument. Moreover, the comprehensive analysis is limited since the MSI is largely based on the qualitative comparison of healthy and diseased samples [521]. Recently, the coupling of

MSI with high-resolution MS involving Orbitrap or Fourier transform ion cyclotron resonance (FT-ICR) has provided deeper insight into the lipidomic complexity of biological samples [522]. One such example is the application of MALDI-Orbitrap using MS/MS spectra to facilitate structural elucidation of even highly complex sulfo-GSL with up to five hexose moieties [173].

1.5 Qualitative analysis of GSL and other lipids

The rapid and direct structural elucidation of GSL and other lipids proves to be critical for studying their functional roles in many biological processes as well as the fundamental mechanism of lipid metabolism and the pathogenesis of various diseases. Although GSL can be relatively easily ionized and fragmented to product ions providing information about the head groups (*i.e.*, lipid class) and type of the ceramide backbone, reps. FAs composition (*i.e.*, lipid species), the precise and in-depth characterization of GSL is quite challenging.

In particular, the biological functions of GSL, as well as other lipids, highly depend on their varying expression levels and structural diversity, including carbon–carbon locations, *cis/trans* isomerism, and the *sn*-position of the fatty acyl chain(s), which further complicate the structural elucidation. Moreover, analysis of complex and heavily glycosylated GSL pose an additional challenge because multistage fragmentation mass spectrometry (MS^n) is usually required to achieve step-by-step cleavage of the glycosidic bonds and ceramide backbones.

An indisputable advantage is also the fact that the fragmentation pathways of GSL can be predicted and structural databases can be constructed *in silico* to identify GSL by matching obtained MS/MS spectra with the database. In addition, the linkages in oligosaccharide head groups may also be determined by MS/MS analysis after the cleavage of glycosidic bond by specific enzymes (see chapter 1.2.3) and removal of the ceramide moiety.

1.5.1 Separation of isomers

One of the current major challenges in lipidomics is difficulty to separate and differentiate isomeric and/or isobaric species due to immense structural variability in head groups, acyl chains, numbers and locations of C=C bonds (cis/trans), and regioisomerism (sn-positions), which inhibit the delineation and assignment of their biological roles [523]. Consequently, the specific functions of isomer have remained largely unknown due to these challenges [523]. Especially, in the case of GSL, the isomer problem is multiplied as many glycans have the

same formula (*e.g.*, Glc vs. Gal) as well as there can be distinct linkages in oligosaccharide chain also with option for either α- or β-glycosidic bond, which further complicate GSL analysis [376,523]. Moreover, the glycosphingolipidome is not only amazingly large, but also expanding with a number of new lipid species. Specifically, GlcCer with less prevalent α-linkage rather than β-linkage have been recently found [116,524,525] together with ceramides either lacking the 1-hydroxyl group [526] or having a fatty acyl attached to the 1-hydroxyl [527] alongside GSL with polyunsaturated very long-chain FAs (C26–C36) [528]. Furthermore, humans only synthesize *cis* (Z) FAs, while *trans* (E) FAs are not endogenously produced but present in human body due to dietary intake. They are well known to play an important role in various physiological processes and therefore, the separation of *cis/trans* isomers is of great interest [529]. In addition, co-elution of different lipid subclasses can lead to ion suppression obscuring the detection of low abundant lipids [529]. To address these issues, improved separation of lipids together with the ability to distinguish and identify GSL isomers is essential and highly advantageous for the investigation of their physiological role and functions in health and disease [523,529]. Although MS is very selective in identifying analytes with different chemical formulas, isomers often provide similar fragmentation spectra. Thus, identification and differentiation of isomers in complex samples require coupling with LC, IM, and/or alternative methods, such as specific fragmentation approaches (chapter 1.5.4) or chemical derivatization (chapter 1.5.5) providing diagnostic ions of each species. Previously, specific chromatographic techniques have been applied to separate lipids according to the number and position of C=C bonds (*i.e.*, Ag-HPLC) [470] or acylglycerols enantiomers (*i.e.*, chiral HPLC) [469]. Most recently, Vaňková *et al.* [462] demonstrated reversed-phase UHPLC method coupled with HRMS using a C18 column with sub-2-µm particles capable of identifying several hundreds of lipid species within a wide range of lipid subclasses, including their isomers and isobars. The developed method has high reliability together with significantly reduced run time. This was further supported by retention dependencies on the number of carbon or C=C bonds in the FAs chain of homologous lipid series (**Fig.36**).

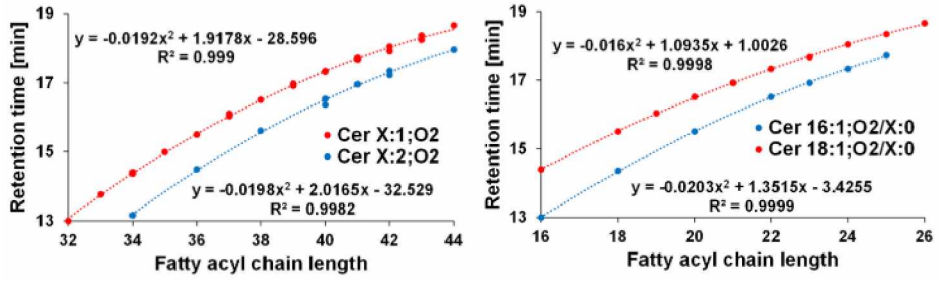

Fig. 36: Example of retention dependency of ceramides with various fatty acyl chain lengths [462].

Remarkable and unique separation power for isomers has been demonstrated using porous graphitized carbon (PGC) columns, even though the retention mechanisms are not yet fully understood but are likely mediated via hydrophobic, polar, and in some cases ionic interactions [404,423]. Specifically, the separation and characterization of GSL-derived oligosaccharide isomers using in-house packed PGC columns have been reported by the group of Teneberg and co-workers [284,530–532]. Moreover, Wuhrer and co-workers [533,534] performed an in-depth studies of GSL-glycan profiles of colorectal cancer and acute myeloid leukemia cell lines and revealed high expression of GSL-glycan isomers including sialyl-Lewis$^{a/x}$ and Lewis$^{b/y}$ antigens in cancer cell lines along with glycans with blood group A, B,, and H antigens in undifferentiated cell lines. Furthermore, a commercial Hypercarb PGC column from Thermo Scientific has been used as well. Mank *et al.* [535] used Hypercarb PGC column for the separation and structural elucidation of human milk oligosaccharides by LC-ESI/MS^2. In addition, Cho *et al.* [536], investigated the separation of permethylated glycans on Hypercarb PGC column using nano-flow-LC/MS. They also investigated the effect of PGC column temperature and revealed that increased temperature drastically improved the peak shape and resolution of some positional permethylated glycan isomers. The major drawback of using PGC column is that the double peaks caused by α and β anomers of the Glc at the reducing end are mostly observed. Although this issue can be overcome by the reduction leading to a single peak, the respective MS/MS spectra of reduced oligosaccharides are then more complicated making the interpretation of the glycan sequence more difficult [423]. Despite PGC columns are able to separate structurally similar glycan isomers, they are still used only by a limited number of research groups.

In recent years, IM has appealed as a suitable technique for the separation of lipid isomers. However, due to the current IM resolving power limitations, lipid isomers cannot be fully resolved by IM alone in complex mixtures [523]. Damen and co-workers [529] have demonstrated the UPLC method coupled to TWIMS-QTOF and using C18 stationary phase incorporating charge surface hybrid technology, which enabled the separation and structural elucidation of lipid isomers including *cis/trans* isomers. Wojcik *et al.* [523] utilized ultra-high resolution IM separation with travelling waves in a serpentine and extended multi-pass SLIM platform for selected lipid and glycolipid isomers. They were able to differentiate C=C bonds positions and their *cis/trans* orientations in phospholipids using multi-pass separation. In case of glycolipid isomers, the partial separation of GlcSph 18:1;O2 vs. GalSph 18:1;O2 and GlcCer 18:1;O2/18:0 vs. GalCer 18:1;O2/18:0 (**Fig. 37**), differing only in the identity of glycan, was achieved after four-passes (~60 m path). Moreover, the baseline separation of GD1a and GD1b

gangliosides, which only differ in the location of SA residue, has been accomplished even with minimal possible path 1.25 m (*i.e.*, without using the multi-pass separation). However, the major issue is the limited number of passes due to increasing peak widths with the increasing number of passes, which reduce the detection and range of mobilities.

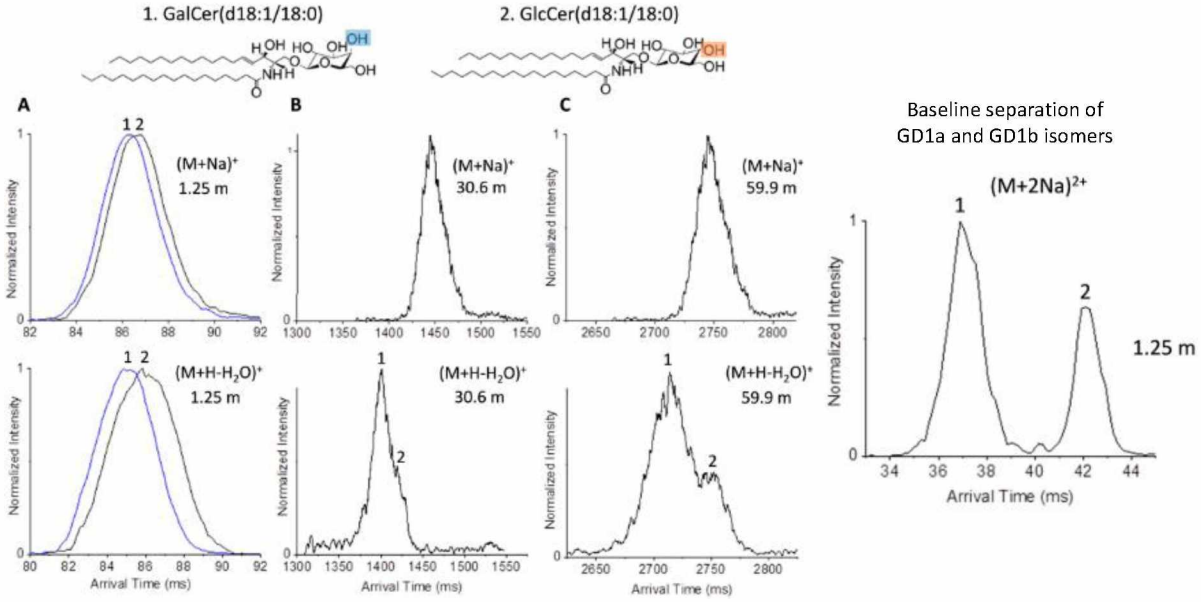

Fig. 37: Examples of separation GSL isomer with IM using SLIM (adopted from [523]).

Next, May *et al.* [537] also resolved GD1a and GD1b gangliosides in a standard mixture as doubly sodiated species $[M+2Na]^{2+}$ along with two pentasaccharide GSL differing in the location and linkage of fucose (**Fig. 38**).

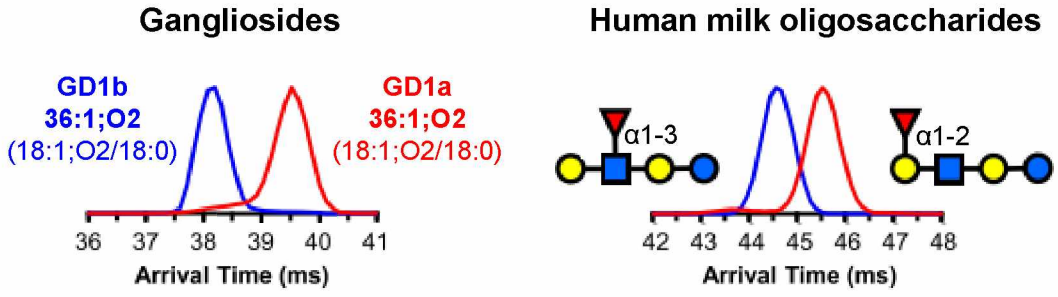

Fig. 38: Separation of GD1a/GD1b isomers and pentasaccharide isomers using IM [537].

Moreover, Djambazova *et al.* [538] have reported a partial separation of GD1a and GD1b isomers with 36:1;O2 and 38:1;O2 ceramide in tissue samples using MALDI-TIMS. Furthermore, Xu *et al.* [539] have shown effective resolution of GlcCer and GalCer species from human plasma and cerebrospinal fluids using DMS coupled to LC-ESI/MS (**Fig. 39**).

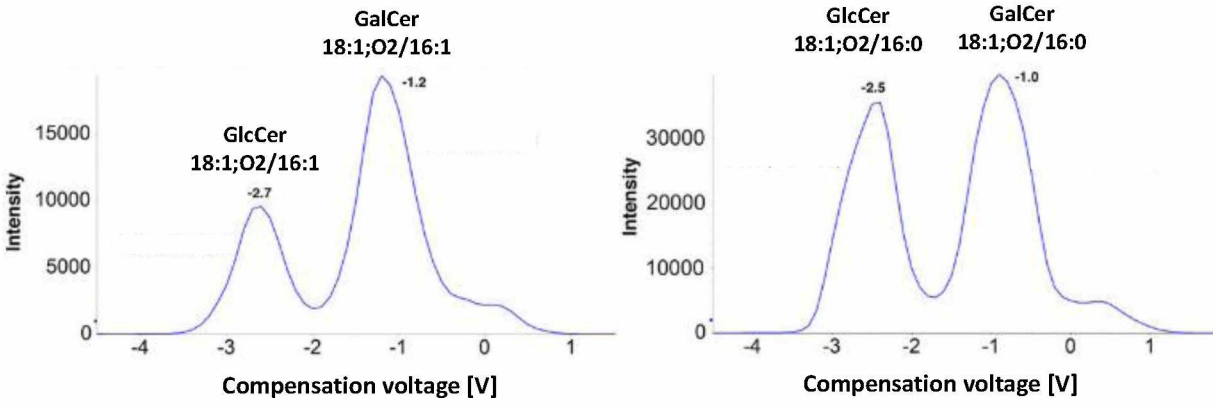

Fig. 39: Separation of HexCer isomers using differential mobility spectrometry (adopted from [539]).

In summary, although the separation of lipid isomers still remains very challenging and only a limited number of lipidomic studies have been carried out to differentiate GSL isomers using IM technologies, recent advances in chromatography and continuous innovation of IM through novel instrumental developments have pushed the popularity of IM forward by enhancing its sensitivity and selectivity. The coupling of IM with LC-MS is thus likely to become a very valuable tool capable of efficiently separating and reliably distinguishing various lipid isomers. However, further progress is still needed as potential applications of IM are still being discovered [496].

1.5.2 Fragmentation (MS^2 and MS^n spectra)

Tandem mass spectrometry (MS/MS) analysis is essential in the structural elucidation of GSL The systematic nomenclature of MS/MS fragments for carbohydrate part of GSL was proposed by Domon and Costello [540] and include fragments containing the non-reducing end (*i.e.*, A, B, and C) and the reducing end (*i.e.*, X, Y, and Z). Fragments B, C, Y, and Z correspond to glycosidic cleavages that determine glycan sequence (**Fig. 40A**), while A and X fragments are cross-ring cleavages allowing the differentiation of linkage positions (**Fig. 40B**). Since the A, B, and C type ions do not include ceramide structure, unlike their X, Y, and Z counterparts, their masses are not affected by a lipid moiety. The naming was later modified by Ann and Adams [541] in order to include more detailed ceramide fragments. The major fragments are shown in **Fig. 40C**, where the N^I and N^{II} fragments are diagnostic of the long-chain base.

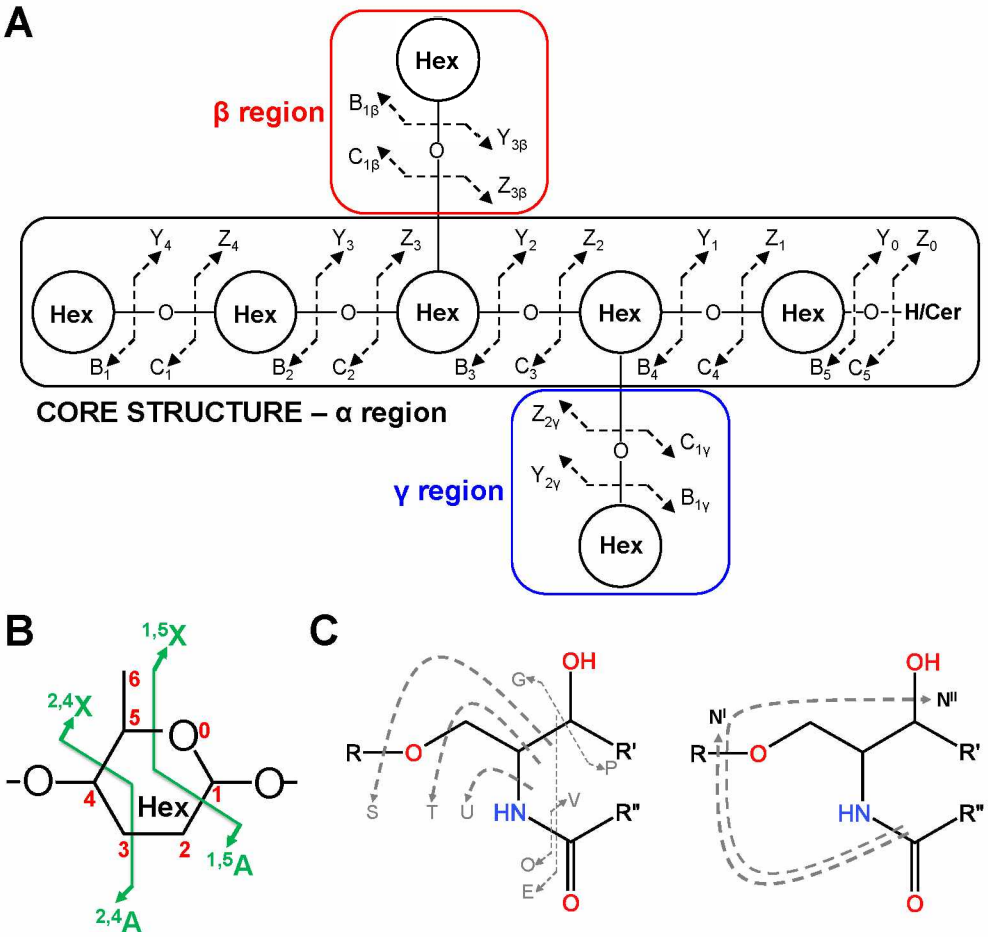

Fig. 40: Fragmentation patterns of GSL (adopted from [540–542]).

Neutral GSL are relatively poorly ionized in the negative ion mode due to their basic (*i.e.*, amino sugar-containing) and acidic counterparts [543], thus neutral GSL are commonly analyzed in the positive ion mode, where GSL are better ionized and provide abundant Y/Z-pair ion series indicative for sequence information accompanied by less common B/C-type fragments. The A/X-type ions involving C–C bond usually require higher energies [64]. Moreover, complex neutral GSL suffer from poor ionization efficiency. It is known that ESI sensitivity decreases with the increasing length of the glycan chain of GSL due to increased hydrophilicity [543,544]. Furthermore, a large majority of GSL share a Gal–Glc disaccharide core linked to the ceramide moiety, which may complicate the product spectral analysis as the Y_0/Z_0, Y_1/Z_1, and Y_2/Z_2 fragments of different GSL species can have the same mass, despite their intensities may vary among GSL species [64]. General fragmentation patterns of neutral GSL have previously been well-demonstrated and extensively studied [396,423,545]. GSL containing 2-hydroxy fatty acyl groups are also typically characterized by abundant fragment ion derived from the loss of the hydroxy-acyl group [546].

In contrast, acidic GSL (*i.e.*, sulfatides and gangliosides) are broadly analyzed in the negative ion mode since the molecule is readily ionisable due to anionic sulphate group and sialic acid residues, respectively [547]. However, the use of positive ion mode is also common [64]. Sulfatides provide prominent diagnostic ion at *m/z* 97 (*i.e.*, loss of HSO_4^-), which is, however, not observed in ion trap MS because of the low-mass cut off, together with B/C-type fragment ions reflecting 3-sulfoGal (*m/z* 259 and 241) and 3-sulfoGal–Glc (*m/z* 419 and 403) residues accompanied by dehydration **(Fig. 41)**. Furthermore, the differentiation of non-hydroxylated and hydroxylated sulfatides has been well documented. The α-hydroxylated fatty acid-containing sulfatides are recognized by the unique and prominent ion cluster originated from primary cleavage of the fatty acyl CO-CH(OH) bond (ion a) accompanied by the direct loss of fatty acyl as a ketene from precursor ion via the NH–CO bond cleavage (ion b), which further undergoes a water loss (ion c) [547–549] (**Fig. 41**).

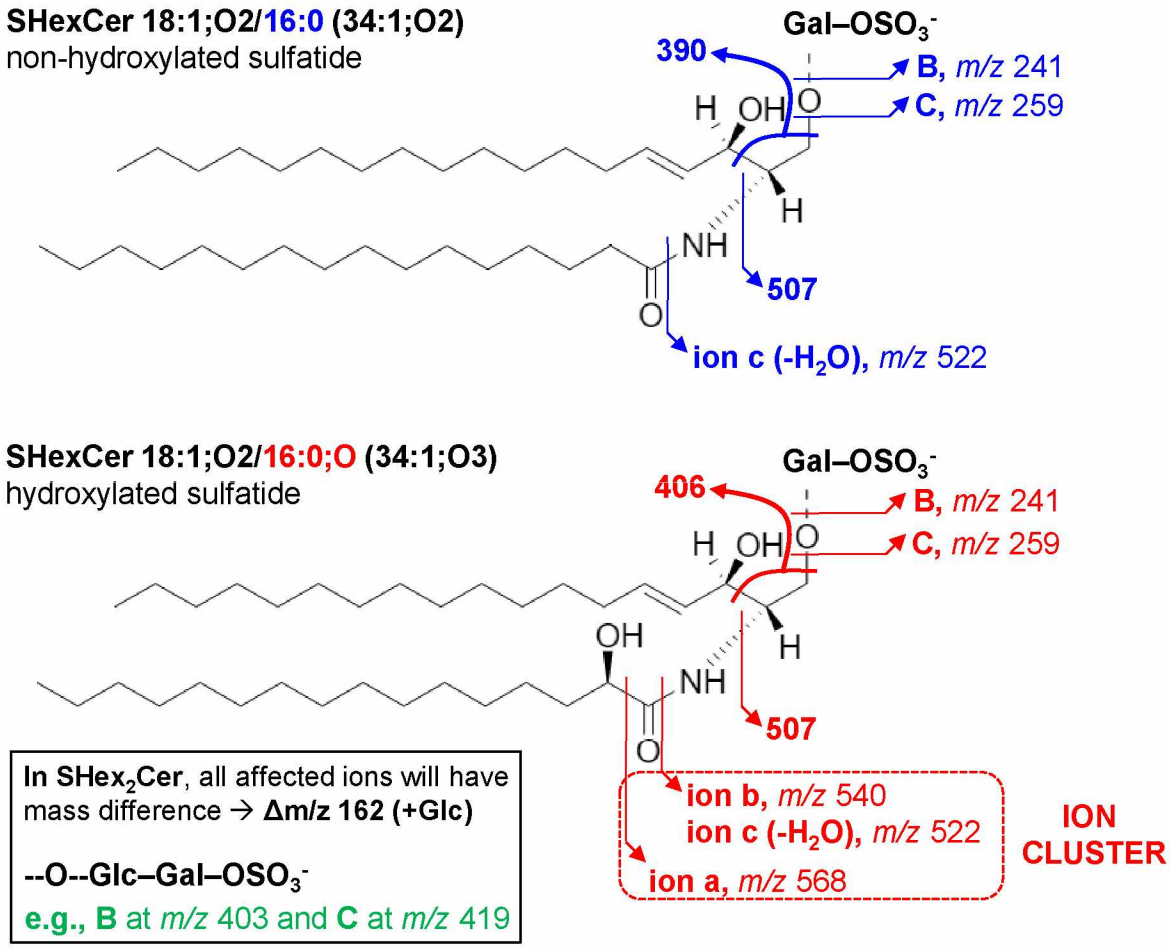

Fig. 41: Typical fragmentation of (non)-hydroxylated sulfatides in negative ion MS/MS [548].

In some cases, the analysis of underivatized GSL-derived oligosaccharides in the negative ion mode may be advantageous for the isomer recognition due to low chemical background noise and low level of cation adducts formation [550,551]. Negative ion MS/MS spectra of oligosaccharides are generally dominated by a series of B/C-type ions providing information about the glycan sequence. More interestingly, C_1 ion can provide additional information about the terminal Gal linked to GlcNAc. The fragmentation of Gal1–4GlcNAc linkage is more facile, and thus can be readily cleaved, while Gal1–3GlcNAc linkage is more resistant. However, when Gal is substituted with Fuc, the 1–3 linkage can be cleaved (**Table 19**) [550].

Table 19: Distinction of 3-/4-linked Gal to GlcNAc with and without Fuc substitution [550].

Linkage	Substitution of Gal	Structure	C_1 ion
Gal**1–4**GlcNAc	non-substituted	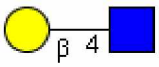	Present at *m/z* 179 (**low** abundance)
	Fuc	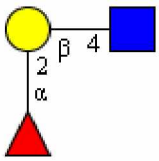	Present at *m/z* 325 (**high** abundance)
Gal**1–3**GlcNAc	non-substituted	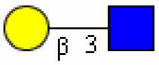	Absent
	Fuc	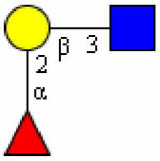	Present at *m/z* 325 (**low** abundance)

Generally, cross-ring fragmentation (*i.e.*, A-type ions) is useful for defining the linkage positions between individual monosaccharides [551]. A cross-ring ^{0,2}A-type cleavage is typical for 4-linked GlcNAc or Glc (*i.e.*, type 2 chain), whereas it is not produced from 3-linked GlcNAc (*i.e.*, type 1 chain). It can be used to discriminate between Gb and iGb as well. In addition, a double glycosidic D-type cleavage (*i.e.*, C–Z double cleavage) is unique to a non-substituted 3-linked GlcNAc/Glc or 4-linked GlcNAc/Glc substituted with Fuc (**Table 20**). Similarly D-type ion indicate 3-linked GlcNAc substituted with Gal at the 4-positions. Taken together, A- and D-type ions are important for differentiations of type 1/2 chain, and blood group H, Le^a, Le^b, Le^x, and Le^y determinants [550].

Table 20: Typical D-type fragments of type ½ chain and blood group determinants [550].

Produced D ion	Residue after cleavage	Chain type + cleavage
***m/z* 202**	3-linked GlcNAc	Type 1 H 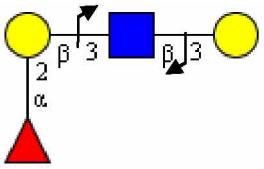
***m/z* 348** (202 + 146)	4-linked Fuc to 3-linked GlcNAc	Type 1 Le^a, Le^b 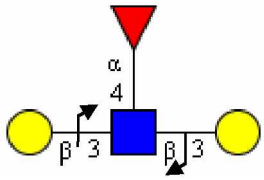
***m/z* 364** (202 + 162)	4-linked Gal to 3-linked GlcNAc	Type 1 Le^x 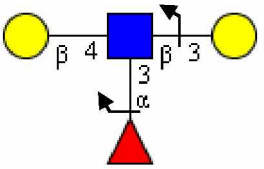
***m/z* 510** (202 + 162 + 146)	4-linked Fuc–Gal to 3-linked GlcNAc	Type 1 Le^y 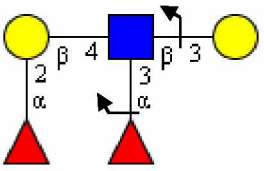

In case of complex branched GSL-derived oligosaccharides, MS/MS spectra can provide complimentary structural information. In the MS/MS spectra of $[M–H]^–$, fragments derived from 6-linked branches (α) are dominant, while those from 3-linked branches (β) are absent. In contrast, fragments from both branches are dominant in the MS/MS spectra of $[M–2H]^{2–}$. Similarly, double cleavage (D-type ion) occurs only at 3-linked branches (**Fig. 42**) [551].

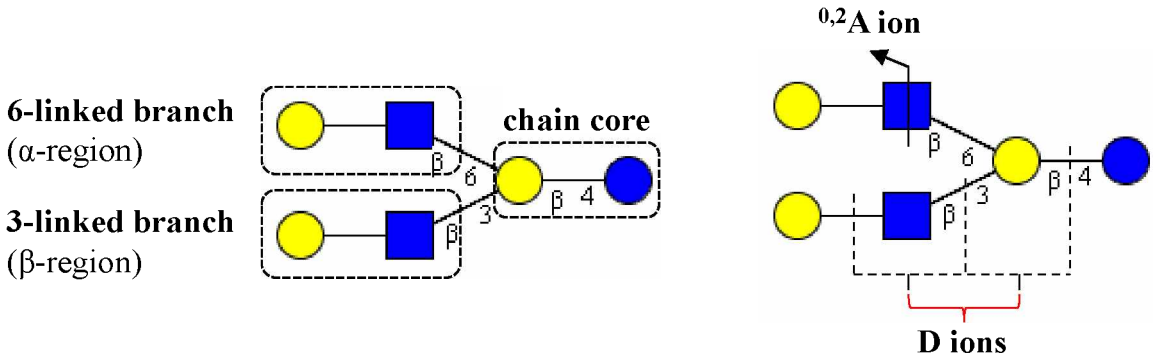

Fig. 42: Illustration of 3- and 6-branched oligosaccharides with typical fragment ions [551].

Additionally, sialylated GSL (*i.e.*, gangliosides) have been considered difficult to analyze as SA is relatively labile and preferentially lost during the ionization process. The loss of SA is favored particularly, when two or more SA are present, but the stability of SA can be improved by the formation of alkali metal adducts (*i.e.*, $[M–2H+Na]^-$). This is a typical feature of MALDI-MS [546,552]. Generally, SA on glycoconjugates can be linked to Gal via 2–3/6 linkage and to GalNAc via 2–6 linkage. There are also α-/β-anomers of SA with α-anomeric form being the most common, while β-anomeric form is typical for free SA. It is also unclear if the β-anomer is present in oligosaccharide chains or ignored/escaped from detection due to low concentration. The linkages positions and anomeric configurations of SA are reflected in the stability of the molecule during ionizations: β2–3 > α2–6 > α2–3 > β2–6 as well as in the characteristic fragmentation patterns in MS/MS spectra (**Table 21**) [552].

Table 21: Differentiation of 2–3/6 and α/β linkages of sialylated oligosaccharides [552].

Linkage and anomeric configuration		**Characteristic fragments**	
2–3-linked NeuAc (SA)	α linkage	$^{2,4}A$-CO_2; B_2-CO_2	
	β linkage		$^{2,4}A$; B_1-CO_2
2–6-linked NeuAc (SA)	α linkage	$^{0,4}A$-CO_2; $^{0,2}A$, $^{2,4}A$	
	β linkage		$^{0,4}A$
D-type ion at *m/z* 493	Internal location of SA on the 3-linked GlcNAc and Glc		

In-depth description of the MS/MS of oligosaccharides can be found in this review [543]. The differentiation of blood group A, B, H and Lewis blood group Le^a, Le^b, Le^x, and Le^y determinants on GSL-derived oligosaccharides has been described in detail as well [530,553]. Additionally, GSL with acidic residues usually facing in-source and/or post-source fragmentation, or produce metastable ions, especially when MALDI-MS is used [544,546].

1.5.3 Dissociation techniques

MS/MS analysis of GSL relies on various dissociation techniques. Each dissociation technique provides a distinct level of structural information since it cleaves bonds at different locations of the molecule. Their combined use can provide complementary structural details of GSL [65]. There are three major types of dissociation techniques including collision-, electron-, and photon-mediated dissociation along with unique radical-directed dissociation.

A) Collision-mediated dissociation

Collision-mediated dissociation is conventional and mostly default dissociation technique employed for MS/MS experiments. It covers three common techniques, namely low-energy collision induced dissociation (CID), higher-energy collisional dissociation (HCD), and surface-induced dissociation (SID). The activation in CID and SID is achieved by single or multiple collisions of precursor ions with an inert gas or with a stationary solid surface. Furthermore, HCD is uniquely used in orbitrap configurations. Both CID and HCD provide structural information aid in elucidating the glycan sequence (*i.e.*, B- and C-type ions) and the lipid part. A supplemental option, implemented exclusively for ion trap MS, is pulsed Q dissociation (PQD), which deposits higher energies on the ions compared to CID and allows the observation of low *m/z* fragments that are usually excluded from CID, however at the cost of reduced fragmentation efficiency [65,554].

Incremental $\Delta m/z$ indicate the loss of a hexose ($\Delta m/z$ 162) and N-acetylhexosamine ($\Delta m/z$ 204). Moreover, sulfatides and gangliosides can be recognized by the loss of sulfate group (*m/z* 97) and sialic acid (*m/z* 290) in the negative mode, respectively [65]. In addition, the ceramide composition, respectively sphingoid bases, can be identified from the specific fragment ions in the positive mode (**Table 22**) [396].

Table 22: Typical N^{II} fragments corresponding to the respective sphingoid base [396].

m/z	**238**	**236**	**266**	**264**	**262**	**294**	**292**	**282**
base	16:0;O2	16:1;O2	18:0;O2	18:1;O2	18:2;O2	20:0;O2	20:1;O2	18:0;O3

One caveat of CID is that to be able to distinguish isomers with subtle structural differences, multi-stage collisional dissociation has to be usually used, even when coupled with the chromatographic separation. This was exemplified in the work of Li *et al.* [555], where MS^n of permethylated GSL allowed differentiation of Gb_4Cer (specific ion at *m/z* 315) and iGb_4Cer (specific ion at *m/z* 357).

B) Electron-mediated dissociation

Electron-mediated dissociation relies on interactions between analyte ions and electrons and is based on the conversion of precursor ions to radical ions followed by the dissociation of the metastable radical ions via intramolecular rearrangements to produce fragments [556]. However, the formation of radical ions differs between electron-capture dissociation (ECD),

electron-detachment dissociation (EDD), and electron-transfer dissociation (ETD) techniques. ECD and EDD operate similarly, the ions pass through a beam of low-energy electrons that are captured by these ions to form radical ions. ECD and EDD apply to multiply-charged positive and negative ions, respectively. Moreover, ECD provides the extensive fragmentation of GSL while EDD is relatively inefficient [65,554]. Both ECD and EDD have been implemented mainly in FT-ICR [557,558], but attempts have been made to integrate them into the more accessible ion trap analyzer, such as orbitrap [559]. EDD technique has been several times used for the structural characterization of oligosaccharides [560–562]. On the contrary, in ETD, precursor ions react with radical ions generated *in situ* finally yielding ceramide backbones fragments and identifying acetylated glycans [65]. Unlike ECD and EDD, ETD can be performed using ion trap mass spectrometers, as shown by Han and Costello [563]. Moreover, there is a so-called electron-induced dissociation (EID) which can be employed for both singly charges and multiple charge precursor ions [554].

C) Photon-mediated dissociation

Photon-mediated dissociation includes three major techniques, specifically infrared multiphoton dissociation (IRMPD), ultraviolet photodissociation (UVPD), and blackbody infrared radiative dissociation (BIRD), which is not discussed here, but is of special interest for investigation of dissociation energetics of rather weak interactions.

In UVPD, the precursor ions are activated and dissociated by the absorption of high-energy photons. Ions are irradiated in a collision cell typically by ns-pulsed UV laser (*e.g.*, 157 nm-F2 and 193 nm-ArF excimer lasers, or 213 nm solid-state laser, depending on the application) delivering a high flux of photons in a short time period. Thereafter, activated ions can undergo one of many competing processes leading to dissociation, such as de-excitation, vibrational redistribution of internal energy, or direct fragmentation. The excitation in UVPD is fast and occurs in a single step rather than in a stepwise fashion. UVPD was first implemented in FT-ICR mass spectrometer and has been mainly used in the combination with ion trap MS. Whereas collision-mediated dissociation methods mainly induce glycosidic bond cleavage, UVPD yields extensive fragmentation patterns of GSL. These include more informative cross-ring fragments of the glycan moieties (A/X-type) and several unique UVPD-specific cleavages at ceramide C–C and C–N bonds that allow differentiation between isomeric glycans and ceramides. In particular, UVPD can reliably locate C=C bonds in ceramide moieties of GSL. Despite the advantages, UVPD is not widely used due to the lack of automated software tools for spectra annotation, however, there are a few lipidomics

applications [554,564,565]. Ryan *et al.* [566] have reported that 193 nm UV irradiation leads to extensive fragmentation of both glycan and ceramide parts in the neutral GSL and gangliosides along with a certain level of fragmentation close to the carbon–carbon double bonds. Recently, Brodbelt and co-workers implemented 193 nm UVPD as well as hybrid triple-stage collision-induced dissociation mass spectrometry (CID-MS^3) coupled with UVPD to localize double bonds and differentiate *sn*-positional isomers of various phospholipid subclasses via the presence of diagnostic fragment pairs [567,568]. 193 nm UVPD was also employed to study neutral and acidic GSL [564]. It should be also noted that the analysis of C=C bonds locations by UVPD is limited by its low fragmentation efficiency caused by low photon absorption by C=C bond, therefore, high-power laser or incorporation of more efficient chromophores in lipids is needed to improve the sensitivity to locate C=C bonds in lipids [569]. The detailed description of UVPD applied to the analysis of various biological molecules can also be found in an excellent review by Brodbelt *et al* [570].

Similarly, IRMPD has similar experimental setup except that infrared lasers (*e.g.*, CO_2 lasers centered around 10.6 μm or Nd:YAG laser) are employed, and the dissociation is induced by sequential absorption of multiple IR photons accompanied by intramolecular vibrational redistribution (IVR) until the cumulatively acquired internal energy exceeds the dissociation barrier resulting in fragmentation (**Fig. 43**) because a single IR photon is not sufficient to cause bond rupture in most biologically relevant molecules. IRMPD was first implemented in FT-ICR mass spectrometers and subsequently integrated into commercial quadrupole ion traps. A major advantage of IRMPD is a certain degree of selectivity as fragmentation can be controlled by the wavelength of the laser and duration of laser irradiation. Moreover, IRMPD does not discriminate between precursor and product ions, thus product ions can be subsequently fragmented via additional photon absorption [554,565].

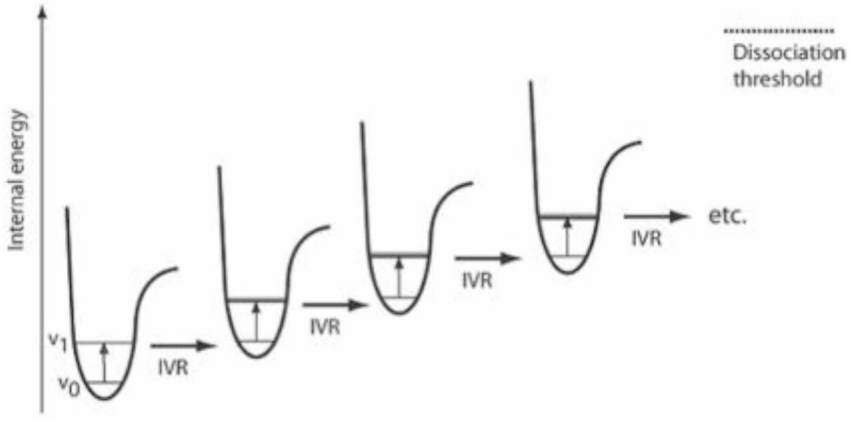

Fig. 43: Schematic representation of multiphoton activation mechanism in IRPMD [554].

Although IRMPD does not usually provide additional information on the lipid structure compared to conventional CID, it proves to be suitable mainly for phosphate-containing compounds [571]. Besides, a few non-phosphorylated lipids were investigated as well [557]. Lee *et al.* used MALDI coupled to FT-ICR mass spectrometer for structural elucidation of gangliosides utilizing both CID and IRMPD for MS/MS experiments, although the IRMPD produced less fragmentation compared to CID [572].

A more detailed description of applications of photon-mediated dissociation techniques in the analysis of biomolecules including a variety of different lipid subclasses, such as GPs, GSL, lipid A, and large lipopolysaccharides have been provided in the following reviews [565,570,573]. The comparison of CID, UVPD, and IRMPD is illustrated in **Fig. 44**

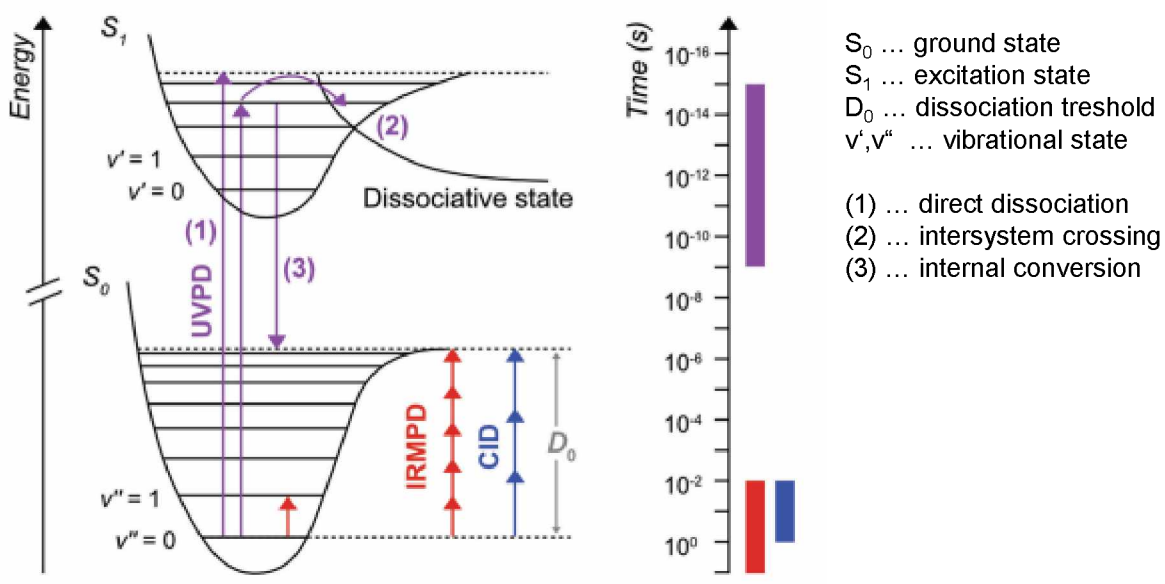

Fig. 44: Comparison of CID, UVPD and IRMPD using Jablonski diagram (adopted from [565]).

D) Radical-directed dissociation (RDD)

Radical-directed dissociation (RDD) is a unique fragmentation technique whose employment for lipidomics was demonstrated by the Blanksby group in 2012 [574]. In the RRD approach, molecules are first derivatized or complexed to introduce UV-labile chromophores (*e.g.*, carbon–iodine bond). The modified molecules are then ionized and subjected to UVPD, where the UV-labile bond breaks via homolytic cleavage to form radicals. These radicals abstract protons from the analyte ions to form radical ions that are finally fragmented using CID [65,574]. Although the application of RDD is limited mainly due to complicated sample preparation, RDD has been shown to distinguish GSL epimers, namely GlcCer and GalCer, based on the inverted abundance of the major fragments caused

by the differential ability of GlcCer and GalCer to lose water (*i.e.*, neutral loss of water is easier in Gal than Glc) [575].

There are also several other dissociation techniques, such as metastable atom-activated dissociation (MAD) [569,576], electron impact excitation of ions from organics (EIEIO) [569,577,578], or charge-remote fragmentation (CRF) [569]. More detailed description of collision-, photon-, and electron-mediated activation techniques can be read from the following papers [554,556,579].

1.5.4 Innovative ion activation technologies (location of C=C bonds)

Nowadays, the collision-induced dissociation tandem mass spectrometry (CID-MS/MS) is well-established dissociation technique providing a head group and ceramide composition. However, the ceramide backbones of GSL as well as other lipids may contain unsaturated FAs with one or more carbon-carbon double bond (C=C), which cannot be located using collision-mediated techniques. The determination of C=C bonds is not trivial and is possible with the use of UVPD or RDD. The determination of C=C bonds has become a hot topic in recent years, thus, several novel and selective ion activation technologies have been developed to address this issue [580,581].

Over the recent years, ambient ionization mass spectrometry (AIMS) techniques coupled with novel ion activation technologies have allowed rapid and direct structural elucidation of carbon–carbon double bond (C=C) locations, *cis/trans* isomers, and *sn*-position isomers of lipids isolated from various complex biological samples with minimal or no sample pretreatment [580]. These novel ion activation methods are discussed below.

A) Paternò-Büchi (PB) reaction

In 2014, Ma and Xia [582] introduced a novel method of pinpointing C=C bond locations by online coupling of the Paternò-Büchi (PB) reaction with tandem mass spectrometry (PB-MS/MS). The PB reaction is photochemical cycloaddition between electronically excited aldehyde or ketone and a C=C bond using typically acetone as PB derivatization reagent for 254-nm UV irradiation. The reaction provides fast and highly specific modification of the C=C bonds in lipids yielding abundant C=C diagnostic fragment ions, which are used for accurate location of C=C bonds (**Fig. 45**) [583].

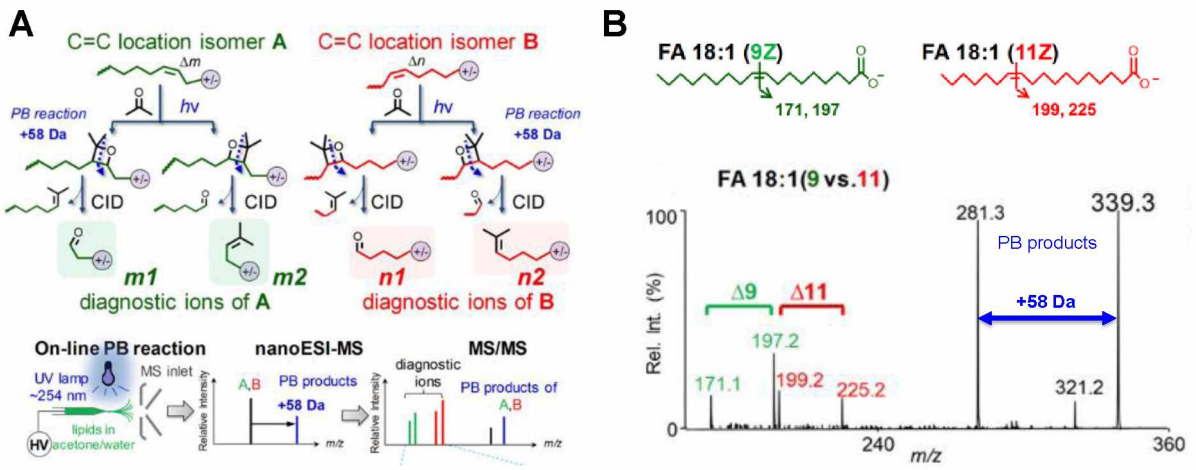

Fig. 45: PB reaction: (A) mechanism and (B) differentiation of FA 18:1 isomers (modified [584]).

This strategy has been applied for the large-scale analysis of C=C location isomers of different lipid subclasses, including non-esterified FAs, GPs, and other lipids in a variety of biological samples, but it also has a potential for the location of C=C bonds in ceramide moieties of GSL [584–586]. PB-MS/MS has a number of unique features, including (1) fast reaction kinetics allowing online coupling with ionization, (2) simple experimental setup without requiring modification of MS instrument, (3) wide applicability to different lipid subclasses, (4) formation of PB products with the specific mass increase from the original molecule, and (5) production of highly abundant diagnostic ions derived from PB products enabling both confident localization of C=C bonds and quantitative analysis [580,581]. Furthermore, PB reaction is compatible with different MS techniques, including DI-MS, LC-MS, and MSI [569].

Moreover, Bednařík *et al.* [587] developed an on-tissues PB reaction for the localization of C=C bonds in phospholipids and glycolipids by MALDI-MS using benzaldehyde. In addition, benzophenone [588,589], 2-acetylpyridine [590], and 2′,4′,6′-trifluoroacetophenone [591] have been shown as potential PB derivatization reagent as well.

B) Ozone-induced dissociation (OzID)

Ozone-induced dissociation (OzID exploits the gas-phase reaction and was firstly implemented in 2008 by Blanksby´s group, who replaced inert collision gas in mass spectrometer with O_3/O_2 mixture so that the ozonolysis can take place inside the collision cell [592]. The reaction is based on cycloaddition of O_3 to unsaturated lipids generating metastable ozonide that spontaneously decays to more stable Criegee and aldehyde diagnostic

ions with a constant mass separation of 16 Da. OzID coupled with soft ionization techniques is highly specific and efficient method for the assignment not only the position of carbon–carbon double bonds, but also their stereochemistry in unsaturated lipids (**Fig. 46**) [569,593]. The major drawbacks are that OzID typically requires modification of commercial instruments and specialized equipment generating ozone as well as requires longer reaction time (0.2–10 s) to accumulate detectable C=C diagnostic ions due to the low ozone density allowed in an ion trap analyzers [583]. This reduces the analysis speed and makes the coupling with LC inefficient, which greatly restricts the application of OzID. To circumvent this limitation, OzID has been implemented in a high-pressure IM cell with high O_3 density significantly accelerating ozonolysis and producing abundant C=C fragment ions [594], which also facilitated a coupling with LC, a novel platform for the analysis of isomer [595]. In addition, online coupling of OzID with HRMS instrument has been reported together with significantly improved ozonolysis efficiency by slowing down ions in the trap region for their prolonged interaction [596].

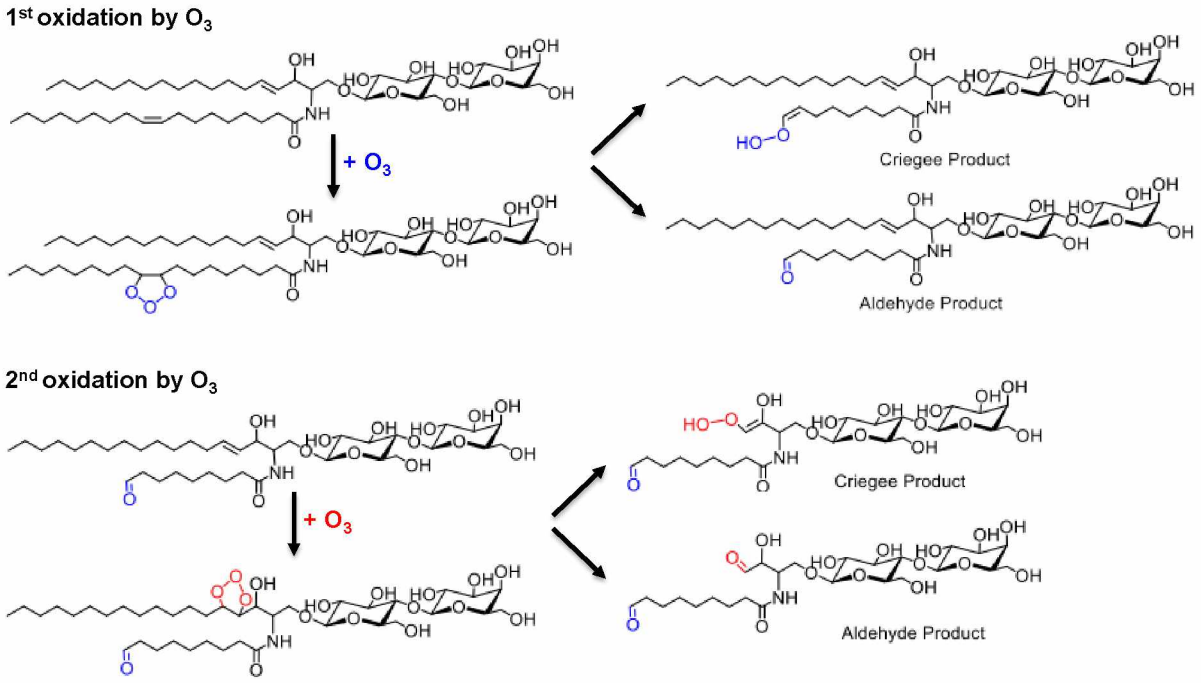

Fig. 46: Mechanism of ozone-induced dissociation (OzID) (modified from [597]).

Marshall *et al.* have also implemented OzID into shotgun lipidomics workflow for fast human plasma lipid profiling [598]. Barrientos and co-workers have demonstrated the structural analysis of sodiated adduct ions of unsaturated GSL using OzID-MS that yielded more informative cross-ring cleavages compared to protonated ions [599]. Later, they

reported that adducts can remarkably influence both the bond cleavage and the fragmentation behavior and illustrated distinct fragmentation patterns of $[M+H]^+$, $[M+Na]^+$, and $[M+Li]^+$ precursor ions of GSL in OzID-MS. Specifically, they reported that $[M+H]^+$ ion primarily undergoes dehydration yielding $[M+H-H_2O]^+$ ion followed by the sequential loss of monosaccharide units, while $[M+Na]^+$ and $[M+Li]^+$ adducts dissociate preferably at the double bonds yielding similar fragmentation patterns, albeit the relative intensities of diagnostic ions were remarkably different (**Fig. 47**) [597].

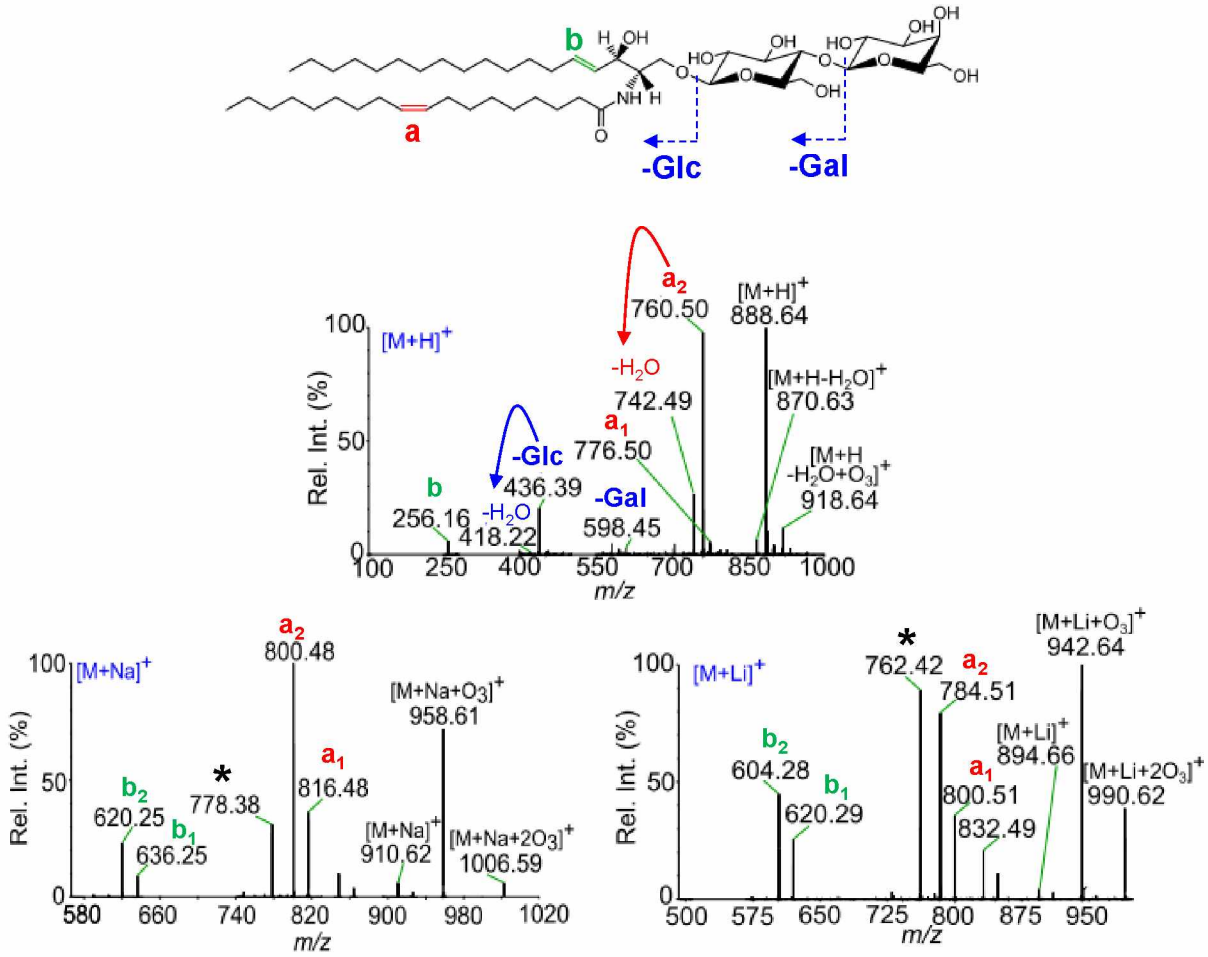

Fig. 47: OzID-MS spectra of LacCer 18:1;O2/18:1;O(9Z) (modified from [597]).

* denotes ozonide stabilized secondary oxidation product of sphingosine n-14 double bond

C) Epoxidation

Recently, Feng *et al.* reported an innovative epoxidation reaction using metachloroperoxybenzoic acid (m-CPBA) coupled with LC-MS/MS for the analysis of unsaturated phospholipids. The m-CPBA epoxidation is completed within minutes and without overoxidized by-products, showing potential for high-throughput analysis [600]. As

a consequence, m-CPBA epoxidation [601] and peracetic acid(PAA)-mediated epoxidation [602] have been used for large-scale identification and spatial mapping of biological C=C isomers. Briefly, epoxidation is initiated by the oxidation of unsaturated lipids via m-CPBA or PAA either in-solution or on-tissue reaction to generate an epoxide product, which is further subjected to CID-MS/MS analysis generating a pair of diagnostic ions pinpointing the location of C=C bond (**Fig. 48**) [602]. The major advantages of the epoxidation are versatility and user-friendly platform with minimal requirements for instrumentation [601].

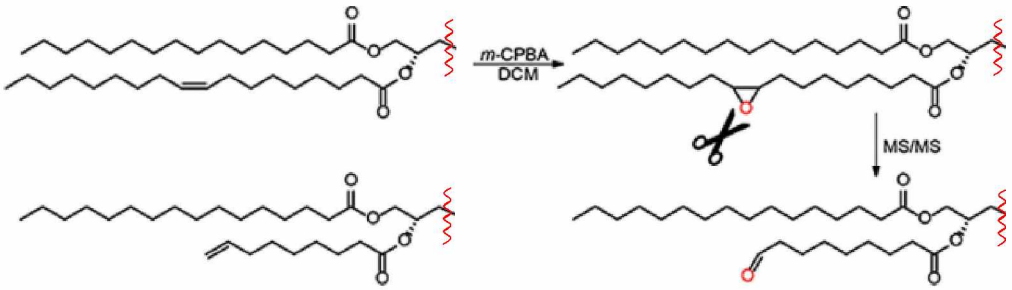

Fig. 48: Schematic illustration of epoxidation reaction (modified from [581]).

Very recently, Zhang *et al.* [603] proposed a rapid light-controlled photoepoxidation using benzoin to locate the positions of C=C double bonds of various isomers of unsaturated lipids in mouse tissue extract, in both positive and negative ion modes. The epoxide formation occurs under UV-light and aerobic conditions. Sawaki and Ogata found that benzoin can transfer oxygen atom in O_2 to benzoyl oxy under UV irradiation, then, acyl peroxy radicals can open the double bonds and photoepoxidation products [604].

In addition, the rapid switch-on/off electrochemical epoxidation controlled simply by tuning the electrospray voltage was recently developed to locate the C=C bond positions in lipids within seconds (**Fig. 49**) [605].

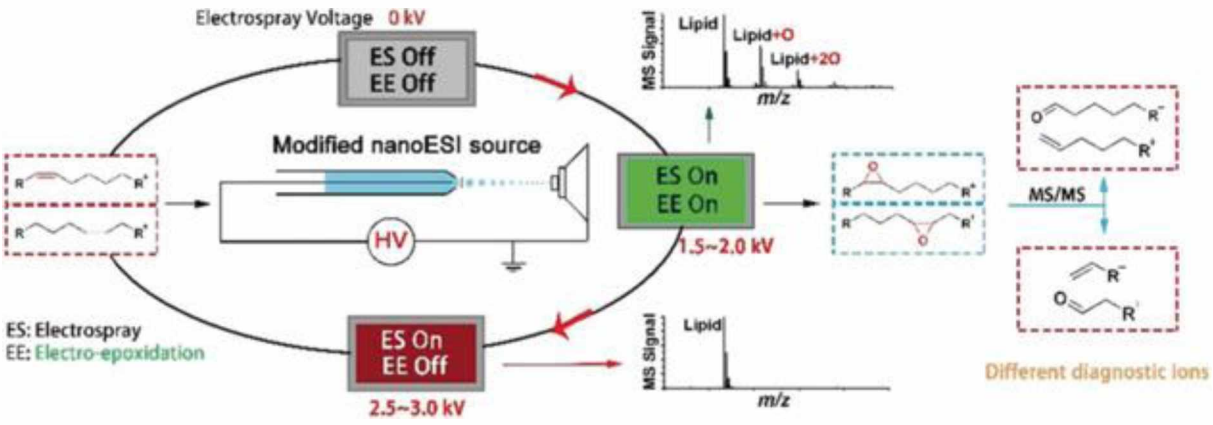

Fig. 49: Schematic representation of electrochemical epoxidation (modified from [605]).

The electrochemical epoxidation can generate on-demand mono- or multiple electro-epoxidized products at different voltages that are further fragmented to generate diagnostic ions to locate the C=C bond [605]. In addition, chloroauric acid ($HAuCl_4$)-dopped solvent introduced into an electrospray has been reported to induce epoxidation [606].

Low-temperature plasma(LTP)-induced epoxidation using atmospheric oxygen as an oxidizing agent without additional need for special solvents can also be used for the assignment of C=C bonds. The reaction is performed by blowing the LTP plasma into the mixture of lipids in acetone/water (50/50, v/v). (**Fig. 50**). The conversion of C=C bonds to the corresponding epoxides is rapid and nearly complete [607]. Moreover, the LTP probe enabled online epoxidation of unsaturated FAs on a paper-based analytical devices [608].

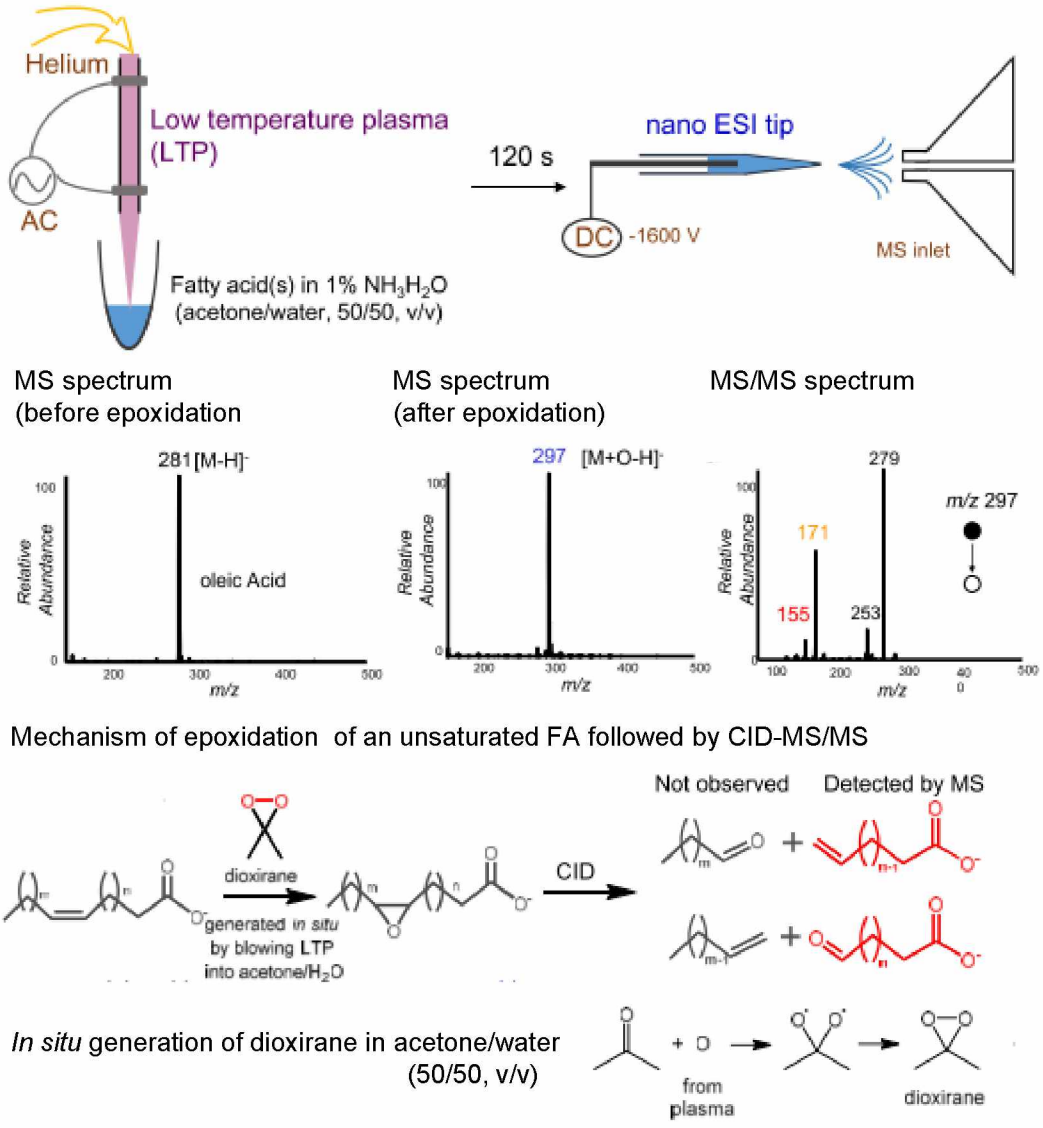

Fig. 50: Schematic representation of epoxidation using low-temperature plasma (modified [607]).

Notably, a novel method based on ambient oxidation (*i.e.*, oxidation reaction in air) coupled with air flow-assisted desorption electrospray ionization (AFADESI) was proposed to conveniently and rapidly characterize spatial distribution of unsaturated lipid isomers using MSI technology (**Fig. 51**) [609].

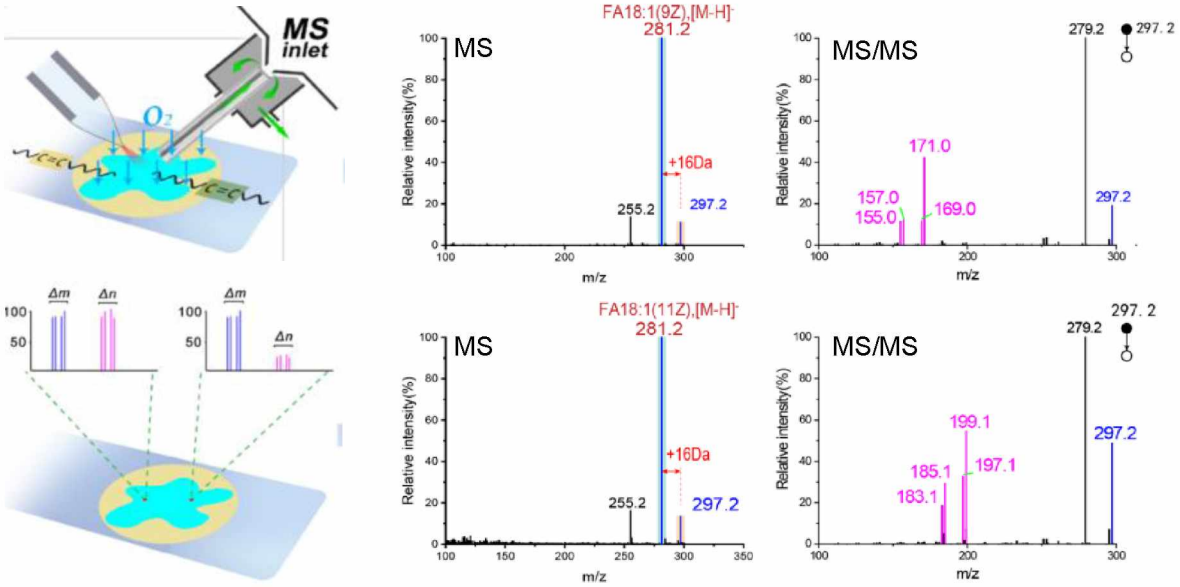

Fig. 51: Set up of AFADESI with MS/MS analysis of two isomers of FA 18:1 (modified from [609]).

A novel, online and selective photosensitized oxidation of C=C bonds induced by singlet oxygen ($^1O_2$) coupled to CID-MS/MS has been proposed to distinguish positional isomers based on the formation of unique lipid hydroperoxide products (neutral losses) generated promptly after laser irradiation. Characteristic neutral losses arise from cleavage at the location of the hydroperoxide group of the respective lipid hydroperoxide, which was produced by the interaction of unsaturated lipids with $^1O_2$ (**Fig. 52**) [610].

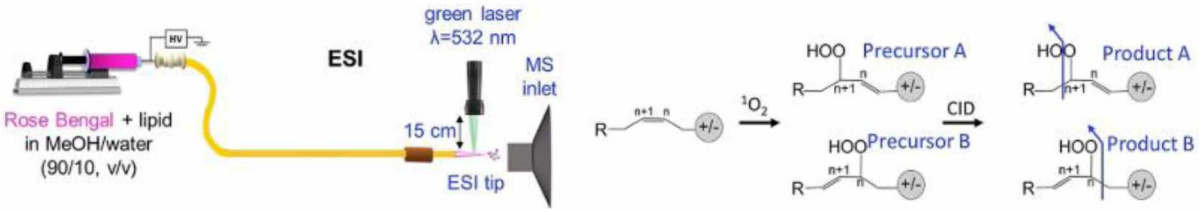

Fig. 52: Schematic depiction of the oxidation of C=C bonds in lipids by $^1O_2$ (adopted from [610]).

In summary, CID commonly generates diagnostic ions of the glycan chain, sphingoid base, or N-fatty acyls composition, while more detailed structural information including branching and linkages in the glycan sequence and double bond positions in the ceramide

backbone can rather be determined using more specialized dissociation techniques (*i.e.*, ECD, EDD, ETD, UVPD, RDD, OzID, $^1O_2$, PB reaction, or epoxidation), see **Fig. 53** [65].

Among the above-mentioned strategies, the PB reaction is the most commonly used method to locate C=C positions in both DI-MS and HPLC-MS/MS workflows, although OzID and epoxidation provide much higher specificity. There is also a common concern regarding the use of UV light and ozone in the PB reactions, OzID, and UVPD as these might pose potential health risks. A more detailed description of applications of AIMS techniques utilizing novel ion activation methods in the elucidation of unsaturated lipids can be found in the following reviews [569,580].

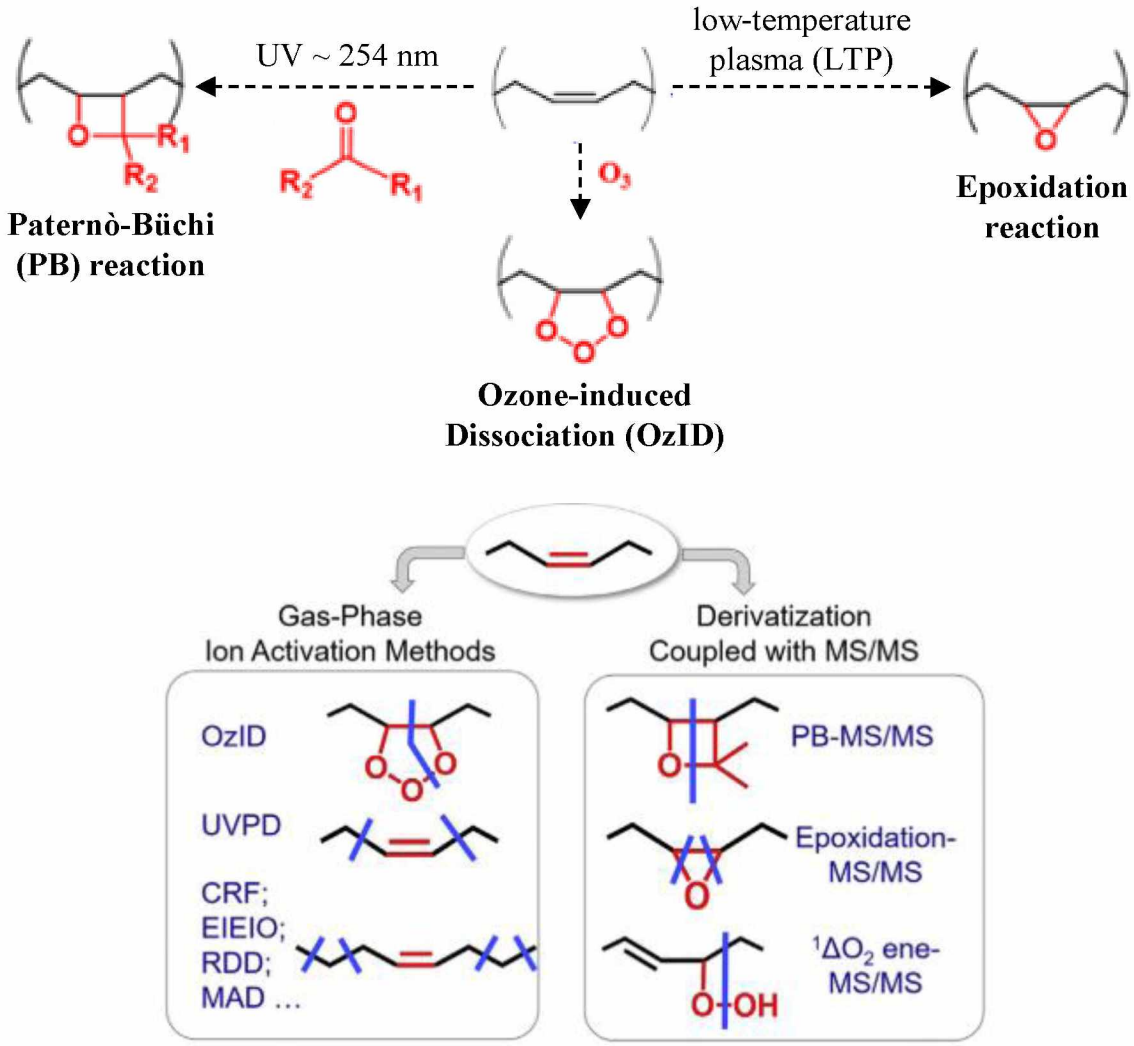

Fig. 53: Approaches utilized for location of C=C bonds in lipids by MS (modified from [569,583]).

1.5.5 Chemical derivatization

Besides LC-MS tools capable of separating isomers and enzymatic digestion utilized for the determination of glycan sequence, linkages, and anomeric configuration in GSL, chemical derivatization of specific functional groups has a great potential to overcome existing analytical barriers in the differentiation of isomeric and/or isobaric compounds to truly comprehensive lipidome coverage [394].

Derivatization in lipidomics serves for two purposes. First, it increases the ionization efficiency of lipids, which is beneficial, in particular, for neutral and heavily glycosylated GSL that suffer from low ionization efficiency. Second, it may allow isomeric separation in combination with UHPLC-MS or IM together with the increased sensitivity either by introducing a specific moiety to scan for selective precursor ions or neutral losses or by incorporating a stable isotopically-labelled moiety for differential quantitation. A great example of such strategy has been applied, for example, to phospholipids [611].

The derivatization reaction should be fast, high yield, precisely controlled, and provide highly abundant diagnostic ions alongside few by-product ions. The reaction device should be simple and convenient without sophisticated MS modifications [603]. Besides decreasing the risk of false identification due to the presence of specific fragments, the derivatization is not as easy as it may seem and can pose a few challenges (*i.e.*, possible contamination or formation of artifacts [361].

A large number of derivatization approaches can potentially be used for the analysis of a variety of lipids, including FAs [612–617], GPs [618–623], GLs [624–626], STs [581,627,628], and SPs. For example, Bollinger *et al.* [612] introduced charge-switch derivatization using N-(4-aminomethylphenyl)pyridinium (AMPP), which has been successfully applied for the analysis of FAs double bond positional isomers providing more than four orders of magnitude improvement in the sensitivity [612,613]. There are also a few modifications of this strategy [614,615] as well as other approaches [616,617]. Furthermore, diazomethane (methylation)-based derivatization approaches, *e.g.*, trimethylation enhancement using ^{13}C-diazomethane (^{13}C-TrEnDi) [618,619] and trimethylsilyldiazomethane (TMSD) [620,621,629], together with 4-(dimethylamino)benzoic acid N-hydroxysuccinimide ester (DMABA-NHS) [622] have been used for the analysis of phospholipids and FAs. One-step *in situ* derivatization of PE and lyso-PE for shotgun lipidomics using 9-fluorenylmethoxyl carbonyl chloride (FMOC-Cl) has been developed by Han *et al.* [623]. Wang *et al.* [624] and Liu *et al.* [625] applied a facile one-step derivatization

approach using N,N-dimethylglycine and N,N-dimethylalanine for differentiation of 1,2-DG and 1,3-DG regioisomers along with Yang *et al.* [626], who utilized acetylation for definitive differentiations of MG. In addition, Liebisch *et al.* [627] established method for simultaneous analysis of cholesterol and CEs using acetyl chloride derivatization. Several other derivatization methods for sterols can be found in the review from Zhao *et al.* [581] along with relatively novel thiyl radical-based method developed by Adhikari and Xia [628]. Reid G. E. and co-workers introduced an ultrahigh resolution accurate mass spectrometry (*i.e.*, mass resolution >100,000 and mass accuracy <1–2 ppm) coupled with the chemical derivatization using d_6-S,S-dimethylthiobutanoylhydroxysuccinimide ester (d_6-DMBNHS). This combined strategy designed for shotgun lipidomics of a wide range of lipids made possible the resolution of both isomeric and isobaric lipids [630,631].

Since this thesis is primarily devoted to GSL, derivatization approaches suitable for analysis of sphingolipids and GSL are discussed in more detail below.

A) Permethylation

Tandem mass spectrometry of permethylated GSL, where the active protons in –OH and $–NH_2$ functional groups of GSL react with methyl iodide in alkaline solution (NaOH) of dimethylsulfoxide (see **Fig. 54**), is a powerful tool for rigorous glycan sequence and linkages determination, and ceramide composition due to the formation of specific fragments. However, the data analysis of permethylated GSL may be complicated since GSL may have different numbers of reaction sites [65].

Permethylation can be carried out using both natural and isotope-labelled methyl iodide (*i.e.*, $^{12}CH_3I$, $^{13}CH_3I$, or $^{12}CD_3I$) [65]. When combined, the so-called differential isotope labelling technique is very useful in the quantitation of intact GSL, resulting in up to 20-fold signal enhancement compared to their low sensitivity in the presence of total lipid extracts. It has also been observed that alkaline conditions during permethylation significantly reduced ion-suppressing ester-linked lipids, thus encouraging the usefulness of the permethylation for quantitation of low-abundant GSL in complex mixtures [427]. In addition, the permethylation process enhances hydrophobicity, volatility, ionization efficiency, and sensitivity [361]. On the contrary, the permethylation in NaOH/DMSO is not suitable for pH-sensitive functional groups of carbohydrates (*e.g.*, O-acetylation) or GSL with polysialic acids, as these may be destroyed under these harsh chemical conditions [377].

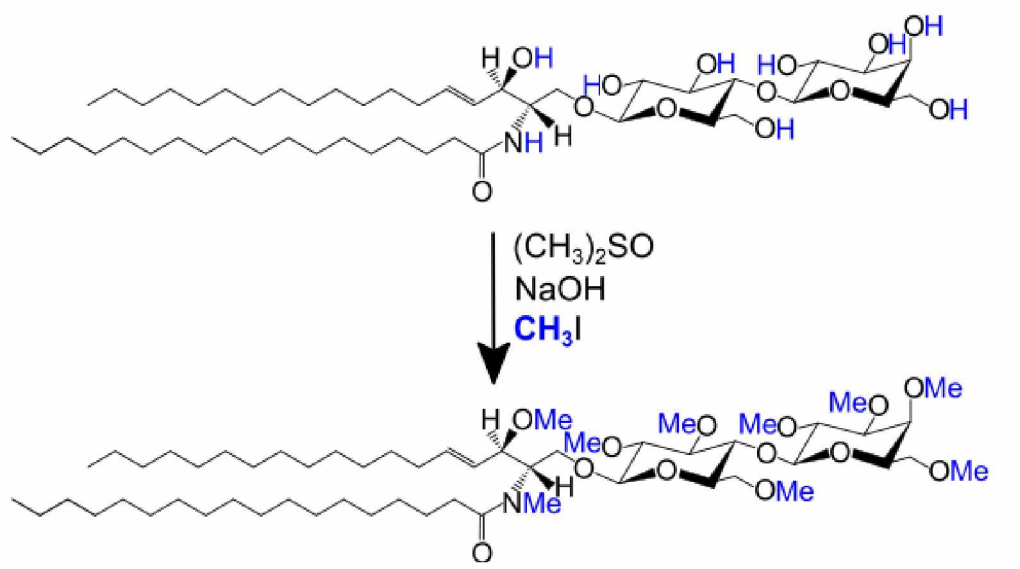

Fig. 54: Example of permethylation process of LacCer 18:1;O2/18:0 (taken from [427]).

The use of permethylation to improve ionization efficiency and structural analysis of GSL in positive-ion mode has been demonstrated [632]. In addition, Ejsing *et al.* reported a shogun-based method for quantitative profiling of long-chain sphingoid bases metabolites by using $^{12}CD_3I$, which significantly enhanced the sensitivity (**Fig. 55**) [633].

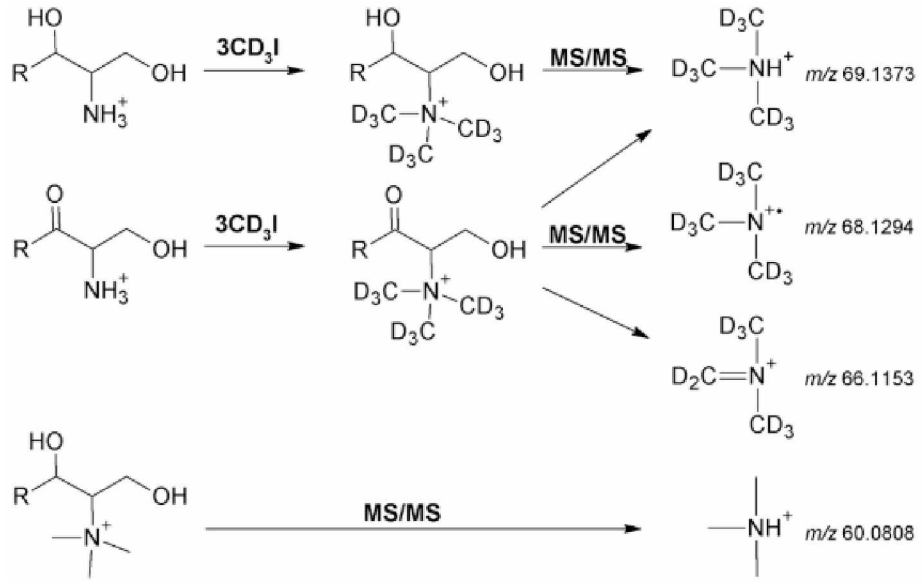

Fig. 55: Methylation of long-chain sphingoid bases using $^{12}CD_3I$ as proposed by Ejsing *et al.* [633].

B) Sialic acid-related derivatization strategies

Acidic GSL, such as gangliosides include a large number of sialyl-linked glycan isomers with α2,3-, α2,6- and α2,8-linked polysialic acids typically on the non-reducing ends of sugars

[634]. Sialylated GSL are commonly analyzed in the negative-ion mode, while they are hard to analyze in the positive-ion mode due to its poor ionization efficiency [635]. Moreover, the treatment under acidic conditions can cleave terminal sialic acids from the oligosaccharide [636]. It should also be stressed that MS cannot fully supply sugar sequence since it has been well-documented that the various sialylated oligosaccharides lose sialic acid during in-source and post-source dissociation, decreasing the sensitivity of molecular ion and dominantly yields product ions lacking sialic acid, representing a major problem in MALDI-MS analysis of sialylated GSL [636,637].

Therefore, distinct chemical derivatizations methods of sialic acids, *e.g.*, esterification [636], amidation [637], permethylation [638], or perbenzoylation [639] have been developed to stabilize the sialylated residues and to improve ionization efficiency of acidic GSL in positive-ion mode. This modification allow highly sensitive and simultaneous identification of both neutral and acidic GSL without ion mode switching, especially for gangliosides with more sialic acids [635]. As another example, Hanamatsu *et al.* [634] developed method based on ring-opening aminolysis for the discrimination between α2,3 and α2,8-linked sialic acids isomers of GSL-glycan by MS. Liu *et al.* [635] labelled the carboxyl group of sialic acid with an easily ionizable tertiary amine, *i.e.*, N,N-dimethylethylenediamine (DMEN), which enhanced the ionization more than 4-fold and provided diagnostic ion to facilitate rapid structural assignments of gangliosides and discrimination of isomers. This strategy was successfully applied for the simultaneous identification of neutral and acidic GSL in human plasma. Moreover, labelling approach using 2-(2-pyridilamino)-ethylamine (PAEA) has been developed by Huang´s group. The method has been applied to plasma using MRM-based LC-MS/MS method, which resulted in 15-fold enhancement of ionization compared to underivatized analogs. However, the derivatization efficiency of PAEA approach was not sufficient, thus only monosialogangliosides (*i.e.*, GM_1, GM_2, and GM_3) were analyzed [640].

C) Isobaric labelling

Isobaric labelling is a relatively novel technique in glycosphingolipidomics, where samples are labelled with isobaric tags consisting of the same molecule with varying placement of isotopes (*e.g.*, ^{13}C and ^{15}N). To date, two versions of commercially available isobaric tags have been applied to GSL: iTRAQ™ (*i.e.*, isobaric tag for relative and absolute quantitation) reacting with free amines [641] and aminoxyTMT™ (aminoxy tandem mass tag) [642] reacting with aldehyde and ketones.

There are also other derivatization strategies that can be used for GSL analysis. Notably, Peterka *et al.* [643] established and optimized a simple, robust, and highly reproducible derivatization of multiple lipid subclasses, including even simple GSL, such as HexCer, using non-hazardous benzoyl chloride. Importantly, Zheng *et al.* [644] developed a highly sensitive method for simultaneous analysis of multiple sphingoid bases using 3-(N,N-dimethylamino)propyl isothiocyanate (DMPI) and its isotopically labelled counterpart (d_4-DMPI). Additionally, naphthalene-2,3-dicarboxyaldehyde (NDA) has been employed for simultaneous quantitation of Cer and Sph [645].

A few other chemical strategies utilized for the elucidation of GSL structures are summarized in **Table 23** as well. The mechanisms of these strategies are illustrated in **Fig. 56**.

Table 23: Summary of chemical oxidation strategies used for the elucidation of GSL.

Strategy	Oxidation of A to B		Ref.
	A	B	
$NaIO_4$ (diluted)	OH group of sialic acid	aldehyde	[646]
DDQ 2,3-dichloro-5,6-dicyano-1,4-benzoquinone	OH group of sphingosine	allyl ketone	[647]
ORNG oxidative release of the natural glycans with NaOCl	glycosidic bond of ceramide	nitrile	[648]

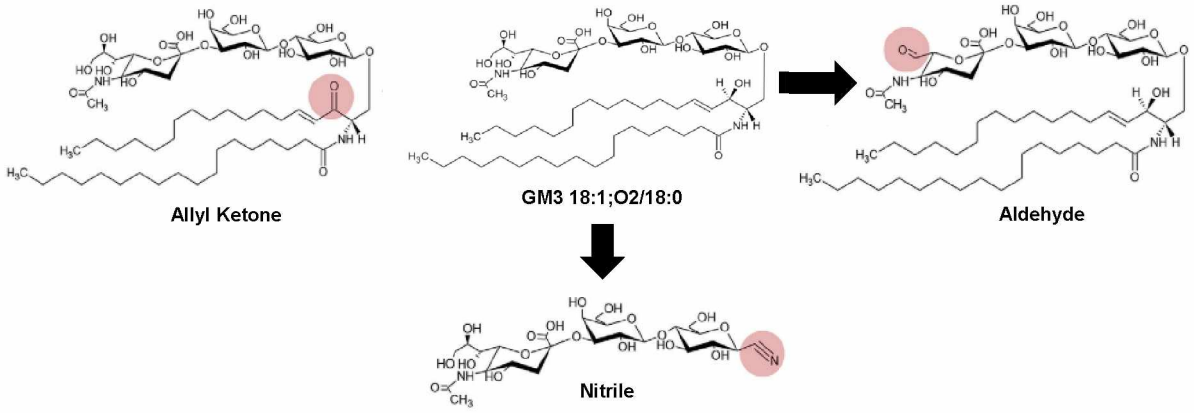

Fig. 56: Illustration of the mechanisms of chemical strategies utilized for GSL (modified from [65]).

More detailed description of chemical derivatization of various functional groups for LC/MS-based analysis of small molecules can be found in the review from Zhang *et al.* [649].

1.6 Quantitative analysis of GSL and other lipids

A major challenge of current lipidomics is to accurately and precisely quantify the lipid species in complex biological samples using appropriate internal standards (ISs) together with standardized annotations and report reliable quantitative results. These issues are crucial to address in order to gain a detailed understanding of functional roles of lipids and to enable a wider acceptance of lipidomics results in various biomarker intra- and inter-laboratory studies [650,651]. Furthermore, due to missing methodological standardization, harmonization, and lack of suitable ISs and reference materials (RMs) providing a sort of quality assurance/quality control (QA/QC), the lipidomic research is challenging and the use of lipid biomarkers in laboratory medicine is limited. This is largely because there are vastly deviated results between various laboratories. Successful inter-laboratory comparisons using appropriate ISs are of utmost importance and will be key to further translating experimental *in vitro* and *in vivo* studies into clinical settings [650,652,653].

1.6.1 Standards and standard mixtures

Standards (*i.e.*, highly pure substances or standard solutions) and their mixtures are generally matrix-free materials with similar or preferably identical chemical structures as naturally occurring lipid species. They are either artificially synthesized or isolated and purified from natural sources. Standard solutions and mixtures are typically premixed in organic solvents [654]. There are 3 major types of standards: (1) endogenous, (2) exogenous, and (3) stable isotopically-labelled (SIL) ISs that are used for both qualitative and quantitative lipidomics (**Table 24**). Nonetheless, SIL ISs are considered ideal and the gold standard for quantitation due to their nearly identical physicochemical properties compared to their naturally occurring endogenous counterparts, nearly replacing the use of endogenous and/or exogenous structural analogues as ISs [655,656]. SIL ISs better mimic their respective unlabeled and naturally occurring lipid species, which is important to ensure similar extraction recoveries, ionization efficiency as well as to correct matrix effect and improve the accuracy and precision of quantitative results [654,655]. However, one should bear in mind that particularly commonly used deuterated ISs can behave differently, sometimes exhibiting slight shifts in retention time or different extraction recoveries [654,655].

Table 24: The characteristics of three major types of standards used in lipidomics [655,657]

Type	Description	Example
Endogenous	Structural analogues naturally occurring in biological samples ***Application:*** qualitative analysis, method optimization	LacCer 18:1;O2/16:0
Exogenous	Structural analogues not commonly found in biological samples *e.g.,* shorter/longer/odd FA chain (C12:0, C14:0, C17:0, C19:0)* ***Application:*** method optimization, validation, quantitation	LacCer 18:1;O2/12:0 LacCer 18:1;O2/17:0
Isotopically-labelled	Synthetic stable isotopically-labelled analogues e.g., ^{2}H (D), ^{13}C, ^{15}N, ^{18}O, ^{31}P ***Application:*** validation, quantitation	LacCer 18:1;O2-d5/15:0

*based on observations that such fatty acyls are not usually found in higher organisms (*e.g.,* mammals) or their endogenous abundance is low (typically <1%)

Moreover, the co-elution of SIL ISs with lipid species can lead to ion suppression or enhancement (details in chapter 1.6.4), which may affect quantitative analysis. Additionally, the use of SIL ISs is very restricted due to the high costs and limited availability, thus structural non-labelled analogues can be useful alternatives in some cases [655].

Although the amount of standards has significantly increased over the past several years, still only a small number of suitable and commercially available SIL ISs are accessible on the market compared to the complexity of the lipidome. Specifically, this issue is multiplied in the case of GSL as only a few SIL ISs are commercially available for simple neutral GSL and some acidic GSL compared to a large number of naturally occurring GSL subclasses. Consequently, the absolute quantitation on a large scale is unrealistic as there are estimated to be between 10,000 and 100,000 distinct lipid species [654]. Moreover, the global quantitative lipidomics in a complex lipidome with thousands of expensive SIL ISs is currently impractical until a suitable stable-isotope labelling method is developed and adopted (more details in the chapter 1.6.3) [658]. The list of currently available endogenous, exogenous and SIL ISs of GSL is summarized in **Table 25**. These standards are readily accessible mainly from the following companies:

- Avanti Polar Lipids (Alabaster, AL, USA, www.avantilipids.com)
- Matreya LLC. (State College, PA, USA, https://www.matreya.com/)
- Cayman chemical (Ann Arbor, MI, USA, https://www.caymanchem.com/)

Table 25: Commercially available standards for GSL analysis, valid as October 31, 2023.

GSL subclass	Endogenous	Exogenous	Isotopically labelled
GalCer	18:1;O2/16:0[a,b,c] 18:1;O2/18:0[a] 18:1;O2/18:0;O[a] 18:1;O2/18:1[a] 18:1;O2/22:0[b,c] 18:1;O2/24:0[a] 18:1;O2/24:1[a]	18:1;O2/8:0[a,b,c] 18:1;O2/12:0[a,b,c] 18:1;O2/15:0[b,c]	18:1-d_7;O2/13:0[a] 18:1-d_7;O2/24:1[a] 18:1;O2/22:0-d_4[b,c] 18:1;O2/18:0-d_{35}[b,c]
GlcCer	18:1;O2/16:0[a] 18:1;O2/18:0[a] 18:1;O2/18:1[a] 18:1;O2/22:0[b,c] 18:1;O2/24:1[a]	18:2;O2/6:0[b,c] 18:1;O2/8:0[a] 18:1;O2/12:0[a] 18:1;O2/17:0[a]	18:1-d_7;O2/15:0[a] 18:1-d_5;O2/18:0[a] 18:1-d_5;O2/18:1[a] 18:1;O2/16:0-d_3[b,c] 18:1;O2/22:0-d_4[b,c]
LacCer	18:1;O2/16:0[a,b,c] 18:1;O2/18:0[a,c] 18:1;O2/18:1[a] 18:1;O2/24:0[a] 18:1;O2/24:1[a]	18:1;O2/8:0[a] 18:1;O2/12:0[a] 18:1;O2/17:0[a,b,c]	18:1-d_7;O2/15:0[a] 18:1-d_7;O2/24:1[a] 18:1;O2/16:0-d_3[b,c]
Ga_2Cer		18:1;O2/17:0[a]	
(i)Gb_3Cer **(i)Gb_4Cer**	18:1;O2/16:0[b,c] 18:1;O2/18:0[b,c]	18:1;O2/17:0[a,b,c] 18:1;O2/17:0[a] (i) 18:1;O2/23:0[b,c]	18:1;O2/18:0-d_3[b,c] 18:1;O2/16:0-d_9[c]
SGalCer	18:1;O2/16:0[b,c] 18:1;O2/18:0[b,c] 18:1;O2/18:0;O[a] 18:1;O2/18:1[b,c] 18:1;O2/24:0[a,b,c] 18:1;O2/24:1[a,b,c]	18:1;O2/2:0[c] 18:1;O2/12:0[a,b,c] 18:1;O2/17:0[a,b,c] 18:1;O2/19:0[a,b,c]	18:1-d_7;O2/13:0[a] 18:1-d_7;O2/24:1[a] 18:1;O2/18:0-d_3[b,c]
SLacCer	18:1;O2/18:0[b]		
GM_1	18:1;O2/16:0[b,c] 18:1;O2/18:0[b,c] 18:1;O2/20:0[a] 18:1;O2/24:1[b,c]	18:1;O2/17:0[a]	18:1;O2/18:0-d_5[a] 18:1;O2/18:0-d_3[b,c] 18:1;O2/16:0-d_9[b,c] 18:1;O2/24:1-d_{18}[b,c]
GM_2	18:1;O2/18:0[b] 18:1;O2/24:1[b,c]		18:1;O2/18:0-d_3[b,c] 18:1;O2/16:0-d_9[b,c]
GM_3	18:1;O2/18:0[a]		18:1;O2/16:0-d_9[b,c] 18:1;O2/18:0-d_5[a] 18:1;O2/18:0-d_3[b,c]
GD_1, GD_2, GD_3	18:1;O2/18:0[a] (GD_{1a})	18:1;O2/17:0[a] (GD_{1a})	18:1;O2/18:0-d_3[b,c] (GD_3)
GT_1, GT_2, GT_3	18:1;O2/18:0[a] (GT_{1b})		
GQ_1	18:1;O2/18:0[b] (GQ_{1b})		

Available from: [a] Avanti Polar Lipids, [b] Matreya LLC, [c] Cayman Chemicals (table do not include lyso-GSL)

The stable isotope is typically introduced in the N-acyl chain of the ceramide (**Table 25**), but it can also be done in the sphingoid base or oligosaccharide head group.

Moreover, new standard mixtures (including deuterated analogues), that qualitatively and quantitatively represent the endogenous lipid subclass distribution in biological samples, have recently been designed and added to the catalogue of the major manufacturers, such as Avanti Polar Lipids, to simplify and permit pre-standardization efforts. These commercial mixtures offer ready and continuous access to qualified and consistent standard mixtures for a particular sample matrix produced with high reproducibility and with well-established stability criteria [372,654] (**Tables 26 and 27**).

On the other hand, mixtures of standards prepared within the laboratory (*i.e.*, in-house standard mixtures) can also provide access to the unique needs of the locally employed methods or where reference materials (RMs) for specific types of sample matrices are not available [654]. These mixtures are generally prepared from a wide range of neat chemical standards available within the laboratory making their preparation affordable and adjustable to specific purposes. Thus, the production of novel labelled standards designed for specific lipid subclass, matrices, and/or applications will facilitate future harmonization toward more accurate quantitation [654].

There are also OxysterolSPLASH and Bile Acid SPLASH containing 13 deuterated oxysterol standards and 17 deuterated bile acids, respectively. Additionally, The Lipidyzer^{TM} platform kits (https://sciex.com/br/products/consumables/lipidyzer-platform-kits) designed to simplify tuning and allow the method validation and normalization of quantitative results have been developed by SCIEX in collaboration with Avanti Polar Lipids and Metabolon. Particularly, the ISs mix contains over 50 deuterated ISs covering 13 lipid subclasses (*i.e.*, PC, LPC, PE, LPE, SM, DG, TG, FFA, CE, Cer, dHCer, HexCer, LacCer) mimicking the natural composition of human plasma [654].

Table 26: Commercially available standard mixtures designed for lipidomics (Avanti Polar Lipids).

	SPLASH Lipidomix I	SPLASH Lipidomix II	Equi SPLASH	Ultimate SPLASH	Light SPLASH	MSI SPLASH	Mouse SPLASH
Solvent	MeOH	MeOH	MeOH	DCM:MeOH (1:1, v/v)	MeOH	Powder	DCM:MeOH (1:1, v/v)
Type	Deuterated	Deuterated	Deuterated	Deuterated	Unlabelled	Deuterated	Deuterated
Number of subclasses	14	12	13	15	13	13	14
Number of ISs	14	12	13	69	13	13	14
Amount	Variable	Variable	100 µg/mL	Variable	100 µg/mL	Variable	Variable
Application	Human plasma*	Human plasma*	Calibration curve generation	Human plasma*	Calibration curve generation	Neurologic tissues (brain)	Mice plasma or tissues
Product No.	330707	330709	330731	330820	330732	330841	330710
PC	✓	✓	✓	✓ (5)	✓	✓	✓
PE	✓	✓	✓	✓ (5)	✓	✓	✓
PS	✓	✓	✓	✓ (5)	✓	✓	✓
PG	✓		✓	✓ (5)	✓	✓	✓
PI	✓	✓	✓	✓ (5)	✓	✓	✓
PA	✓					✓	✓
LPC	✓	✓	✓	✓ (3)	✓	✓	✓
LPE	✓	✓	✓	✓ (3)	✓	✓	✓
LPS				✓ (3)			
LPG				✓ (3)			
LPI				✓ (3)			
Plasm-PC		✓					✓
Plasm-PE		✓					✓
MG	✓		✓		✓		
DG	✓	✓	✓	✓ (5)	✓		✓
TG	✓	✓	✓	✓ (9)	✓		✓
SM	✓	✓	✓	✓ (5)	✓	✓	✓
Cholesterol	✓						
CE	✓	✓	✓	✓ (5)	✓		✓
Cer			✓	✓ (5)	✓	✓	
GlcCer						✓	
LacCer						✓	
SGalCer						✓	

** also used for tissue samples*

Table 27: Commercially available standard mixtures designed for lipidomics (Avanti Polar Lipids).

	Ceramide Lipidomix	**Deuterated Ceramide Lipidomix**	**Cer/Sph Mixture I**	**Cer/Sph Mixture II**	**Sphingo SPLASH I**	**Sphingo SPLASH II**	**Sphingo SPLASH III**
Solvent	DCM:MeOH (1:1, v/v)	DCM:MeOH (1:1, v/v)	EtOH	EtOH	MeOH	MeOH	MeOH
Type	Unlabelled	Deuterated	Unlabelled	Unlabelled	Deuterated	Deuterated	Deuterated
Number of subclasses	1	1	5	5	5	1	5
Number of ISs	4	4	10	9	6	4	5
Amount	Variable	Variable	~10 µg/ml	~10 µg/ml	Variable	10 µM	10 µM
Application	Human blood samples	Human blood samples	Sphingolipid profiling	Sphingolipid profiling	Study of Cer metabolism	Study of Sph metabolism	Study of Sph metabolism
Product No.	330712	330713	LM6002	LM6005	330734	330735	330737
Lipid species	Cer C16:0	Cer-d7 C16:0	Sph C17:0	Sph C17:0	dHCer-d7 C13:0	3-KSph C18:0-d7	GlcSph C18:1-d7
	Cer C18:0	Cer-d7 C18:0	Sph C17:1	Sph C17:1	Cer-d7 C15:0	Sph C18:0-d7	GalSph C18:1-d7
	Cer C24:0	Cer-d7 C24:0	Sph-1-P C17:0	Sph-1-P C17:0	GlcCer-d7 C15:0	Sph C18:1-d7	LacSph C18:1-d7
	Cer C24:1	Cer-d7 C24:1	Sph-1-P C17:1	Sph-1-P C17:1	GalCer-d7 C15:0	Sph C18:2-d7	SGalSph C18:1-d7
			Cer C12:0	Cer C12:0	LacCer-d7 C15:0		Lyso-SM-d9 C18:1
			Cer C25:0	Cer-1-P C12:0	SM-d9 C15:0		
			Cer-1-P C12:0	GlcCer C12:0			
			GlcCer C12:0	LacCer C12:0			
			LacCer C12:0	SM C12:0			
			SM C12:0				

1.6.2 Artificial synthesis of GSL and standards

Since GSL are amphiphilic molecules with immense structural heterogeneity, acquiring specific GSL species via isolation and purification from natural sources is very difficult, making their artificial synthesis the most viable option [659,660]. From a synthetic point of view, the direct coupling of glycans to ceramides is extremely difficult, primarily because of the substantially reduced nucleophilicity of the ceramide caused by high steric hindrance (*i.e., the* large size of the ceramide) and hydrogen bonding between the –OH and $–NH_2$ groups in

the ceramide moiety [659]. Although the discovery of bacterial GTFs that are superior to mammalian GTFs (e.g., higher abundance, stability, and substrate range) has significantly enriched the GTFs pool, streamlined syntheses of GSL through their natural synthetic pathways are still beyond our capabilities due to the absence of some key enzymes involved in the ceramide glycosylation, so that glycan–ceramide coupling to access primers required for GTFs-catalyzed glycosylation remains dependent on the chemical synthesis [660]. Consequently, chemoenzymatic synthesis or other rapid, simple, and efficient methods for the synthesis of GSL are highly desirable as they could address the lack of appropriate standards. These reactions can also be adapted for the synthesis of non-natural and more complex glycolipids, which could have useful applications in GSL-related research [659,661].

Notably, Chiang *et al.* reported a viable and straightforward chemoenzymatic method for the synthesis of globo-series GSL, namely Gb_3Cer, Gb_4Cer, Gb_5Cer, Globo H and S-Gb_5Cer [662] along with Globo A, Globo B, and (para)-Forsmann GSL [661]. This strategy uses a lactoside acceptor with a partial ceramide structure (*i.e.*, LacβSph, **Fig. 57**), which represents a common substrate for unique glycan extension via the action of a panel of GTFs in a highly efficient one-pot multienzyme procedure. In addition, the late-stage N-acylation allows the incorporation of various FAs to produce distinct ceramide parts in the GSL molecules to permit easy access to different GSL forms [661,662].

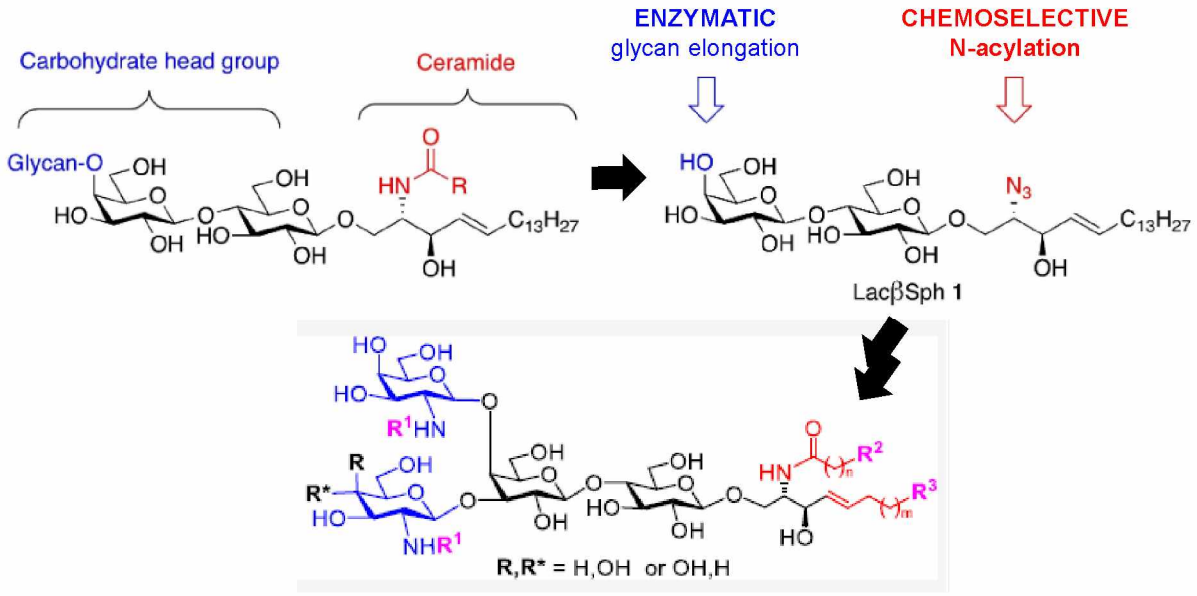

Fig. 57: Retrosynthetic analysis of globo-series GSL (modified from [659,662]).

Remarkably, Rohokale *et al.* [659] established a novel diversity-oriented strategy to prepare GSL and their derivatives using the similar strategy and starting material as in the

works published by Chiang et al. [661,662]. In this strategy, the stepwise elongation of the glycan is achieved via chemical glycosylation and on-site remodeling of the lipid through chemoselective cross-metathesis and N-acylation (**Fig. 57**). Moreover, the formation of lipid part in the diversity-oriented strategies is conducted at the late stage compared to conventional chemoenzymatic synthesis, allowing dual diversification of both glycans and lipids to achieve broader application scope [660]. In contrast, the early-stage incorporation of the FA chains into the ceramide of lactosyl substrate causes solubility issues leading to low glycosylation efficiency, the major reason why smaller lipid groups (*e.g.*, sphingosine) have been ubiquitously adopted in the initial acceptors [660]. Additionally, a detailed overview of the common strategies designed for the synthesis of GSL, including their limitations has been published by Rohokale *et al.* [659] **(Fig. 58)**.

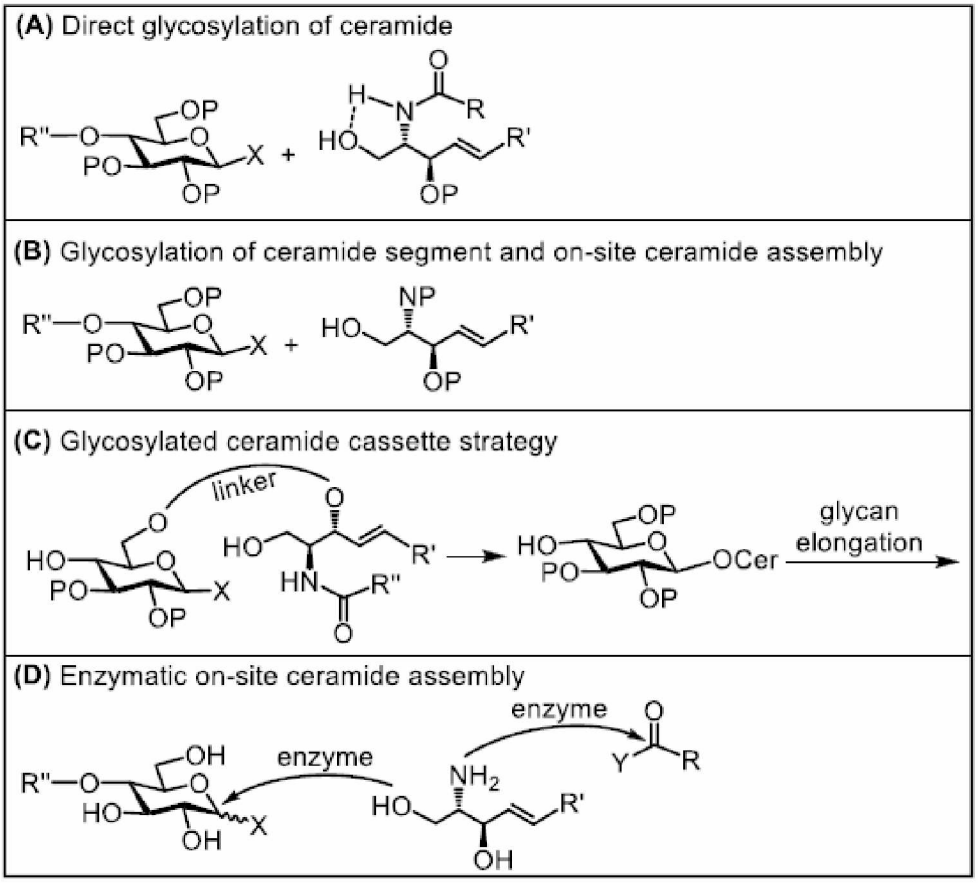

Fig. 58: Overview of common strategies developed for the synthesis of GSL (adopted from [659]).

Last but not least, Mills *et al.* [663] reported the synthesis of deuterated (d_4, d_{47}) ISs composed of C16- and C24-isoforms of GalCer, LacCer, Gb_3Cer, SGalCer, SM and GM_1, GM_2, and GM_3 gangliosides from their respective lyso-forms.

1.6.3 Stable isotope labelling (*in vivo*)

Recently, SIL compounds synthesized *in vivo* have become key for MS-based qualitative and quantitative analysis [652]. For instance, the internal standardization by uniformly ^{13}C-labelled cell extracts was already introduced in 2005 [664]. Over the last decades, libraries of SIL metabolites (^{2}H, ^{13}C, ^{15}N, ^{34}S) have been generated using various organisms (*e.g.,* bacteria, yeast, or plants) growing on labelled growth media or fed with labelled materials. A summary of SIL biomass materials can be found in the work of Rampler *et al.* [652]. More importantly, *in vivo* stable isotope labelling has become a fundamental technique for monitoring metabolic pathways and dynamics [656]. Specifically, Rampler *et al.* [665] introduced lipidome isotope labelling of yeast (LILY), a fast and efficient *in vivo* labelling strategy induced in *Pichia pastoris* to generate a library of ^{13}C-labelled ISs, paving the way for normalization and reliable quantitation in lipidomics. The method is based on growing yeast on a fully ^{13}C-labelled glucose as a carbon source, resulting in almost complete (>99.5%) labelling efficiency of yeast metabolites with the ^{13}C isotope [656]. Jaber *et al.* [666] investigated a comparative study of *in vivo* ^{13}C-labelling strategy to synthesize ^{13}C-labelled ISs in four species, namely *Escherichia coli, Arthrospira platensis, Saccharomyces cerevisae, and Pichia pastoris*. Out of these four species, the *P. pastoris* provided the best match to the human plasma lipidome, thus providing the best source of labelled ISs mixture from tested species for quantitative lipidomics of human plasma samples by isotope dilution.

The biologically generated ^{13}C-labelled ISs mixtures provide a cost-effective and promising alternative avoiding expensive or difficult-to-obtain commercial SIL ISs. Moreover, they can significantly reduce unwanted variations introduced during the lipidomic workflow compared to other normalization approaches (*e.g.,* total ion counts, deuterated ISs mixtures). Although fully-labelled ISs mixtures have limited coverage of the mammalian lipidome, this strategy could eventually be applied to a variety of mammalian samples and compensate for the lack of available SIL ISs. It should also be noted that batch-to-batch variability may occur in any biosynthesized lipid mixture, therefore, a sufficient amount of material should be produced to meet the requirements of any lipidomics study [666].

Despite the great advances in GSL synthesis that have allowed the successful synthesis of a number of GSL using various target-oriented strategies (*i.e.,* synthetic method adapted to the preparation of specific GSL of interest), GSL synthesis and access to GSL and related derivatives remain a significant challenge [659,660].

1.6.4 Relative and absolute quantitation

Depending on the nature of the analyte and the biological matrix (*i.e.*, authentic, surrogate, artificial, *etc.*), different quantitation strategies can be considered to estimate the analyte concentration–response functions, in particular the analytical calibration [667]. The amount of lipid species in MS-based studies can be determined using relative, semi, and absolute quantitation. Relative quantitation is performed by analyzing the sample before and after an alteration or compared to a control situation, such as degradation (*i.e.*, measuring differences between sample groups – intensity fold change, **Fig. 59A**). In semi-quantitative analysis, the calibration function is established using standards similar to the analytes of interest or other matrices comparable to one of the study samples (*e.g.*, neat solutions, artificial matrices). The instrument response is then converted into concentration using another reference (**Fig. 59B**). Finally, absolute quantitation relies on the use of authentic ISs and matrix to construct the calibration function from which concentrations are back-calculated, and requires proper standardization and method validation (**Fig. 59C**) [652,667].

The relative quantitation approach is useful and common for biomarker discovery and readout after treatment or stimulation, but nowadays, lipidomics is progressing towards absolute quantitation, as it is critical to elucidate the biochemical mechanism(s) responsible for changes in order to discover corresponding biomarkers [658] based on the comparison of reported lipid species concentrations of the cellular lipidome of interest against the consensus values [668]. The overview of relative, semi, and absolute quantitation is shown in **Fig. 59**.

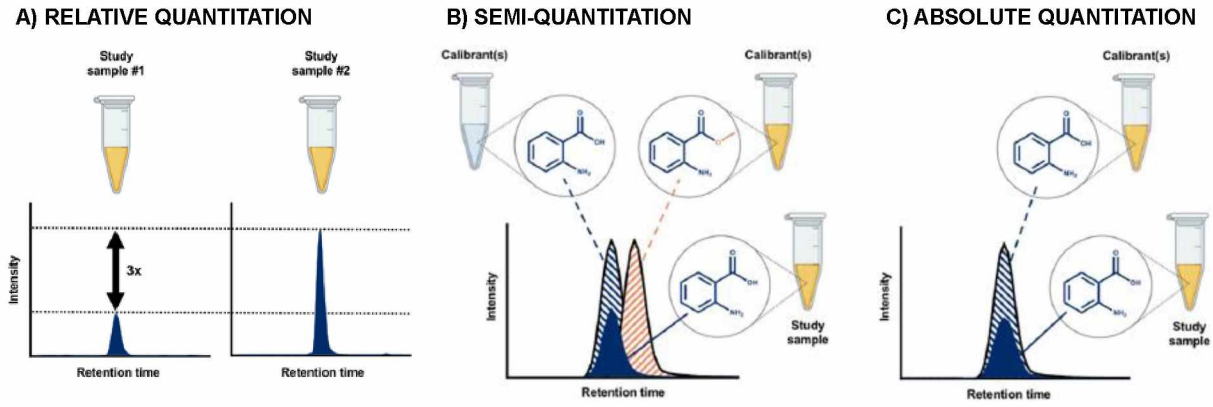

Fig. 59: Overview of **(A)** relative, **(B)** semi, and **(C)** absolute quantitation approaches (modified [667]).

The calibration function can be constructed as the external calibration (EC, *i.e.*, out-sample), which uses only one calibration curve that can be used for many study samples. Conversely, internal calibration (IC, *i.e.*, in-sample) is performed directly on the study

samples, thus, one calibration curve is obtained for each sample. EC can implement different configurations (discussed in more detail here [667]) depending on the availability of an analyte and matrix: (a) authentic analyte in authentic matrix, (b) authentic analyte in surrogate matrix, (c) surrogate analyte in authentic matrix, and (d) surrogate analyte in surrogate matrix.

In contrast, IC relies solely on the availability of the analyte (authentic or surrogate) as there is no choice of matrix. The standard addition method is one of the most commonly used IC methodology in analytical chemistry, where the study sample is divided into identical aliquots and the calibration curve is obtained by spiking of known amounts of authentic analyte at various concentrations covering the expected concentration range of endogenous species. Nonetheless, this approach is quite impractical in high-throughput lipidomics for several reasons: (1) limited availability of authentic standards, (2) limited availability of sufficient sample quantity, (3) method is time-consuming due to the need to prepare multiple samples, and (4) multiple additions at different concentration levels are required as the levels of the lipids in biological samples vary widely [667]. A summary of ISs-based quantitation established in lipidomics and metabolomics is shown in **Table 28**.

Table 28: Established ISs-based quantitation strategies [652,667].

Authentic ISs		**Surrogate ISs** (SIL ISs or exogenous ISs)	
Fully labelled ISs (compound specific)	**Partially labelled ISs** (compound-specific)		
Isotope dilution One-point calibration	**Isotope dilution** (multiple linear regression)	**Multi-point calibration**	**One-point calibration**
+ high potential for accuracy	+ potential for accuracy	+ reduced number of ISs	
- high number of species specific ISs		- cannot compensate for differences in ionization and extraction recovery	

One-point calibrations are estimates that are based on the comparison of peak intensities of an analyte and the corresponding IS multiplied by the concentration of the IS [669]. Thus, fully validated concentrations can only be obtained by using of calibration curves with authentic and isotopically-labelled ISs [651].

Isotope dilution using a known amount of fully or partially labelled ISs represents a method of high metrological order. Nevertheless, in the absence of compound-specific ISs, surrogate ISs (*i.e.*, structurally similar and isotopically labelled or non-endogenous ISs) can

be used. Surrogate calibration is also accepted in lipidomics, provided that the lipid subclass co-ionize with the ISs and the use of response factors is ensured [652].

When using SIL-ISs as surrogate calibrators, the potential presence of interference with endogenous species must be investigated. Two methods can then be considered (**Fig. 60**). The first one, called isotopic pattern deconvolution, is considered when partially SIL-ISs are used and the contribution from SIL-ISs is observed in the MS signal (*i.e.*, overlapping isotopic envelopes). This approach is based on the alteration of the natural isotopic pattern with an enriched isotopically-labelled analogue. It is typically used by chemical manufacturers to calculate the isotopic enrichment and purity of SIL-ISs. The second one, called direct internal calibration, is considered when the fully SIL-ISs are used together with the absence of significant interference from the SIL-ISs. In this approach, which is one of the most promising methodologies in modern absolute quantitation based on LC-MS, the authentic analyte and the surrogate calibrant are measured together in the study sample and the analyte concentration is obtained directly from their area ratio [667]. A more detailed discussion of the quantitative strategies can be found in the following reviews [652,667].

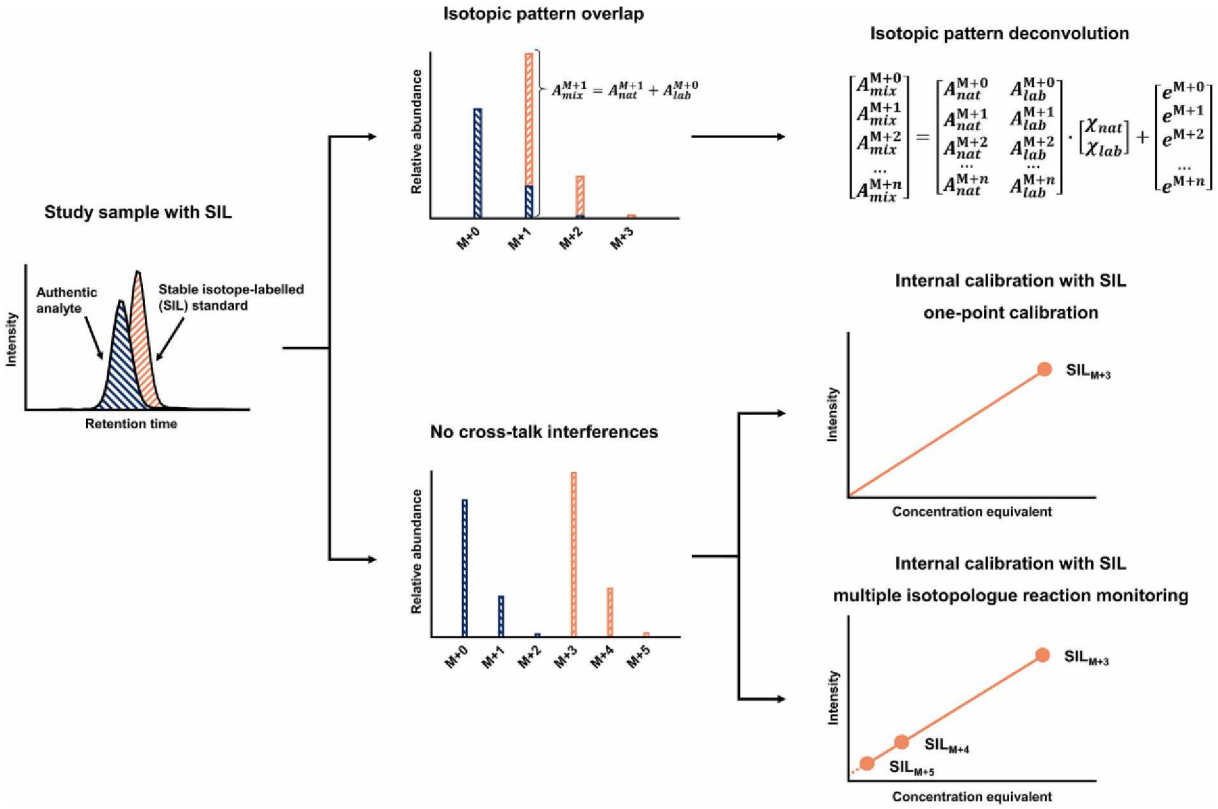

Fig. 60: Principle of isotope pattern deconvolution and direct internal calibration (modified [667]).

A useful tool for predicting isotope distributions from chemical formulae as well as their combination can be calculated using either IsoPatrn© software [670] or web-based platform called enviPat (https://www.envipat.eawag.ch/index.php).

In lipidomics, the most commonly used quantitation approach is internal standardization of external calibration using authentic SIL-ISs. Multi-point external calibration at the working range is used and defined by lower limit of quantitation (LLOQ) and upper limit of quantitation (ULOQ) based on the natural abundance of endogenous species. In addition, other external calibration strategies could meet the recommendations of widely accepted (bio)analytical method validation guidelines, as long as they properly employ internal standardization [652]. Before drawing biological conclusions and evaluating the clinical perspectives of newly discovered lipidomic signatures, it is important to know the normal levels of lipid subclasses and lipid species, including the ranges of their variations (**Fig. 61**).

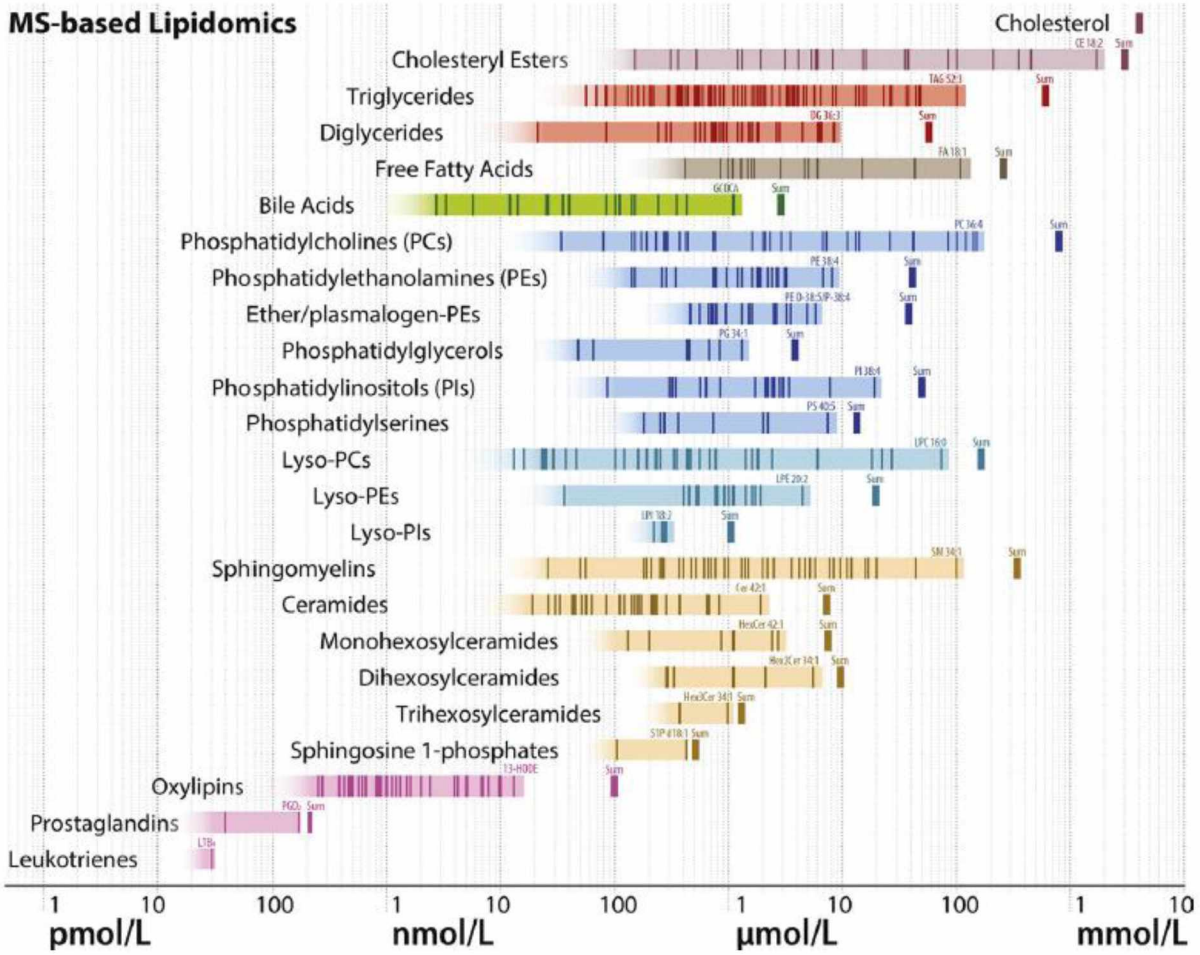

Fig. 61: Estimated ranges of molar concentrations of lipid subclasses (colored horizontal bands) and individual lipid species (vertical lines) within lipid subclass based on the inter-laboratory comparative analysis of reference human plasma (NIST SRM 1950) (adopted from [671]).

It should also be considered whether the corresponding lipid species are observed in similar concentrations in other pathophysiological contexts, as many lipids have no apparent direct link to disease pathophysiology [668]. Furthermore, care must be taken when using pooled matrices, as concentrations may vary due to intra- and inter-sample variation, potentially leading to variable results [667]. In addition, the abundances of lipids and other metabolites may be related to the abundance of proteins involved in their metabolism [668].

It is also worth mentioning the use of differential isotope labelling by permethylation for the relative quantitation of intact neutral GSL analyzed using RPLC-MS. In this strategy, each individual sample and a pooled sample are permethylated using $^{12}CH_3I$ and $^{13}CH_3I$. The ratio of the peak areas between the ^{12}C- and ^{13}C-labelled GSL serves as a measure of their relative concentrations. This method could also address the lack of SIL IS by using a pooled ^{13}C-labelled sample serving as an omnipresent internal standard. Permethylation has been shown to increase the ionization efficiency of neutral GSL, while significantly reducing the analytical background by eliminating highly abundant ester-linked lipids (*e.g.*, GPs, GL). This is advantageous when analyzing particularly low abundant GSL, whose ionization may be suppressed by better ionizing phospholipids when they co-elute [427].

Requirements for ISs

The best practice in quantitative lipidomics involves the use of series of multiple ISs spiked into all study samples, ideally at the earliest stage of the sample processing. This helps to control the variability in extraction recoveries, ionization, fragmentation, and matrix effects [669]. The main criterion for the selection of ISs is the absence or very low abundance (*i.e.*, << 1% of the most abundant lipid species within the lipid subclass) of planned ISs in the study sample. This is particularly important when using non-labelled ISs. Additionally, the selected ISs should not overlap, or at least overlap as little as possible (<1%), with the endogenous lipid species to minimize the effect on the ionization. These conditions must be pre-determined by analyzing lipid extract without ISs [372,658]. It is also necessary to assume that the behavior of ISs is representative of each analyzed lipid subclass [654].

Number of ISs

The quantitation requires at least one non-endogenous IS per lipid subclass, but ideally, two or more ISs eluting at different times (*i.e.*, covering the whole FA chains heterogeneity) would be more appropriate for reliable quantitation [650,658]. Generally, one IS per lipid subclass is sufficient for polar lipid species as their ionization efficiency is predominantly

dependent on the inherent charge of the polar head group and only slightly affected by structural modifications in FA chains [658]. In contrast, neutral lipids are substantially affected by the number of carbon atoms and double bonds in their FA chains as they often span a greater range in terms of FA chains, thus three or more ISs are required to efficiently cover a wide range of FA chains heterogeneity [672]. Consequently, the structure-response relationship within and in between each lipid subclass should be bear in mind as it vary to a certain extent [651,658]. Moreover, the signal response of lipid species also vary markedly based on the composition of solvent at the time of ionization. The instrument responses for both saturated and unsaturated phospholipids decrease with the increasing FA chain length [669]. These issues can be addressed by the application of response factor models (*e.g.,* type I and II isotopic effects, see chapter 1.6.5).

Lipids are typically quantified using either DI-MS, where lipid subclasses are separated based on a characteristic scan event (*i.e.,* precursor ion or neutral loss scans) or lipid subclass separation approach (*e.g.,* HILIC-MS or SFC-MS), where all native lipid species within particular lipid subclass co-elute and co-ionize with ISs guaranteeing the same or comparable and matrix effects originating from the same or similar solvent composition during ionization [372,654]. Therefore, HILIC is believed to be best suited for lipidomic quantitation [673] (**Fig. 62A**). Conversely, the use of RPLC-MS approach provides superior lipid species separation based on the differences in FA chains, however, the co-ionization of ISs and analytes from particular lipid subclass does not follow the logic of HILIC (**Fig. 62B**), thus, such approach should be avoided whenever possible until the suitable SIL method is developed [372,674]. Nevertheless, RPLC-MS has to be used in the case, where the separation of several isomers (*e.g.,* oxylipins [675] and oxysterols[676]) is required [372]. Similarly, 2D-HPLC poses the same issues since the first mode typically resolves lipid classes (HILIC or NPLC), while the second mode separate lipid species (RPLC) or provide specific interactions [465,468].

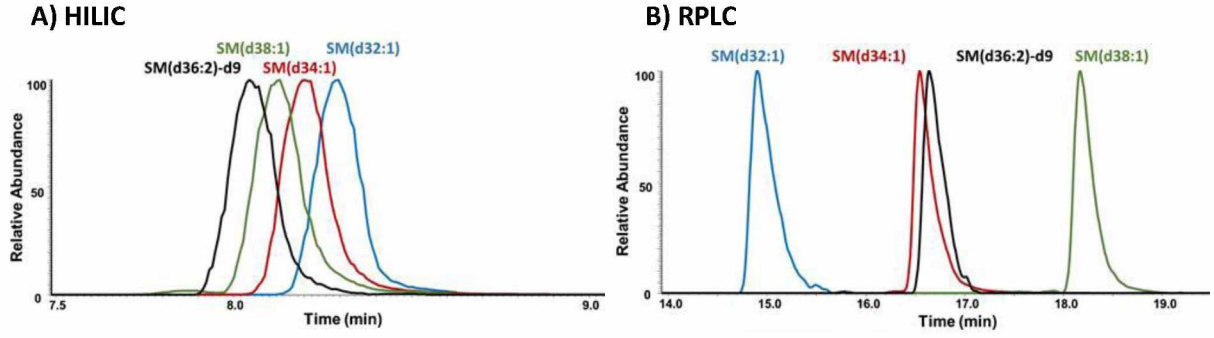

Fig. 62: Quantitation using **(A)** lipid class (HILIC) and **(B)** lipid species (RPLC) approach [673].

Effect of amount of ISs

Precise and accurate quantitation of lipids also relies on the use of an appropriate amount of ISs correlating with the physiological values of the endogenous species (**Fig.63**), as too much or too little amount of ISs can lead to large experimental errors [650,658]. If too much ISs is added (**Fig. 63A**), the ionization of endogenous lipid can be suppressed, eventually hindering the quantitation of low-abundance species. If too little ISs is added (**Fig. 63B**), then the ionization of SIL IS can be suppressed by endogenous species and any small error caused by ISs will be amplified [658,667]. Consequently, it is generally recommended to optimize the added amount of ISs to make the relative intensity of the ISs peak close to mid-point (*i.e.*, 30–50% (**Fig. 63C**) compared to the ion peak that corresponds to the most abundant lipid species in the lipid subclass. Accordingly, the optimal amounts of ISs needed for quantitation can vary widely between various types of samples [658]. In addition, care must be taken when selecting ISs as the chemical impurities from SIL ISs become relevant when the concentration is close to upper limit of quantitation [667].

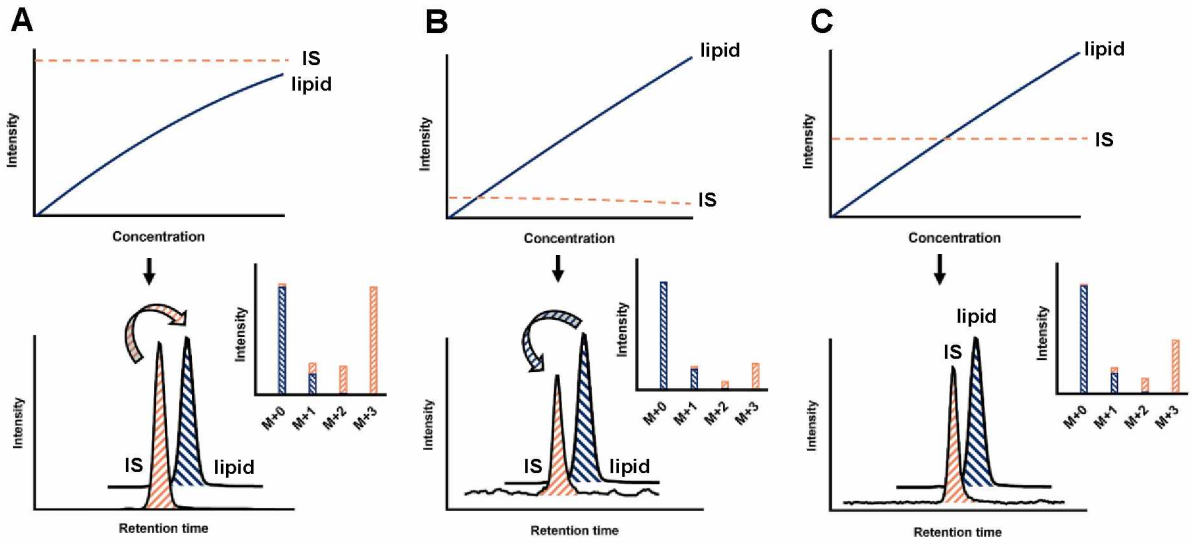

Fig. 63: Effect of added amount of ISs on quantitation (modified from [667]).

1.6.5 Type I and II isotopic effects

Type I isotopic effect is caused by the natural abundance of ^{13}C atom. The intensity of M+0 isotopolog relative to the summed ion intensity of all isotopologs M+0, M+1, M+2, *etc.*) decreases with the increasing number of carbon atoms [651,673,677]. This effect can be simply corrected based on the calculated isotopic pattern or by extrapolating the peak

intensities for the corresponding isotopolog based on the number of carbons in the molecule, natural abundance of ^{13}C, and the intensity of the monoisotopic mass [673].

Type II isotopic effect is caused by DB series within a lipid subclass leading to the overlap of isotopic envelopes of lipid species differing in one DB numbers (*i.e.*, overlap of M+0 and M+2 isotopologs. Moreover, isobaric peak overlap may also occur between lipid species from different lipid subclass, whose isotopologs overlap with the isotopologs of the other lipid [651,677]. This effect can be corrected by subtracting the calculated peak area of the M+2 isotopolog from the M+0 isotopolog. Such correction is only needed when two lipid species differing in one DB cannot be chromatographically resolved, such as in HILIC. When using LRMS, this effect is typically corrected by calculating isotopic patterns, while HRMS with Orbitrap or ICR can resolve this isobaric overlap due to sufficient resolving power [673].

For example, some natural GSL, such as GM1 gangliosides have a large molecular weight and a high ^{13}C isotope abundance up to the M+5. Here, the GM1 gangliosides have their natural M+3 isotope very abundant as well as having almost the same mass as its d_3-labeled IS, thus the overlap can contribute to the variability in the deuterated IS and can negatively impact quantitation. Thus, d_9-labelled IS might overcome this issue because it does not interfere with natural isotopes of GM1, however, the physicochemical properties may differ slightly due to the high degree of deuteration as mentioned above.

1.6.6 Method validation

Bioanalytical methods must meet strict requirements to provide accurate and precise results. Method validation is a fundamental process to confirm that the quantitative results obtained for an analyte in a certain biological matrix using the developed method are reliable [678,679]. There are three types of validation that are summarized in **Table 29**.

Table 29: Summary of three types of method validation [678].

Type of validation	Applicability
Full	Newly developed bioanalytical method
Partial	Modification of already validated bioanalytical method (*e.g.*, change in sample processing, sample matrix, calibration range)
Cross-validation	Two or more bioanalytical methods are used within the same study

In addition, the depth of method validation can be limited when addressing research questions based on semi-quantitative results. However, the full method validation in accordance with regulatory requirements is an indispensable part of any quantitative clinical trial [651]. Method validation in bioanalysis is regulated by approved authorities (**Table 30**) who have issued guidelines detailing every aspect of method validation, including definitions and criteria. Although the key parameters are similar, these guidelines differ in experimental design and evaluation approaches [494]. Full method validation should include: linearity (calibration curve), accuracy, precision, selectivity, stability, recovery rate, carry-over, dilution integrity, repeatability, robustness, limit of detection (LOD), limit of quantitation (LOQ), and matrix effects [494,678]. Although the full validation has not been frequently applied in lipidomics, the situation is changing due to several harmonization efforts.

Table 30: Method validation guidelines from approved authorities.

Authority	Guideline	Ref.
EMA European Medicines Agency	Guideline on bioanalytical method validation	[680]
FDA Food and Drug Administration	Bioanalytical Method Validation: Guidance for Industry	[681]

Important note: ICH guideline M10 published on July 2022 has formally replaced the previously enforced EMA guideline and should be used in all method validations without exception as of the date of coming into effect on 21 January 2023.

The individual parameters required by various authorities along with acceptance criteria are summarized in the following works [494,678,682]. To date, there are still no standardized guidelines for the lipidomic workflow including the entire process along with a variety of commercially available MS instruments from various manufacturers with different instrumentation settings. Taken together, these issues may have a significant impact on the quantitative results and currently represent a major limitation in translation of lipidomics into clinical practice [650]. Over the last few years, several lipidomics communities devoted considerable effort towards the standardization that should allow reproducible and reliable interlaboratory comparisons independent on the MS platform used to address the discrepancies not only in confidence of structural assignments but also in quantitative results, and to raise transparency and overall quality of published data [650,651,674].

Although the standardization is currently underway, community-wide harmonization efforts were focused more on broadly defining the lipidome rather than on harmonizing

lipidomics workflow [654]. Thus, common problems of improper annotation of lipid species, misidentifications, and over-reporting among others will continue until the minimal guidelines have been published and implemented into the lipidomic workflows [674].

Specifically, Köfeler *et al.* [677] have pointed out that exclusive reliance on software-assisted lipid assignments without an independent inspection of MS spectra has a significant impact leading to over-reporting, potentially misguiding other lipidomics laboratories. Nowadays, guidelines and recommendations for interpreting and reporting lipidomic data in order to reduce potential experimental errors have been provided and refined as a result of collaboration of lipidomic communities including the International Lipidomics Society (ILS, https://lipidomicssociety.org/), the Lipidomics Standards Initiative (LSI, https://lipidomics-standardsinitiative.org/), and LIPID MAPS [651].

As a consequence, continuous efforts leading to the standardization of lipid workflows and definition of the minimum of quality requirements are of paramount importance to provide reliable and accurate quantitative readouts as well as to translate lipidomics into a high-throughput clinical settings [653,673].

1.6.7 Reference materials

Reference materials (RMs) are standards with certified values and/or consensus estimates that should be incorporated into routine lipidomic analyses as quality assurance (QA) and quality control (QC) samples to reduce variances and allow a comparability of lipidomic results [654,683]. RMs are critical tools that serve as benchmarks for the determination of lipid concentrations in various biological matrices when measured in parallel with study samples, paving the way towards reproducibility and most importantly inter-assay commutability [650,653]. Consequently, QA/QC is key aspect for the data standardization from different instrumental platforms across different laboratories [654].

Biological RMs are typically pooled matrix-based materials derived from natural sources and designed to be representative of the biochemical complexity observed in a particular type of sample. They are frequently used as QC samples. Ideally, these materials should be (1) matrix-specific, (2) inexpensive, and (3) available on a long-term basis [654].

One of the commercially available standard reference materials (SRMs) with certified values for various metabolites designed for the use in lipidomics has been developed by the National Institute of Standards and Technology (NIST) in collaboration with the National Institute of Health (NIH). This RM is called the NIST SRM 1950 Metabolites in Frozen

Human Plasma and is considered a "universal matrix", consisting of plasma from 100 individuals (equal numbers of men and women) between the ages of 40 and 50 years, reflecting the racial distribution of donors in the US population at the time of implementation (more details can be found here https://tsapps.nist.gov/srmext/certificates/1950.pdf) [684,685]. It is routinely used as community-wide quantitative benchmark for intra- and inter-laboratory quality control and analytical method validation [654]. It has also been shown that normalization to commonly available RMs (*e.g.*, the NIST SRM 1950) can largely correct for quantitative biases and significantly improve quantitative data obtained from the same samples across different methods in different laboratories. Nevertheless, one should bear in mind the drawbacks associated with the use of the NIST SRM 1950, such as relatively high cost and limited long-term availability due to extensive use (stocks will run out) [685], which makes its use as a routine and forever-sustained RM material impractical [654].

To meet QA/QC requirements, cheaper and matrix-specific references (*i.e.*, QC samples) can be produced *in-house*. These QC samples represent a pool of aliquots from all study samples with the average abundance of lipid species present in all samples [685].

Alternatively, a flexible and easily adaptable method, applicable to any type of matrix, called iterative batch averaging (IBAT), can be used to produce *in-house* RMs. In IBAT, multiple batches of starting material are produced from a common source of material and homogeneous aliquots from different batches are then pooled into a single tube, containing only small amounts of newly produced material. This allows continuous generation of reference material over time with minor variances [686] (**Fig. 64**).

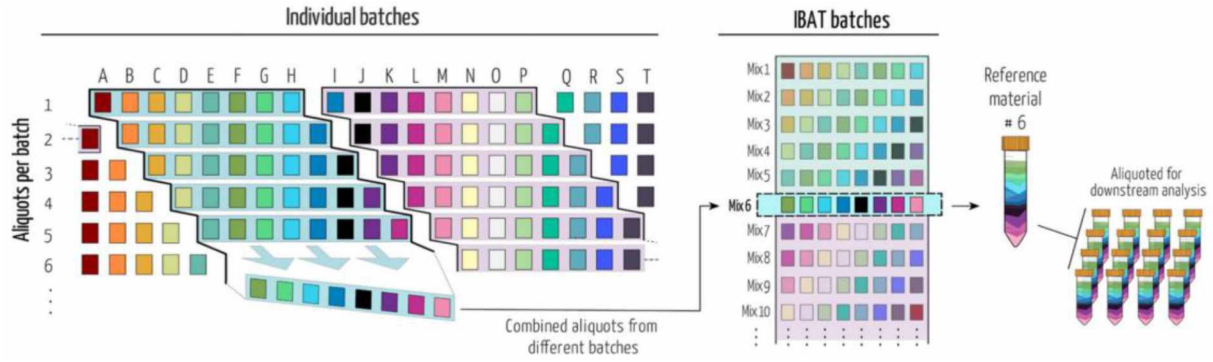

Fig. 64: Schematic illustration of iterative batch averaging (IBAT) process (adopted from [686]).

The unavailability of appropriate and diverse RMs designed adequately for specific applications poses a significant challenge for current lipidomics [683], primarily due to the complexity of the RMs design process, which limits the production of RMs for any common

matrix. Moreover, the limited supply of human tissues amplifies this challenge. To address this issue, NIST has initiated the development of tissue-based RMs specifically for untargeted analysis. In addition, the time and expense of adding metrological traceability increases the cost of RMs, another limitation to the wider harmonization [654]. A summary of available and potential RMs is listed in the **Table 31**.

Table 31: Reference materials (RMs) used in lipidomics and metabolomics [652].

Reference material	Type of sample	Ref.
NIST SRM 1950	Pooled human plasma	[684,687,688]
CHEAR	Pooled human plasma	[688]
Qstd3	Pooled human plasma	
NIST candidate 8231-1*	Diabetic plasma	[683]
NIST candidate 8231-2*	High triglyceride plasma	
NIST candidate 8231-3*	African-American plasma	
Candidate 8462[a]	Frozen Human Liver Suite	Under development (NIST) [654]
Suite of pooled urine[b]	Pooled urine suite	

* candidate RMs means the values has not been certified (*i.e.*, only semi-quantitate analysis)

[a] RM composed of cryogenically homogenized and freeze-dried liver tissues that will be characterized for differential expression of lipids, metabolites and proteins

[b] RM composed of both male and female smokers and non-smokers

1.6.8 Intra- and inter-laboratory comparison

Intra-laboratory and especially inter-laboratory studies, often referred to as ring trials, are useful to assess the differences in lipidomic workflows to validate the overall process and methodology. More importantly, studies utilizing RMs are an effective tool to identify sources of variation or challenges that affect lipidomics results [654].

Inter-laboratory studies

In 2017, Bowden *et al.* [687] initiated and conducted a large-scale international ring trial to compare the lipid concentrations in the NIST SRM 1950. The ring trial was attended by a total of 31 laboratories from all over the world using non-standardized, laboratory-independent lipidomic workflows, and their preferred MS-based methods. As expected, the study revealed significant disparities in the quantitative results and lipid profiles reported by

the participating laboratories, most likely due to the different lipidomic workflows used including the use of different ISs. Besides that, the inter-laboratory comparison included 1,527 unique lipid species and provided consensus mean values with associated uncertainties for 339 lipids in the NIST SRM 1950, including 5 major lipid classes (*i.e.*, FAs, GLs, GPs, SPs, and STs). Nevertheless, GSL, which constitute a large proportion of SPs, are covered by only a few simple GSL species, leaving the more complex neutral and acidic GSL (*i.e.*, sulfatides and gangliosides) unnoticed. Consequently, the use of the NIST SRM 1950 in glycosphingolipidomics is very restricted until a more comprehensive characterization of GSL in the NIST SRM 1950 becomes available.

Another example, Triebl *et al.* [685] have systematically investigated the variability of results using multiple lipidomic approaches considering (1) different sample induction methods, (2) different MS instruments, and (3) inter-laboratory differences in comparable analytical platforms. They demonstrated different quantitative results caused by each of these analytical variables, even with the inclusion of SIL-ISs for individual lipid subclasses.

Furthermore, Ghorasaini *et al.* [653] presented a cross-laboratory comparison using standardized lipidomics protocols that allowed highly reproducible analysis of several hundred of lipids in human plasma across 9 laboratories. They compared two lipid extraction protocols (*i.e.*, MTBE and Bligh-Dyer using dichloromethane instead of chloroform) and incorporated clinically relevant disease-related plasma materials to demonstrate that the harmonized protocols can provide excellent inter-laboratory data. The limitation of this study is that only one experimental platform was use for this comparison.

Intra-laboratory studies

Quehenberger *et al.* [689,690] published a semi-quantitative estimates of lipid concentrations in a widely adopted plasma reference material NIST SRM 1950, identifying and quantifying nearly 600 distinct lipid molecular species within 6 major lipid classes together with their relative distribution (SLs and PKs were not included). This was the first attempt to define the human plasma lipidome, which also indicated that lipids are the major metabolites of human plasma [690].

In 2017, Čajka *et al.* [669] compared 9 different LC/MS-based platforms under identical conditions for human plasma lipidomics in an intra-laboratory study and found highly comparable quantitative results even when different MS instruments were used. Moreover, Lange and Fedorova [673] compared lipidomics workflows for the quantitation of five lipid subclasses (PC, LPC, PE, LPE, and SM) in human plasma based on HILIC- and RPLC-MS

and found out that the concentration determined were comparable for most of the lipids studied, except for highly unsaturated PC. Furthermore, Chocholoušková *et al.* [650] investigated the intra-laboratory comparison of four platforms, including two HILIC and two UHPSFC methods coupled to two different QTOF analyzers, in human plasma.

More recently, Zhang *et al.* [674] developed a multiplexed NPLC-HILIC-QqQ-MS method that allows the quantitation of 900 lipid species from across over 20 lipid subclasses spanning a wide range of polarities in a single 20-minute run, using multiple fragment MRM experiments for each lipid species for deeper information. However, only HexCer and Hex_2Cers were measured in this study, leaving more complex GSL unrevealed or unnoticed.

1.7 Software tools and online resources

Unequivocal identification of diverse lipids is a fundamental challenge and key component of lipidomics studies, which significantly affects the interpretation and significance of analyses aimed at revealing the associations of lipids with underlying cellular mechanisms, understanding their complex interactions as well as highlighting their biological relevance [691,692].

Over the last years, advances in MS-based platforms, mainly improved sensitivity and resolution, have allowed considerable progress in the analyses of lipidomic data, enabling researchers to routinely identify hundreds of unique lipid species in a variety of complex biological samples, an important step to integrate lipidomics MS data into a biochemical or medical context [692,693]. This is evidenced by the increasing number of lipidomic studies that generate extremely large datasets. Nonetheless, manual data processing of these large raw datasets is labor- and time-intensive and represents a significant bottleneck in the analysis of numerous complex biological samples. Therefore, increased efforts and sophisticated solutions to support the automation in the data processing are highly desirable to reduce the bias and burden associated with the extensive manual inspection [693–696]. Although data processing is rather demanding, it represents an important step in keeping the integrity and quality of lipidomic data. Consequently, the automated data processing is required to ensure fast, reliable, and consistent lipid species identification along with the relative or absolute quantitation [372].

To address this issue, numerous commercial, open-source, and in-house software packages have been developed and tailored to enable effective computational processing of the data and automated lipid species annotation based on MS/MS spectra [693,694]. These tools improve the confidence of lipid identifications, enable mutual interconnection of identified lipids with biological knowledge via the use of databases and libraries, and integrate lipidomics data with

other classes of molecules for the cellular and molecular understanding of lipid homeostasis and metabolism [692].

However, these tools face four major issues [677], namely (1) isomeric and/or isobaric lipid species from different lipid subclasses often yield similar fragments, thus do not allow unambiguous identification, (2) the abundance of fragment ions strongly depends on experimental conditions, (3) fragmentation of co-isolated precursor ions originating from different lipid classes often yields highly convoluted spectra, and (4) missing adaptation of standardized nomenclature and reporting.

What is more, current software tools face the major challenge of keeping pace with rapid technological progress as high accuracy and high throughput MS technologies continue to improve and enable more comprehensive characterization of the lipidome [691,693]. Therefore, novel and comprehensive open-source bioinformatics tools are urgently needed to capture the data as well as to facilitate their automated processing [691,692]. Otherwise, the rapidly evolving lipidomics would be slowed down by the scarcity of suitable bioanalytical tools able to handle the big datasets [691]. Care must also be taken as exclusive reliance on annotations by a single software without additional means of validation usually leads to unacceptably high rates of false positive identification, thus, further inspection is indispensable for MS spectra [677]

It should also be noted that most vendors of MS instruments use proprietary or non-standard data formats. These strict formatting requirements do not allow data processing from all MS platforms, thus limiting the possibility of universal use, mutual result comparison, or data exchange [691,693]. The interoperability is also limited or completely prevented by the development of software tools dedicated to specific MS instrument or a preferred MS/MS-based method. For simplicity, developers should publish their source code under an open-source license in publicly available repositories to improve overall data quality [693,694].

To date, numerous freely available bioinformatics tools used in lipidomics have been summarized and described in the following reviews [370,461,695]. Notably, Hoffmann *et al.* [693] recently compiled an up-to-date encyclopedia of bioinformatics tools, data formats, and resources for MS-based lipidomics. This excellent work catalogs in detail freely available software tools, libraries, databases, repositories, and other resources that support lipidomics data analysis including those suited for both targeted and non-targeted analysis together with their brief description. Furthermore, Wolrab *et al.* [694] developed a vendor-independent and freely available script for automated data processing in lipid class separation lipidomics called LipidQuant 1.0, which can be run on every computer with Microsoft Excel. This simple tool

works with *m/z* values and their corresponding intensities in txt tables acquired by any peak-picking software and provides the full flexibility to modify (1) the extent of the embedded lipid database (*i.e.,* the addition of another lipid class, lipid species, or IS), (2) choice of IS (*i.e.,* simultaneous application of up to three IS at various concentrations), and (3) mass tolerance window. Recently, Lin *et al.* [691] developed a highly flexible and user-friendly web-based platform called LipidSig designed for easy and efficient data mining to help the user identify significant lipid-related features in order to advance lipid biology. In addition, Ni *et al.* [695] provided guidance for the appropriate choice of tools and software for lipidomics applications as well as evaluated the data processing pipelines.

Despite the current evolution and ever-increasing interest in IM-MS technology, only a few software tools are available, reflecting the still restricted adoption of ion mobility as well as software support. Indeed, only two free and open-source software tools (*i.e.,* Skyline and MS-DIAL) are capable of performing a complete analysis of IM-MS lipidomics data, emphasizing the software pool for data analysis by IM-MS is surprisingly insufficient [696]. Notably, Ross *et al.* [696] provided a survey and in-depth evaluation of two essential bioinformatics software tools for IM-MS analysis of lipidomics data utilizing total lipid extracts from NIST 1950 SRM plasma. They also highlighted the identification discrepancies between the two software tools that are likely attributed to (1) a lack of coverage for some lipid subclasses in the internal (reference) databases, (2) the specific difference in data extraction and processing, and (3) biases introduced through the manual inspection of results by the user. Specifically, the latter two factors are often less discussed despite their possible significant impact on the reproducibility of the results. It is also possible that the factors contributing to lipid identification (*i.e.,* retention time, isotope patterns, and MS/MS spectral matching) differ between those two software tools. Moreover, Zhou *et al.* [697] have developed LipidCCS Predictor for precise prediction of lipid CCS values from SMILE structures, including database with >15,000 lipids and >63,000 CCS values. The Predictor covers three major categories of lipids, *i.e.,* GPs, GLs, and SPs, and the CCS values are predicted for 5 common adducts, *i.e.,* $[M+H]^+$, $[M-H]^-$, $[M+Na]^+$, $[M+NH_4]^+$, and $[M+HCOO^-]^-$. The prediction precision was externally validated with a median relative error of ~1% across different instruments and laboratories using independent datasets. Nonetheless, there are two major limitations: (1) inability to accurately predict CCS values of isomers differing in position or geometry (cis/trans) primarily due to the missing isomeric lipid standards in the training data set and (2) insufficient resolution of the used IM instrument.

Very recently, [499] summarized characteristics of the current CCS predictive tools and CCS predictive databases, including CCS compendium [698], CCS base [699], and AllCCS [700] together with the list of publications in which CCS values were used for lipid identification.

Another issue is the lack of experimentally obtained reference spectra for MS/MS as in GC/MS, which causes problems when attempting to identify low-abundant analytes. To address this issue, a number of software tools called *in-silico* fragmenters (*e.g.*, MetFrag 2.2, CSI:FinderID, or CFM-ID) employing a more computational approach have been developed over the last decade [370]. Last but not least, Lipid MAPS provides a free MS/MS prediction tool (http://lipidmaps.org/resources/tools/index.php) and the structure database library (http://lipidmaps.org/data/classification/LM_classification_exp.php) allowing data easier data handling in lipidomics.

1.8 Statistical analysis

Statistical evaluation is performed using multivariate data analysis methods. Metabolic correlation and significance analyses of lipids are conducted with a set of visual chemometric tools and statistical methods. Chemometric tools provide an overview of analytes trends and outliers in relationship to their observation using non-supervised principal component analysis (PCA) [372,451]. PCA attempts to flatten a large dataset with multiple variables to find two most important sources of variation (*i.e.*, principal components) that ultimately lead to the differentiation of study compounds into distinct groups[372,701]. Similarly, systematic but uncorrelated variations between lipidome states can be found with partial least-squares regression discriminant analysis (PLS-DA) or supervised orthogonal projection to latent structures discriminant analysis (OPLS-DA), which help to differentiate healthy and diseased groups and to find the most dysregulated lipids, which could be potentially applied as biomarkers for studied disease. PLS-DA seeks to flatten multivariate data to find the most fitting parallel 2D-plane representing the whole dataset, whereas OPLS-DA reduces the dataset to an orthogonal plane found with the partial least square plateau of the dataset [372,451].

PCA, PLS-DA, and OPLS-DA, represent the most common tools used for visualizing analyte grouping (PCA) and metabolic changes (PLS-DA, OPLS-DA), which in combination with the metabolic knowledge highlight certain lipids from others to determine the most viable biomarkers. In addition, the concentration evaluation can be made with boxplots or a heat map visualization for significant outlier detection, analyte interaction, or metabolic interlinkage of lipid species via hierarchical cluster analysis (HCA), often accompanied with heat map analysis,

interactive network, or pathways analysis. The comparison can also be made by using Venn diagrams [461].

1.9 Summary of lipidomics workflow

The lipidomic workflow is a highly complex set of individual steps (**Fig. 65**) that must be performed to achieve reliable quantitation of lipid species in various biological samples. However, each step can introduce unwanted variation that can lead to biased quantitative results. The sources of unwanted variation covering the whole lipidomics workflow have recently been reviewed in detail [702] and are summarized in **Table 32**.

Briefly, most of the unwanted variations from pre-analytical steps can be reasonably captured and dealt with in the subsequent analysis by the addition of ISs immediately after sampling or by the use of QC samples. To maintain the integrity of the sample, flash-freezing in liquid nitrogen is commonly used along with other minor approaches, such as heat treatment, addition of antioxidants or enzyme inhibitors. In addition, the systematic variation may be adjustable if ISs are used and samples are randomized [702].

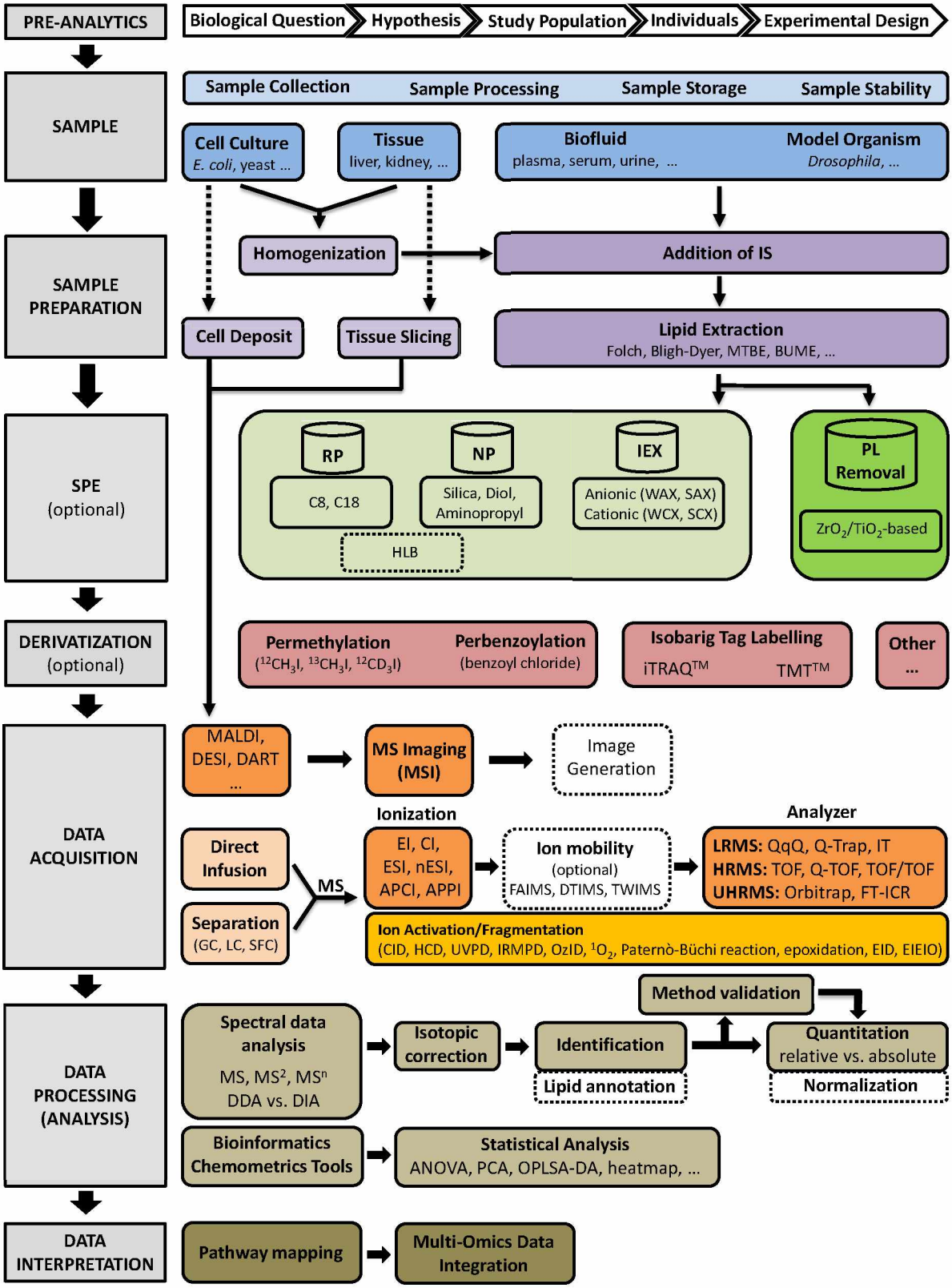

Fig. 65: General scheme of lipidomics workflow.

Table 32: Overview of sources of unwanted variations in lipidomics [702].

Type of variations		Description
PRE-ANALYTICAL	sample-related factors	• type of sample (*i.e.,* tissues, biofluids, and cells) • genotype/phenotype (*i.e.,* gender, age, racial, and ethical factors) • fasting status (*i.e.,* diets, length of fasting) • other factors (*i.e.,* alcohol, drugs, medication, physical conditions – BMI)
	sample collection	• collection centers and/or countries variability • diurnal patterns (i.e., sampling time) • collection tubes (i.e., anticoagulants: EDTA, heparin, citrate) • time-controlled serum coagulation (too short/too long – hemolysis) • plasma vs. serum (reduced matrix effect due to lower protein fraction)
	sample processing	• time spent at room temperature before centrifugation (chemical degradation, enzymatic activity - (per)oxidation or hydrolysis
	sample storage	• storage temperature and time (RT, 4°C (<24h), -20°C, -80°C (>6 months) • storage conditions (temperature fluctuations, freeze-thaw cycles) • lipids stability (hydrolysis, enzymatic activity → degradation)
ANALYTICAL	sample processing	• quantity (biofluids – volume, tissues/cells – wet vs. dry weight) • batch vs. real-time preparation • randomization (+ use of quality control samples) • chemical and oxidative reactions, other spontaneous processes
	sample extraction	• incomplete and/or variable recovery • variable volumes of extraction solvents (equilibrium), solvent strength • poor and insufficient selection of internal standards • relative vs. absolute quantitation
	instrumental variations	• acquisition time (hours, days, weeks, or months) • intra-/inter-day variations (retention time shift, peak area) • signal deterioration (contamination of ion source, ion optics) • detector saturation (decreased sensitivity) • instrumental maintenance (solvent replacement, cleaning, tuning, and calibrating)
	measurement variations	• changes in solvent compositions (signal suppression/enhancement) • different matrix effects (effect of co-eluting compounds and interferents) • instrument response (dynamic range)
POST-ANALYTICAL	peak alignment and integration	• retention time alignment (correspondence of peaks) • peak assignment (isotopes, adducts, dimers, multiply charged ions, fragments) • peak integration
	lipid annotation	• correct annotation (development of software tools for automation) • false positive annotation using only software (inspection required), overreporting • standardized reporting
	imputation of missing values	• variation between imputation methods (impact on data) • substantiating the reason of the missing values (unsuccessful peak alignment, peak picking, and integration, analytical factors, matrix effects, etc.) • prediction of missing values using available signals in the dataset
DATA ANALYSIS	transformation and scaling	• distortion of data and loss of information • impact on downstream analysis (peak area variability – large studies/long runs)
	normalization	• variation between normalization results • success in removing unwanted variations • control features
	control samples	• QC samples – quality assurance (NIST SRM 1950 human plasma)

1.10 Future challenges and prospective

Aberrant expression of specific GSL and related enzymes have been repeatedly associated with the tumor initiation and progression. Consequently, advances in the understanding of how the biosynthesis and turnover of GSL and other lipids regulate cellular function under normal and abnormal conditions will allow the development of a relatively unexploited area of cancer therapy leading to exciting and novel clinical applications.

Despite steady increase in the lipid coverage together with the integration of lipidomics data with other omics disciplines improves our understanding of lipid metabolic pathways and their dynamic changes, we are still far from unravelling and exploiting the particular roles and therapeutic potential of majority GSL, leaving them for future research.

Although recent developments of high-sensitive MS-based analytical platforms represent powerful tools that have boosted lipidomics, there are still a number of limitations restricting the translation of lipidomics into clinical practice that should be addressed in the foreseeable future. Specifically, (1) the separation of multiple isomers can still be difficult despite ion mobility techniques has recently provided the ability to overcome this limitation (*i.e.,* isomers separation issue), (2) LC-MS also suffers from a limited ability to perform high throughput screening, although 96-well plate formats, platforms coupled to robotic systems, and software for automated data processing are becoming available (*i.e.,* automation issue), (3) commercially available ISs for various important lipid subclasses or suitable methods for *in-house* synthesis of ISs are still lacking (*i.e.,* quantitation issue), (4) many lipidomic studies do not follow the same standard operating procedures for collection, storage, and processing of samples including method validation (*i.e.,* standardization issue), and (5) lack of large population-based studies with minimally invasive or non-invasive methods.

One of the major perspectives is to obtain information about the lipid metabolic flow by utilizing stable isotope precursors in combination with MS [703] and the isotopomer analysis [704]. This would allow the localization of specific lipid species during a metabolic process to determine the place where they come from and the way in which they are removed.

2 AIMS

The goal of this work is to provide a broad overview of both neutral and acidic GSL and other lipids together with isolation, purification, and concentration strategies required for their comprehensive identification, structural characterization and in-depth profiling in various biological samples using (U)HPLC-ESI-MS^2. The in-depth GSL and lipid profiling has potential in discovery of novel biomarkers in cancer-related research.

A. Lipid class separation I – characterization of simple GSL

- Described in ***Section 3.1*** and ***Annex A***
- Determination of neutral and acidic GSL using untargeted HILIC-ESI/MS^2
- Optimization of lipid preparation and structural elucidation of GSL and other lipids
- Generation of lipid species profiles in human plasma

B. Lipid class separation II – characterization of complex GSL

- Described in ***Section 3.2*** and ***Annex B***
- Determination of complex GSL using HPLC-ESI/MS^2 on HILIC and PGC columns
- Differentiation of glycan isomers with the use of endoglycoceramidase digestion
- Mutual comparison of GSL profiles of human normal and tumor pancreatic tissues

C. Plasma lipid profiles of three types of cancer (partial contribution)

- Described in ***Section 3.3*** and ***Annex C***
- Differentiation of kidney, breast, and prostate cancer from healthy controls
- Discovery of potential screening biomarkers for kidney, breast, and prostate cancer

D. Review: Analysis of GSL in biological samples (submitted)

- Described in ***Section 3.4*** and ***Annex D***
- Recent advances, challenges and future directions in the analysis of GSL

3 EXPERIMENTAL PART

The experimental part of the thesis consists of the author's published papers and manuscripts, which are put into context. Experimental part, representing a pivotal part of this thesis, is dedicated mainly to a systematic and detailed characterization of neutral and acidic GSL isolated from human plasma and tissues. The strong emphasis is given to structural elucidation, which is accomplished by a combination of various techniques, such as high-performance tin-layer chromatography (HPTLC), chemical staining, carbohydrate-recognizing binding assays (antibodies, lectins, and bacteria), and LC/ESI-MS and/or LC/ESI-MS^2 analysis. Full versions of all manuscripts are attached in the Annex section.

3.1 Comprehensive characterization of simple glycosphingolipids and other lipids in human plasma using HILIC-ESI/MS^2

Glycosphingolipids (GSL) are amphipathic and extremely diverse glycolipids covering a wide range of polarities, mainly from the polar to ionic region. Several studies have shown the association between alterations of GSL and onset of various human diseases including cancer. Therefore, one of the major attention has been devoted to the characterization of GSL and their role in progression and development of various pathophysiological processes.

Given that GSL are typically low abundant in biofluids compared to other lipids and also suffer from low ionization efficiency, especially those heavily glycosylated, their isolation, detection, and complex structural analysis in biological samples poses a challenging task. We developed and optimized extraction protocol using monophasic ethanol–water solvent system in combination with solid phase extraction (SPE) designed for isolation, purification, and concentration of GSL from human plasma samples (250 µl). The following parameters were optimized: deproteinization solvent (*i.e.,* acetonitrile, MeCN,; methanol, MeOH; ethanol, EtOH; acetone, ACE), the suitability of SPE column (*i.e.,* normal-phase, reversed-phase, polymeric-phase, and ZrO_2-based sorbents; in total 14 SPE columns were tested), and effect of methanol in the loading step (i.e., 0–20% of MeOH). The optimal results were achieved for EtOH as a protein precipitation reagent in combination with Spe-ed C18/18 SPE cartridge and deionized water in the loading step. Optimized method was then applied to the analysis of human plasma.

The analysis of GSL and other polar lipids, namely phospholipids, was performed on liquid chromatograph Ultimate 3000 (Thermo) coupled with mass spectrometer detector

Velos Pro (Thermo) with dual-pressure linear ion trap analyzer. The separation was accomplished on the Ascentis Si column (150 × 2.1 mm, 2.1 µm) within 25 min run time using a modified method from Hájek *et al.* 2017 [476].

In total, 154 GSL species within 8 subclasses (*i.e.,* GlcCer, GalCer, LacCer, Gb_3Cer, Gb_4Cer, SHexCer, $SHex_2Cer$, and GM_3) and 77 phospholipids from 4 subclasses (*i.e.,* PI, LPI, PE, LPE) were explicitly identified in human plasma using hydrophilic interaction liquid chromatography electrospray ionization tandem mass spectrometry (HILIC-ESI/MS^2). Few other compounds, such as FA, Cer, PC, LPC, and SM were also detected. The identification and in-depth structural elucidation of individual lipid species were based on their retention times, *m/z* of precursor and product ions, and monitoring specific MS^2/MS^3 fragmentation patterns, such as glycan sequence and composition of the ceramide part of the GSL molecule in positive and negative ion modes. The individual mass spectra are included in an extensive part of the Supplementary Material. Moreover, the normalized collision energy (NCE) of MS^2 transitions of GSL species with 34:1;O2 ceramide was optimized on the scale 10–100 % using commercially available TLC neutral GSL mixture (Matreya, LLC.). The optimal NCE for all investigated neutral GSL subclasses was obtained at 40% NCE.

Furthermore, the lipid profile of human plasma was generated upon identification. The lipid profiling revealed that the most abundant GSL species within particular subclasses were composed of ceramide 18:1;O2/16:0, respectively 34:1;O2, alongside numerous other usually low abundant GSL species. The only exception was sulfatide SHexCer, dominated by hydroxylated ceramide with the composition 18:1;O2/16:0;O, respectively 34:1;O3. It was also found that the majority of identified lipid species consisted of 18:1;O2 sphingosine.

In addition, the extraction recovery at a medium concentration level using 1–2 IS per each lipid subclass (*i.e.,* exogenous and deuterated) was performed in triplicates. The purpose of this step was to illustrate that the developed and optimized method effectively extracts the GSL of interest and may be further used for future studies in biological samples. The extraction recovery of GSL ranged from 80.8 to 101.7% with relative standard deviation (RSD) varying from 4.0 to 12.5%. Most of the exogenous IS also fulfilled the requirement (*i.e.,* RSD ≤ 15%), except GlcCer (RSD 18.8%) and GM3 (RSD 17.0 %). Consequently, the developed HILIC-ESI-MS^2 method can be a useful tool for GSL profiling and may be used for further biological research of GSL in the biological samples.

The following part is not included in the published paper.

Last but not least, the GSL profile of NIST plasma SRM 1950 (*i.e.*, standard reference material) was constructed (**Fig. 66**) and compared with the GSL profile of human plasma.

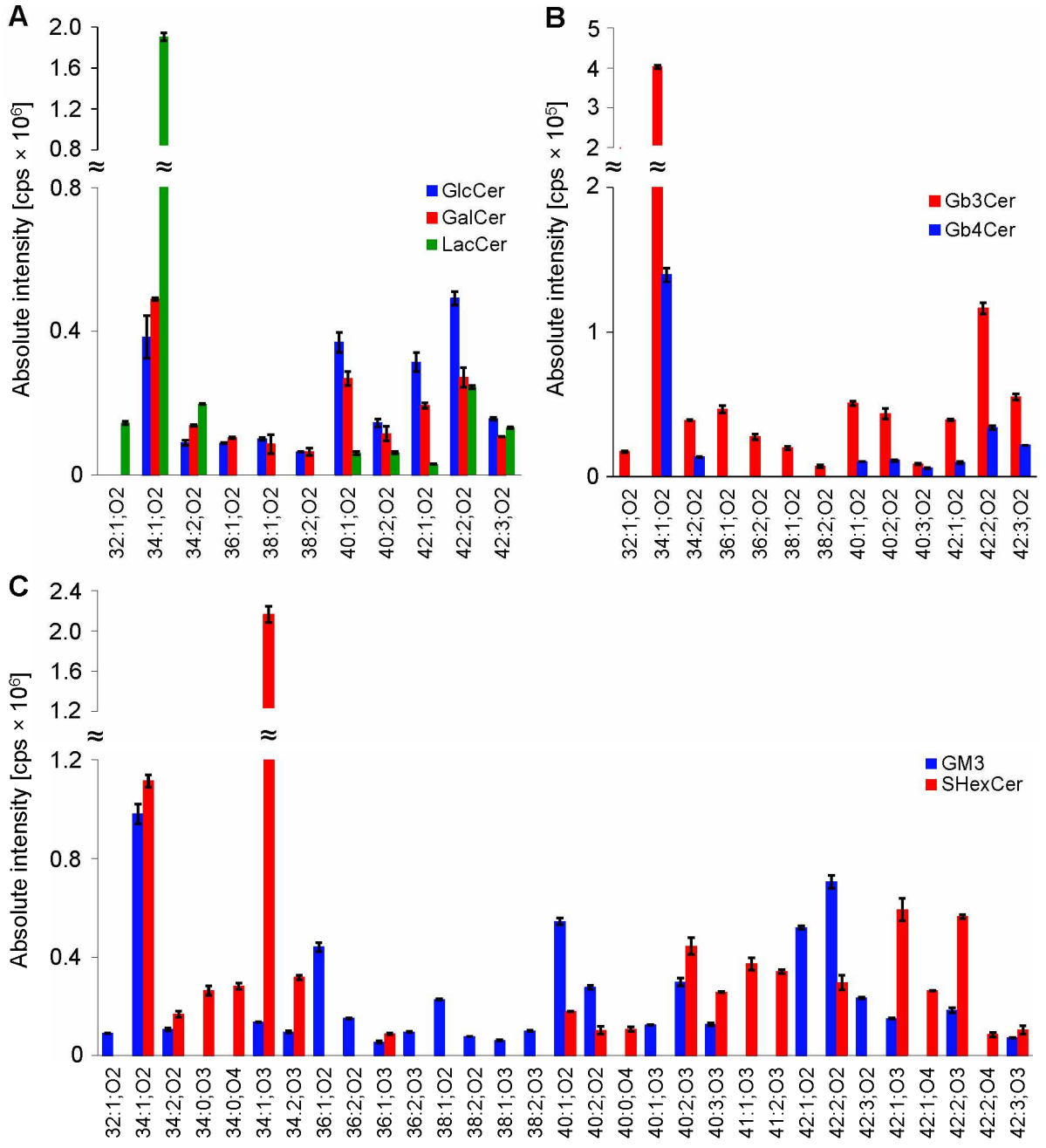

Fig. 66: NIST SRM 1950 human plasma profile of neutral and acidic GSL: **(A)** glucosyl-, galactosyl-, and lactosyl-ceramides (GlcCer, GalCer, LacCer), **(B)** globotri- and globotetra-osylceramides (Gb3Cer and Gb4Cer), and **(C)** monosialodihexosylgangliosides (GM3) with monohexosylsulfatides (SHexCer). The intensities of GSL with error bars are depicted as the mean intensity ± RSD (n = 2) and expressed as a function of sum composition.

The GSL profile of NIST plasma was comparable to that of human plasma, although the number and amounts of particular lipid species were higher in NIST plasma. However, the identified GSL species were in line with previously published data [687,689,705]. Moreover, the identification of some previously reported species, such as HexCer 32:1;O2, 36:2;O2, 44:1;O2, 44:2;O2, Hex2Cer 44:1;O2 and 44:2;O2 were not confirmed. On the contrary, we described considerably more GM3 gangliosides in NIST plasma, including less abundant hydroxylated ones together with Gb_4Cer and SHexCer subclasses that were not reported in NIST plasma.

My contribution to this manuscript:

I was responsible for designing the extraction procedure. I performed all experimental work, including data evaluation, and I prepared the first draft of the manuscript (including Figures, Tables, and Supplementary Material) in close collaboration with co-authors and contributed to revisions.

Reference

Annex A.

Hořejší, K., Jirásko, R., Chocholoušková, M., Wolrab, D., Kahoun, D., and Holčapek, M. Comprehensive Identification of Glycosphingolipids in Human Plasma Using Hydrophilic Interaction Liquid Chromatography–Electrospray Ionization Mass Spectrometry. *Metabolites* **11** (2021) 140. doi: 10.3390/metabo11030140.

3.2 Comprehensive characterization of complex glycosphingolipids in human pancreatic cancer tissues using HPLC-ESI/MS^2

Plasma and/or serum are not the only biological samples suitable for lipidomic analysis. Lipid profiling can also be performed in other biological matrices, such as whole blood, urine, saliva, cerebrospinal fluid, and notably tissues. A vast number of GSL have been shown to be implicated in various diseases including cancer. However, most of these studies are restricted only to simple GSL, such as GlcCer, GalCer, LacCer, and Gb_3Cer, together with several gangliosides and sulfatides, while altered complex GSL are shown only in a few studies.

Consequently, special attention is devoted to the isolation and purification of complex GSL from tumors and adjacent normal tissues of PDAC patients, since the pancreas is one of the organs in which substantial amounts of ABH and Lewis antigens are present in epithelial cells of mainly pancreatic ducts. In addition, ABH antigens are suggested to be related to the tumorigenesis of the pancreas [706]. Pancreatic cancer tissues were prioritized based on an assumption that complex GSL could be more abundant in tissues compared to body fluids.

The isolation and purification of GSL were carried out using a micro method according to Barone *et al.* [442]. Despite this procedure is rather laborious and time-consuming, it has been shown to be particularly advantageous for less abundant complex GSL for which efficient isolation by traditional methods has not yet been reported. In total, 24 paired tissue samples were collected from 12 PDAC patients, pooled (tumor vs. adjacent normal tissues), and used for extraction. In addition, enzymatic digestion using recombinant endoglycoceramidase II (rEGCase II) from *Rhodococcus spp.* was used to release glycans from neutral GSL fractions in order to enhance the capability of isomeric separation.

Analyses were carried out using an Accela 600 binary pump (Thermo) coupled with LTQ XL linear quadrupole ion trap mass spectrometer (Thermo). The separation of GSL-derived glycans and acid GSL was achieved on porous graphitic carbon (PGC) and silica-based capillary column, respectively, using methods described under Method S1 and S2 in Supporting Material of Appendix B. The MS^2 patterns of GSL-derived glycans investigated in negative ion mode allowed clear distinction of isomers and deduction of glycan sequence and linkages positions via typical B- and C-type fragment ions and specific diagnostic fragments.

The major neutral GSL identified were GSL with 4 to 7 monosaccharide units bearing terminal blood group A, B, H, Le^a, Le^x, Le^b, Le^y, P1, and PX2 determinants alongside globo- (Gb_3Cer and Gb_4Cer), and neolacto-series GSL (nLc_4Cer and nLc_6Cer). Moreover, sulfatides and GM3 gangliosides were predominant acidic GSL together with minor sialyl-

nLc$_4$Cer/nLc$_6$Cer and sialyl-Le^a/Le^x. On the contrary, the analysis of neutral GSL using the HILIC column provided a limited number of reliably identified GSL species due to sensitivity issues. Furthermore, the double peak formation resulting probably from the existence of both α and β anomer of Glc at the reducing end was observed in most GSL subclasses, with the identical composition confirmed by MS^2 experiments.

TLC with anisaldehyde and resorcinol staining together with carbohydrate-recognizing binding assays using antibodies (*i.e.*, anti-Le^a, anti-Le^b, anti-A, anti-Neu5Acα3-nLc4, anti-Neu5Acα3-Lc4, anti-sLe^a, anti-sLe^x), lectins (*i.e.*, *Erythrina crystagalli, Groffionia simplicifolia* IB4), and bacteria (*i.e.*, ^{35}S-labeled P-fimbriated *E. coli* strain 291-15) were tested to substantiate the data obtained from LC-ESI/MS^2. TLC staining revealed that major bands migrated in the regions with 1 to 4 monosaccharide units along with some minor slow-migrating compounds with 5 to 7 monosaccharide units. The outcomes of binding assays clearly illustrated the differences in GSL expression between tumor and adjacent normal pancreatic tissues in line with the LC-ESI/MS^2.

Glycan profiling of tumor and adjacent normal pancreatic tissues revealed differences in the region from 4 to 7 sugar units, and in type 1/2 core chains. Specifically, tumor pancreatic tissues were dominated by GSL with blood group Le^a and Le^b determinants (*i.e.*, type 1 chain) alongside nLc$_4$Cer, while the predominant GSL of adjacent normal pancreatic tissues were GSL with blood group A and B determinants (*i.e.*, type 2 chain). Other glycans including GSL with blood group Le^x, Le^y, H determinants, and nLc$_6$Cer were found in both tissues, while P1 and PX2 pentaosylceramides along with Le^y heptaosylceramides were minor components of tumor pancreatic tissues. Additionally, binding assays confirmed the presence of Gb$_3$Cer and Gb$_4$Cer, although they were not identified by LC-ESI/MS^2. In the case of acid GSL, the major GSL were sulfatides and GM3 gangliosides with 34:1;O2 and 34:1;O3 ceramides together with minor s-nLc$_4$Cer/nLc$_6$Cer. Sialylated GSL, such as sLe^a (*i.e.*, CA 19-9 biomarker) and sLe^x, were determined by binding assays despite not being identified by LC-ESI/MS^2.

Modifications of expression of ABH and Lewis blood group-related antigens are characteristic features of various carcinomas. The major changes in the glycosylation in most human cancers occur on type 2 chain, which is also the major carrier for the blood group ABH determinant of human red blood cells [533,707]. These changes are inevitably connected with the dysregulation of glycosyltransferases, namely fucosyltransferases (FUTs), which are responsible for the formation of Lewis blood group determinants. Namely, FUT1 has been shown to preferentially glycosylate type 2 chain. Conversely, FUT2 and FUT3

prioritize type 1 chain. This is in line with the observed predominance of fucosylated type 1 chain GSL (*i.e.*, Le^a-5 and Le^b-6) in tumor tissues and dominance of GSL with blood group A and B determinants (*i.e.*, A6-2, B6-2, and B7-2) on type 2 chain in adjacent normal tissues in this study. Therefore, the overexpression of Lewis blood group antigens in PDAC may be associated with the upregulation of FUT2 and/or FUT3. In contrast, the accumulation of nLc_4Cer along with the absence of blood group A and B associated GSL (*i.e.*, type 2 chain) may be in line with the downregulation of FUT1, the enzyme responsible for the formation of the H type 2 GSL, and the precursor of blood group A and B determinants on type 2 chain. These findings are interesting and opposite of what was found by Hattori [707], *i.e.*, presence of type 1 chain only in normal and both type 1 and 2 chain in tumor tissues. Finally, the relative amounts of GSL varied between tumor and adjacent normal pancreatic tissues.

The extensive investigation of complex GSL in human pancreatic cancer extends the coverage of GSL that are not routinely analyzed by traditional lipidomic methods. Furthermore, it provides an important platform for further studies of GSL alterations, such as glycosylation, sialylation, and/or fucosylation that are an integral part of many pathophysiological processes. It could also contribute to the development of new biomarkers and therapeutic approaches. The future perspective is to simplify the isolation protocol and to incorporate complex GSL into the body fluids-based screening methods of PDAC and possibly other cancers. However, future studies should clarify these results and investigate whether these differences translate into GSL profiles between patients and healthy subjects.

The following part is not included in the published paper.

In this study, we also tried to compare the profiles of GSL-derived glycans in tumor and normal pancreatic tissues of three individuals (**Table 33**) using a similar isolation protocol (extraction in glass test tubes instead of Soxhlet extractor) to increase the value of the data.

Table 33: The amounts of tissue samples of the three individuals before lyophilisation.

Sample No.	Tumour tissue			Normal tissue		
	672	685	791	672	685	791
Amount [mg]	87	116	149	227	195	149

The expression of the blood group A, B, H and Lewis type GSL should be in line with the ABH and Lewis phenotypes of the patients (**Table 34**), however, the presence of incompatible blood group antigens was already reported as a probable consequence of neosynthesis in cancer tissues [707].

Table 34: Expression of ABH and Lewis type GSL related to phenotypes [708].

Genotype	OO	AO	AA	BO	BB	AB
Phenotype	O	A		B		AB
Expressed antigens	H	A		B		AB

ABH phenotype	**Lewis phenotype**	**FUT2**	**FUT3**	**Expressed antigens**
A, B, AB, O	Le(a-b+)	active	active	H, A and/or B, Le^a, Le^b
A, B, AB, O	Le(a+b-)	inactive	active	Le^a
A, B, AB, O	Le(a-b-)	active	inactive	H, A and/or B
A, B, AB, O		inactive	inactive	type 1 precursor glycans
A, B, AB, O	Le(a+b+)	this combination is very rare		

However, we were able to identify and characterize GSL-derived glycans only in 3 out of 6 samples (*i.e.*, two individual patients, **Fig. 67**) probably due to sensitivity issues.

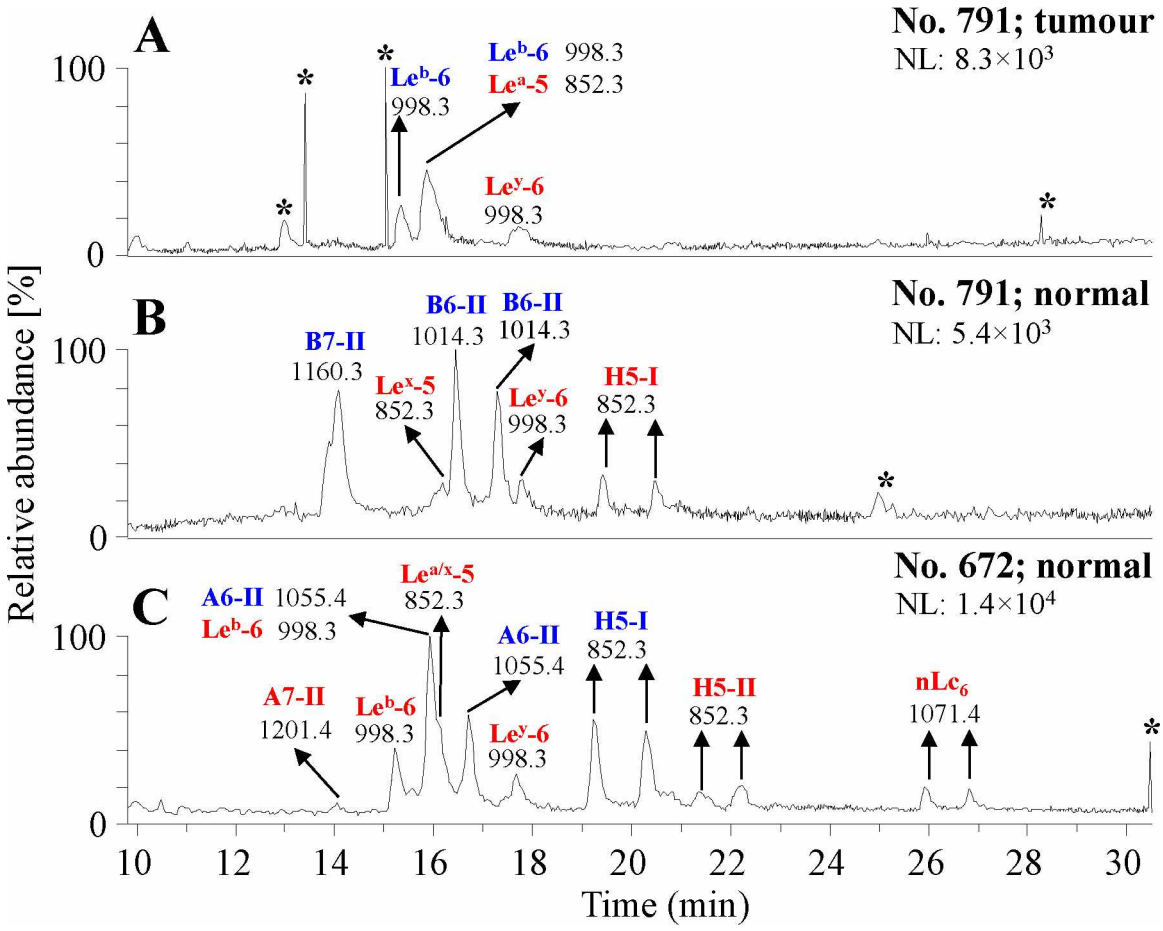

Fig. 67: Reconstructed ion current (RIC) chromatograms of GSL-derived glycans of individual PDAC patients: **(A)** tumor and **(B)** normal tissue of single individual No. 791, and **(C)** normal tissue of single individual No. 672 (blue, major glycans; red, minor or less abundant glycans; *, non-GSL).

Nevertheless, the observed GSL patterns were in accordance with those found in pooled pancreatic tissues, *i.e.*, GSL with Lewis blood group determinants predominate in tumor tissue (**Fig. 67A**), while GSL with blood group B (**Fig. 67B**) and blood group A (**Fig. 67C**) determinants prevailed in normal tissues. Since we did not obtain information on the blood type of the patients from clinicians, we can only assume that the patient No. 791 probably has the blood type B, and patient No. 672 has the blood type A.

However, a few studies suggesting that individuals carrying non-O blood group have an increased risk of pancreatic cancer compared to those with O blood group were reported by Wolpin *et al.* [709], and more recently by Rahbari *et al.* [710] and Antwi *et al.* [711]. It has also been shown that individuals with pancreatic cancer express either blood group A or B antigens corresponding to the respective blood group or are characterized by loss of the expression of the blood group antigens in most cases [706,712,713], which supports our findings. Moreover, one case–control study investigated by Annese *et al.* [714] indicated that individuals with blood group B seem to be more prone to development of pancreatic cancer. Furthermore, Aird *et al.* [715] and Rizzato *et al.* [716] reported an increase in the incidence of pancreatic cancer in blood group A individuals. Last but not least, Mahajan *et al.* [717] unveiled that glycolipid-associated pathways, including dysregulation of complex lipids in plasma of PDAC patients, differ substantially among the specific subtypes of PDAC.

We can only speculate whether individuals carrying blood groups A and B determinants may incline to develop pancreatic cancer, as the linkage between GSL metabolism with pancreatic cancer progression needs to be clarified by future studies using a larger set of samples. Consequently, the significance of the linkage remains debatable.

My contribution to this manuscript:

I carried out the majority of practical work and a few binding assays. I was responsible for performing HPLC/MS^2 experiments along with data evaluation in collaboration with S. Teneberg. I also prepared the manuscript in close consultation with co-authors.

Reference

Annex B.

Hořejší, K., Jin, Ch., Vaňková, Z., Jirásko, R., Strouhal, O., Melichar, B., Teneberg, S., and Holčapek, M. Comprehensive characterization of complex glycosphingolipids in human pancreatic cancer tissues. *J. Biol. Chem.* **299** (2023) 3. doi: 10.1016/j.jbc.2023.102923

3.3 Lipid profiles of kidney, breast and prostate cancer patients differ from healthy controls

Another study comparing the plasma lipid profiles of healthy volunteers and patients with kidney, breast, and prostate cancer was carried out using UHPSFC-MS and DI-MS with the aim to differentiate cancer patients from healthy controls.

In total, 289 samples of cancer patients (*i.e.,* 119 kidney, 103 breast, and 67 prostate) and 192 samples of healthy volunteers were collected and analyzed. Samples were divided into training set (ca 75%) and validation set (ca 25%) in a similar percentage representation of individual types of samples. The analysis resulted in the quantitation of 138 lipids from GL, GP, and SP subclasses, from which 91 lipids were selected for multivariate data analysis. Then, the number of lipid species was further reduced to seven lipids by applying additional statistical criteria, such as fold change, *p*-value, VIP value, and Bonferroni correction. Models of cancer prediction were characterized by high sensitivity, specificity, and accuracy.

Statistically, the most dysregulated lipids were CE 16:0, Cer 42:1;O2, LPC 18:2, PC 36:2, PC 36:3, SM 32:1;O2, and SM 41:1;O2, which may represent potential biomarkers to differentiate kidney, breast, and prostate cancer from healthy volunteers based on human plasma profiling. In conclusion, the data indicated the potential of lipid profiling with the use of multivariate data analysis as a diagnostic tool for all three studied types of cancer.

My contribution to this manuscript:

I read, reviewed, and edited the manuscript. I also provide a critical and valuable comments.

Reference

Annex C.

Wolrab, D., Jirásko, R., Peterka, O., Idkowiak, J., Chocholoušková, M., Vaňková, Z. **Hořejší, K.**, Brabcová, I., Vrána, D., Študentová, H., Melichar, B., and Holčapek, M. Plasma lipidomic profiles of kidney, breast and prostate cancer patients differ from healthy controls. *Sci. Rep.* **11** (2021) 20322. doi: 10.1038/s41598-021-99586-1

3.4 Recent advances, challenges and future direction in the analysis of glycosphingolipids in biological samples

The last part of my work is a review article. The review first discusses technological advances in GSL analysis, such as the replacement of conventional HPLC columns with sub-2-µm particles, offering enhanced separation efficiency and high-throughput analysis, the use of 2D SFC/RPLC-MS and UHPSFC-MS for improved lipidomic coverage, selectivity, and sensitivity, or implementation of IM technologies, adding a fourth dimension of separation, together with recent innovations (*e.g.,* PASEF, SLIM) enhancing the separation of isomers. These advancements contribute to a comprehensive understanding of GSL in a biological context. The next section addresses the challenges in the GSL analysis, focusing on sample pre-treatment and extraction and purification strategies that are crucial to maintaining the integrity of the sample. The need for innovative isolation protocols for efficient GSL extraction from complex matrices is emphasized as the well-established protocols are not sufficient. The challenges, such as achieving rapid and uniform extraction, along with the complete removal of interfering substances (*e.g.,* alkaline hydrolysis, ZrO_2/TiO_2-based SPE, and silica-based or weak-anion exchange chromatography) that persist are highlighted. Then the review is focused on issues related to the separation of isomers, as the baseline separation of GSL isomers is still challenging even when applying IM with innovative technologies, such as PASEF or SLIM. Various derivatization techniques, such as permethylation, isobaric labelling, or benzoyl derivatization, designed to increase the ionization efficiency of GSL and/or to aid in the structural elucidation by introducing specific fragment ions are discussed as well. The section addressing quantitative analysis and validation emphasizes the limited availability of suitable ISs for quantitation and suggests alternative strategies, such as chemoenzymatic synthesis or *in vivo* stable isotope labeling, a promising approaches to reliable and accurate quantitation addressing the lack of ISs for GSL. The importance of method validation and harmonized protocols or guidelines is also discussed together with the absence of well-defined and certified reference materials that complicate the inter-laboratory comparisons. Furthermore, the development of novel, comprehensive, and open-source bioinformatics tools is crucial, as lipidomic analyses generate large datasets, to support lipidomics' potential for clinical diagnostics and understanding the roles of lipids in various pathophysiological processes. Although lipidomics is promising for monitoring diseases, including cancer, through non-invasive biomarkers obtained from body fluids, there are not so

many GSL biomarkers that are used as diagnostic or prognostic markers. Moreover, the lack of extensive population-based clinical trials hinders the translation into clinical lipidomics

Consequently, future directions should focus on the efficient isolation of more complex and minor GSL, increased ionization efficiency, enhanced separation of GSL isomers, and development of stable-isotope labelling method for accurate absolute quantitation. In conclusion, continuous efforts are crucial to address these limitations to fully reveal the potential of glycosphingolipidomics for clinical translation as comprehensive high-throughput GSL profiling in biological samples remains very challenging.

My contribution:

I prepared the review proposal together with a detailed outline. I wrote the majority of the manuscript, except validation and quantitation, and prepared tables and 3 out of 4 figures and discussed it with close collaboration with co-authors.

Reference

Annex D.

Hořejší, K., Kolářová D., Jirásko, R., and Holčapek, M. Recent advances, challenges, and future directions in the mass spectrometry analysis of glycosphingolipids in biological samples. *Trac-Trends Anal. Chem.* **178** (2024) 117827. doi: 10.1016/j.trac.2024.117827

4 CONCLUSIONS

This dissertation deals with the development and optimization of methods for detailed structural characterization and profiling of GSL, GSL-derived glycans, and other lipids in biological samples using HPLC-ESI-MS/MS.

The theoretical part provides a detailed and comprehensive review describing the structure, classification, nomenclature, and biological functions of GSL together with their associations with various diseases including cancers. Various sample preparation methods and analytical methods, with the emphasis on the qualitative and quantitative analysis of GSL and other lipids, are discussed in detail as well.

The experimental part is devoted to the development and optimization of new liquid-liquid extraction followed by solid-phase extraction using the HILIC-ESI-MS/MS method. This method enabled the identification and characterization of 154 simple GSL species within 7 lipid subclasses in human plasma together with 77 phospholipids and several ceramides and fatty acids. The HPLC-ESI-MS/MS method using a PGC column capable of separating structural isomers was applied for the analysis of GSL-derived glycans extracted and isolated from human pancreatic cancer tissues and adjacent normal pancreatic tissues. This method primarily allowed the profiling of more complex GSL. The analysis also revealed striking differences in glycosylation, mainly fucosylation and sialylation, between the tumor and adjacent normal tissues. It was found that the type 1 core chain represented by GSL carrying Le^a and Le^b determinants along with nLc_4Cer predominated in tumor tissues, while the type 2 core chain represented by GSL with blood group A and B determinants were preferentially found in adjacent normal tissues. These findings were also supported by chromatogram binding assays using specific antibodies, bacteria, and lectins. UHPSFC-MS method has been applied for the differentiation of patients with kidney, breast and prostate cancer from healthy controls based on the quantitative lipid profiling, where lipids were extracted from human plasma. Finally, recent advances, current challenges, and future directions in the analysis of GSL in biological samples were reviewed.

The related works demonstrate that the coupling of chromatographic techniques with mass spectrometry for the analysis of GSL has recently greatly advanced. However, there are still a few issues complicating the reliable identification and quantitation, namely (1) variability in extraction protocols that do not effectively extract a wide range of GSL, (2) lack of appropriate ISs for accurate quantitation, and (3) inability to differentiate isomers and/or

isobars. Although the latter has recently been greatly improved by utilizing novel dissociation techniques and IM, much more effort is still needed to elucidate C=C positions, *sn*-positions, and branched-chain isomers. Future directions should also focus on the development of novel and unique extraction protocols capable of isolating simple as well as more complex and even minor GSL subclasses together with the development of suitable methods for the synthesis of ISs that could compensate for the lack of ISs. These improvements are necessary to improve the possibilities of finding suitable biomarkers that could provide valuable information and enable the detection of various diseases in the early stages and assure timely treatment to improve clinical outcomes.

5 SCIENTIFIC CONTRIBUTION

Submitted papers in impact journals

1. **Hořejší K.,** and Holčapek M. Unraveling the complexity of glycosphingolipidome: The key role of mass spectrometry in the structural analysis of glycosphingolipids. *Anal. Bioanal. Chem.* (2024). (Q1; IF = 4.3; CIn = 0.93; submitted)

Published papers in impact journals

1. **Hořejší K.,** Kolářová D., Jirásko R., and Holčapek M. Recent advances, challenges and future direction in the mass spectrometry analysis of glycosphingolipids in biological samples. *Trac-Trends Anal. Chem.* **178** (2024) **117827**. doi: 10.1016/j.trac.2024.117827. (Q1(D1); IF = 13.1; CIn = 1.31, number of citations: 0)

2. **Hořejší K.,** Jin Ch., Vaňková Z., Jirásko R., Strouhal O., Melichar B., Teneberg S., and Holčapek M. Comprehensive characterization of complex glycosphingolipids in human pancreatic cancer tissues. *J. Biol. Chem.* **299** (2023) **102923**. doi: 10.1016/j.jbc.2023.102923 (Q2; IF = 4.8; CIn = 0.87; number of citations: 6)

3. Wolrab D., Jirásko R., Peterka O., Idkowiak J., Chocholoušková M., Vaňková Z., **Hořejší K.,** Brabcová I., Vrána D., Študentová H., Melichar B., and Holčapek M. Plasma lipidomic profiles of kidney, breast and prostate cancer patients differ from healthy controls. *Sci. Rep.* **11** (2021) **20322**. doi: 10.1038/s41598-021-99586-1 (Q2; IF = 4.6; CIn = 1.06; number of citations: 16)

4. **Hořejší K.,** Jirásko R., Chocholoušková M., Wolrab D., Kahoun D., and Holčapek M. Comprehensive Identification of Glycosphingolipids in Human Plasma Using Hydrophilic Interaction Liquid Chromatography–Electrospray Ionization Mass Spectrometry. *Metabolites.* **11** (2021) **140**. doi: 10.3390/metabo11030140 (Q2; IF = 4.1; CIn = 0.71; number of citations: 7)

The following paper is not related to Ph.D. thesis

1. Pexová Kalinová J., Tříska J., and **Hořejší K**. Comparison of the Main Constituents in Two Varieties of Proso Millet Using GC-MS, *Foods* **12** (2023), **2294**. doi: 10.3390/foods12122294 (Q1; IF = 5.2; CIn = 0.97; number of citations: 1)

The value of impact factor (IF), citation indicator (CIn), and quartile (Q) stated are based on the data from the Web of Science (valid for 2022) along with the number of citations, excluding self-citation, valid to date May 31, 2024.

Lectures

1. Holčapek, M., **Hořejší, K.**, Peterka, O., Vaňková, Z., Kolářová, D., Veseli, V., Šubrtová, V., Jirásko, R., Dolečková, Z., and Kanásová, M. Dysregulation of (Glyco)sphingolipids in Pancreatic Cancer. GRC Glycolipid and Sphingolipid Biology, Galvestone, Texas, USA, February 18–23, 2024

2. Holčapek, M., Vaňková, Z., Peterka, O., Wolrab, D., **Hořejší, K.**, Kolářová, D., Šubrtová, V., Chocholoušková, M., and Jirásko, R. Potential of Various Chromatography Modes for Detailed Characterization of Lipidome. HPLC 2023, June 18–22, Düsseldorf, Germany

3. Holčapek M., **Hořejší K.,** Hájek R., Chocholoušková M., Jirásko R., and Wolrab D. Characterization of Neutral and Anionic Glycosphingolipids Using HILIC-UHPLC/MS. COST online seminar, May 4, 2021

4. Holčapek M., Wolrab D., Jirásko R., Chocholoušková M., Peterka O., Vaňková Z., and **Hořejší K.** Chromatography of Lipids – Potential for Separation of Various Types of Lipid Isomers. LIPID MAPS Spring School, online, April 12–14, 2021

5. **Hořejší K.,** Jirásko R., Chocholoušková M., Kahoun D., and Holčapek M. Stuctural Analysis of Glycosphingolipids in Human Plasma Using HILIC-ESI-MS/MS. 21st School of mass spectrometry, September 13–18, 2020, Srní, Czech Republic

The following lecture is not related to Ph.D. thesis

6. **Hořejší K.,** Kahoun D., and Hauer. T. Development, optimization and valiation of an analytical method for determination of neurotoxin β-N-methylamino-L-alanine in water using LC-MS. The Karel Štulík Award for the best student research work in analytical chemistry, February 8–9, 2017, České Budějovice, Czech Republic

Posters

1. **Hořejší K.,** Jin Ch., Vaňková Z., Jirásko R., Strouhal O., Melichar B., Teneberg S., and Holčapek M. Comprehensive characterization of glycosphingolipids in human pancreatic cancer tissues. 23rd School of mass spectrometry, September 4–9, 2022, Milovy, Czech Republic

2. **Hořejší K.,** Jin Ch., Vaňková Z., Jirásko R., Strouhal O., Melichar B., Teneberg S., and Holčapek M. Analysis of complex glycosphingolipids of human pancreatic cancer revealed differences in lipid profile between normal and tumor pancreatic tissues. HPLC 2022, June 18–23, San Diego, California, USA
3. **Hořejší K.,** Chocholoušková M., Wolrab D., Jirásko R, and Holčapek M. Validation of bioanalytical method for determination of glycosphingolipids in human plasma using HILIC-HPLC/MS. 22nd School of mass spectrometry, September 5–10, 2021, Srní, Czech Republic

4. **Hořejší K.,** Jirásko R., Chocholoušková M., Kahoun D., and Holčapek M. Structural characterization of glycosphingolipids in human plasma using HILIC-ESI-MS/MS. 21st School of mass spectrometry, September 13–18, 2020, Srní, Czech Republic

5. **Hořejší K.,** Jirásko R., Kahoun D., and Holčapek M. Lipidomic analysis of glycosphingolipids in human blood plasma using HILIC-HPLC/MS. 20th School of mass spectrometry, September 9–13, 2019, Špindlerův Mlýn, Czech Republic

The following posters are not related to Ph.D. thesis

6. **Hořejší K.,** Kahoun D., and Hauer. T. Development, optimization and validation of an analytical method for determination of the neurotoxin β-N-methylamino-L-alanine in water and cyanobacteria using LC-MS. 19th School of mass spectrometry, September 10–14, 2018, Špindlerův Mlýn, Czech Republic

7. **Hořejší K.,** Kahoun D., and Hauer. T. Development, optimization and validation of an analytical method for determination of the neurotoxin β-N-methylamino-L-alanine in water using LC-MS. Czech Mass Spectrometry Conference, March 29–31, 2017, Olomouc, Czech Republic

Contributions in proceedings (not related to Ph.D. thesis)

1. **Hořejší K.,** Kahoun D., and Hauer T. Development, optimization and valiation of an analyticalmethod fordetermination of the neurotoxin β-N-methylamino-L-alanine in water using LC/MS, *Czech Chem. Soc. Symp. Ser.* 15 (2017), 49-100.

Research internships

1. **University of Gothenburg,** Sahlgrenska Academy, Institute of Biochemistry, Department of Medical Biochemistry and Cell Biology, Göteborg, Sweden, **Supervisor:** prof. Susann Teneberg
   09-12/2021, 2021 (3 months), 08/2022 (10 days), and 06/2023 (2 weeks)

Achievements and Awards

1. **Travel grant recipient from California Separation Science Society (CASSS)**, support of active participation in HPLC 2022, June 18–23, 2022, San Diego, California, USA

2. **Nominated for a lecture for the best young scientist in the Youth Forward section,** 21st School of mass spectrometry, September 17, 2020, Srní, Czech Republic

The following achievements and awards are not related to Ph.D. thesis

3. **Dean's Award for excellent results published in diploma thesis**, University of South Bohemia in České Budějovice, Faculty of Science, June 25, 2018, Czech Republic

4. **Special Committee Awards, The Karel Štulík Award,** February 8–9, 2017, České Budějovice, Czech Republic

Attended courses and seminars

1. **Lipidomic analysis,** lecturer: Holčapek M., Jirásko R., Peterka O., Chocholoušková M. 22nd School of mass spectrometry, September 6, 2021, Srní, Czech Republic

2. **Lipidomic analysis,** lecturer: Liebisch G. 21st School of mass spectrometry, September 14, 2020, Srní, Czech Republic

3. **Statistical data evaluation in bioanalytical chemistry,** lecturer: Friedecký D. 21st School of mass spectrometry, September 13, 2020, Srní, Czech Republic

4. **Statistical data analysis,** lecturer: Friedecký D. 20th School of mass spectrometry, September 9, 2019, Špindlerův Mlýn, Czech Republic

5. **Development of LC-MS methods for small molecules,** lecturer: Holčapek M., Nováková L. 20th School of mass spectrometry, September 8, 2019, Špindlerův Mlýn, Czech Republic

6. **Workflow in metabolomics,** lecturer: Kohler I. 19th School of mass spectrometry, September 10, 2018, Špindlerův Mlýn, Czech Republic
7. **Troubleshooting in LC-MS,** lecturer: Nováková L., Kotland O., Buček J. 19th School of mass spectrometry, September 9, 2018, Špindlerův Mlýn, Czech Republic

8. **Interpretation of EI spectra,** lecturer: Polášek M., Cvačka J., Holčapek M., Čáslavský J. 18th School of mass spectrometry, September 10–11, 2017, Luhačovice, Czech Republic

The following courses are not related to Ph.D. thesis

9. **GC/MS training,** lecturer: Čáslavský J, Petrus K. Pragolab s.r.o, November 13–14, 2018, Praha, Czech Republic

10. **Modern chromatographic techniques for 'smart' analysis in the field of food and environment,** seminar, University of Chemistry and Technology, May 5 , 2017, Praha, Czech Republic

6 REFERENCES

1. Holčapek, M.; Liebisch, G.; Ekroos, K. Lipidomic analysis. *Anal. Bioanal. Chem.* **2020**, *412*, 2187–2189, doi:10.1007/s00216-020-02419-9.
2. Han, X. *Lipidomics: Comprehensive Mass Spectrometry of Lipids*; Desiderio, D.M., Loo, J.A., Eds.; 1st ed.; John Wiley & Sons, Inc.: Hoboken, NJ, USA, 2016; ISBN 9781118893128.
3. Fahy, E.; Subramaniam, S.; Brown, H.A.; Glass, C.K.; Merrill, A.H.; Murphy, R.C.; Raetz, C.R.H.; Russell, D.W.; Seyama, Y.; Shaw, W.; et al. A comprehensive classification system for lipids. *J. Lipid Res.* **2005**, *46*, 839–861, doi:10.1194/jlr.E400004-JLR200.
4. Fahy, E.; Subramaniam, S.; Murphy, R.C.; Nishijima, M.; Raetz, C.R.H.; Shimizu, T.; Spener, F.; Van Meer, G.; Wakelam, M.J.O.; Dennis, E.A. Update of the LIPID MAPS comprehensive classification system for lipids. *J. Lipid Res.* **2009**, *50*, S9–S14, doi:10.1194/jlr.R800095-JLR200.
5. Schnaar, R.L.T.; Kinoshita, T. Glycosphingolipids. In *Essentials of Glycobiology 3rd Edition*; 2017; pp. 1–11.
6. Yamakawa, T. A reflection on the early history of glycosphingolipids. *Glycoconj. J.* **1996**, *13*, 123–126, doi:10.1007/BF00731485.
7. Merrill, A.H.; Wang, M.D.; Park, M.; Sullards, M.C. (Glyco)sphingolipidology: an amazing challenge and opportunity for systems biology. *Trends Biochem. Sci.* **2007**, *32*, 457–468, doi:10.1016/j.tibs.2007.09.004.
8. Zhang, X.; Kiechle, F.L. Review: Glycosphingolipids in Health and Disease. *Ann. Clin. Lab. Sci.* **2004**, *34*, 3–13.
9. Lingwood, D.; Simons, K. Lipid rafts as a membrane-organizing principle. *Science (80-.).* **2010**, *327*, 46–50, doi:10.1126/science.1174621.
10. Skotland, T.; Kavaliauskiene, S.; Sandvig, K. The role of lipid species in membranes and cancer-related changes. *Cancer Metastasis Rev.* **2020**, *39*, 343–360, doi:10.1007/s10555-020-09872-z.
11. Hakomori, S. Glycosphingolipids. *Sci. Am.* **1986**, *254*, 44–53, doi:10.1038/scientificamerican0586-44.
12. Senn, H. -J; Orth, M.; Fitzke, E.; Wieland, H.; Gerok, W. Gangliosides in normal human serum: Concentration, pattern and transport by lipoproteins. *Eur. J. Biochem.* **1989**, *181*, 657–662, doi:10.1111/j.1432-1033.1989.tb14773.x.
13. Mullen, T.D.; Hannun, Y.A.; Obeid, L.M. Ceramide synthases at the centre of sphingolipid metabolism and biology. *Biochem. J.* **2012**, *441*, 789–802, doi:10.1042/BJ20111626.
14. Levy, M.; Futerman, A.H. Mammalian ceramide synthases. *IUBMB Life* **2010**, *62*, 347–356, doi:10.1002/iub.319.
15. Grösch, S.; Schiffmann, S.; Geisslinger, G. Chain length-specific properties of ceramides. *Prog. Lipid Res.* **2012**, *51*, 50–62, doi:10.1016/j.plipres.2011.11.001.
16. Jennemann, R.; Gröne, H.J. Cell-specific in vivo functions of glycosphingolipids: Lessons from genetic deletions of enzymes involved in glycosphingolipid synthesis. *Prog. Lipid Res.* **2013**, *52*, 231–248, doi:10.1016/j.plipres.2013.02.001.
17. Gault, C.R.; Obeid, L.M.; Hannun, Y.A. An overview of sphingolipid metabolism: from synthesis to breakdown. *Adv. Exp. Med. Biol.* **2010**, *688*, 1–23, doi:10.1007/978-1-4419-6741-1_1.
18. Hanada, K.; Kumagai, K.; Yasuda, S.; Miura, Y.; Kawano, M.; Fukasawa, M.; Nishijima, M. Molecular machinery for non-vesicular trafficking of ceramide. *Nature*

2003, *426*, 803–809, doi:10.1038/nature02188.
19. D'Angelo, G.; Capasso, S.; Sticco, L.; Russo, D. Glycosphingolipids: Synthesis and functions. *FEBS J.* **2013**, *280*, 6338–6353, doi:10.1111/febs.12559.
20. Glick, B.S.; Luini, A. Models for Golgi traffic: A critical assessment. *Cold Spring Harb. Perspect. Biol.* **2011**, *3*, doi:10.1101/cshperspect.a005215.
21. D'Angelo, G.; Polishchuk, E.; Tullio, G. Di; Santoro, M.; Campli, A. Di; Godi, A.; West, G.; Bielawski, J.; Chuang, C.C.; Van Der Spoel, A.C.; et al. Glycosphingolipid synthesis requires FAPP2 transfer of glucosylceramide. *Nature* **2007**, *449*, 62–67, doi:10.1038/nature06097.
22. D'Angelo, G.; Uemura, T.; Chuang, C.C.; Polishchuk, E.; Santoro, M.; Ohvo-Rekilä, H.; Sato, T.; Di Tullio, G.; Varriale, A.; D'Auria, S.; et al. Vesicular and non-vesicular transport feed distinct glycosylation pathways in the Golgi. *Nature* **2013**, *501*, 116–120, doi:10.1038/nature12423.
23. Halter, D.; Neumann, S.; Van Dijk, S.M.; Wolthoorn, J.; De Mazière, A.M.; Vieira, O. V.; Mattjus, P.; Klumperman, J.; Van Meer, G.; Sprong, H. Pre- and post-Golgi translocation of glucosylceramide in glycosphingolipid synthesis. *J. Cell Biol.* **2007**, *179*, 101–115, doi:10.1083/jcb.200704091.
24. De Rosa, M.F.; Sillence, D.; Ackerley, C.; Lingwood, C. Role of Multiple Drug Resistance Protein 1 in Neutral but Not Acidic Glycosphingolipid Biosynthesis. *J. Biol. Chem.* **2004**, *279*, 7867–7876, doi:10.1074/jbc.M305645200.
25. van Meer, G.; Hoetzl, S. Sphingolipid topology and the dynamic organization and function of membrane proteins. *FEBS Lett.* **2010**, *584*, 1800–1805, doi:10.1016/j.febslet.2009.10.020.
26. Merrill, A.H. Sphingolipid and glycosphingolipid metabolic pathways in the era of sphingolipidomics. *Chem. Rev.* **2011**, *111*, 6387–6422, doi:10.1021/cr2002917.
27. MacCioni, H.J.F.; Quiroga, R.; Ferrari, M.L. Cellular and molecular biology of glycosphingolipid glycosylation. *J. Neurochem.* **2011**, *117*, 589–602, doi:10.1111/j.1471-4159.2011.07232.x.
28. Van Meer, G.; Voelker, D.R.; Feigenson, G.W. Membrane lipids: Where they are and how they behave. *Nat. Rev. Mol. Cell Biol.* **2008**, *9*, 112–124, doi:10.1038/nrm2330.
29. Uemura, S.; Go, S.; Shishido, F.; Inokuchi, J.I. Expression machinery of GM4: The excess amounts of GM3/GM4S synthase (ST3GAL5) are necessary for GM4 synthesis in mammalian cells. *Glycoconj. J.* **2014**, *31*, 101–108, doi:10.1007/s10719-013-9499-1.
30. Liang, Y.J.; Kuo, H.H.; Lin, C.H.; Chen, Y.Y.; Yang, B.C.; Cheng, Y.Y.; Yu, A.L.; Khoo, K.H.; Yu, J. Switching of the core structures of glycosphingolipids from globo- and lacto- to ganglio-series upon human embryonic stem cell differentiation. *Proc. Natl. Acad. Sci. U. S. A.* **2010**, *107*, 22564–22569, doi:10.1073/pnas.1007290108.
31. Taube, S.; Jiang, M.; Wobus, C.E. Glycosphingolipids as receptors for non-enveloped viruses. *Viruses* **2010**, *2*, 1011–1049, doi:10.3390/v2041011.
32. Kuan, C.T.; Chang, J.; Mansson, J.E.; Li, J.; Pegram, C.; Fredman, P.; McLendon, R.E.; Bigner, D.D. Multiple phenotypic changes in mice after knockout of the B3gnt5 gene, encoding Lc3 synthase - A key enzyme in lacto-neolacto ganglioside synthesis. *BMC Dev. Biol.* **2010**, *10*, doi:10.1186/1471-213X-10-114.
33. Westman, J.S.; Benktander, J.; Storry, J.R.; Peyrard, T.; Hult, A.K.; Hellberg, Å.; Teneberg, S.; Olsson, M.L. Identification of the molecular and genetic basis of PX2, a glycosphingolipid blood group antigen lacking on globoside-deficient erythrocytes. *J. Biol. Chem.* **2015**, *290*, 18505–18518, doi:10.1074/jbc.M115.655308.
34. Aureli, M.; Loberto, N.; Chigorno, V.; Prinetti, A.; Sonnino, S. Remodeling of sphingolipids by plasma membrane associated enzymes. *Neurochem. Res.* **2011**, *36*, 1636–1644, doi:10.1007/s11064-010-0360-7.

35. Coant, N.; Sakamoto, W.; Mao, C.; Hannun, Y.A. Ceramidases, roles in sphingolipid metabolism and in health and disease. *Adv. Biol. Regul.* **2017**, *63*, 122–131, doi:10.1016/j.jbior.2016.10.002.
36. Kitatani, K.; Idkowiak-Baldys, J.; Hannun, Y.A. The sphingolipid salvage pathway in ceramide metabolism and signaling. *Cell. Signal.* **2008**, *20*, 1010–1018, doi:10.1016/j.cellsig.2007.12.006.
37. Yu, R.K.; Ando, S. Structures of some new complex gangliosides of fish brain. *Adv. Exp. Med. Biol.* **1980**, *125*, 33–45, doi:10.1007/978-1-4684-7844-0_5.
38. Jennemann, R.; Sandhoff, R.; Wang, S.; Kiss, E.; Gretz, N.; Zuliani, C.; Martin-Villalba, A.; Jäger, R.; Schorle, H.; Kenzelmann, M.; et al. Cell-specific deletion of glucosylceramide synthase in brain leads to severe neural defects after birth. *Proc. Natl. Acad. Sci. U. S. A.* **2005**, *102*, 12459–12464, doi:10.1073/pnas.0500893102.
39. Ma, Z.; Yang, H.; Peng, L.; Kuhn, C.; Chelariu-Raicu, A.; Mahner, S.; Jeschke, U.; von Schönfeldt, V. Expression of the Carbohydrate Lewis Antigen, Sialyl Lewis A, Sialyl Lewis X, Lewis X, and Lewis Y in the Placental Villi of Patients With Unexplained Miscarriages. *Front. Immunol.* **2021**, *12*, 1–12, doi:10.3389/fimmu.2021.679424.
40. Cooling, L. Blood groups in infection and host susceptibility. *Clin. Microbiol. Rev.* **2015**, *28*, 801–870, doi:10.1128/CMR.00109-14.
41. Daniels, G. *Human blood groups*; second.; Alden Press: Oxford, 2002; ISBN 0-632-056460.
42. Reid, M.E.; Lomas-Francis, C.; Olsson, M.L. ABO Blood Group System. In *The Blood Group Antigen FactsBook*; 2012; pp. 27–51 ISBN 9780124158498.
43. Shan, M.; Yang, D.; Dou, H.; Zhang, L. *Fucosylation in cancer biology and its clinical applications*; 1st ed.; Elsevier Inc., 2019; Vol. 162; ISBN 9780128177389.
44. Ravn, V.; Dabelsteen, E. Tissue distribution of histo-blood group antigens. *Apmis* **2000**, *108*, 1–28, doi:10.1034/j.1600-0463.2000.d01-1.x.
45. Cooling, L.; Down, T. Immunohematology. In *Henry's Clinical diagnosis and Management by Laboratory Methods*; McPherson, R.A., Pincus, M.R., Eds.; Elsevier Saunders: Philadelphia, PA, 2011; pp. 674–730 ISBN 9781437709742.
46. Yamamoto, M.; Yamamoto, F.; Luong, T.T.; Williams, T.; Kominato, Y.; Yamamoto, F. Expression profiling of 68 glycosyltransferase genes in 27 different human tissues by the systematic multiplex reverse transcription-polymerase chain reaction method revealed clustering of sexually related tissues in hierarchial clustering algorithm analy. *Electrophoresis* **2003**, *24*, 2295–2307, doi:10.1002/elps.200305459.
47. Ångström, J.; Larsson, T.; Hansson, G.C.; Karlsson, K.A.; Henry, S. Default biosynthesis pathway for blood group-related glycolipids in human small intestine as defined by structural identification of linear and branched glycosylceramides in a group O Le(a-b-) nonsecretor. *Glycobiology* **2004**, *14*, 1–12, doi:10.1093/glycob/cwh003.
48. Henry, S.M. (a,b); Oriol, R. (c); Samuelsson, B.E. (b) Detection and Characterization of Lewis Antigens in Plasma of Lewis-Negative Individuals. *Vox Sang.* **1994**, *67*, 387–396, doi:10.1159/000462644.
49. Schenkel-Brunner, H. ABO(H) System, Lewis System and Antigens Lex and Ley. In *Human blood groups: chemical and biochemical basis of antigen specificity*; Springer Vienna: Wien, 2000; pp. 54–248 ISBN 978-3-211-83471-8.
50. Dotz, V.; Wuhrer, M. Histo-blood group glycans in the context of personalized medicine. *Biochim. Biophys. Acta - Gen. Subj.* **2016**, *1860*, 1596–1607, doi:10.1016/j.bbagen.2015.12.026.
51. Pruett, S.T.; Bushnev, A.; Hagedorn, K.; Adiga, M.; Haynes, C.A.; Sullards, M.C.; Liotta, D.C.; Merrill, A.H. Biodiversity of sphingoid bases ("sphingosines") and related amino alcohols. *J. Lipid Res.* **2008**, *49*, 1621–1639, doi:10.1194/jlr.R800012-JLR200.

52. Haynes, C.A.; Allegood, J.C.; Sims, K.; Wang, E.W.; Sullards, M.C.; Merrill, A.H. Quantitation of fatty acyl-coenzyme As in mammalian cells by liquid chromatography-electrospray ionization tandem mass spectrometry. *J. Lipid Res.* **2008**, *49*, 1113–1125, doi:10.1194/jlr.D800001-JLR200.
53. Renkonen, O.; Hirvisalo, E.L. Structure of plasma sphingadienine. *J. Lipid Res.* **1969**, *10*, 687–693, doi:10.1016/s0022-2275(20)43032-9.
54. Stewart, M.E.; Downing, D.T. Free Sphingosines of Human Skin Include 6-Hydroxysphingosine and Unusually Long-Chain Dihydrosphingosines. *J. Invest. Dermatol.* **1995**, *105*, 613–618, doi:10.1111/1523-1747.ep12323736.
55. Stewart, M.E.; Downing, D.T. A new 6-hydroxy-4-sphingenine-containing ceramide in human skin. *J. Lipid Res.* **1999**, *40*, 1434–1439, doi:10.1016/s0022-2275(20)33385-x.
56. Merrill, A.H.; Williams, R.D. Utilization of different fatty acyl-CoA thioesters by serine palmitoyltransferase from rat brain. *J. Lipid Res.* **1984**, *25*, 185–188, doi:10.1016/s0022-2275(20)37838-x.
57. Farwanah, H.; Pierstorff, B.; Schmelzer, C.E.H.; Raith, K.; Neubert, R.H.H.; Kolter, T.; Sandhoff, K. Separation and mass spectrometric characterization of covalently bound skin ceramides using LC/APCI-MS and Nano-ESI-MS/MS. *J. Chromatogr. B Anal. Technol. Biomed. Life Sci.* **2007**, *852*, 562–570, doi:10.1016/j.jchromb.2007.02.030.
58. Sonnino, S.; Chigorno, V. Ganglioside molecular species containing C18- and C20-sphingosine in mammalian nervous tissues and neuronal cell cultures. *Biochim. Biophys. Acta - Rev. Biomembr.* **2000**, *1469*, 63–77, doi:10.1016/S0005-2736(00)00210-8.
59. Keränen, A. Fatty acids and long-chain bases of gangliosides of human gastrointestinal mucosa. *Chem. Phys. Lipids* **1976**, *17*, 14–21, doi:10.1016/0009-3084(76)90032-3.
60. Han, X. Lipidomics for studying metabolism. *Nat. Rev. Endocrinol.* **2016**, *12*, 668–679, doi:10.1038/nrendo.2016.98.
61. Karlsson, K.A. Sphingolipid long chain bases. *Lipids* **1970**, *5*, 878–891, doi:10.1007/BF02531119.
62. Karlsson, K.A. On the chemistry and occurrence of sphingolipid long-chain bases. *Chem. Phys. Lipids* **1970**, *5*, 6–43, doi:10.1016/0009-3084(70)90008-3.
63. Degroote, S.; Wolthoorn, J.; Van Meer, G. The cell biology of glycosphingolipids. *Semin. Cell Dev. Biol.* **2004**, *15*, 375–387, doi:10.1016/j.semcdb.2004.03.007.
64. Guo, Z. The structural diversity of natural glycosphingolipids (GSLs). *J. Carbohydr. Chem.* 2022, *41*, 63–154.
65. Barrientos, R.C.; Zhang, Q. Recent advances in the mass spectrometric analysis of glycosphingolipidome – A review. *Anal. Chim. Acta* **2020**, *1132*, 134–155, doi:10.1016/j.aca.2020.05.051.
66. Liebisch, G.; Fahy, E.; Aoki, J.; Dennis, E.A.; Durand, T.; Ejsing, C.S.; Fedorova, M.; Feussner, I.; Griffiths, W.J.; Köfeler, H.; et al. Update on LIPID MAPS classification, nomenclature, and shorthand notation for MS-derived lipid structures. *J. Lipid Res.* **2020**, *61*, 1539–1555, doi:10.1194/jlr.S120001025.
67. Liebisch, G.; Ahrends, R.; Arita, M.; Arita, M.; Bowden, J.A.; Ejsing, C.S.; Griffiths, W.J.; Holčapek, M.; Köfeler, H.; Mitchell, T.W.; et al. Lipidomics needs more standardization. *Nat. Metab.* **2019**, *1*, 745–747, doi:10.1038/s42255-019-0094-z.
68. O'Donnell, V.B.; Ekroos, K.; Liebisch, G.; Wakelam, M. Lipidomics: Current state of the art in a fast moving field. *Wiley Interdiscip. Rev. Syst. Biol. Med.* **2019**, *12*, 1–6, doi:10.1002/wsbm.1466.
69. Chester, M.A. IUPAC-IUB Joint Commission on Biochemical Nomenclature (JCBN). Nomenclature of glycolipids--recommendations 1997. *Eur. J. Biochem.* **1998**, *257*,

293–298, doi:10.1046/j.1432-1327.1998.2570293.x.
70. Liebisch, G.; Vizcaíno, J.A.; Köfeler, H.; Trötzmüller, M.; Griffiths, W.J.; Schmitz, G.; Spener, F.; Wakelam, M.J.O. Shorthand notation for lipid structures derived from mass spectrometry. *J. Lipid Res.* **2013**, *54*, 1523–1530, doi:10.1194/jlr.M033506.
71. Varki, A.; Cummings, R.D.; Aebi, M.; Packer, N.H.; Seeberger, P.H.; Esko, J.D.; Stanley, P.; Hart, G.; Darvill, A.; Kinoshita, T.; et al. Symbol nomenclature for graphical representations of glycans. *Glycobiology* **2015**, *25*, 1323–1324, doi:10.1093/glycob/cwv091.
72. Neelamegham, S.; Aoki-Kinoshita, K.; Bolton, E.; Frank, M.; Lisacek, F.; Lütteke, T.; O'Boyle, N.; Packer, N.H.; Stanley, P.; Toukach, P.; et al. Updates to the Symbol Nomenclature for Glycans guidelines. *Glycobiology* **2019**, *29*, 620–624, doi:10.1093/glycob/cwz045.
73. Groux-Degroote, S.; Guérardel, Y.; Delannoy, P. Gangliosides: Structures, Biosynthesis, Analysis, and Roles in Cancer. *ChemBioChem* **2017**, *18*, 1146–1154, doi:10.1002/cbic.201600705.
74. Schnaar, R.L. Gangliosides of the Vertebrate Nervous System. *J. Mol. Biol.* **2016**, *428*, 3325–3336, doi:10.1016/j.jmb.2016.05.020.
75. Hakomori, S. itiroh Traveling for the glycosphingolipid path. *Glycoconj. J.* **2000**, *17*, 627–647, doi:10.1023/A:1011086929064.
76. Zhang, T.; De Waard, A.A.; Wuhrer, M.; Spaapen, R.M. The role of glycosphingolipids in immune cell functions. *Front. Immunol.* **2019**, *10*, 1–22, doi:10.3389/fimmu.2019.00090.
77. Furukawa, K.; Ohmi, Y.; Ohkawa, Y.; Bhuiyan, R.H.; Zhang, P.; Tajima, O.; Hashimoto, N.; Hamamura, K.; Furukawa, K. New era of research on cancer-associated glycosphingolipids. *Cancer Sci.* **2019**, *110*, 1544–1551, doi:10.1111/cas.14005.
78. Low, J.A.; Magnuson, B.; Tsai, B.; Imperiale, M.J. Identification of Gangliosides GD1b and GT1b as Receptors for BK Virus. *J. Virol.* **2006**, *80*, 1361–1366, doi:10.1128/jvi.80.3.1361-1366.2006.
79. Tsai, B.; Gilbert, J.M.; Stehle, T.; Lencer, W.; Benjamin, T.L.; Rapoport, T.A. Gangliosides are receptors for murine polyoma virus and SV40. *EMBO J.* **2003**, *22*, 4346–4355, doi:10.1093/emboj/cdg439.
80. Kitamura, M.; Takamiya, K.; Aizawa, S.; Furukawa, K.; Furukawa, K. Gangliosides are the binding substances in neural cells for tetanus and botulinum toxins in mice. *Biochim. Biophys. Acta - Mol. Cell Biol. Lipids* **1999**, *1441*, 1–3, doi:10.1016/S1388-1981(99)00140-7.
81. Lingwood, C.A.; Law, H.; Richardson, S.; Petric, M.; Brunton, J.L.; De Grandis, S.; Karmali, M. Glycolipid binding of purified and recombinant Escherichia coli produced verotoxin in vitro. *J. Biol. Chem.* **1987**, *262*, 8834–8839, doi:10.1016/s0021-9258(18)47490-x.
82. Schnaar, R.L. Glycolipid-mediated cell-cell recognition in inflammation and nerve regeneration. *Arch. Biochem. Biophys.* **2004**, *426*, 163–172, doi:10.1016/j.abb.2004.02.019.
83. Hakomori, S.I. The glycosynapse. *Proc. Natl. Acad. Sci. U. S. A.* **2002**, *99*, 225–232, doi:10.1073/pnas.012540899.
84. Schnaar, R.L. Glycosphingolipids in cell surface recognition. *Glycobiology* **1991**, *1*, 477–485, doi:10.1093/glycob/1.5.477.
85. Hakomori, S. Bifunctional role of glycosphingolipids. Modulators for transmembrane signaling and mediators for cellular interactions. *J. Biol. Chem.* **1990**, *265*, 18713–18716, doi:10.1016/s0021-9258(17)30565-3.

86. Hakomori, S.; Handa, K.; Iwabuchi, K.; Yamamura, S.; Prinetti, A. Glyco-Forum section. **1998**, *8*.
87. Iwabuchi, K.; Handa, K.; Hakomori, S. Separation of " Glycosphingolipid Signaling Domain " from Caveolin-containing Membrane Fraction in Mouse Melanoma B16 Cells and Its Role in Cell Adhesion Coupled with Signaling *. **1998**, *273*, 33766–33773.
88. Yates, A.J.; Rampersaud, A. Sphingolipids as receptor modulators: An overview. *Ann. N. Y. Acad. Sci.* **1998**, *845*, 57–71, doi:10.1111/j.1749-6632.1998.tb09662.x.
89. Ho, W.L.; Hsu, W.M.; Huang, M.C.; Kadomatsu, K.; Nakagawara, A. Protein glycosylation in cancers and its potential therapeutic applications in neuroblastoma. *J. Hematol. Oncol.* **2016**, *9*, 1–15, doi:10.1186/s13045-016-0334-6.
90. Nardy, A.F.F.R.; Freire-de-Lima, L.; Freire-de-Lima, C.G.; Morrot, A. The sweet side of immune evasion: Role of Glycans in the Mechanisms of Cancer Progression. *Front. Oncol.* **2016**, *6*, 1–7, doi:10.3389/fonc.2016.00054.
91. Cadena, A.P.; Cushman, T.R.; Welsh, J.W. Glycosylation and Antitumor Immunity. *Int. Rev. Cell Mol. Biol.* **2019**, *343*, 111–127, doi:10.1016/bs.ircmb.2018.05.014.
92. Krengel, U.; Bousquet, P.A. Molecular recognition of gangliosides and their potential for cancer immunotherapies. *Front. Immunol.* **2014**, *5*, 1–11, doi:10.3389/fimmu.2014.00325.
93. Lingwood, C.A.; Hakomori, S. Selective inhibition of cell growth and associated changes in glycolipid metabolism induced by monovalent antibodies to gly. *Exp. Cell Res.* **1977**, *108*, 385–391.
94. Bremer, E.G.; Hakomori, S. GM3 ganglioside induces hamster fibroblast growth inhibition in chemically-defined medium: ganglioside may regulate growth factor receptor function. *Biochem. Biophys. Res. Commun.* **1982**, *106*, 711–718, doi:10.1016/0006-291x(82)91769-7.
95. Bremer, E.; Schlessinger, J.; Hakomori, S. Ganglioside-mediated modulation of cell growth. *J. Biol. Chem.* **1986**, *261*, 2434–2440, doi:10.1016/S0021-9258(17)35954-9.
96. Bremer, E.G.; Hakomori, S.I.; Bowen-Pope, D.F. Ganglioside-mediated modulation of cell growth, growth factor binding, and receptor phosphorylation. *J. Biol. Chem.* **1984**, *259*, 6818–6825, doi:10.1016/s0021-9258(17)39801-0.
97. Ono, M.; Handa, K.; Withers, D.A.; Hakomori, S.I. Motility inhibition and apoptosis are induced by metastasis-suppressing gene product CD82 and its analogue CD9, with concurrent glycosylation. *Cancer Res.* **1999**, *59*, 2335–2339.
98. Zhou, J.; Cox, N.R.; Ewald, S.J.; Morrison, N.E.; Basker, H.J. Evaluation of GMI ganglioside-mediated apoptosis in feline thymocytes. *Vet. Immunol. Immunopathol.* **1998**, *66*, 25–42, doi:10.1016/S0165-2427(98)00180-9.
99. Garcia-Ruiz, C.; Morales, A.; Fernández-Checa, J.C. Glycosphingolipids and cell death: One aim, many ways. *Apoptosis* **2015**, *20*, 607–620, doi:10.1007/s10495-015-1092-6.
100. Lahiri, S.; Futerman, A.H. The metabolism and function of sphingolipids and glycosphingolipids. *Cell. Mol. Life Sci.* **2007**, *64*, 2270–2284, doi:10.1007/s00018-007-7076-0.
101. Hannun, Y.A.; Obeid, L.M. Sphingolipids and their metabolism in physiology and disease. *Nat. Rev. Mol. Cell Biol.* **2018**, *19*, 175–191, doi:10.1038/nrm.2017.107.
102. Groux-Degroote, S.; Rodríguez-Walker, M.; Dewald, J.H.; Daniotti, J.L.; Delannoy, P. Gangliosides in Cancer Cell Signaling. *Prog. Mol. Biol. Transl. Sci.* **2018**, *156*, 197–227, doi:10.1016/bs.pmbts.2017.10.003.
103. Wong, M.; Xu, G.; Park, D.; Barboza, M.; Lebrilla, C.B. Intact glycosphingolipidomic analysis of the cell membrane during differentiation yields extensive glycan and lipid

changes. *Sci. Rep.* **2018**, *8*, 1–10, doi:10.1038/s41598-018-29324-7.
104. Lingwood, C.A. Glycosphingolipid functions. *Cold Spring Harb. Perspect. Biol.* **2011**, *3*, 1–26, doi:10.1101/cshperspect.a004788.
105. Grayson, G.U.Y.; Ladisch, S. Immunosuppression by Human Gangliosides. **1992**, *29*, 18–29.
106. Biswas, S.; Biswas, K.; Richmond, A.; Ko, J.; Ghosh, S.; Simmons, M.; Rayman, P.; Rini, B.; Gill, I.; Tannenbaum, C.S.; et al. Elevated Levels of Select Gangliosides in T Cells from Renal Cell Carcinoma Patients Is Associated with T Cell Dysfunction. *J. Immunol.* **2009**, *183*, 5050–5058, doi:10.4049/jimmunol.0900259.
107. Ando, I.; Hoon, D.S.B.; Suzuki, Y.; Saxton, R.E.; Golub, S.H.; Irie, R.F. Ganglioside GM2 on the K562 cell line is recognized as a target structure by human natural killer cells. *Int. J. Cancer* **1987**, *40*, 12–17, doi:10.1002/ijc.2910400104.
108. Popa, I.; Portoukalian, J. Distribution of Gangliosides in Human Epidermis, Dermis and Whole Skin. *J. Clin. Exp. Dermatol. Res.* **2015**, *6*, 1000282, doi:10.4172/2155-9554.1000282.
109. Coetzee, T.; Suzuki, K.; Popko, B. New perspectives on the function of myelin galactolipids. *Trends Neurosci.* **1998**, *21*, 126–130, doi:10.1016/S0166-2236(97)01178-8.
110. Jennemann, R.; Sandhoff, R.; Langbein, L.; Kaden, S.; Rothermel, U.; Gallala, H.; Sandhoff, K.; Wiegandt, H.; Gröne, H.J. Integrity and barrier function of the epidermis critically depend on glucosylceramide synthesis. *J. Biol. Chem.* **2007**, *282*, 3083–3094, doi:10.1074/jbc.M610304200.
111. Holleran, W.M.; Takagi, Y.; Uchida, Y. Epidermal sphingolipids: Metabolism, function, and roles in skin disorders. *FEBS Lett.* **2006**, *580*, 5456–5466, doi:10.1016/j.febslet.2006.08.039.
112. Patwardhan, G.A.; Liu, Y.Y. Sphingolipids and expression regulation of genes in cancer. *Prog. Lipid Res.* **2011**, *50*, 104–114, doi:10.1016/j.plipres.2010.10.003.
113. Butler, L.M.; Perone, Y.; Dehairs, J.; Lupien, L.E.; de Laat, V.; Talebi, A.; Loda, M.; Kinlaw, W.B.; Swinnen, J. V. Lipids and cancer: Emerging roles in pathogenesis, diagnosis and therapeutic intervention. *Adv. Drug Deliv. Rev.* **2020**, *159*, 245–293, doi:10.1016/j.addr.2020.07.013.
114. Reis, C.A.; Osorio, H.; Silva, L.; Gomes, C.; David, L. Alterations in glycosylation as biomarkers for cancer detection. *J. Clin. Pathol.* **2010**, *63*, 322–329, doi:10.1136/jcp.2009.071035.
115. Munkley, J. The glycosylation landscape of pancreatic cancer (Review). *Oncol. Lett.* **2019**, *17*, 2569–2575, doi:10.3892/ol.2019.9885.
116. Reza, S.; Ugorski, M.; Suchański, J. Glucosylceramide and galactosylceramide, small glycosphingolipids with significant impact on health and disease. *Glycobiology* **2021**, *31*, 1416–1434, doi:10.1093/glycob/cwab046.
117. Meikle, P.J.; Wong, G.; Barlow, C.K.; Kingwell, B.A. Lipidomics: Potential role in risk prediction and therapeutic monitoring for diabetes and cardiovascular disease. *Pharmacol. Ther.* **2014**, *143*, 12–23, doi:10.1016/j.pharmthera.2014.02.001.
118. Jeyakumar, M.; Butters, T.D.; Dwek, R.A.; Platt, F.M. Glycosphingolipid lysosomal storage diseases: Therapy and pathogenesis. *Neuropathol. Appl. Neurobiol.* **2002**, *28*, 343–357, doi:10.1046/j.1365-2990.2002.00422.x.
119. Schulze, H.; Sandhoff, K. Lysosomal lipid storage diseases. *Cold Spring Harb. Perspect. Biol.* **2011**, *3*, 1–19, doi:10.1101/cshperspect.a004804.
120. Sandhoff, K.; Harzer, K. Gangliosides and gangliosidoses: Principles of molecular and metabolic pathogenesis. *J. Neurosci.* **2013**, *33*, 10195–10208, doi:10.1523/JNEUROSCI.0822-13.2013.

121. Van Eijk, M.; Ferra, M.J.; Boot, R.G.; Aerts, J.M.F.G. Lyso-glycosphingolipids: Presence and consequences. *Essays Biochem.* **2020**, *64*, 565–578, doi:10.1042/EBC20190090.
122. Choy, F.Y.M.; Campbell, T.N. Gaucher disease and cancer: Concept and controversy. *Int. J. Cell Biol.* **2011**, *2011*, doi:10.1155/2011/150450.
123. Bird, S.; Hadjimichael, E.; Mehta, A.; Ramaswami, U.; Hughes, D. Fabry disease and incidence of cancer. *Orphanet J. Rare Dis.* **2017**, *12*, 1–8, doi:10.1186/s13023-017-0701-6.
124. Aerts, J.M.; Groener, J.E.; Kuiper, S.; Donker-Koopman, W.E.; Strijland, A.; Ottenhoff, R.; Van Roomen, C.; Mirzaian, M.; Wijburg, F.A.; Linthorst, G.E.; et al. Elevated globotriaosylsphingosine is a hallmark of Fabry disease. *Proc. Natl. Acad. Sci. U. S. A.* **2008**, *105*, 2812–2817, doi:10.1073/pnas.0712309105.
125. Heywood, W.E.; Doykov, I.; Spiewak, J.; Hallqvist, J.; Mills, K.; Nowak, A. Global glycosphingolipid analysis in urine and plasma of female Fabry disease patients. *Biochim. Biophys. Acta - Mol. Basis Dis.* **2019**, *1865*, 2726–2735, doi:10.1016/j.bbadis.2019.07.005.
126. Willison, H.J.; Yuki, N. Peripheral neuropathies and anti-glycolipid antibodies. *Brain* **2002**, *125*, 2591–2625, doi:10.1093/brain/awf272.
127. Fredman, P. The Role of Antiglycolipid Antibodies in Neurological Disorders. *Ann. New York Acad. Sci.* **1988**, *19*, 341–352, doi:10.1111/j.1749-6632.1998.tb09686.x.
128. Yuki, N. Infectious origins of, and molecular mimicry in, Guillain-Barré and Fisher syndromes. *Lancet Infect. Dis.* **2001**, *1*, 29–37, doi:10.1016/S1473-3099(01)00019-6.
129. Jacobs, B.C.; Van Doorn, P.A.; Schmitz, P.I.M.; Tio-Gillen, A.P.; Herbrink, P.; Visser, L.H.; Hooijkaas, H.; Van Der Meché, F.G.A. Campylobacter jejuni infections and anti-GM1 antibodies in Guillain- Barre syndrome. *Ann. Neurol.* **1996**, *40*, 181–187, doi:10.1002/ana.410400209.
130. Takigawa, T.; Yasuda, H.; Kikkawa, R.; Shigeta, Y.; Saida, T.; Kitasato, H. Antibodies against GM1 ganglioside affect K+ and NA+ currents in isolated rat myelinated nerve fibers. *Ann. Neurol.* **1995**, *37*, 436–442, doi:10.1002/ana.410370405.
131. Wirguin, I.; Rosoklija, G.; Trojaborg, W.; Hays, A.P.; Latov, N. Axonal degeneration accompanied by conduction block induced by toxin mediated immune reactivity to GM1 ganglioside in rat nerves. *J. Neurol. Sci.* **1995**, *130*, 17–21, doi:10.1016/0022-510X(94)00270-X.
132. Rosenbluth, J.; Liang, W.L.; Schiff, R.; Dou, W.K. Spinal cord dysmyelination induced in vivo by IgM antibodies to three different myelin glycolipids. *Glia* **1997**, *19*, 58–66, doi:10.1002/(SICI)1098-1136(199701)19:1<58::AID-GLIA6>3.0.CO;2-6.
133. Franklin, R.J.M.; Ffrench-Constant, C. Regenerating CNS myelin - From mechanisms to experimental medicines. *Nat. Rev. Neurosci.* **2017**, *18*, 753–769, doi:10.1038/nrn.2017.136.
134. Cuatrecasas, P. Vibrio cholerae Choleragenoid. Mechanism of Inhibition of Cholera Toxin Action. *Biochemistry* **1973**, *12*, 3577–3581, doi:10.1021/bi00742a034.
135. Svennerholm, L. Interaction of cholera toxin and ganglioside G(M1). *Adv. Exp. Med. Biol.* **1976**, *71*, 191–204, doi:10.1007/978-1-4614-4614-9_12.
136. Merritt, E.A.; Sarfaty, S.; Akker, F. Van Den; L'Hoir, C.; Martial, J.A.; Hol, W.G.J. Crystal structure of cholera toxin B-pentamer bound to receptor GM1 pentasaccharide. *Protein Sci.* **1994**, *3*, 166–175, doi:10.1002/pro.5560030202.
137. Galen, J.E.; Ketley, J.M.; Fasano, A.; Richardson, S.H.; Wasserman, S.S.; Kaper, J.B. Role of Vibrio cholerae neuraminidase in the function of cholera toxin. *Infect. Immun.* **1991**, *60*, 406–415, doi:10.1128/iai.60.2.406-415.1992.
138. Lindner, J.; Geczy, A.F.; Russell-Jones, G.J. Identification of the Site of Uptake of the

E. coli Heat-labile Enterotoxin, LTB. *Scand. J. Immunol.* **1994**, *40*, 564–572, doi:10.1111/j.1365-3083.1994.tb03505.x.
139. Zalem, D.; Ribeiro, J.P.; Varrot, A.; Lebens, M.; Imberty, A.; Teneberg, S. Biochemical and structural characterization of the novel sialic acid-binding site of Escherichia coli heat-labile enterotoxin LT-IIb. *Biochem. J.* **2016**, *473*, 3923–3936, doi:10.1042/BCJ20160575.
140. Tzipori, S.; Chow, C.W.; Powell, H.R. Cerebral infection with Escherichia coli 0157:H7 in humans and gnotobiotic piglets. *J. Clin. Pathol.* **1988**, *41*, 1099–1103, doi:10.1136/jcp.41.10.1099.
141. Karmali, M.A.; Petric, M.; Lim, C.; Fleming, P.C.; Arbus, G.S.; Lior, H. The association between idiopathic hemolytic uremic syndrome and infection by verotoxin-producing Escherichia coli. 1985. *J. Infect. Dis.* **2004**, *189*, 556–563, doi:10.1086/jid/189.3.566.
142. Karmali, M.A.; Gannon, V.; Sargeant, J.M. Verocytotoxin-producing Escherichia coli (VTEC). *Vet. Microbiol.* **2010**, *140*, 360–370, doi:10.1016/j.vetmic.2009.04.011.
143. Mahdavi, J.; Sondén, B.; Hurtig, M.; Olfat, F.O.; Forsberg, L.; Roche, N.; Ångström, J.; Larsson, T.; Teneberg, S.; Karlsson, K.A.; et al. Helicobacter pylori sabA adhesin in persistent infection and chronic inflammation. *Science (80-.).* **2002**, *297*, 573–578, doi:10.1126/science.1069076.
144. Roche, N.; Ångström, J.; Hurtig, M.; Larsson, T.; Borén, T.; Teneberg, S. Helicobacter pylori and Complex Gangliosides. *Infect. Immun.* **2004**, *72*, 1519–1529, doi:10.1128/IAI.72.3.1519-1529.2004.
145. Ångström, J.; Teneberg, S.; Milh, M.A.; Larsson, T.; Leonardsson, I.; Olsson, B.M.; Halvarsson, M.Ö.; Danielsson, D.; Näslund, I.; Ljungh, Å.; et al. The lactosylceramide binding specificity of Helicobacter pylori. *Glycobiology* **1998**, *8*, 297–309, doi:10.1093/glycob/8.4.297.
146. Roche, N.; Ilver, D.; Ångström, J.; Barone, S.; Telford, J.L.; Teneberg, S. Human gastric glycosphingolipids recognized by Helicobacter pylori vacuolating cytotoxin VacA. *Microbes Infect.* **2007**, *9*, 605–614, doi:10.1016/j.micinf.2007.01.023.
147. Kurek, K.; Łukaszuk, B.; Piotrowska, D.M.; Wiesiołek, P.; Chabowska, A.M.; Zendzian-Piotrowska, M. Metabolism, physiological role, and clinical implications of sphingolipids in gastrointestinal tract. *Biomed Res. Int.* **2013**, *2013*, doi:10.1155/2013/908907.
148. Miyoshi, E.; Moriwaki, K.; Nakagawa, T. Biological function of fucosylation in cancer biology. *J. Biochem.* **2008**, *143*, 725–729, doi:10.1093/jb/mvn011.
149. Delannoy, C.P.; Rombouts, Y.; Groux-Degroote, S.; Holst, S.; Coddeville, B.; Harduin-Lepers, A.; Wuhrer, M.; Elass-Rochard, E.; Guérardel, Y. Glycosylation Changes Triggered by the Differentiation of Monocytic THP-1 Cell Line into Macrophages. *J. Proteome Res.* **2017**, *16*, 156–169, doi:10.1021/acs.jproteome.6b00161.
150. Schömel, N.; Geisslinger, G.; Wegner, M.S. Influence of glycosphingolipids on cancer cell energy metabolism. *Prog. Lipid Res.* **2020**, *79*, 101050, doi:10.1016/j.plipres.2020.101050.
151. Don, A.S.; Lim, X.Y.; Couttas, T.A. Re-configuration of sphingolipid metabolism by oncogenic transformation. *Biomolecules* 2014, *4*, 315–353.
152. Wennekes, T.; Van Den Berg, R.J.B.H.N.; Boot, R.G.; Van Der Marel, G.A.; Overkleeft, H.S.; Aerts, J.M.F.G. Glycosphingolipids - Nature, function, and pharmacological modulation. *Angew. Chemie - Int. Ed.* **2009**, *48*, 8848–8869, doi:10.1002/anie.200902620.
153. Astudillo, L.; Therville, N.; Colacios, C.; Ségui, B.; Andrieu-Abadie, N.; Levade, T.

Glucosylceramidases and malignancies in mammals. *Biochimie* **2016**, *125*, 267–280, doi:10.1016/j.biochi.2015.11.009.
154. Natoli, T.A.; Smith, L.A.; Rogers, K.A.; Wang, B.; Komarnitsky, S.; Budman, Y.; Belenky, A.; Bukanov, N.O.; Dackowski, W.R.; Husson, H.; et al. Inhibition of glucosylceramide accumulation results in effective blockade of polycystic kidney disease in mouse models. *Nat. Med.* **2010**, *16*, 788–792, doi:10.1038/nm.2171.
155. Russo, D.; Capolupo, L.; Loomba, J.S.; Sticco, L.; D'Angelo, G. Glycosphingolipid metabolism in cell fate specification. *J. Cell Sci.* **2018**, *131*, 1–11, doi:10.1242/jcs.219204.
156. Giussani, P.; Tringali, C.; Riboni, L.; Viani, P.; Venerando, B. Sphingolipids: Key regulators of apoptosis and pivotal players in cancer drug resistance. *Int. J. Mol. Sci.* **2014**, *15*, 4356–4392, doi:10.3390/ijms15034356.
157. Hakomori, S. itiroh Aberrant Glycosylation In Tumors And Tumor-Associated Carbohydrate Antigens. *Adv. Cancer Res.* **1989**, *52*, 257–331, doi:10.1016/S0065-230X(08)60215-8.
158. Jennemann, R.; Rodden, A.; Bauer, B.L.; Mennel, H.D.; Wiegandt, H. Glycosphingolipids of Human Gliomas. *Cancer Res.* **1990**, *50*, 7444–7449.
159. Pukel, C.S.; Lloyd, K.O.; Travassos, L.R.; Dippold, W.G.; Oettgen, H.F.; Old, L.J. GD3, a prominent ganglioside of human melanoma. Detection and characterisation by mouse monoclonal antibody. *J. Exp. Med.* **1982**, *155*, doi:10.1084/jem.155.4.1133.
160. Baumann, H.; Nudelman, E.; Watanabe, K.; Hakomori, S.I. Neutral Fucolipids and Fucogangliosides of Rat Hepatoma HTC and H35 Cells, Rat Liver, and Hepatocytes. *Cancer Res.* **1979**, *39*, 2637–2643.
161. Lai, T.Y.; Chen, I.J.; Lin, R.J.; Liao, G.S.; Yeo, H.L.; Ho, C.L.; Wu, J.C.; Chang, N.C.; Lee, A.C.L.; Yu, A.L. Fucosyltransferase 1 and 2 play pivotal roles in breast cancer cells. *Cell Death Discov.* **2019**, *5*, doi:10.1038/s41420-019-0145-y.
162. Yang, J.M.; Byrd, J.C.; Siddiki, B.B.; Chung, Y.S.; Okuno, M.; Sowa, M.; Kim, Y.S.; Matta, K.L.; Brockhausen, I. Alterations of O-glycan biosynthesis in human colon cancer tissues. *Glycobiology* **1994**, *4*, 873–884, doi:10.1093/glycob/4.6.873.
163. Yang, X.S.; Liu, S.; Liu, Y.J.; Liu, J.W.; Liu, T.J.; Wang, X.Q.; Yan, Q. Overexpression of fucosyltransferase IV promotes A431 cell proliferation through activating MAPK and PI3K/Akt signaling pathways. *J. Cell. Physiol.* **2010**, *225*, 612–619, doi:10.1002/jcp.22250.
164. Liang, L.; Gao, C.; Li, Y.; Sun, M.; Xu, J.; Li, H.; Jia, L.; Zhao, Y. MiR-125a-3p/FUT5-FUT6 axis mediates colorectal cancer cell proliferation, migration, invasion and pathological angiogenesis via PI3K-Akt pathway. *Cell Death Dis.* **2017**, *8*, e2968-10, doi:10.1038/cddis.2017.352.
165. Guo, Q.; Guo, B.; Wang, Y.; Wu, J.; Jiang, W.; Zhao, S.; Qiao, S.; Wu, Y. Functional analysis of α1,3/4-fucosyltransferase VI in human hepatocellular carcinoma cells. *Biochem. Biophys. Res. Commun.* **2012**, *417*, 311–317, doi:10.1016/j.bbrc.2011.11.106.
166. Liang, J. xiao; Gao, W.; Cai, L. Fucosyltransferase VII promotes proliferation via the EGFR/AKT/mTOR pathway in A549 cells. *Onco. Targets. Ther.* **2017**, *10*, 3971–3978, doi:10.2147/OTT.S140940.
167. Yang, X.; Liu, Y.; Liu, J.; Wang, X.; Yan, Q. Cyclophosphamide-induced apoptosis in A431 cells is inhibited by fucosyltransferase IV. *J. Cell. Biochem.* **2011**, *112*, 1376–1383, doi:10.1002/jcb.23054.
168. Daniels, G. Blood groups on red cells, platelets and neutrophils. In *Blood and Bone Marrow Pathology: Expert Consult*; Elsevier Ltd, 2011; pp. 599–617 ISBN 9780702045356.

169. Miyoshi, E.; Moriwaki, K.; Terao, N.; Tan, C.C.; Terao, M.; Nakagawa, T.; Matsumoto, H.; Shinzaki, S.; Kamada, Y. Fucosylation is a promising target for cancer diagnosis and therapy. *Biomolecules* **2012**, *2*, 34–45, doi:10.3390/biom2010034.
170. Zhuo, D.; Li, X.; Guan, F. Biological roles of aberrantly expressed glycosphingolipids and related enzymes in human cancer development and progression. *Front. Physiol.* **2018**, *9*, 1–9, doi:10.3389/fphys.2018.00466.
171. Hakomori, S.I. Cancer-associated glycosphingolipid antigens: Their structure, organization, and function. *Acta Anat. (Basel).* **1998**, *161*, 79–90, doi:10.1159/000046451.
172. Hakomori, S.I.; Zhang, Y. Glycosphingolipid antigens and cancer therapy. *Chem. Biol.* **1997**, *4*, 97–104, doi:10.1016/S1074-5521(97)90253-2.
173. Jirásko, R.; Holčapek, M.; Khalikova, M.; Vrána, D.; Študent, V.; Prouzová, Z.; Melichar, B. MALDI Orbitrap Mass Spectrometry Profiling of Dysregulated Sulfoglycosphingolipids in Renal Cell Carcinoma Tissues. *J. Am. Soc. Mass Spectrom.* **2017**, *28*, 1562–1574, doi:10.1007/s13361-017-1644-9.
174. Hájek, R.; Lísa, M.; Khalikova, M.; Jirásko, R.; Cífková, E.; Študent, V.; Vrána, D.; Opálka, L.; Vávrová, K.; Matzenauer, M.; et al. HILIC/ESI-MS determination of gangliosides and other polar lipid classes in renal cell carcinoma and surrounding normal tissues. *Anal. Bioanal. Chem.* **2018**, *410*, 6585–6594, doi:10.1007/s00216-018-1263-8.
175. Sakakibara, N.; Gasa, S.; Kamio, K.; Makita, A.; Koyanagi, T. Association of Elevated Sulfatides and Sulfotransferase Activities with Human Renal Cell Carcinoma. *Cancer Res.* **1989**, *49*, 335–339.
176. Jirásko, R.; Idkowiak, J.; Wolrab, D.; Kvasnička, A.; Friedecký, D.; Polański, K.; Študentová, H.; Študent, V.; Melichar, B.; Holčapek, M. Altered Plasma, Urine, and Tissue Profiles of Sulfatides and Sphingomyelins in Patients with Renal Cell Carcinoma. *Cancers (Basel).* **2022**, *14*, 1–19, doi:10.3390/cancers14194622.
177. Kim, I.C.; Bang, G.; Lee, J.H.; Kim, K.P.; Kim, Y.H.; Kim, H.K.; Chung, J. Low C24-OH and C22-OH sulfatides in human renal cell carcinoma. *J. Mass Spectrom.* **2014**, *49*, 409–416, doi:10.1002/jms.3358.
178. Morichika, H.; Hamanaka, Y.; Tai, T.; Ishizuka, I. Sulfatides as a predictive factor of lymph node metastasis in patients with colorectal adenocarcinoma. *Cancer* **1996**, *78*, 43–47, doi:10.1002/(SICI)1097-0142(19960701)78:1<43::AID-CNCR8>3.0.CO;2-I.
179. Liu, Y.; Chen, Y.; Momin, A.; Shaner, R.; Wang, E.; Bowen, N.J.; Matyunina, L. V.; Walker, L.D.; McDonald, J.F.; Sullards, M.C.; et al. Elevation of sulfatides in ovarian cancer: An integrated transcriptomic and lipidomic analysis including tissue-imaging mass spectrometry. *Mol. Cancer* **2010**, *9*, 1–13, doi:10.1186/1476-4598-9-186.
180. Honke, K.; Tsuda, M.; Hirahara, Y.; Miyao, N.; Tsukamoto, T.; Satoh, M.; Wada, Y. Cancer-associated expression of glycolipid sulfotransferase gene in human renal cell carcinoma cells. *Cancer Res.* **1998**, *58*, 3800–3805.
181. Wu, X.Z.; Honke, K.; Zhang, Y.L.; Zha, X.L.; Taniguchi, N. Lactosylsulfatide expression in hepatocellular carcinoma cells enhances cell adhesion to vitronectin and intrahepatic metastasis in nude mice. *Int. J. Cancer* **2004**, *110*, 504–510, doi:10.1002/ijc.20127.
182. Hiraiwa, N.; Kannagi, R.; Hiraiwa, N.; Fukuda, Y.; Imura, H.; Tadano-Aritomi, K.; Nagai, K.I.; Ishizuka, I. Accumulation of Highly Acidic Sulfated Glycosphingolipids in Human Hepatocellular Carcinoma Defined by a Series of Monoclonal Antibodies. *Cancer Res.* **1990**, *50*, 2917–2928.
183. Shida, K.; Misonou, Y.; Korekane, H.; Seki, Y.; Noura, S.; Ohue, M.; Honke, K.; Miyamoto, Y. Unusual accumulation of sulfated glycosphingolipids in colon cancer

cells. *Glycobiology* **2009**, *19*, 1018–1033, doi:10.1093/glycob/cwp083.
184. Kwak, D.H.; Ryu, J.S.; Kim, C.H.; Ko, K.; Ma, J.Y.; Hwang, K.A.; Choo, Y.K. Relationship between ganglioside expression and anti-cancer effects of the monoclonal antibody against epithelial cell adhesion molecule in colon cancer. *Exp. Mol. Med.* **2011**, *43*, 693–701, doi:10.3858/emm.2011.43.12.080.
185. Portoukalian, J.; Zwingelstein, G.; Doré, J. -F Lipid Composition of Human Malignant Melanoma Tumors at Various Levels of Malignant Growth. *Eur. J. Biochem.* **1979**, *94*, 19–23, doi:10.1111/j.1432-1033.1979.tb12866.x.
186. Tsuchida, T.; Irie, R.F.; Ishibashi, Y. Gangliosides of Human Melanoma. *Pigment Cell Res.* **1990**, *3*, 147–150, doi:10.1111/j.1600-0749.1990.tb00365.x.
187. Hamilton, W.B.; Helling, F.; Lloyd, K.O.; Livingston, P.O. Ganglioside expression on human malignant melanoma assessed by quantitative immune thin-layer chromatography. *Int. J. Cancer* **1993**, *53*, 566–573, doi:10.1002/ijc.2910530407.
188. Tai, T.; Paulson, J.C.; Cahan, L.D.; Irie, R.F. Ganglioside GM2 as a human tumor antigen (OFA-I-1). *Proc. Natl. Acad. Sci. U. S. A.* **1983**, *80*, 5392–5396, doi:10.1073/pnas.80.17.5392.
189. Yuko Yuyama, V.D.; Dohi, T.; Morita, H.; Furukawa, K.; Oshima, M. Enhanced expression of GM2/GD2 synthase mRNA in human gastrointestinal cancer. *Cancer* **1995**, *75*, 1273–1280, doi:10.1002/1097-0142(19950315)75:6<1273::AID-CNCR2820750609>3.0.CO;2-O.
190. Yamada, T.; Bando, H.; Takeuchi, S.; Kita, K.; Li, Q.; Wang, W.; Akinaga, S.; Nishioka, Y.; Sone, S.; Yano, S. Genetically engineered humanized anti-ganglioside GM2 antibody against multiple organ metastasis produced by GM2-expressing small-cell lung cancer cells. *Cancer Sci.* **2011**, *102*, 2157–2163, doi:10.1111/j.1349-7006.2011.02093.x.
191. Liang, Y.J.; Ding, Y.; Levery, S.B.; Lobaton, M.; Handa, K.; Hakomori, S.I. Differential expression profiles of glycosphingolipids in human breast cancer stem cells vs. cancer non-stem cells. *Proc. Natl. Acad. Sci. U. S. A.* **2013**, *110*, 4968–4973, doi:10.1073/pnas.1302825110.
192. Sasaki, N.; Hirabayashi, K.; Michishita, M.; Takahashi, K.; Hasegawa, F.; Gomi, F.; Itakura, Y.; Nakamura, N.; Toyoda, M.; Ishiwata, T. Ganglioside GM2, highly expressed in the MIA PaCa-2 pancreatic ductal adenocarcinoma cell line, is correlated with growth, invasion, and advanced stage. *Sci. Rep.* **2019**, *9*, 1–13, doi:10.1038/s41598-019-55867-4.
193. Sarbu, M.; Clemmer, D.E.; Zamfir, A.D. Ion mobility mass spectrometry of human melanoma gangliosides. *Biochimie* **2020**, *177*, 226–237, doi:10.1016/j.biochi.2020.08.011.
194. Yoshida, S.; Fukumoto, S.; Kawaguchi, H.; Sato, S.; Ueda, R.; Furukawa, K. Ganglioside GD2 in small cell lung cancer cell lines: Enhancement of cell proliferation and mediation of apoptosis. *Cancer Res.* **2001**, *61*, 4244–4252.
195. Lin, L.; Huang, Z.; Gao, Y.; Chen, Y.; Hang, W.; Xing, J.; Yan, X. LC-MS-based serum metabolic profiling for genitourinary cancer classification and cancer type-specific biomarker discovery. *Proteomics* **2012**, *12*, 2238–2246, doi:10.1002/pmic.201200016.
196. Saito, S.; Orikasa, S.; Ohyama, C.; Satoh, M.; Fukushi, Y. Changes in glycolipids in human renal-cell carcinoma and their clinical significance. *Int. J. Cancer* **1991**, *49*, 329–334, doi:10.1002/ijc.2910490303.
197. Wang, Z.; Wen, L.; Ma, X.; Chen, Z.; Yu, Y.; Zhu, J.; Wang, Y.; Liu, Z.; Liu, H.; Wu, D.; et al. High expression of lactotriaosylceramide, a differentiation-associated glycosphingolipid, in the bone marrow of acute myeloid leukemia patients.

Glycobiology **2012**, *22*, 930–938, doi:10.1093/glycob/cws061.
198. Wang, H.; Isaji, T.; Satoh, M.; Li, D.; Arai, Y.; Gu, J. Antitumor effects of exogenous ganglioside gm3 on bladder cancer in an orthotopic cancer model. *Urology* **2013**, *81*, 210.e11-210.e15, doi:10.1016/j.urology.2012.08.015.
199. Prinetti, A.; Cao, T.; Illuzzi, G.; Prioni, S.; Aureli, M.; Gagliano, N.; Tredici, G.; Rodriguez-Menendez, V.; Chigorno, V.; Sonnino, S. A glycosphingolipid/caveolin-1 signaling complex inhibits motility of human ovarian carcinoma cells. *J. Biol. Chem.* **2011**, *286*, 40900–40910, doi:10.1074/jbc.M111.286146.
200. Chung, T.W.; Choi, H.J.; Kim, S.J.; Kwak, C.H.; Song, K.H.; Jin, U.H.; Chang, Y.C.; Chang, H.W.; Lee, Y.C.; Ha, K.T.; et al. The ganglioside GM3 is associated with cisplatin-induced apoptosis in human colon cancer cells. *PLoS One* **2014**, *9*, doi:10.1371/journal.pone.0092786.
201. Popa, I.; Pons, A.; Mariller, C.; Tai, T.; Zanetta, J.P.; Thomas, L.; Portoukalian, J. Purification and structural characterization of de-N-acetylated form of GD3 ganglioside present in human melanoma tumors. *Glycobiology* **2007**, *17*, 367–373, doi:10.1093/glycob/cwm006.
202. Yan, Q.; Bach, D.Q.; Gatla, N.; Sun, P.; Liu, J.W.; Lu, J.Y.; Paller, A.S.; Wang, X.Q. Deacetylated GM3 promotes uPAR-associated membrane molecular complex to activate p38 MAPK in metastatic melanoma. *Mol. Cancer Res.* **2013**, *11*, 665–675, doi:10.1158/1541-7786.MCR-12-0270-T.
203. Sung, C. -C; Pearl, D.K.; Coons, S.W.; Scheithauer, B.W.; Johnson, P.C.; Yates, A.J. Gangliosides as diagnostic markers of human astrocytomas and primitive neuroectodermal tumors. *Cancer* **1994**, *74*, 3010–3022, doi:10.1002/1097-0142(19941201)74:11<3010::AID-CNCR2820741119>3.0.CO;2-I.
204. Marquina, G.; Waki, H.; Fernandez, L.E.; Kon, K.; Carr, A.; Valiente, O.; Perez, R.; Ando, S. Gangliosides expressed in human breast cancer. *Cancer Res.* **1996**, *56*, 5165–5171.
205. van Cruijsen, H.; Ruiz, M.; van der Valk, P.; de Gruijl, T.D.; Giaccone, G. Tissue micro array analysis of ganglioside N-glycolyl GM3 expression and signal transducer and activator of transcription (STAT)-3 activation in relation to dendritic cell infiltration and microvessel density in non-small cell lung cancer. *BMC Cancer* **2009**, *9*, 1–9, doi:10.1186/1471-2407-9-180.
206. Higashi, H.; Fukui, Y.; Ueda, S.; Kato, S.; Matsumoto, M.; Naiki, M. Characterization of N-Glycolylneuraminic Acid-containing Gangliosides as Tumor-associated Hanganutziu-Deicher Antigen in Human Colon Cancer. *Cancer Res.* **1985**, *45*, 3796–3802.
207. Labrada, M.; Dorvignit, D.; Hevia, G.; Rodríguez-Zhurbenko, N.; Hernández, A.M.; Vázquez, A.M.; Fernández, L.E. GM3(Neu5Gc) ganglioside: an evolution fixed neoantigen for cancer immunotherapy. *Semin. Oncol.* 2018, *45*, 41–51.
208. Hatano, K.; Miyamoto, Y.; Nonomura, N.; Kaneda, Y. Expression of gangliosides, GD1a, and sialyl paragloboside is regulated by NF-κB-dependent transcriptional control of α2,3-sialyltransferase I, II, and VI in human castration-resistant prostate cancer cells. *Int. J. Cancer* **2011**, *129*, 1838–1847, doi:10.1002/ijc.25860.
209. Comas, T.C.; Tai, T.; Kimmel, D.; Scheithauer, B.W.; Burger, P.C.; Pearl, D.K.; Jewell, S.D.; Yates, A.J. Immunohistochemical staining for ganglioside GD1b as a diagnostic and prognostic marker for primary human brain tumors. *Neuro. Oncol.* **1999**, *1*, 261–267, doi:10.1093/neuonc/1.4.261.
210. Ha, S.H.; Lee, J.M.; Kwon, K.M.; Kwak, C.H.; Abekura, F.; Park, J.Y.; Cho, S.H.; Lee, K.; Chang, Y.C.; Lee, Y.C.; et al. Exogenous and endogeneous disialosyl ganglioside GD1b induces apoptosis of MCF-7 human breast cancer cells. *Int. J. Mol.*

Sci. **2016**, *17*, 1–16, doi:10.3390/ijms17050652.
211. Navid, F.; Santana, V.M.; Barfield, R.C. Anti-GD2 Antibody Therapy for GD2-Expressing Tumors. *Curr. Cancer Drug Targets* **2010**, *10*, 200–209.
212. Cheresh, D.A.; Pierschbacher, M.D.; Herzig, M.A.; Mujoo, K. Disialogangliosides GD2 and GD3 are involved in the attachment of human melanoma and neuroblastoma cells to extracellular matrix proteins. *J. Cell Biol.* **1986**, *102*, 688–696, doi:10.1083/jcb.102.3.688.
213. Saito, K.; Yu, R.K.; Cheung, N.K. V. Ganglioside GD2 specificity of monoclonal antibodies to human neuroblastoma cell. *Biochem. Biophys. Res. Commun.* **1985**, *127*, 1–7, doi:10.1016/s0006-291x(85)80117-0.
214. Schengrund, C.L.; Shochat, S.J. Gangliosides in Neuroblastomas. *Neurochem. Pathol.* **1988**, *8*, 189–202, doi:10.1007/BF03160146.
215. Hettmer, S.; Ladisch, S.; Kaucic, K. Low complex ganglioside expression characterizes human. **2005**, *225*, 141–149, doi:10.1016/j.canlet.2004.11.036.
216. Wu, Z.L.; Schwartz, E.; Ladisch, S.; Seeger, R. Expression of GD2 ganglioside by untreated primary human neuroblastomas. *Cancer Res.* **1986**, *46*, 440–443.
217. Mujoo, K.; Cheresh, D.A.; Yang, H.M.; Reisfeld, R.A. Disialoganglioside GD2 on Human Neuroblastoma Cells: Target Antigen for Monoclonal Antibody-mediated Cytolysis and Suppression of Tumor Growth. *Cancer Res.* **1987**, *47*, 1098–1104.
218. Cahan, L.D.; Irie, R.F.; Singh, R.; Cassidenti, A.; Paulson, J.C. Identification of a human neuroectodermal tumor antigen (OFA-I-2) as ganglioside GD2. *Proc. Natl. Acad. Sci. U. S. A.* **1982**, *79*, 7629–7633, doi:10.1073/pnas.79.24.7629.
219. Yang, R.K.; Sondel, P.M. Anti-GD2 strategy in the treatment of neuroblastoma. *Drugs Future* 2010, *35*, 665–673.
220. Shibuya, H.; Hamamura, K.; Hotta, H.; Matsumoto, Y.; Nishida, Y.; Hattori, H.; Furukawa, K.; Ueda, M.; Furukawa, K. Enhancement of malignant properties of human osteosarcoma cells with disialyl gangliosides GD2/GD3. *Cancer Sci.* **2012**, *103*, 1656–1664, doi:10.1111/j.1349-7006.2012.02344.x.
221. Dobrenkov, K.; Ostrovnaya, I.; Gu, J.; Cheung, I.Y.; Cheung, N.K. V. Oncotargets GD2 and GD3 are highly expressed in sarcomas of children, adolescents, and young adults. *Pediatr. Blood Cancer* **2016**, *63*, 1780–1785, doi:10.1002/pbc.26097.
222. Cheresh, D.A.; Rosenberg, J.; Mujoo, K.; Hirschowitz, L.; Reisfeld, R.A. Biosynthesis and Expression of the Disialoganglioside GD2, a Relevant Target Antigen on Small Cell Lung Carcinoma for Monoclonal Antibody-mediated Cytolysis. *Cancer Res.* **1986**, *46*, 5112–5118, doi:10.1016/s0169-5002(87)80034-x.
223. Cazet, A.; Bobowski, M.; Rombouts, Y.; Lefebvre, J.; Steenackers, A.; Popa, I.; Guérardel, Y.; Le Bourhis, X.; Tulasne, D.; Delannoy, P. The ganglioside GD2 induces the constitutive activation of c-Met in MDA-MB-231 breast cancer cells expressing the GD3 synthase. *Glycobiology* **2012**, *22*, 806–816, doi:10.1093/glycob/cws049.
224. Cazet, A.; Groux-Degroote, S.; Teylaert, B.; Kwon, K.M.; Lehoux, S.; Slomianny, C.; Kim, C.H.; Le Bourhis, X.; Delannoy, P. GD3 synthase overexpression enhances proliferation and migration of MDA-MB-231 breast cancer cells. *Biol. Chem.* **2009**, *390*, 601–609, doi:10.1515/BC.2009.054.
225. Battula, V.L.; Shi, Y.; Evans, K.W.; Wang, R.Y.; Spaeth, E.L.; Jacamo, R.O.; Guerra, R.; Sahin, A.A.; Marini, F.C.; Hortobagyi, G.; et al. Ganglioside GD2 identifies breast cancer stem cells and promotes tumorigenesis. *J. Clin. Invest.* **2012**, *122*, 2066–2078, doi:10.1172/JCI59735.
226. Lin, J.J.; Huang, C.S.; Yu, J.; Liao, G.S.; Lien, H.C.; Hung, J.T.; Lin, R.J.; Chou, F.P.; Yeh, K.T.; Yu, A.L. Malignant phyllodes tumors display mesenchymal stem cell features and aldehyde dehydrogenase/disialoganglioside identify their tumor stem cells.

Breast Cancer Res. **2014**, *16*, 1–13, doi:10.1186/bcr3631.
227. Portoukalian, J.; David, M. -J; Richard, M.; Gain, P. Shedding of GD2 ganglioside in patients with retinoblastoma. *Int. J. Cancer* **1993**, *53*, 948–951, doi:10.1002/ijc.2910530614.
228. Furukawa, K.; Kambe, M.; Miyata, M.; Ohkawa, Y.; Tajima, O.; Furukawa, K. Ganglioside GD3 induces convergence and synergism of adhesion and hepatocyte growth factor/Met signals in melanomas. *Cancer Sci.* **2014**, *105*, 52–63, doi:10.1111/cas.12310.
229. Kaneko, K.; Ohkawa, Y.; Hashimoto, N.; Ohmi, Y.; Kotani, N.; Honke, K.; Ogawa, M.; Okajima, T.; Furukawa, K.; Furukawa, K. Neogenin, defined as a GD3-associated molecule by enzyme-mediated activation of radical sources, confers malignant properties via intracytoplasmic domain in melanoma cells. *J. Biol. Chem.* **2016**, *291*, 16630–16643, doi:10.1074/jbc.M115.708834.
230. Makino, Y.; Hamamura, K.; Takei, Y.; Bhuiyan, R.H.; Ohkawa, Y.; Ohmi, Y.; Nakashima, H.; Furukawa, K.; Furukawa, K. A therapeutic trial of human melanomas with combined small interfering RNAs targeting adaptor molecules p130Cas and paxillin activated under expression of ganglioside GD3. *Biochim. Biophys. Acta - Gen. Subj.* **2016**, *1860*, 1753–1763, doi:10.1016/j.bbagen.2016.04.005.
231. Cheresh, D.A.; Honsik, C.J.; Staffileno, L.K.; Jung, G.; Reisfeld, R.A. Disialoganglioside GD3 on human melanoma serves as a relevant target antigen for monoclonal antibody-mediated tumor cytolysis. *Proc. Natl. Acad. Sci. U. S. A.* **1985**, *82*, 5155–5159, doi:10.1073/pnas.82.15.5155.
232. Merritt, W.D.; Casper, J.T.; Lauer, S.J.; Reaman, G.H. Expression of GD3 Ganglioside in Childhood T-Cell Lymphoblastic Malignancies1. **1987**, 1724–1730.
233. Fredman, P.; von Holst, H.; Collins, V.P.; Dellheden, B.; Svennerholm, L. Expression of Gangliosides GD3 and 3′-isoLM1 in Autopsy Brains from Patients with Malignant Tumors. *J. Neurochem.* **1993**, *60*, 99–105, doi:10.1111/j.1471-4159.1993.tb05827.x.
234. Berra, B.; Gaini, S.M.; Riboni, L. Correlation between ganglioside distribution and histological grading of human astrocytomas. *Int. J. Cancer* **1985**, *36*, 363–366, doi:10.1002/ijc.1985.36.3.363.
235. Webb, T.J.; Li, X.; Giuntoli, R.L.; Lopez, P.H.H.; Heuser, C.; Schnaar, R.L.; Tsuji, M.; Kurts, C.; Oelke, M.; Schneck, J.P. Molecular identification of GD3 as a suppressor of the innate immune response in ovarian cancer. *Cancer Res.* **2012**, *72*, 3744–3752, doi:10.1158/0008-5472.CAN-11-2695.
236. Fuentes, R.; Allman, R.; Mason, M.D. Ganglioside expression in lung cancer cell lines. *Lung Cancer* **1997**, *18*, 21–33, doi:10.1016/S0169-5002(97)00049-4.
237. Brezicka, T.; Bergman, B.; Olling, S.; Fredman, P. Reactivity of monoclonal antibodies with ganglioside antigens in human small cell lung cancer tissues. *Lung Cancer* **2000**, *28*, 29–36, doi:10.1016/S0169-5002(99)00107-5.
238. Sivasubramaniyan, K.; Harichandan, A.; Schilbach, K.; Mack, A.F.; Bedke, J.; Stenzl, A.; Kanz, L.; Niederfellner, G.; Bühring, H.J. Expression of stage-specific embryonic antigen-4 (SSEA-4) defines spontaneous loss of epithelial phenotype in human solid tumor cells. *Glycobiology* **2015**, *25*, 902–917, doi:10.1093/glycob/cwv032.
239. Höfner, T.; Klein, C.; Eisen, C.; Rigo-Watermeier, T.; Haferkamp, A.; Sprick, M.R. Protein profile of basal prostate epithelial progenitor cells-stage-specific embryonal antigen 4 expressing cells have enhanced regenerative potential in vivo. *J. Cell. Mol. Med.* **2016**, *20*, 721–730, doi:10.1111/jcmm.12785.
240. Aloia, A.; Petrova, E.; Tomiuk, S.; Bissels, U.; Déas, O.; Saini, M.; Zickgraf, F.M.; Wagner, S.; Spaich, S.; Sütterlin, M.; et al. The sialyl-glycolipid stage-specific embryonic antigen 4 marks a subpopulation of chemotherapy-resistant breast cancer

cells with mesenchymal features. *Breast Cancer Res.* **2015**, *17*, 1–17, doi:10.1186/s13058-015-0652-6.
241. Lou, Y.W.; Wang, P.Y.; Yeh, S.C.; Chuang, P.K.; Li, S.T.; Wu, C.Y.; Khoo, K.H.; Hsiao, M.; Hsu, T.L.; Wong, C.H. Stage-specific embryonic antigen-4 as a potential therapeutic target in glioblastoma multiforme and other cancers. *Proc. Natl. Acad. Sci. U. S. A.* **2014**, *111*, 2482–2487, doi:10.1073/pnas.1400283111.
242. Saito, S.; Levery, S.B.; Salyan, M.E.K.; Goldberg, R.I.; Hakomori, S.I. Common tetrasaccharide epitope NeuAcα2→3Galβ1→3(NeuAcα2→6)GalNAc, presented by different carrier glycosylceramides or O-linked peptides, is recognized by different antibodies and ligands having distinct specificities. *J. Biol. Chem.* **1994**, *269*, 5644–5652, doi:10.1016/s0021-9258(17)37509-9.
243. Satoh, M.; Handa, K.; Saito, S.; Tokuyama, S.; Ito, A.; Miyao, N.; Orikasa, S.; Hakomori, S.I. Disialosyl galactosylgloboside as an adhesion molecule expressed on renal cell carcinoma and its relationship to metastatic potential. *Cancer Res.* **1996**, *56*, 1932–1938.
244. Kawasaki, Y.; Ito, A.; Kakoi, N.; Shimada, S.; Itoh, J.; Mitsuzuka, K.; Arai, Y. Ganglioside, disialosyl globopentaosylceramide (DSGB5), enhances the migration of renal cell carcinoma cells. *Tohoku J. Exp. Med.* **2015**, *236*, 1–7, doi:10.1620/tjem.236.1.
245. Shimada, S.; Ito, A.; Kawasaki, Y.; Kakoi, N.; Taima, T.; Mitsuzuka, K.; Watanabe, M.; Saito, S.; Arai, Y. Ganglioside disialosyl globopentaosylceramide is an independent predictor of PSA recurrence-free survival following radical prostatectomy. *Prostate Cancer Prostatic Dis.* **2014**, *17*, 199–205, doi:10.1038/pcan.2014.9.
246. Wu, C.S.; Yen, C.J.; Chou, R.H.; Li, S.T.; Huang, W.C.; Ren, C.T.; Wu, C.Y.; Yu, Y.L. Cancer-associated carbohydrate antigens as potential biomarkers for hepatocellular carcinoma. *PLoS One* **2012**, *7*, 1–8, doi:10.1371/journal.pone.0039466.
247. Von Holst, H.; Nygren, C.; Boström, K.; Collins, V.P.; Fredman, P. The presence of foetal ganglioside antigens 3'-IsoLM1 and 3'6'-IsoLD1 in both glioma tissue and surrounding areas from human brain. *Acta Neurochir. (Wien).* **1997**, *139*, 141–145, doi:10.1007/BF02747194.
248. Nilsson, O.; Månsson, J.E.; Lindholm, L.; Holmgren, J.; Svennerholm, L. Sialosyllactotetraosylceramide, a novel ganglioside antigen detected in human carcinomas by a monoclonal antibody. *FEBS Lett.* **1985**, *182*, 398–402, doi:10.1016/0014-5793(85)80341-0.
249. Chatterjee, S.; Alsaeedi, N.; Hou, J.; Bandaru, V.V.R.; Wu, L.; Halushka, M.K.; Pili, R.; Ndikuyeze, G.; Haughey, N.J. Use of a Glycolipid Inhibitor to Ameliorate Renal Cancer in a Mouse Model. *PLoS One* **2013**, *8*, 1–10, doi:10.1371/journal.pone.0063726.
250. Schwamb, J.; Feldhaus, V.; Baumann, M.; Patz, M.; Brodesser, S.; Brinker, R.; Claasen, J.; Pallasch, C.P.; Hallek, M.; Wendtner, C.M.; et al. B-cell receptor triggers drug sensitivity of primary CLL cells by controlling glucosylation of ceramides. *Blood* **2012**, *120*, 3978–3985, doi:10.1182/blood-2012-05-431783.
251. Weinkove, R.; Brooks, C.R.; Carter, J.M.; Hermans, I.F.; Ronchese, F. Functional invariant natural killer T-cell and CD1d axis in chronic lymphocytic leukemia: Implications for immunotherapy. *Haematologica* **2013**, *98*, 376–384, doi:10.3324/haematol.2012.072835.
252. Hasegawa, H.; Yamashita, K.; Otubo, D.; Fujii, S.I.; Kamigaki, T.; Kuroda, D.; Kakeji, Y. Allogeneic DCG promote lung NK cell activation and antitumor effect after invariant NKT cell activation. *Anticancer Res.* **2014**, *34*, 3411–3417.
253. Ando, T.; Ito, H.; Arioka, Y.; Ogiso, H.; Seishima, M. Combination therapy with α-

galactosylceramide and a Toll-like receptor agonist exerts an augmented suppressive effect on lung tumor metastasis in a mouse model. *Oncol. Rep.* **2015**, *33*, 826–832, doi:10.3892/or.2014.3634.

254. Albertini, M.R.; Ranheim, E.A.; Zuleger, C.L.; Sondel, P.M.; Hank, J.A.; Bridges, A.; Newton, M.A.; McFarland, T.; Collins, J.; Clements, E.; et al. Phase I study to evaluate toxicity and feasibility of intratumoral injection of α-gal glycolipids in patients with advanced melanoma. *Cancer Immunol. Immunother.* **2016**, *65*, 897–907, doi:10.1007/s00262-016-1846-1.
255. Neumann, S.; Young, K.; Compton, B.; Anderson, R.; Painter, G.; Hook, S. Synthetic TRP2 long-peptide and α-galactosylceramide formulated into cationic liposomes elicit CD8+ T-cell responses and prevent tumour progression. *Vaccine* **2015**, *33*, 5838–5844, doi:10.1016/j.vaccine.2015.08.083.
256. Yoshioka, K.; Ueno, Y.; Tanaka, S.; Nagai, K.; Onitake, T.; Hanaoka, R.; Watanabe, H.; Chayama, K. Role of natural killer t cells in the mouse colitis-associated colon cancer model. *Scand. J. Immunol.* **2012**, *75*, 16–26, doi:10.1111/j.1365-3083.2011.02607.x.
257. Dong, T.; Yi, T.; Yang, M.; Lin, S.; Li, W.; Xu, X.; Hu, J.; Jia, L.; Hong, X.; Niu, W. Co-operation of α-galactosylceramide-loaded tumour cells and TLR9 agonists induce potent anti-Tumour responses in a murine colon cancer model. *Biochem. J.* **2016**, *473*, 7–19, doi:10.1042/BJ20150129.
258. Skotland, T.; Ekroos, K.; Kauhanen, D.; Simolin, H.; Seierstad, T.; Berge, V.; Sandvig, K.; Llorente, A. Molecular lipid species in urinary exosomes as potential prostate cancer biomarkers. *Eur. J. Cancer* **2017**, *70*, 122–132, doi:10.1016/j.ejca.2016.10.011.
259. Zhu, T.; Xu, L.; Xu, X.; Wang, Z.; Zhu, J.; Xie, Q.; Zhang, B.; Wang, Y.; Ju, L.; He, Y.; et al. Analysis of breast cancer-associated glycosphingolipids using electrospray ionization-linear ion trap quadrupole mass spectrometry. *Carbohydr. Res.* **2015**, *402*, 189–199, doi:10.1016/j.carres.2014.10.006.
260. Fukuda, M.N.; Bothner, B.; Lloyd, K.O.; Rettig, W.J.; Tiller, P.R.; Dell, A. Structures of glycosphingolipids isolated from human embryonal carcinoma cells. The presence of mono- and disialosyl glycolipids with blood group type 1 sequence. *J. Biol. Chem.* **1986**, *261*, 5145–5153, doi:10.1016/s0021-9258(19)89226-8.
261. Alam, S.; Anugraham, M.; Huang, Y.L.; Kohler, R.S.; Hettich, T.; Winkelbach, K.; Grether, Y.; López, M.N.; Khasbiullina, N.; Bovin, N. V; et al. Altered (neo-) lacto series glycolipid biosynthesis impairs α2-6 sialylation on N-glycoproteins in ovarian cancer cells. *Sci. Rep.* **2017**, *7*, 1–18, doi:10.1038/srep45367.
262. Van Slambrouck, S.; Hilkens, J.; Bisoffi, M.; Steelant, W.F.A. AsialoGM1 and integrin α2β1 mediate prostate cancer progression. *Int. J. Oncol.* **2009**, *35*, 693–699, doi:10.3892/ijo_00000381.
263. Van Slambrouck, S.; Groux-Degroote, S.; Krzewinski-Recchi, M.A.; Cazet, A.; Delannoy, P.; Steelant, W.F.A. Carbohydrate-to-carbohydrate interactions between α2,3-linked sialic acids on α2 integrin subunits and asialo-GM1 underlie the bone metastatic behaviour of LNCAP-derivative C4-2B prostate cancer cells. *Biosci. Rep.* **2014**, *34*, 546–557, doi:10.1042/BSR20140096.
264. Guan, F.; Handa, K.; Hakomori, S.I. Specific glycosphingolipids mediate epithelial-to-mesenchymal transition of human and mouse epithelial cell lines. *Proc. Natl. Acad. Sci. U. S. A.* **2009**, *106*, 7461–7466, doi:10.1073/pnas.0902368106.
265. Wiels, J.; Fellous, M.; Tursz, T. Monoclonal antibody against a Burkitt lymphoma-associated antigen. *Proc. Natl. Acad. Sci. U. S. A.* **1981**, *78*, 6485–6488, doi:10.1073/pnas.78.10.6485.
266. Mangeney, M.; Lingwood, C.A.; Taga, S.; Caillou, B.; Tursz, T.; Wiels, J. Apoptosis

Induced in Burkitt's Lymphoma Cells via Gb3/CD77, a Glycolipid Antigen. *Cancer Res.* **1993**, *53*, 5314–5319.
267. Johansson, D.; Kosovac, E.; Moharer, J.; Ljuslinder, I.; Brännström, T.; Johansson, A.; Behnam-Motlagh, P. Expression of verotoxin-1 receptor Gb3 in breast cancer tissue and verotoxin-1 signal transduction to apoptosis. *BMC Cancer* **2009**, *9*, 1–9, doi:10.1186/1471-2407-9-67.
268. Falguières, T.; Maak, M.; Von Weyhern, C.; Sarr, M.; Sastre, X.; Poupon, M.F.; Robine, S.; Johannes, L.; Janssen, K.P. Human colorectal tumors and metastases express Gb3 and can be targeted by an intestinal pathogen-based delivery tool. *Mol. Cancer Ther.* **2008**, *7*, 2498–2508, doi:10.1158/1535-7163.MCT-08-0430.
269. Distler, U.; Souady, J.; Hülsewig, M.; Drmić-Hofman, I.; Haier, J.; Friedrich, A.W.; Karch, H.; Senninger, N.; Dreisewerd, K.; Berkenkamp, S.; et al. Shiga toxin receptor Gb3Cer/CD77: Tumor-association and promising therapeutic target in pancreas and colon cancer. *PLoS One* **2009**, *4*, doi:10.1371/journal.pone.0006813.
270. Bien, T.; Perl, M.; MacHmüller, A.C.; Nitsche, U.; Conrad, A.; Johannes, L.; Müthing, J.; Soltwisch, J.; Janssen, K.P.; Dreisewerd, K. MALDI-2 Mass Spectrometry and Immunohistochemistry Imaging of Gb3Cer, Gb4Cer, and Further Glycosphingolipids in Human Colorectal Cancer Tissue. *Anal. Chem.* **2020**, *92*, 7096–7105, doi:10.1021/acs.analchem.0c00480.
271. Kovbasnjuk, O.; Mourtazina, R.; Baibakov, B.; Wang, T.; Elowsky, C.; Choti, M.A.; Kane, A.; Donowitz, M. The glycosphingolipid globotriaosylceramide in the metastatic transformation of colon cancer. *Proc. Natl. Acad. Sci. U. S. A.* **2005**, *1*, 1–6.
272. Arab, S.; Russel, E.; Chapman, W.B.; Rosen, B.; Lingwood, C.A. Expression of the verotoxin receptor glycolipid, globotriaosylceramide, in ovarian hyperplasias. *Oncol. Res.* **1997**, *9*, 553–563.
273. Kang, J.; Rajpert-De Meyts, E.; Skakkebæk, N.; Wiels, J. Expression of the glycolipid globotriaosylceramide (Gb3) in testicular carcinoma in situ. *Virchows Arch.* **1995**, *426*, 369–374, doi:10.1007/BF00191346.
274. Sawada, R.; Hotta, H.; Chung, Y.S.; Sowa, M.; Tai, T.; Yano, I. Globotriaosyl ceramide and globoside as major glycolipid components of fibroblasts in scirrhous gastric carcinoma tissues. *Japanese J. Cancer Res.* **1998**, *89*, 167–176, doi:10.1111/j.1349-7006.1998.tb00545.x.
275. Geyer, P.E.; Maak, M.; Nitsche, U.; Perl, M.; Novotny, A.; Slotta-Huspenina, J.; Dransart, E.; Holtorf, A.; Johannes, L.; Janssen, K.P. *Gastric adenocarcinomas express the glycosphingolipid Gb3/CD77: Targeting of gastric cancer cells with Shiga toxin B-subunit*; 2016; Vol. 15; ISBN 4989414020.
276. Tyler, A.; Johansson, A.; Karlsson, T.; Gudey, S.K.; Brännström, T.; Grankvist, K.; Behnam-Motlagh, P. Targeting glucosylceramide synthase induction of cell surface globotriaosylceramide (Gb3) in acquired cisplatin-resistance of lung cancer and malignant pleural mesothelioma cells. *Exp. Cell Res.* **2015**, *336*, 23–32, doi:10.1016/j.yexcr.2015.05.012.
277. Park, S.Y.; Kwak, C.Y.; Shayman, J.A.; Kim, J.H. Globoside promotes activation of ERK by interaction with the epidermal growth factor receptor. *Biochim. Biophys. Acta - Gen. Subj.* **2012**, *1820*, 1141–1148, doi:10.1016/j.bbagen.2012.04.008.
278. Schrump, D.S.; Furukawa, K.; Yamaguchi, H.; Lloyd, K.O.; Old, L.J. Recognition of galactosylgloboside by monoclonal antibodies derived from patients with primary lung cancer. *Proc. Natl. Acad. Sci. U. S. A.* **1988**, *85*, 4441–4445, doi:10.1073/pnas.85.12.4441.
279. Ohyama, C.; Orikasa, S.; Kawamura, S.; Satoh, M.; Saito, S.; Fukushi, Y.; Levery, S.B.; Hakomori, S. -I Galactosylgloboside expression in seminoma. Inverse correlation

with metastatic potential. *Cancer* **1995**, *76*, 1043–1050, doi:10.1002/1097-0142(19950915)76:6<1043::AID-CNCR2820760619>3.0.CO;2-A.
280. Chang, W.W.; Chien, H.L.; Lee, P.; Lin, J.; Hsu, C.W.; Hung, J.T.; Lin, J.J.; Yu, J.C.; Shao, L.E.; Yu, J.; et al. Expression of Globo H and SSEA3 in breast cancer stem cells and the involvement of fucosyl transferases 1 and 2 in Globo H synthesis (Proceedings of the National Academy of Sciences of the United States of America (2008) 105, (11667-11672) DOI: 10.1073/pn. *Proc. Natl. Acad. Sci. U. S. A.* **2008**, *105*, 17206, doi:10.1073/pnas.0808811105.
281. Cheung, S.K.C.; Chuang, P.K.; Huang, H.W.; Hwang-Verslues, W.W.; Cho, C.H.H.; Yang, W. Bin; Shen, C.N.; Hsiao, M.; Hsu, T.L.; Chang, C.F.; et al. Stage-specific embryonic antigen-3 (SSEA-3) and β3GalT5 are cancer specific and significant markers for breast cancer stem cells. *Proc. Natl. Acad. Sci. U. S. A.* **2016**, *113*, 960–965, doi:10.1073/pnas.1522602113.
282. Suzuki, Y.; Haraguchi, N.; Takahashi, H.; Uemura, M.; Nishimura, J.; Hata, T.; Takemasa, I.; Mizushima, T.; Ishii, H.; Doki, Y.; et al. SSEA-3 as a novel amplifying cancer cell surface marker in colorectal cancers. *Int. J. Oncol.* **2013**, *42*, 161–167, doi:10.3892/ijo.2012.1713.
283. Jacob, F.; Anugraham, M.; Pochechueva, T.; Tse, B.W.C.; Alam, S.; Guertler, R.; Bovin, N. V.; Fedier, A.; Hacker, N.F.; Huflejt, M.E.; et al. The glycosphingolipid P1 is an ovarian cancer-associated carbohydrate antigen involved in migration. *Br. J. Cancer* **2014**, *111*, 1634–1645, doi:10.1038/bjc.2014.455.
284. Jin, C.; Teneberg, S. Characterization of novel nonacid glycosphingolipids as biomarkers of human gastric adenocarcinoma. *J. Biol. Chem.* **2022**, *298*, 101732, doi:10.1016/j.jbc.2022.101732.
285. Goupille, C.; Marionneau, S.; Bureau, V.; Hallouin, F.; Meichenin, M.; Rocher, J.; Le Pendu, J. A1,2Fucosyltransferase Increases Resistance To Apoptosis of Rat Colon Carcinoma Cells. *Glycobiology* **2000**, *10*, 375–382, doi:10.1093/glycob/10.4.375.
286. Mejías-Luque, R.; López-Ferrer, A.; Garrido, M.; Fabra, À.; de Bolós, C. Changes in the invasive and metastatic capacities of HT-29/M3 cells induced by the expression of fucosyltransferase 1. *Cancer Sci.* **2007**, *98*, 1000–1005, doi:10.1111/j.1349-7006.2007.00484.x.
287. Bremer, E.G.; Levery, S.B.; Sonnino, S.; Ghidoni, R.; Canevari, S.; Kannagi, R.; Hakomori, S. Characterization of a glycosphingolipid antigen defined by the monoclonal antibody MBr1 expressed in normal and neoplastic epithelial cells of human mammary gland. *J. Biol. Chem.* **1984**, *259*, 14773–14777, doi:10.1016/s0021-9258(17)42669-x.
288. Zhu, J.; Wang, Y.; Yu, Y.; Wang, Z.; Zhu, T.; Xu, X.; Liu, H.; Hawke, D.; Zhou, D.; Li, Y. Aberrant fucosylation of glycosphingolipids in human hepatocellular carcinoma tissues. *Liver Int.* **2014**, *34*, 147–160, doi:10.1111/liv.12265.
289. Cheng, S.P.; Yang, P.S.; Chien, M.N.; Chen, M.J.; Lee, J.J.; Liu, C.L. Aberrant expression of tumor-associated carbohydrate antigen Globo H in thyroid carcinoma. *J. Surg. Oncol.* **2016**, *114*, 853–858, doi:10.1002/jso.24479.
290. Kajiwara, H.; Yasuda, M.; Kumaki, N.; Shibayama, T.; Osamura, Y. Expression of carbohydrate antigens (SSEA-1, sialyl-Lewis X, DU-PAN-2 and CA19-9) and E-selectin in urothelial carcinoma of the renal pelvis, ureter, and urinary bladder. *Tokai J. Exp. Clin. Med.* **2005**, *30*, 177–182.
291. Vangsted, A.J.; Kjcldsen, T.B.; White, T.; Sweeney, B.; Hakomori, S. Immunochemical Detection of a Small Cell Lung Cancer-associated Ganglioside (FucGivii)Antigen in Serum. *Cancer Res.* **1991**, *51*, 2879–2884, doi:10.1016/0169-5002(92)90246-g.

292. Nilsson, O.; MÅnsson, J.E.; Brezicka, T.; Holmgren, J.; Lindholm, L.; Sörenson, S.; Yngvason, F.; Svennerholm, L. Fucosyl-GM1 - A ganglioside associated with small cell lung carcinomas. *Glycoconj. J.* **1984**, *1*, 43–49, doi:10.1007/BF01875411.
293. Ranasinghe, A.; Mehl, J.; D'Arienzo, C.; Nabbie, F.; Chiu, C.; Thevanayagam, L.; Srinivasan, M.; Hogan, J.; Ponath, P.; Olah, T. Fucosyl monosialoganglioside: Quantitative analysis of specific potential biomarkers of lung cancer in biological matrices using immunocapture extraction/tandem mass spectrometry. *Rapid Commun. Mass Spectrom.* **2018**, *32*, 1481–1490, doi:10.1002/rcm.8194.
294. Brezicka, F.T.; Olling, S.; Nilsson, O.; Bergh, J.; Holmgren, J.; Sörenson, S.; Yngvason, F.; Lindholm, L. Immunohistological detection of fucosyl-GM1 ganglioside in human lung cancer and normal tissues with monoclonal antibodies. *Cancer Res.* **1989**, *49*, 1300–1305.
295. Brezicka, F.T.; Olling, S.; Bergman, B.; Berggren, H.; Engström, C.P.; Hammarström, S.; Holmgren, J.; Larsson, S.; Lindholm, L. Coexpression of ganglioside antigen Fuc-GM1, neural-cell adhesion molecule, carcinoembryonic antigen, and carbohydrate tumor-associated antigen CA 50 in lung cancer. *Tumor Biol.* **1992**, *13*, 308–315, doi:10.1159/000217780.
296. Kasai, K.; Kameya, T.; Okuda, T.; Terasaki, P.I.; Iwaki, Y. Immunohistochemical examination of lung cancers using monoclonal antibodies reacting with sialosylated Lewisx and sialosylated Lewisa. *Virchows Arch. A Pathol. Anat. Histopathol.* **1987**, *410*, 253–261, doi:10.1007/BF00710832.
297. Ferreira, I.G.; Carrascal, M.; Mineiro, A.G.; Bugalho, A.; Borralho, P.; Silva, Z.; Dall'Olio, F.; Videira, P.A. Carcinoembryonic antigen is a sialyl Lewis x/a carrier and an E-selectin ligand in non-small cell lung cancer. *Int. J. Oncol.* **2019**, *55*, 1033–1048, doi:10.3892/ijo.2019.4886.
298. Herlyn, M.; Sears, H.F.; Steplewski, Z.; Koprowski, H. Monoclonal antibody detection of a circulating tumor-associated antigen. I. Presence of antigen in sera of patients with colorectal, gastric, and pancreatic carcinoma. *J. Clin. Immunol.* **1982**, *2*, 135–140, doi:10.1007/BF00916897.
299. Paschos, K.A.; Canovas, D.; Bird, N.C. The engagement of selectins and their ligands in colorectal cancer liver metastases. *J. Cell. Mol. Med.* **2010**, *14*, 165–174, doi:10.1111/j.1582-4934.2009.00852.x.
300. Nakagoe, T.; Sawai, T.; Tsuji, T.; Jibiki, M.A.; Nanashima, A.; Yamaguchi, H.; Kurosaki, N.; Yasutake, T.; Ayabe, H. Circulating sialyl Lewisx, sialyl Lewisa, and sialyl Tn antigens in colorectal cancer patients: Multivariate analysis of predictive factors for serum antigen levels. *J. Gastroenterol.* **2001**, *36*, 166–172, doi:10.1007/s005350170124.
301. Carrascal, M.A.; Silva, M.; Ramalho, J.S.; Pen, C.; Martins, M.; Pascoal, C.; Amaral, C.; Serrano, I.; Oliveira, M.J.; Sackstein, R.; et al. Inhibition of fucosylation in human invasive ductal carcinoma reduces E-selectin ligand expression, cell proliferation, and ERK1/2 and p38 MAPK activation. *Mol. Oncol.* **2018**, *12*, 579–593, doi:10.1002/1878-0261.12163.
302. Ohyama, C. Glycosylation in bladder cancer. *Int. J. Clin. Oncol.* **2008**, *13*, 308–313, doi:10.1007/s10147-008-0809-8.
303. Borsig, L.; Imbach, T.; Höchli, M.; Berger, E.G. α1,3fucosyltransferase VI is expressed in HepG2 cells and codistributed with β1,4galactosyltransferase I in the Golgi apparatus and monensin-induced swollen vesicles. *Glycobiology* **1999**, *9*, 1273–1280, doi:10.1093/glycob/9.11.1273.
304. Kleeff, J.; Korc, M.; Apte, M.; La Vecchia, C.; Johnson, C.D.; Biankin, A. V.; Neale, R.E.; Tempero, M.; Tuveson, D.A.; Hruban, R.H.; et al. Pancreatic cancer. *Nat. Rev.*

Dis. Prim. **2016**, *2*, 1–23, doi:10.1038/nrdp.2016.22.
305. Sarantis, P.; Koustas, E.; Papadimitropoulou, A.; Papavassiliou, A.G.; Karamouzis, M. V. Pancreatic ductal adenocarcinoma: Treatment hurdles, tumor microenvironment and immunotherapy. *World J. Gastrointest. Oncol.* **2020**, *12*, 173–181, doi:10.4251/wjgo.v12.i2.173.
306. Schawkat, K.; Manning, M.A.; Glickman, J.N.; Mortele, K.J. Pancreatic ductal adenocarcinoma and its variants: Pearls and perils. *Radiographics* **2020**, *40*, 1219–1239, doi:10.1148/rg.2020190184.
307. Orth, M.; Metzger, P.; Gerum, S.; Mayerle, J.; Schneider, G.; Belka, C.; Schnurr, M.; Lauber, K. Pancreatic ductal adenocarcinoma: Biological hallmarks, current status, and future perspectives of combined modality treatment approaches. *Radiat. Oncol.* **2019**, *14*, 1–20, doi:10.1186/s13014-019-1345-6.
308. Sung, H.; Ferlay, J.; Siegel, R.L.; Laversanne, M.; Soerjomataram, I.; Jemal, A.; Bray, F. Global Cancer Statistics 2020: GLOBOCAN Estimates of Incidence and Mortality Worldwide for 36 Cancers in 185 Countries. *CA. Cancer J. Clin.* **2021**, *71*, 209–249, doi:10.3322/caac.21660.
309. Wong, M.C.S.; Jiang, J.Y.; Liang, M.; Fang, Y.; Yeung, M.S. Global temporal patterns of pancreatic cancer and association with socioeconomic development. **2020**, 1–9, doi:10.1038/s41598-017-02997-2.
310. Ushio, J.; Kanno, A.; Ikeda, E.; Ando, K.; Nagai, H.; Miwata, T.; Kawasaki, Y.; Tada, Y.; Yokoyama, K.; Numao, N.; et al. Pancreatic ductal adenocarcinoma: Epidemiology and risk factors. *Diagnostics* **2021**, *11*, 1–13, doi:10.3390/diagnostics11030562.
311. International Agency for Research on Cancer. Data Visualization Tools for Exploring the Global Cancer Burden in 2020 Available online: https://gco.iarc.fr/today (accessed on Dec 5, 2022).
312. Mayo, S.C.; Nathan, H.; Cameron, J.L.; Olino, K.; Edil, B.H.; Herman, J.M.; Hirose, K.; Schulick, R.D.; Choti, M.A.; Wolfgang, C.L.; et al. Conditional survival in patients with pancreatic ductal adenocarcinoma resected with curative intent. *Cancer* **2012**, *118*, 2674–2681, doi:10.1002/cncr.26553.
313. Liot, S.; Balas, J.; Aubert, A.; Prigent, L.; Mercier-Gouy, P.; Verrier, B.; Bertolino, P.; Hennino, A.; Valcourt, U.; Lambert, E. Stroma Involvement in Pancreatic Ductal Adenocarcinoma: An Overview Focusing on Extracellular Matrix Proteins. *Front. Immunol.* **2021**, *12*, 1–12, doi:10.3389/fimmu.2021.612271.
314. Becker, A.E.; Hernandez, Y.G.; Frucht, H.; Lucas, A.L. Pancreatic ductal adenocarcinoma: Risk factors, screening, and early detection. *World J. Gastroenterol.* **2014**, *20*, 11182–11198, doi:10.3748/wjg.v20.i32.11182.
315. Klein, A.P.; De Andrade, M.; Hruban, R.H.; Bondy, M.; Schwartz, A.G.; Gallinger, S.; Lynch, H.T.; Syngal, S.; Rabe, K.G.; Goggins, M.G.; et al. Linkage analysis of chromosome 4 in families with familial pancreatic cancer. *Cancer Biol. Ther.* **2007**, *6*, 320–323, doi:10.4161/cbt.6.3.3721.
316. Turati, F.; Edefonti, V.; Bosetti, C.; Ferraroni, M.; Malvezzi, M.; Franceschi, S.; Talamini, R.; Montella, M.; Levi, F.; Dal Maso, L.; et al. Family history of cancer and the risk of cancer: A network of case-control studies. *Ann. Oncol.* **2013**, *24*, 2651–2656, doi:10.1093/annonc/mdt280.
317. Risch, H.A.; Yu, H.; Lu, L.; Kidd, M.S. ABO blood group, helicobacter pylori seropositivity, and risk of pancreatic cancer: A case-control study. *J. Natl. Cancer Inst.* **2010**, *102*, 502–505, doi:10.1093/jnci/djq007.
318. Egawa, N.; Lin, Y.; Tabata, T.; Kuruma, S.; Hara, S.; Kubota, K.; Kamisawa, T. ABO blood type, long-standing diabetes, and the risk of pancreatic cancer. *World J. Gastroenterol.* **2013**, *19*, 2537–2542, doi:10.3748/wjg.v19.i16.2537.

319. Amundadottir, L.; Kraft, P.; Stolzenberg-Solomon, R.Z.; Fuchs, C.S.; Petersen, G.M.; Arslan, A.A.; Bueno-De-Mesquita, H.B.; Gross, M.; Helzlsouer, K.; Jacobs, E.J.; et al. Genome-wide association study identifies variants in the ABO locus associated with susceptibility to pancreatic cancer. *Nat. Genet.* **2009**, *41*, 986–990, doi:10.1038/ng.429.
320. Lowenfels, A.B.; Maisonneuve, P.; Whitcomb, D.C.; Lerch, M.M.; DiMagno, E.P. Cigarette smoking as a risk factor for pancreatic cancer in patients with hereditary pancreatitis. *J. Am. Med. Assoc.* **2001**, *286*, 169–170, doi:10.1001/jama.286.2.169.
321. Lowenfels, A.B.; Maisonneuve, P. Epidemiology and risk factors for pancreatic cancer. *Best Pract. Res. Clin. Gastroenterol.* **2006**, *20*, 197–209, doi:10.1016/j.bpg.2005.10.001.
322. Iodice, S.; Gandini, S.; Maisonneuve, P.; Lowenfels, A.B. Tobacco and the risk of pancreatic cancer: A review and meta-analysis. *Langenbeck's Arch. Surg.* **2008**, *393*, 535–545, doi:10.1007/s00423-007-0266-2.
323. Zhang, S.; Wang, C.; Huang, H.; Jiang, Q.; Zhao, D.; Tian, Y.; Ma, J.; Yuan, W.; Sun, Y.; Che, X.; et al. Effects of alcohol drinking and smoking on pancreatic ductal adenocarcinoma mortality: A retrospective cohort study consisting of 1783 patients. *Sci. Rep.* **2017**, *7*, 1–8, doi:10.1038/s41598-017-08794-1.
324. Gapstur, S.M.; Jacobs, E.J.; Deka, A.; McCullough, M.L.; Patel, A. V.; Thun, M.J. Association of alcohol intake with pancreatic cancer mortality in never smokers. *Arch. Intern. Med.* **2011**, *171*, 444–451, doi:10.1001/archinternmed.2010.536.
325. Beaney, A.J.; Banim, P.J.R.; Luben, R.; Lentjes, M.A.H.; Khaw, K.; Hart, A.R. Risk of Developing Pancreatic Cancer in an Age-Dependent Manner and Are Modified by Plasma Antioxidants A Prospective Cohort Study (EPIC-Norfolk) Using Data From Food Diaries. **2017**, 672–678, doi:10.1097/MPA.0000000000000819.
326. Ojajärvi, A.; Partanen, T.; Ahlbom, A.; Hakulinen, T.; Kauppinen, T.; Weiderpass, E.; Wesseling, C. Estimating the relative risk of pancreatic cancer associated with exposure agents in job title data in a hierarchical Bayesian meta-analysis. *Scand. J. Work. Environ. Heal.* **2007**, *33*, 325–335, doi:10.5271/sjweh.1153.
327. Ghaneh, P.; Costello, E.; Neoptolemos, J.P. Biology and management of pancreatic cancer. *Postgrad. Med. J.* **2008**, *84*, 478–497, doi:10.1136/gut.2006.103333.
328. Hruban, R.H.; Maitra, A.; Goggins, M. Update on Pancreatic Intraepithelial Neoplasia. *Int. J. Clin. Exp. Pathol.* **2008**, *1*, 306–316.
329. Corbo, V.; Tortora, G.; Scarpa, A. Molecular Pathology of Pancreatic Cancer: From Bench-to-Bedside Translation. *Curr. Drug Targets* **2012**, *13*, 744–752, doi:10.2174/138945012800564103.
330. Oberstein, P.E.; Olive, K.P. Pancreatic cancer: Why is it so hard to treat? *Therap. Adv. Gastroenterol.* **2013**, *6*, 321–337, doi:10.1177/1756283X13478680.
331. Roalsø, M.; Aunan, J.R.; Søreide, K. Refined TNM-staging for pancreatic adenocarcinoma – Real progress or much ado about nothing? *Eur. J. Surg. Oncol.* **2020**, *46*, 1554–1557, doi:10.1016/j.ejso.2020.02.014.
332. Ansari, D.; Gustafsson, A.; Andersson, R. Update on the management of pancreatic cancer: Surgery is not enough. *World J. Gastroenterol.* **2015**, *21*, 3157–3165, doi:10.3748/wjg.v21.i11.3157.
333. Adamska, A.; Domenichini, A.; Falasca, M. Pancreatic ductal adenocarcinoma: Current and evolving therapies. *Int. J. Mol. Sci.* **2017**, *18*, doi:10.3390/ijms18071338.
334. Grasso, C.; Jansen, G.; Giovannetti, E. Drug resistance in pancreatic cancer: Impact of altered energy metabolism. *Crit. Rev. Oncol. Hematol.* **2017**, *114*, 139–152, doi:10.1016/j.critrevonc.2017.03.026.
335. Werner, J.; Combs, S.E.; Springfeld, C.; Hartwig, W.; Hackert, T.; Büchler, M.W. Advanced-stage pancreatic cancer: Therapy options. *Nat. Rev. Clin. Oncol.* **2013**, *10*,

323–333, doi:10.1038/nrclinonc.2013.66.
336. Haab, B.B.; Huang, Y.; Balasenthil, S.; Partyka, K.; Tang, H.; Anderson, M.; Allen, P.; Sasson, A.; Zeh, H.; Kaul, K.; et al. Definitive characterization of CA 19-9 in resectable pancreatic cancer using a reference set of serum and plasma specimens. *PLoS One* **2015**, *10*, 1–18, doi:10.1371/journal.pone.0139049.
337. Fong, Z.V.; Winter, J.M. Biomarkers in Pancreatic Cancer: Diagnostic, Prognostic, and Predictive. *Cancer J.* **2012**, *18*, 530–538, doi:10.1097/PPO.0b013e31827654ea.
338. Winter, J.M.; Yeo, C.J.; Brody, J.R. Diagnostic, prognostic, and predictive biomarkers in pancreatic cancer. *J. Surg. Oncol.* **2013**, *107*, 15–22, doi:10.1002/jso.23192.
339. E. Poruk, K.; Z. Gay, D.; Brown, K.; D. Mulvihill, J.; M. Boucher, K.; L. Scaife, C.; A. Firpo, M.; J. Mulvihill, S. The Clinical Utility of CA 19-9 in Pancreatic Adenocarcinoma: Diagnostic and Prognostic Updates. *Curr. Mol. Med.* **2013**, *13*, 340–351, doi:10.2174/1566524011313030003.
340. Tang, H.; Partyka, K.; Hsueh, P.; Sinha, J.Y.; Kletter, D.; Zeh, H.; Huang, Y.; Brand, R.E.; Haab, B.B. Glycans Related to the CA19-9 Antigen Are Increased in Distinct Subsets of Pancreatic Cancers and Improve Diagnostic Accuracy Over CA19-9. *Cell. Mol. Gastroenterol. Hepatol.* **2016**, *2*, 210–221, doi:10.1016/j.jcmgh.2015.12.003.
341. Goonetilleke, K.S.; Siriwardena, A.K. Systematic review of carbohydrate antigen (CA 19-9) as a biochemical marker in the diagnosis of pancreatic cancer. *Eur. J. Surg. Oncol.* **2007**, *33*, 266–270, doi:10.1016/j.ejso.2006.10.004.
342. Mayerle, J.; Kalthoff, H.; Reszka, R.; Kamlage, B.; Peter, E.; Schniewind, B.; González Maldonado, S.; Pilarsky, C.; Heidecke, C.D.; Schatz, P.; et al. Metabolic biomarker signature to differentiate pancreatic ductal adenocarcinoma from chronic pancreatitis. *Gut* **2018**, *67*, 128–137, doi:10.1136/gutjnl-2016-312432.
343. Nishihara, S.; Yazawa, S.; Iwasaki, H.; Nakazato, M.; Kudo, T.; Ando, T.; Narimatsu, H. α(1,3/1,4)Fucosyltransferase (FucT-III) gene is inactivated by a single amino acid substitution in Lewis histo-blood type negative individuals. *Biochem. Biophys. Res. Commun.* 1993, *196*, 624–631.
344. Hernandez, J.M.; Cowgill, S.M.; Al-Saadi, S.; Collins, A.; Ross, S.B.; Cooper, J.; Villadolid, D.; Zervos, E.; Rosemurgy, A. CA 19-9 velocity predicts disease-free survival and overall survival after pancreatectomy of curative intent. *J. Gastrointest. Surg.* **2009**, *13*, 349–353, doi:10.1007/s11605-008-0696-3.
345. Wolrab, D.; Jirásko, R.; Cífková, E.; Höring, M.; Mei, D.; Chocholoušková, M.; Peterka, O.; Idkowiak, J.; Hrnčiarová, T.; Kuchař, L.; et al. Lipidomic profiling of human serum enables detection of pancreatic cancer. *Nat. Commun.* **2022**, *13*, 1–16, doi:10.1038/s41467-021-27765-9.
346. Zhang, T.; van Die, I.; Tefsen, B.; van Vliet, S.J.; Laan, L.C.; Zhang, J.; ten Dijke, P.; Wuhrer, M.; Belo, A.I. Differential O- and Glycosphingolipid Glycosylation in Human Pancreatic Adenocarcinoma Cells With Opposite Morphology and Metastatic Behavior. *Front. Oncol.* **2020**, *10*, 1–19, doi:10.3389/fonc.2020.00732.
347. Mohamed Abd-El-Halim, Y.; El Kaoutari, A.; Silvy, F.; Rubis, M.; Bigonnet, M.; Roques, J.; Cros, J.; Nicolle, R.; Iovanna, J.; Dusetti, N.; et al. A glycosyltransferase gene signature to detect pancreatic ductal adenocarcinoma patients with poor prognosis. *EBioMedicine* **2021**, *71*, 103541, doi:10.1016/j.ebiom.2021.103541.
348. Yu, J.; Hung, J.T.; Wang, S.H.; Cheng, J.Y.; Yu, A.L. Targeting glycosphingolipids for cancer immunotherapy. *FEBS Lett.* **2020**, 1–17, doi:10.1002/1873-3468.13917.
349. Schuster, M.; Nechansky, A.; Loibner, H.; Kircheis, R. Cancer immunotherapy. *Biotechnol. J.* **2006**, *1*, 138–147, doi:10.1002/biot.200500044.
350. Fredman, P.; Hedberg, K.; Brezicka, T. Gangliosides as therapeutic targets for cancer. *BioDrugs* **2003**, *17*, 155–167, doi:10.2165/00063030-200317030-00002.

351. Heimburg-Molinaro, J.; Lum, M.; Vijay, G.; Jain, M.; Almogren, A.; Rittenhouse-Olson, K. Cancer vaccines and carbohydrate epitopes. *Vaccine* **2011**, *29*, 8802–8826, doi:10.1016/j.vaccine.2011.09.009.
352. Dippold, W.G.; Lloyd, K.O.; Li, L.T.C.; Ikeda, H.; Oettgen, H.F. Cell surface antigens of human malignant melanoma: Definition of six antigenic systems with mouse monoclonal antibodies. *Proc. Natl. Acad. Sci. U. S. A.* **1980**, *77*, 6114–6118, doi:10.1073/pnas.77.10.6114.
353. Houghton, A.N.; Mintzer, D.; Cordon-Cardo, C.; Welt, S.; Fliegel, B.; Vadhan, S.; Carswell, E.; Melamed, M.R.; Oettgen, H.F.; Old, L.J. Mouse monoclonal IgG3 antibody detecting G(D3) ganglioside: A phase I trial in patients with malignant melanoma. *Proc. Natl. Acad. Sci. U. S. A.* **1985**, *82*, 1242–1246, doi:10.1073/pnas.82.4.1242.
354. Scott, A.M.; Lee, F.T.; Hopkins, W.; Cebon, J.S.; Wheatley, J.M.; Liu, Z.; Smyth, F.E.; Murone, C.; Sturrock, S.; MacGregor, D.; et al. Specific targeting, biodistribution, and lack of immunogenicity of chimeric anti-GD3 monoclonal antibody KM871 in patients with metastatic melanoma: Results of a phase I trial. *J. Clin. Oncol.* **2001**, *19*, 3976–3987, doi:10.1200/JCO.2001.19.19.3976.
355. Ho, M.Y.; Yu, A.L.; Yu, J. Glycosphingolipid dynamics in human embryonic stem cell and cancer: their characterization and biomedical implications. *Glycoconj. J.* **2017**, *34*, 765–777, doi:10.1007/s10719-016-9715-x.
356. Zajonc, D.M.; Kronenberg, M. CD1 mediated T cell recognition of glycolipids. *Curr. Opin. Struct. Biol.* **2007**, *17*, 521–529, doi:10.1016/j.sbi.2007.09.010.
357. Speak, A.O.; Cerundolo, V.; Platt, F.M. CD1d presentation of glycolipids. *Immunol. Cell Biol.* **2008**, *86*, 588–597, doi:10.1038/icb.2008.42.
358. Root, A.; Allen, P.; Tempst, P.; Yu, K. Protein biomarkers for early detection of pancreatic ductal adenocarcinoma: Progress and challenges. *Cancers (Basel).* **2018**, *10*, 1–12, doi:10.3390/cancers10030067.
359. Hyötyläinen, T.; Orešič, M. Bioanalytical techniques in nontargeted clinical lipidomics. *Bioanalysis* **2016**, *8*, 351–364.
360. Stevens, V.L.; Hoover, E.; Wang, Y.; Zanetti, K.A. Pre-analytical factors that affect metabolite stability in human urine, plasma, and serum: A review. *Metabolites* **2019**, *9*, doi:10.3390/metabo9080156.
361. Jurowski, K.; Kochan, K.; Walczak, J.; Barańska, M.; Piekoszewski, W.; Buszewski, B. Comprehensive review of trends and analytical strategies applied for biological samples preparation and storage in modern medical lipidomics: State of the art. *TrAC - Trends Anal. Chem.* **2017**, *86*, 276–289, doi:10.1016/j.trac.2016.10.014.
362. Reis, G.B.; Rees, J.C.; Ivanova, A.A.; Kuklenyik, Z.; Drew, N.M.; Pirkle, J.L.; Barr, J.R. Stability of lipids in plasma and serum: Effects of temperature-related storage conditions on the human lipidome. *J. Mass Spectrom. Adv. Clin. Lab* **2021**, *22*, 34–42, doi:10.1016/j.jmsacl.2021.10.002.
363. Wolrab, D.; Chocholoušková, M.; Jirásko, R.; Peterka, O.; Mužáková, V.; Študentová, H.; Melichar, B.; Holčapek, M. Determination of one year stability of lipid plasma profile and comparison of blood collection tubes using UHPSFC/MS and HILIC-UHPLC/MS. *Anal. Chim. Acta* **2020**, *1137*, 74–84, doi:10.1016/j.aca.2020.08.061.
364. Kronenberg, F.; Lobentanz, E.M.; Konig, P.; Utermann, G.; Dieplinger, H. Effect of sample storage on the measurement of lipoprotein[a], apolipoproteins B and A-IV, total and high density lipoprotein cholesterol and triglycerides. *J. Lipid Res.* **1994**, *35*, 1318–1323, doi:10.1016/s0022-2275(20)39975-2.
365. Matthan, N.R.; Ip, B.; Resteghini, N.; Ausman, L.M.; Lichtenstein, A.H. Long-term fatty acid stability in human serum cholesteryl ester, triglyceride, and phospholipid

fractions. *J. Lipid Res.* **2010**, *51*, 2826–2832, doi:10.1194/jlr.D007534.
366. Hammad, S.M.; Pierce, J.S.; Soodavar, F.; Smith, K.J.; Al Gadban, M.M.; Rembiesa, B.; Klein, R.L.; Hannun, Y.A.; Bielawski, J.; Bielawska, A. Blood sphingolipidomics in healthy humans: Impact of sample collection methodology. *J. Lipid Res.* **2010**, *51*, 3074–3087, doi:10.1194/jlr.D008532.
367. Zivkovic, A.M.; Wiest, M.M.; Nguyen, U.T.; Davis, R.; Watkins, S.M.; German, J.B. Effects of sample handling and storage on quantitative lipid analysis in human serum. *Metabolomics* **2009**, *5*, 507–516, doi:10.1007/s11306-009-0174-2.
368. Klibanov, A.M. Improving enzymes by using them in organic solvents. *Nature* **2001**, *409*, 241–246, doi:10.1038/35051719.
369. Teo, C.C.; Chong, W.P.K.; Tan, E.; Basri, N.B.; Low, Z.J.; Ho, Y.S. Advances in sample preparation and analytical techniques for lipidomics study of clinical samples. *TrAC - Trends Anal. Chem.* **2015**, *66*, 1–18, doi:10.1016/j.trac.2014.10.010.
370. Züllig, T.; Trötzmüller, M.; Köfeler, H.C. Lipidomics from sample preparation to data analysis: a primer. *Anal. Bioanal. Chem.* **2020**, *412*, 2191–2209, doi:10.1007/s00216-019-02241-y.
371. Saini, R.K.; Prasad, P.; Shang, X.; Keum, Y.S. Advances in lipid extraction methods—a review. *Int. J. Mol. Sci.* **2021**, *22*, 1–19, doi:10.3390/ijms222413643.
372. Holčapek, M.; Liebisch, G.; Ekroos, K. Lipidomic Analysis. *Anal. Chem.* **2018**, *90*, 4249–4257, doi:10.1021/acs.analchem.7b05395.
373. Wolf, C.; Quinn, P.J. Lipidomics: Practical aspects and applications. *Prog. Lipid Res.* **2008**, *47*, 15–36, doi:10.1016/j.plipres.2007.09.001.
374. Römisch-Margl, W.; Prehn, C.; Bogumil, R.; Röhring, C.; Suhre, K.; Adamski, J. Procedure for tissue sample preparation and metabolite extraction for high-throughput targeted metabolomics. *Metabolomics* **2012**, *8*, 133–142, doi:10.1007/s11306-011-0293-4.
375. Reis, A.; Rudnitskaya, A.; Blackburn, G.J.; Fauzi, N.M.; Pitt, A.R.; Spickett, C.M. A comparison of five lipid extraction solvent systems for lipidomic studies of human LDL. *J. Lipid Res.* **2013**, *54*, 1812–1824, doi:10.1194/jlr.M034330.
376. Merrill, A.H.; Sullards, M.C. Opinion article on lipidomics: Inherent challenges of lipidomic analysis of sphingolipids. *Biochim. Biophys. Acta - Mol. Cell Biol. Lipids* **2017**, *1862*, 774–776, doi:10.1016/j.bbalip.2017.01.009.
377. Smith, D.F.; Prieto, P.A. Special Considerations for Glycolipids and Their Purification. *Curr. Protoc. Mol. Biol.* **1993**, *22*, 1–13, doi:10.1002/0471142727.mb1703s22.
378. Folch, J.; Lees, M.; Sloane Stanley, G.H. A simple method for the isolation and purification of total lipides from animal tissues. *J. Biol. Chem.* **1957**, *226*, 497–509, doi:10.1016/s0021-9258(18)64849-5.
379. Bligh, E.G. and Dyer, W.J. A Rapid Method of Total Lipid Extraction and Purification. *Can. J. Biochem. Physiol.* **1959**, *37*, 911–917, doi:10.1139/o59-099.
380. Matyash, V.; Liebisch, G.; Kurzchalia, T. V.; Shevchenko, A.; Schwudke, D. Lipid extraction by methyl-terf-butyl ether for high-throughput lipidomics. *J. Lipid Res.* **2008**, *49*, 1137–1146, doi:10.1194/jlr.D700041-JLR200.
381. Löfgren, L.; Ståhlman, M.; Forsberg, G.B.; Saarinen, S.; Nilsson, R.; Hansson, G.I. The BUME method: A novel automated chloroform-free 96-well total lipid extraction method for blood plasma. *J. Lipid Res.* **2012**, *53*, 1690–1700, doi:10.1194/jlr.D023036.
382. Löfgren, L.; Forsberg, G.B.; Ståhlman, M. The BUME method: A new rapid and simple chloroform-free method for total lipid extraction of animal tissue. *Sci. Rep.* **2016**, *6*, doi:10.1038/srep27688.
383. Alshehry, Z.H.; Barlow, C.K.; Weir, J.M.; Zhou, Y.; McConville, M.J.; Meikle, P.J. An efficient single phase method for the extraction of plasma lipids. *Metabolites* **2015**,

5, 389–403, doi:10.3390/metabo5020389.
384. Wong, M.W.K.; Braidy, N.; Pickford, R.; Sachdev, P.S.; Poljak, A. Comparison of single phase and biphasic extraction protocols for lipidomic studies using human plasma. *Front. Neurol.* **2019**, *10*, 1–11, doi:10.3389/fneur.2019.00879.
385. Vale, G.; Martin, S.A.; Mitsche, M.A.; Thompson, B.M.; Eckert, K.M.; McDonald, J.G. Three-phase liquid extraction: A simple and fast method for lipidomic workflows. *J. Lipid Res.* **2019**, *60*, 694–706, doi:10.1194/jlr.D090795.
386. Iverson, S.J.; Lang, S.L.C.; Cooper, M.H. Comparison of the bligh and dyer and folch methods for total lipid determination in a broad range of marine tissue. *Lipids* **2001**, *36*, 1283–1287, doi:10.1007/s11745-001-0843-0.
387. Byeon, S.K.; Lee, J.Y.; Moon, M.H. Optimized extraction of phospholipids and lysophospholipids for nanoflow liquid chromatography-electrospray ionization-tandem mass spectrometry. *Analyst* **2012**, *137*, 451–458, doi:10.1039/c1an15920h.
388. Schmid, P.; Hunter, E.; Calvert, J.O.H.N. Extraction and purification of lipids. III. Serious limitations of chloroform and chloroform-methanol in lipid investigations. *Physiol. Chem. Phys. Med. NMR* **1973**, *5*, 151–155.
389. Höring, M.; Stieglmeier, C.; Schnabel, K.; Hallmark, T.; Ekroos, K.; Burkhardt, R.; Liebisch, G. Benchmarking One-Phase Lipid Extractions for Plasma Lipidomics. *Anal. Chem.* **2022**, *94*, 12292–12296, doi:10.1021/acs.analchem.2c02117.
390. Sarafian, M.H.; Gaudin, M.; Lewis, M.R.; Martin, F.P.; Holmes, E.; Nicholson, J.K.; Dumas, M.E. Objective set of criteria for optimization of sample preparation procedures for ultra-high throughput untargeted blood plasma lipid profiling by ultra performance liquid chromatography-mass spectrometry. *Anal. Chem.* **2014**, *86*, 5766–5774, doi:10.1021/ac500317c.
391. Cham, B.E.; Knowles, B.R. A solvent system for delipidation of plasma or serum without protein precipitation. *J. Lipid Res.* **1976**, *17*, 176–181, doi:10.1016/s0022-2275(20)37003-6.
392. Hara, A.; Radin, N.S. Lipid Extraction of Tissues with a Low/Toxicitz Solvents. *Anal. Biochem.* **1978**, *90*, 420–426.
393. Retra, K.; Bleijerveld, O.B.; van Gestel, R.A.; Tielens, A.G.M.; van Hellemond, J.J.; Brouwers, J.F. A simple and universal method for the separation and identification of phospholipid molecular species. *Rapid Commun. Mass Spectrom.* **2008**, *22*, 1853–1862, doi:10.1002/rcm.3562 A.
394. Lydic, T.A.; Busik, J. V.; Reid, G.E. A monophasic extraction strategy for the simultaneous lipidome analysis of polar and nonpolar retina lipids. *J. Lipid Res.* **2014**, *55*, 1797–1809, doi:10.1194/jlr.D050302.
395. Lee, D.Y.; Kind, T.; Yoon, Y.R.; Fiehn, O.; Liu, K.H. Comparative evaluation of extraction methods for simultaneous mass-spectrometric analysis of complex lipids and primary metabolites from human blood plasma. *Anal. Bioanal. Chem.* **2014**, *406*, 7275–7286, doi:10.1007/s00216-014-8124-x.
396. Hořejší, K.; Jirásko, R.; Chocholoušková, M.; Wolrab, D.; Kahoun, D.; Holčapek, M. Comprehensive identification of glycosphingolipids in human plasma using hydrophilic interaction liquid chromatography—electrospray ionization mass spectrometry. *Metabolites* **2021**, *11*, 1–24, doi:10.3390/metabo11030140.
397. Ejsing, C.S.; Sampaio, J.L.; Surendranath, V.; Duchoslav, E.; Ekroos, K.; Klemm, R.W.; Simons, K.; Shevchenko, A. Global analysis of the yeast lipidome by quantitative shotgun mass spectrometry. *Proc. Natl. Acad. Sci. U. S. A.* **2009**, *106*, 2136–2141, doi:10.1073/pnas.0811700106.
398. Phenomenex The Complete Guide to Solid Phase Extraction (SPE): A method development and application guide. *Phenomenex* 2017, 1–15.

399. Song, Z.; Duan, C.; Shi, M.; Li, S.; Guan, Y. One-step preparation of ZrO2/SiO2 microspheres and modification with D-fructose 1,6-bisphosphate as stationary phase for hydrophilic interaction chromatography. *J. Chromatogr. A* **2017**, *1522*, 30–37, doi:10.1016/j.chroma.2017.09.046.
400. Noda, A.; Kato, M.; Miyazaki, S.; Kyogashima, M. Separation of glycosphingolipids with titanium dioxide. *Glycoconj. J.* **2018**, *35*, 493–498, doi:10.1007/s10719-018-9844-5.
401. Nagasawa, H.; Miyazaki, S.; Kyogashima, M. Simple separation of glycosphingolipids in the lower phase of a Folch's partition from crude lipid fractions using zirconium dioxide. *Glycoconj. J.* **2022**, *39*, 789–795, doi:10.1007/s10719-022-10080-w.
402. Ahmad, S.; Kalra, H.; Gupta, A.; Raut, B.; Hussain, A.; Rahman, M.A. HybridSPE: A novel technique to reduce phospholipid-based matrix effect in LC-ESI-MS Bioanalysis. *J. Pharm. Bioallied Sci.* **2012**, *4*, 267–275, doi:10.4103/0975-7406.103234.
403. Khoury, S.; Masson, E.; Sibille, E.; Cabaret, S.; Berdeaux, O. Rapid sample preparation for ganglioside analysis by liquid chromatography mass spectrometry. *J. Chromatogr. B Anal. Technol. Biomed. Life Sci.* **2020**, *1137*, 121956, doi:10.1016/j.jchromb.2019.121956.
404. Ruhaak, L.R.; Deelder, A.M.; Wuhrer, M. Oligosaccharide analysis by graphitized carbon liquid chromatography-mass spectrometry. *Anal. Bioanal. Chem.* **2009**, *394*, 163–174, doi:10.1007/s00216-009-2664-5.
405. Appelblad, P.; Jonsson, T.; Jiang, W. *A Practical Guide to HILIC including ZIC-HILIC applications*; 1st ed.; Merck SeQuant AB: Darmstadt (Germany), 2009; ISBN 978-91-631-8370-6.
406. Uchikata, T.; Matsubara, A.; Fukusaki, E.; Bamba, T. High-throughput phospholipid profiling system based on supercritical fluid extraction-supercritical fluid chromatography/mass spectrometry for dried plasma spot analysis. *J. Chromatogr. A* **2012**, *1250*, 69–75, doi:10.1016/j.chroma.2012.06.031.
407. Le Faouder, P.; Soullier, J.; Tremblay-Franco, M.; Tournadre, A.; Martin, J.F.; Guitton, Y.; Carlé, C.; Caspar-Bauguil, S.; Denechaud, P.D.; Bertrand-Michel, J. Untargeted lipidomic profiling of dry blood spots using sfc-hrms. *Metabolites* **2021**, *11*, doi:10.3390/metabo11050305.
408. Pizarro, C.; Arenzana-Rámila, I.; Pérez-Del-Notario, N.; Pérez-Matute, P.; González-Sáiz, J.M. Plasma lipidomic profiling method based on ultrasound extraction and liquid chromatography mass spectrometry. *Anal. Chem.* **2013**, *85*, 12085–12092, doi:10.1021/ac403181c.
409. Teo, C.C.; Chong, W.P.K.; Ho, Y.S. Development and application of microwave-assisted extraction technique in biological sample preparation for small molecule analysis. *Metabolomics* **2013**, *9*, 1109–1128, doi:10.1007/s11306-013-0528-7.
410. Ramluckan, K.; Moodley, K.G.; Bux, F. An evaluation of the efficacy of using selected solvents for the extraction of lipids from algal biomass by the soxhlet extraction method. *Fuel* **2014**, *116*, 103–108, doi:10.1016/j.fuel.2013.07.118.
411. Zgoła-Grześkowiak, A.; Grześkowiak, T. Dispersive liquid-liquid microextraction. *TrAC - Trends Anal. Chem.* **2011**, *30*, 1382–1399, doi:10.1016/j.trac.2011.04.014.
412. Pusvaskiene, E.; Januskevic, B.; Prichodko, A.; Vickackaite, V. Simultaneous derivatization and dispersive liquid-liquid microextraction for fatty acid GC determination in water. *Chromatographia* **2009**, *69*, 271–276, doi:10.1365/s10337-008-0885-y.
413. Li, Y.T.; Chou, C.W.; Li, S.C.; Kobayashi, U.; Ishibashi, Y.H.; Ito, M. Preparation of homogenous oligosaccharide chains from glycosphingolipids. *Glycoconj. J.* **2009**, *26*, 929–933, doi:10.1007/s10719-008-9125-9.

414. Ito, M.; Yamagata, T. A Novel Glycosphingolipid-degrading Enzyme Cleaves of the Linkage of Neutral and Acidic between the Oligosaccharide and Ceramide Glycosphingolipids *. *J. Biol. Chem.* **1986**, *261*, 14278–14282, doi:10.1016/S0021-9258(18)67015-2.
415. Li, S.-C.; DeGasperi, R.; Muldrey, J.E.; Li, Y.-T. A unique glycosphingolipid-splitting enzyme (ceramide-glycanase fromv leech) cleaves the linkage between oligosaccharide and the ceramide. *Biochem. Biophys. Res. Commun.* **1986**, *141*, 346–352, doi:10.1016/s0006-291x(86)80375-8.
416. Chakraberty, R.; Reiz, B.; Cairo, C.W. Profiling of glycosphingolipids with SCDase digestion and HPLC-FLD-MS. *Anal. Biochem.* **2021**, *631*, 114361, doi:10.1016/j.ab.2021.114361.
417. Wiegandt, H.; BÜCKING, H.W. Carbohydrate Components of Extraneuronal Gangliosides from Bovine and Human Spleen, and Bovine Kidney. *Eur. J. Biochem.* **1970**, *15*, 287–292, doi:10.1111/j.1432-1033.1970.tb01006.x.
418. Hakomori, S.I. Release of carbohydrates from sphingoglycolipid by osmium-catalyzed periodate oxidation followed by treatment with mild alkali. *J. Lipid Res.* **1966**, *7*, 789–792, doi:10.1016/s0022-2275(20)38958-6.
419. Ito, M.; Yamagata, T. Purification and characterization of glycosphingolipid-specific endoglycosidases (endoglycoceramidases) from a mutant strain of Rhodococcus sp. Evidence for three molecular species of endoglycoceramidase with different specificities. *J. Biol. Chem.* **1989**, *264*, 9510–9519, doi:10.1016/S0021-9258(18)60561-7.
420. Han, Y. Bin; Chen, L.Q.; Li, Z.; Tan, Y.M.; Feng, Y.; Yang, G.Y. Structural insights into the broad substrate specificity of a novel endoglycoceramidase i belonging to a new subfamily of GH5 glycosidases. *J. Biol. Chem.* **2017**, *292*, 4789–4800, doi:10.1074/jbc.M116.763821.
421. Albrecht, S.; Vainauskas, S.; Stöckmann, H.; McManus, C.; Taron, C.H.; Rudd, P.M. Comprehensive Profiling of Glycosphingolipid Glycans Using a Novel Broad Specificity Endoglycoceramidase in a High-Throughput Workflow. *Anal. Chem.* **2016**, *88*, 4795–4802, doi:10.1021/acs.analchem.6b00259.
422. Ishibashi, Y.; Kobayashi, U.; Hijikata, A.; Sakaguchi, K.; Goda, H.M.; Tamura, T.; Okino, N.; Ito, M. Preparation and characterization of EGCase I, applicable to the comprehensive analysis of GSLs, using a rhodococcal expression system. *J. Lipid Res.* **2012**, *53*, 2242–2251, doi:10.1194/jlr.D028951.
423. Karlsson, H.; Halim, A.; Teneberg, S. Differentiation of glycosphingolipid-derived glycan structural isomers by liquid chromatography/mass spectrometry. *Glycobiology* **2010**, *20*, 1103–1116, doi:10.1093/glycob/cwq070.
424. Fujitani, N.; Takegawa, Y.; Ishibashi, Y.; Araki, K.; Furukawa, J.I.; Mitsutake, S.; Igarashi, Y.; Ito, M.; Shinohara, Y. Qualitative and quantitative cellular glycomics of glycosphingolipids based on rhodococcal endoglycosylceramidase-assisted glycan cleavage, glycoblotting-assisted sample preparation, and matrix-assisted laser desorption ionization tandem time-of-flight ma. *J. Biol. Chem.* **2011**, *286*, 41669–41679, doi:10.1074/jbc.M111.301796.
425. Karlsson, K.-A. Preparation of Total Nonacid Glycolipids for Overlay Analysis of Receptors for Bacteria and Viruses and for Other Studies. *Methods Enzymol.* **1987**, *138*, 212–220, doi:10.1016/0076-6879(87)38018-8.
426. van Echten-Decker, G. Sphingolipid extraction and analysis by thin-layer chromatography. *Prog. Brain Res.* **1994**, *101*, 139.
427. Barrientos, R.C.; Zhang, Q. Differential Isotope Labeling by Permethylation and Reversed-Phase Liquid Chromatography-Mass Spectrometry for Relative

Quantification of Intact Neutral Glycolipids in Mammalian Cells. *Anal. Chem.* **2019**, *91*, 9673–9681, doi:10.1021/acs.analchem.9b01206.
428. Li, M.; Yang, L.; Bai, Y.; Liu, H. Analytical methods in lipidomics and their applications. *Anal. Chem.* **2014**, *86*, 161–175, doi:10.1021/ac403554h.
429. Haynes, C.A.; Allegood, J.C.; Park, H.; Sullards, M.C. Sphingolipidomics: Methods for the comprehensive analysis of sphingolipids. *J. Chromatogr. B Anal. Technol. Biomed. Life Sci.* **2009**, *877*, 2696–2708, doi:10.1016/j.jchromb.2008.12.057.
430. Wilson, R.; Sargent, J.R. High-resolution separation of polyunsaturated fatty acids by argentation thin-layer chromatography. *J. Chromatogr. A* **1992**, *623*, 403–407, doi:10.1016/0021-9673(92)80385-8.
431. Dobson, G.; Christie, W.W.; Nikolova-Damyanova, B. Silver ion chromatography of lipids and fatty acids. *J. Chromatogr. B* **1995**, *671*, 197–222.
432. Fuchs, B.; Süß, R.; Teuber, K.; Eibisch, M.; Schiller, J. Lipid analysis by thin-layer chromatography-A review of the current state. *J. Chromatogr. A* **2011**, *1218*, 2754–2774, doi:10.1016/j.chroma.2010.11.066.
433. Schnaar, R.L. and Cm is the product of the percent molar incidence of. *Methods* **1994**, *230*, 348–370.
434. Svennerholm, L. Quantitive estimation of sialic acids. *Biochim. Biophys. Acta* **1957**, *24*, 604–611, doi:10.1016/0006-3002(57)90254-8.
435. Svennerholm, L.; Fredman, P. A procedure for the quantitative isolation of brain gangliosides. *Biochim. Biophys. Acta (BBA)/Lipids Lipid Metab.* **1980**, *617*, 97–109, doi:10.1016/0005-2760(80)90227-1.
436. Svennerholm, L.; Rynmark, B. -M; Vilbergsson, G.; Fredman, P.; Gottfries, J.; Månsson, J. -E; Percy, A. Gangliosides in Human Fetal Brain. *J. Neurochem.* **1991**, *56*, 1763–1768, doi:10.1111/j.1471-4159.1991.tb02078.x.
437. Svennerholm, L. the Quantitative Estimation of Cerebrosides in Nervous Tissue. *J. Neurochem.* **1956**, *1*, 42–53, doi:10.1111/j.1471-4159.1956.tb12053.x.
438. Stübiger, G.; Pittenauer, E.; Belgacem, O.; Rehulka, P.; Widhalm, K.; Allmaier, G. Analysis of human plasma lipids and soybean lecithin by means of high-performance thin-layer chromatography and matrix-assisted laser desorption/ionization mass spectrometry. *Rapid Commun. Mass Spectrom.* **2009**, *23*, 2711–2723, doi:10.1002/rcm.4173.
439. Paglia, G.; Ifa, D.R.; Wu, C.; Corso, G.; Graham Cooks, R. Desorption electrospray ionization mass spectrometry analysis of lipids after two-dimensional high-performance thin-layer chromatography partial separation. *Anal. Chem.* **2010**, *82*, 1744–1750, doi:10.1021/ac902325j.
440. Magnani, J.L.; Smith, D.F.; Ginsburg, V. Detection of gangliosides that bind cholera toxin: Direct binding of 125I-labeled toxin to thin-layer chromatograms. *Anal. Biochem.* **1980**, *109*, 399–402, doi:10.1016/0003-2697(80)90667-3.
441. Meisen, I.; Mormann, M.; Müthing, J. Thin-layer chromatography, overlay technique and mass spectrometry: A versatile triad advancing glycosphingolipidomics. *Biochim. Biophys. Acta - Mol. Cell Biol. Lipids* **2011**, *1811*, 875–896, doi:10.1016/j.bbalip.2011.04.006.
442. Barone, A.; Benktander, J.; Teneberg, S.; Breimer, M.E. Characterization of acid and non-acid glycosphingolipids of porcine heart valve cusps as potential immune targets in biological heart valve grafts. *Xenotransplantation* **2014**, *21*, 510–522, doi:10.1111/xen.12123.
443. Barone, A.; Benktander, J.; Whiddon, C.; Jin, C.; Galli, C.; Teneberg, S.; Breimer, M.E. Glycosphingolipids of porcine, bovine, and equine pericardia as potential immune targets in bioprosthetic heart valve grafts. *Xenotransplantation* **2018**, *25*, 1–15,

doi:10.1111/xen.12406.
444. Barone, A.; Benktander, J.; Ångström, J.; Aspegren, A.; Björquist, P.; Teneberg, S.; Breimer, M.E. Structural complexity of non-acid glycosphingolipids in human embryonic stem cells grown under feeder-free conditions. *J. Biol. Chem.* **2013**, *288*, 10035–10050, doi:10.1074/jbc.M112.436162.
445. Sweeley, C.C.; Nunez, H.A. Structural analysis of glycoconjugates by mass spectrometry and nuclear magnetic resonance spectroscopy. *Ann. Rev. Biochem.* **1985**, *54*, 765–801, doi:10.1201/9780203485286.ch3.
446. Wenk, M.R. The emerging field of lipidomics. *Nat. Rev. Drug Discov.* **2005**, *4*, 594–610, doi:10.1038/nrd1776.
447. Koerner, T.A.W.; Prestegard, J.H.; Demou, P.C.; Yu, R.K. High-Resolution Proton NMR Studies of Gangliosides. 1. Use of Homonuclear Two-Dimensional Spin-Echo J-Correlated Spectroscopy for Determination of Residue Composition and Anomeric Configurations. *Biochemistry* **1983**, *22*, 2676–2687, doi:10.1021/bi00280a014.
448. Wolrab, D.; Jirásko, R.; Chocholoušková, M.; Peterka, O.; Holčapek, M. Oncolipidomics: Mass spectrometric quantitation of lipids in cancer research. *Trends Anal. Chem.* **2019**, *121*, 115480.
449. Li, J.; Vosegaard, T.; Guo, Z. Applications of nuclear magnetic resonance in lipid analyses: An emerging powerful tool for lipidomics studies. *Prog. Lipid Res.* **2017**, *68*, 37–56, doi:10.1016/j.plipres.2017.09.003.
450. Garádi, Z.; Tóth, A.; Gáti, T.; Dancsó, A.; Béni, S. Utilizing the 1H-15N NMR Methods for the Characterization of Isomeric Human Milk Oligosaccharides. *Int. J. Mol. Sci.* **2023**, *24*, doi:10.3390/ijms24032180.
451. Wu, Z.; Bagarolo, G.I.; Thoröe-Boveleth, S.; Jankowski, J. "Lipidomics": Mass spectrometric and chemometric analyses of lipids. *Adv. Drug Deliv. Rev.* **2020**, *159*, 294–307, doi:10.1016/j.addr.2020.06.009.
452. Li, M.; Zhou, Z.; Nie, H.; Bai, Y.; Liu, H. Recent advances of chromatography and mass spectrometry in lipidomics. *Anal. Bioanal. Chem.* **2011**, *399*, 243–249, doi:10.1007/s00216-010-4327-y.
453. Hauff, S.; Vetter, W. Quantification of fatty acids as methyl esters and phospholipids in cheese samples after separation of triacylglycerides and phospholipids. *Anal. Chim. Acta* **2009**, *636*, 229–235, doi:10.1016/j.aca.2009.01.056.
454. Han, L. Da; Xia, J.F.; Liang, Q.L.; Wang, Y.; Wang, Y.M.; Hu, P.; Li, P.; Luo, G.A. Plasma esterified and non-esterified fatty acids metabolic profiling using gas chromatography-mass spectrometry and its application in the study of diabetic mellitus and diabetic nephropathy. *Anal. Chim. Acta* **2011**, *689*, 85–91, doi:10.1016/j.aca.2011.01.034.
455. Sánchez-Ávila, N.; Mata-Granados, J.M.; Ruiz-Jiménez, J.; Luque de Castro, M.D. Fast, sensitive and highly discriminant gas chromatography-mass spectrometry method for profiling analysis of fatty acids in serum. *J. Chromatogr. A* **2009**, *1216*, 6864–6872, doi:10.1016/j.chroma.2009.08.045.
456. Hejazi, L.; Ebrahimi, D.; Guilhaus, M.; Hibbert, D.B. Determination of the composition of fatty acid mixtures using GC × FI-MS: A comprehensive two-dimensional separation approach. *Anal. Chem.* **2009**, *81*, 1450–1458, doi:10.1021/ac802277c.
457. Martin, C.A.; de Oliveira, C.C.; Visentainer, J.V.; Matsushita, M.; de Souza, N.E. Optimization of the selectivity of a cyanopropyl stationary phase for the gas chromatographic analysis of trans fatty acids. *J. Chromatogr. A* **2008**, *1194*, 111–117, doi:10.1016/j.chroma.2008.04.033.
458. Destaillats, F.; Cruz-Hernandez, C.; Nagy, K.; Dionisi, F. Identification of

monoacylglycerol regio-isomers by gas chromatography-mass spectrometry. *J. Chromatogr. A* **2010**, *1217*, 1543–1548, doi:10.1016/j.chroma.2010.01.016.
459. Son, H.H.; Moon, J.Y.; Seo, H.S.; Kim, H.H.; Chung, B.C.; Choi, M.H. High-temperature GC-MS-based serum cholesterol signatures may reveal sex differences in vasospastic angina. *J. Lipid Res.* **2014**, *55*, 155–162, doi:10.1194/jlr.D040790.
460. Ge, P.; Luo, Y.; Chen, H.; Liu, J.; Guo, H.; Xu, C.; Qu, J.; Zhang, G.; Chen, H. Application of Mass Spectrometry in Pancreatic Cancer Translational Research. *Front. Oncol.* **2021**, *11*, 1–16, doi:10.3389/fonc.2021.667427.
461. Avela, H.F.; Sirén, H. Advances in analytical tools and current statistical methods used in ultra-high-performance liquid chromatography-mass spectrometry of glycero-, glycerophospho- and sphingolipids. *Int. J. Mass Spectrom.* **2020**, *457*, doi:10.1016/j.ijms.2020.116408.
462. Vaňková, Z.; Peterka, O.; Chocholoušková, M.; Wolrab, D.; Jirásko, R.; Holčapek, M. Retention dependences support highly confident identification of lipid species in human plasma by reversed-phase UHPLC/MS. *Anal. Bioanal. Chem.* **2022**, *414*, 319–331, doi:10.1007/s00216-021-03492-4.
463. Ovčačíková, M.; Lísa, M.; Cífková, E.; Holčapek, M. Retention behavior of lipids in reversed-phase ultrahigh-performance liquid chromatography-electrospray ionization mass spectrometry. *J. Chromatogr. A* **2016**, *1450*, 76–85, doi:10.1016/j.chroma.2016.04.082.
464. Gao, F.; Tian, X.; Wen, D.; Liao, J.; Wang, T.; Liu, H. Analysis of phospholipid species in rat peritoneal surface layer by liquid chromatography/electrospray ionization ion-trap mass spectrometry. *Biochim. Biophys. Acta - Mol. Cell Biol. Lipids* **2006**, *1761*, 667–676, doi:10.1016/j.bbalip.2006.03.022.
465. Lísa, M.; Cífková, E.; Holčapek, M. Lipidomic profiling of biological tissues using off-line two-dimensional high-performance liquid chromatography-mass spectrometry. *J. Chromatogr. A* **2011**, *1218*, 5146–5156, doi:10.1016/j.chroma.2011.05.081.
466. Lísa, M.; Cífková, E.; Khalikova, M.; Ovčačíková, M.; Holčapek, M. Lipidomic analysis of biological samples: Comparison of liquid chromatography, supercritical fluid chromatography and direct infusion mass spectrometry methods. *J. Chromatogr. A* **2017**, *1525*, 96–108, doi:10.1016/j.chroma.2017.10.022.
467. Cífková, E.; Holčapek, M.; Lísa, M.; Vrána, D.; Gatěk, J.; Melichar, B. Determination of lipidomic differences between human breast cancer and surrounding normal tissues using HILIC-HPLC/ESI-MS and multivariate data analysis. *Anal. Bioanal. Chem.* **2015**, *407*, 991–1002, doi:10.1007/s00216-014-8272-z.
468. Holčapek, M.; Ovčačíková, M.; Lísa, M.; Cífková, E.; Hájek, T. Continuous comprehensive two-dimensional liquid chromatography–electrospray ionization mass spectrometry of complex lipidomic samples. *Anal. Bioanal. Chem.* **2015**, *407*, 5033–5043, doi:10.1007/s00216-015-8528-2.
469. Lísa, M.; Holčapek, M. Characterization of triacylglycerol enantiomers using chiral HPLC/APCI-MS and synthesis of enantiomeric triacylglycerols. *Anal. Chem.* **2013**, *85*, 1852–1859, doi:10.1021/ac303237a.
470. Holčapek, M.; Lísa, M. Silver-Ion Liquid Chromatography - Mass Spectrometry. In *Handbook of Advanced Chromatography/Mass Spectrometry Techniques*; Holčapek, M., Byrdwell, W.C., Eds.; Elsevier: London, UK, 2017; p. 520 ISBN 9780128117323.
471. Deng, L.; Nakano, H.; Iwasaki, Y. Direct separation of monoacylglycerol isomers by enantioselective high-performance liquid chromatography. *J. Chromatogr. A* **2008**, *1198–1199*, 67–72, doi:10.1016/j.chroma.2008.03.095.
472. Ho, C.S.; Lam, C.W.K.; Chan, M.H.M.; Cheung, R.C.K.; Law, L.K.; Lit, L.C.W.; Ng, K.F.; Suen, M.W.M.; Tai, H.L. Electrospray ionisation mass spectrometry: principles

and clinical applications. *Clin. Biochem. Rev.* **2003**, *24*, 3–12.
473. Parr, M.K.; Wüst, B.; Teubel, J.; Joseph, J.F. Splitless hyphenation of SFC with MS by APCI, APPI, and ESI exemplified by steroids as model compounds. *J. Chromatogr. B Anal. Technol. Biomed. Life Sci.* **2018**, *1091*, 67–78, doi:10.1016/j.jchromb.2018.05.017.
474. Stephenson, D.J.; Hoeferlin, L.A.; Chalfant, C.E. Lipidomics in translational research and the clinical significance of lipid-based biomarkers. *Transl. Res.* **2017**, *189*, 13–29, doi:10.1016/j.trsl.2017.06.006.
475. Banerjee, S.; Mazumdar, S. Electrospray Ionization Mass Spectrometry: A Technique to Access the Information beyond the Molecular Weight of the Analyte. *Int. J. Anal. Chem.* **2012**, *2012*, 1–40, doi:10.1155/2012/282574.
476. Hájek, R.; Jirásko, R.; Lísa, M.; Cífková, E.; Holčapek, M. Hydrophilic Interaction Liquid Chromatography-Mass Spectrometry Characterization of Gangliosides in Biological Samples. *Anal. Chem.* **2017**, *89*, 12425–12432, doi:10.1021/acs.analchem.7b03523.
477. Farwanah, H.; Wirtz, J.; Kolter, T.; Raith, K.; Neubert, R.H.H.; Sandhoff, K. Normal phase liquid chromatography coupled to quadrupole time of flight atmospheric pressure chemical ionization mass spectrometry for separation, detection and mass spectrometric profiling of neutral sphingolipids and cholesterol. *J. Chromatogr. B Anal. Technol. Biomed. Life Sci.* **2009**, *877*, 2976–2982, doi:10.1016/j.jchromb.2009.07.008.
478. Van Smeden, J.; Hoppel, L.; Van Der Heijden, R.; Hankemeier, T.; Vreeken, R.J.; Bouwstra, J.A. LC/MS analysis of stratum corneum lipids: Ceramide profiling and discovery. *J. Lipid Res.* **2011**, *52*, 1211–1221, doi:10.1194/jlr.M014456.
479. Sato, Y.; Suzuki, I.; Nakamura, T.; Bernier, F.; Aoshima, K.; Oda, Y. Identification of a new plasma biomarker of Alzheimer's disease using metabolomics technology. *J. Lipid Res.* **2012**, *53*, 567–576, doi:10.1194/jlr.M022376.
480. Wolrab, D.; Peterka, O.; Chocholoušková, M.; Holčapek, M. Ultrahigh-performance supercritical fluid chromatography / mass spectrometry in the lipidomic analysis. *TrAC - Trends Anal. Chem.* **2022**, *149*, doi:10.1016/j.trac.2022.116546.
481. Haag, A.M. Mass Analyzers and Mass Spectrometers. *Adv. Exp. Med. Biol.* **2016**, *919*, 157–169, doi:10.1007/978-3-319-41448-5_7.
482. de Hoffmann, E.; Stroobant, V. *Mass Spectrometry: Pricniples and Applications*; 3rd ed.; John Wiley & Sons, Ltd., 2007; ISBN 978-0-470-03310-4.
483. Holčapek, M.; Jirásko, R.; Lísa, M. Recent developments in liquid chromatography-mass spectrometry and related techniques. *J. Chromatogr. A* **2012**, *1259*, 3–15, doi:10.1016/j.chroma.2012.08.072.
484. van de Velde, B.; Guillarme, D.; Kohler, I. Supercritical fluid chromatography – Mass spectrometry in metabolomics: Past, present, and future perspectives. *J. Chromatogr. B Anal. Technol. Biomed. Life Sci.* **2020**, *1161*, 122444, doi:10.1016/j.jchromb.2020.122444.
485. Pilařová, V.; Plachká, K.; Khalikova, M.A.; Svec, F.; Nováková, L. Recent developments in supercritical fluid chromatography – mass spectrometry: Is it a viable option for analysis of complex samples? *TrAC - Trends Anal. Chem.* **2019**, *112*, 212–225, doi:10.1016/j.trac.2018.12.023.
486. West, C. Current trends in supercritical fluid chromatography. *Anal. Bioanal. Chem.* **2018**, *410*, 6441–6457, doi:10.1007/s00216-018-1267-4.
487. Tarafder, A. Metamorphosis of supercritical fluid chromatography to SFC: An Overview. *TrAC - Trends Anal. Chem.* **2016**, *81*, 3–10, doi:10.1016/j.trac.2016.01.002.
488. Yamada, T.; Uchikata, T.; Sakamoto, S.; Yokoi, Y.; Nishiumi, S.; Yoshida, M.;

Fukusaki, E.; Bamba, T. Supercritical fluid chromatography/orbitrap mass spectrometry based lipidomics platform coupled with automated lipid identification software for accurate lipid profiling. *J. Chromatogr. A* **2013**, *1301*, 237–242, doi:10.1016/j.chroma.2013.05.057.

489. Sakai, M.; Hayakawa, Y.; Funada, Y.; Ando, T.; Fukusaki, E.; Bamba, T. Development of a split-flow system for high precision variable sample introduction in supercritical fluid chromatography. *J. Chromatogr. A* **2017**, *1515*, 218–231, doi:10.1016/j.chroma.2017.07.077.
490. Suzuki, M.; Nishiumi, S.; Kobayashi, T.; Sakai, A.; Iwata, Y.; Uchikata, T.; Izumi, Y.; Azuma, T.; Bamba, T.; Yoshida, M. Use of on-line supercritical fluid extraction-supercritical fluid chromatography/tandem mass spectrometry to analyze disease biomarkers in dried serum spots compared with serum analysis using liquid chromatography/tandem mass spectrometry. *Rapid Commun. Mass Spectrom.* **2017**, *31*, 886–894, doi:10.1002/rcm.7857.
491. Wolrab, D.; Chocholoušková, M.; Jirásko, R.; Peterka, O.; Holčapek, M. Validation of lipidomic analysis of human plasma and serum by supercritical fluid chromatography–mass spectrometry and hydrophilic interaction liquid chromatography–mass spectrometry. *Anal. Bioanal. Chem.* **2020**, *412*, 2375–2388, doi:10.1007/s00216-020-02473-3.
492. Lísa, M.; Holčapek, M. High-Throughput and Comprehensive Lipidomic Analysis Using Ultrahigh-Performance Supercritical Fluid Chromatography-Mass Spectrometry. *Anal. Chem.* **2015**, *87*, 7187–7195, doi:10.1021/acs.analchem.5b01054.
493. Yang, L.; Nie, H.; Zhao, F.; Song, S.; Meng, Y.; Bai, Y.; Liu, H. A novel online two-dimensional supercritical fluid chromatography/reversed phase liquid chromatography–mass spectrometry method for lipid profiling. *Anal. Bioanal. Chem.* **2020**, *412*, 2225–2235, doi:10.1007/s00216-019-02242-x.
494. Kočová Vlčková, H.; Pilařová, V.; Svobodová, P.; Plíšek, J.; Švec, F.; Nováková, L. Current state of bioanalytical chromatography in clinical analysis. *Analyst* **2018**, *143*, 1305–1325, doi:10.1039/c7an01807j.
495. May, J.C.; McLean, J.A. Ion mobility-mass spectrometry: Time-dispersive instrumentation. *Anal. Chem.* **2015**, *87*, 1422–1436, doi:10.1021/ac504720m.
496. Dodds, J.N.; Baker, E.S. Ion Mobility Spectrometry: Fundamental Concepts, Instrumentation, Applications, and the Road Ahead. *J. Am. Soc. Mass Spectrom.* **2019**, *30*, 2185–2195, doi:10.1007/s13361-019-02288-2.
497. Camunas-Alberca, S.M.; Moran-Garrido, M.; Sáiz, J.; Gil-de-la-Fuente, A.; Barbas, C.; Gradillas, A. Integrating the potential of ion mobility spectrometry-mass spectrometry in the separation and structural characterisation of lipid isomers. *Front. Mol. Biosci.* **2023**, *10*, 1–21, doi:10.3389/fmolb.2023.1112521.
498. Paglia, G.; Kliman, M.; Claude, E.; Geromanos, S.; Astarita, G. Applications of ion-mobility mass spectrometry for lipid analysis. *Anal. Bioanal. Chem.* **2015**, *407*, 4995–5007, doi:10.1007/s00216-015-8664-8.
499. Moran-Garrido, M.; Camunas-Alberca, S.M.; Gil-de-la Fuente, A.; Mariscal, A.; Gradillas, A.; Barbas, C.; Sáiz, J. Recent developments in data acquisition, treatment and analysis with ion mobility-mass spectrometry for lipidomics. *Proteomics* **2022**, *22*, doi:10.1002/pmic.202100328.
500. Sarbu, M.; Fabris, D.; Vukelić, Ž.; Clemmer, D.E.; Zamfir, A.D. Ion Mobility Mass Spectrometry Reveals Rare Sialylated Glycosphingolipid Structures in Human Cerebrospinal Fluid. *Molecules* **2022**, *27*, 1–13, doi:10.3390/molecules27030743.
501. Gabelica, V.; Shvartsburg, A.A.; Afonso, C.; Barran, P.; Benesch, J.L.P.; Bleiholder, C.; Bowers, M.T.; Bilbao, A.; Bush, M.F.; Campbell, J.L.; et al. Recommendations for

reporting ion mobility Mass Spectrometry measurements. *Mass Spectrom. Rev.* **2019**, *38*, 291–320, doi:10.1002/mas.21585.
502. May, J.C.; Morris, C.B.; McLean, J.A. Ion mobility collision cross section compendium. *Anal. Chem.* **2017**, *89*, 1032–1044, doi:10.1021/acs.analchem.6b04905.
503. Paglia, G.; Astarita, G. Metabolomics and lipidomics using traveling-wave ion mobility mass spectrometry. *Nat. Protoc.* **2017**, *12*, 797–813, doi:10.1038/nprot.2017.013.
504. Hu, C.; Wang, C.; He, L.; Han, X. Novel strategies for enhancing shotgun lipidomics for comprehensive analysis of cellular lipidomes. *TrAC - Trends Anal. Chem.* **2019**, *120*, doi:10.1016/j.trac.2018.11.028.
505. Han, X.; Gross, R.W. Electrospray ionization mass spectroscopic analysis of human erythrocyte plasma membrane phospholipids. *Proc. Natl. Acad. Sci. U. S. A.* **1994**, *91*, 10635–10639, doi:10.1073/pnas.91.22.10635.
506. Ståhlman, M.; Ejsing, C.S.; Tarasov, K.; Perman, J.; Borén, J.; Ekroos, K. High-throughput shotgun lipidomics by quadrupole time-of-flight mass spectrometry. *J. Chromatogr. B Anal. Technol. Biomed. Life Sci.* **2009**, *877*, 2664–2672, doi:10.1016/j.jchromb.2009.02.037.
507. Han, X. Multi-dimensional mass spectrometry-based shotgun lipidomics and the altered lipids at the mild cognitive impairment stage of Alzheimer's disease. *Biochim. Biophys. Acta - Mol. Cell Biol. Lipids* **2010**, *1801*, 774–783, doi:10.1016/j.bbalip.2010.01.010.
508. Yang, K.; Zhao, Z.; Gross, R.W.; Han, X. Systematic analysis of choline-containing phospholipids using multi-dimensional mass spectrometry-based shotgun lipidomics. *J. Chromatogr. B Anal. Technol. Biomed. Life Sci.* **2009**, *877*, 2924–2936, doi:10.1016/j.jchromb.2009.01.016.
509. Manicke, N.E.; Wiseman, J.M.; Ifa, D.R.; Cooks, R.G. Desorption Electrospray Ionization (DESI) Mass Spectrometry and Tandem Mass Spectrometry (MS/MS) of Phospholipids and Sphingolipids: Ionization, Adduct Formation, and Fragmentation. *J. Am. Soc. Mass Spectrom.* **2008**, *19*, 531–543, doi:10.1016/j.jasms.2007.12.003.
510. Nemes, P.; Woods, A.S.; Vertes, A. Simultaneous imaging of small metabolites and lipids in rat brain tissues at atmospheric pressure by laser ablation electrospray ionization mass spectrometry. *Anal. Chem.* **2010**, *82*, 982–988, doi:10.1021/ac902245p.
511. Muck, A.; Stelzner, T.; Hübner, U.; Christiansen, S.; Svatoš, A. Lithographically patterned silicon nanowire arrays for matrix free LDI-TOF/MS analysis of lipids. *Lab Chip* **2010**, *10*, 320–325, doi:10.1039/b913212k.
512. Han, X.; Yang, K.; Gross, R.W. Microfluidics-based electrospray ionization enhances the intrasource separation of lipid classes and extends identification of individual molecular species through multi-dimensional mass spectrometry: development of an automated high-throughput platform f. *Rapid Commun. Mass Spectrom.* **2008**, *22*, 2115–2124, doi:10.1002/rcm.3595 Microfluidics-based.
513. Idkowiak, J.; Jirásko, R.; Kolářová, D.; Bártl, J.; Hájek, T.; Antonelli, M.; Vaňková, Z.; Wolrab, D.; Hrstka, R.; Študentová, H.; et al. Robust and high-throughput lipidomic quantitation of human blood samples using flow injection analysis with tandem mass spectrometry for clinical use. *Anal. Bioanal. Chem.* **2023**, *415*, 935–951, doi:10.1007/s00216-022-04490-w.
514. Hsu, F.F. Mass spectrometry-based shotgun lipidomics – a critical review from the technical point of view. *Anal. Bioanal. Chem.* **2018**, *410*, 6387–6409, doi:10.1007/s00216-018-1252-y.
515. Wang, J.; Han, X. Analytical challenges of shotgun lipidomics at different resolution of measurements. *TrAC - Trends Anal. Chem.* **2019**, *121*, 115697,

doi:10.1016/j.trac.2019.115697.
516. Harvey, D.J. Matrix-Assisted Laser Desorption/Ionization Mass Spectrometry of Carbohydrates. *Mass Spectrom. Rev.* **1999**, *18*, 349–451, doi:10.1002/(sici)1098-2787(1999)18:6<349::aid-mas1>3.0.co;2-h.
517. Cheng, H.; Sun, G.; Yang, K.; Gross, R.W.; Han, X. Selective desorption/ionization of sulfatides by MALDI-MS facilitated using 9-aminoacridine as matrix. *J. Lipid Res.* **2010**, *51*, 1599–1609, doi:10.1194/jlr.D004077.
518. Leopold, J.; Popkova, Y.; Engel, K.M.; Schiller, J. Recent developments of useful MALDI matrices for the mass spectrometric characterization of lipids. *Biomolecules* **2018**, *8*, doi:10.3390/biom8040173.
519. Torretta, E.; Fania, C.; Vasso, M.; Gelfi, C. HPTLC-MALDI MS for (glyco)sphingolipid multiplexing in tissues and blood: A promising strategy for biomarker discovery and clinical applications. *Electrophoresis* **2016**, *37*, 2036–2049, doi:10.1002/elps.201600094.
520. Furukawa, J.I.; Sakai, S.; Yokota, I.; Okada, K.; Hanamatsu, H.; Kobayashi, T.; Yoshida, Y.; Higashino, K.; Tamura, T.; Igarashi, Y.; et al. Quantitative GSL-glycome analysis of human whole serum based on an EGCase digestion and glycoblotting method. *J. Lipid Res.* **2015**, *56*, 2399–2407, doi:10.1194/jlr.D062083.
521. Norris, J.L.; Caprioli, R.M. Analysis of tissue specimens by matrix-assisted laser desorption/ionization imaging mass spectrometry in biological and clinical research. *Chem. Rev.* **2013**, *113*, 2309–2342, doi:10.1021/cr3004295.
522. Ellis, S.R.; Paine, M.R.L.; Eijkel, G.B.; Pauling, J.K.; Husen, P.; Jervelund, M.W.; Hermansson, M.; Ejsing, C.S.; Heeren, R.M.A. Automated, parallel mass spectrometry imaging and structural identification of lipids. *Nat. Methods* **2018**, *15*, 515–518, doi:10.1038/s41592-018-0010-6.
523. Wojcik, R.; Webb, I.K.; Deng, L.; Garimella, S.V.B.; Prost, S.A.; Ibrahim, Y.M.; Baker, E.S.; Smith, R.D. Lipid and glycolipid isomer analyses using ultra-high resolution ion mobility spectrometry separations. *Int. J. Mol. Sci.* **2017**, *18*, 1–12, doi:10.3390/ijms18010183.
524. Kain, L.; Webb, B.; Anderson, B.L.; Deng, S.; Holt, M.; Constanzo, A.; Zhao, M.; Self, K.; Teyton, A.; Everett, C.; et al. The Identification of the Endogenous Ligands of Natural Killer T Cells Reveals the Presence of Mammalian α-Linked Glycosylceramides. *Immunity* **2014**, *41*, 543–554, doi:10.1016/j.immuni.2014.08.017.
525. Von Gerichten, J.; Schlosser, K.; Lamprecht, D.; Morace, I.; Eckhardt, M.; Wachten, D.; Jennemann, R.; Gröne, H.J.; Mack, M.; Sandhoff, R. Diastereomer-specific quantification of bioactive hexosylceramides from bacteria and mammals. *J. Lipid Res.* **2017**, *58*, 1247–1258, doi:10.1194/jlr.D076190.
526. Duan, J.; Merrill, A.H. 1-deoxysphingolipids encountered exogenously and made de novo: Dangerous mysteries inside an enigma. *J. Biol. Chem.* **2015**, *290*, 15380–15389, doi:10.1074/jbc.R115.658823.
527. Shayman, J.A.; Abe, A.; Hiraoka, M. A turn in the road: How studies on the pharmacology of glucosylceramide synthase inhibitors led to the identification of a lysosomal phospholipase A2 with ceramide transacylase activity. *Glycoconj. J.* **2003**, *20*, 25–32, doi:10.1023/B:GLYC.0000016739.32089.55.
528. Sandhoff, R. Very long chain sphingolipids: Tissue expression, function and synthesis. *FEBS Lett.* **2010**, *584*, 1907–1913, doi:10.1016/j.febslet.2009.12.032.
529. Damen, C.W.N.; Isaac, G.; Langridge, J.; Hankemeier, T.; Vreeken, R.J. Enhanced lipid isomer separation in human plasma using reversed-phase UPLC with ion-mobility/high-resolution MS detection. *J. Lipid Res.* **2014**, *55*, 1772–1783, doi:10.1194/jlr.D047795.

530. Hořejší, K.; Jin, C.; Vaňková, Z.; Jirásko, R.; Strouhal, O.; Melichar, B.; Teneberg, S.; Holčapek, M. Comprehensive characterization of complex glycosphingolipids in human pancreatic cancer tissues. *J. Biol. Chem.* **2023**, *299*, 1–22, doi:10.1016/j.jbc.2023.102923.
531. Säljö, K.; Thornell, A.; Jin, C.; Stålberg, P.; Norlén, O.; Teneberg, S. Characterization of glycosphingolipids in the human parathyroid and thyroid glands. *Int. J. Mol. Sci.* **2021**, *22*, 7044, doi:10.3390/ijms22137044.
532. Säljö, K.; Thornell, A.; Jin, C.; Norlén, O.; Teneberg, S. Characterization of human medullary thyroid carcinoma glycosphingolipids identifies potential cancer markers. *Int. J. Mol. Sci.* **2021**, *22*, doi:10.3390/ijms221910463.
533. Wang, D.; Madunić, K.; Zhang, T.; Mayboroda, O.A.; Lageveen-Kammeijer, G.S.M.; Wuhrer, M. High Diversity of Glycosphingolipid Glycans of Colorectal Cancer Cell Lines Reflects the Cellular Differentiation Phenotype. *Mol. Cell. Proteomics* **2022**, *21*, 0–14, doi:10.1016/j.mcpro.2022.100239.
534. Wang, D.; Zhang, T.; Madunić, K.; De Waard, A.A.; Blöchl, C.; Mayboroda, O.A.; Griffioen, M.; Spaapen, R.M.; Huber, C.G.; Lageveen-Kammeijer, G.S.M.; et al. Glycosphingolipid-Glycan Signatures of Acute Myeloid Leukemia Cell Lines Reflect Hematopoietic Differentiation. *J. Proteome Res.* **2022**, *21*, 1029–1040, doi:10.1021/acs.jproteome.1c00911.
535. Mank, M.; Welsch, P.; Heck, A.J.R.; Stahl, B. Label-free targeted LC-ESI-MS2 analysis of human milk oligosaccharides (HMOS) and related human milk groups with enhanced structural selectivity. *Anal. Bioanal. Chem.* **2019**, *411*, 231–250, doi:10.1007/s00216-018-1434-7.
536. Cho, B.G.; Peng, W.; Mechref, Y. Separation of permethylated o-glycans, free oligosaccharides, and glycosphingolipid-glycans using porous graphitized carbon (Pgc) column. *Metabolites* **2020**, *10*, 1–12, doi:10.3390/metabo10110433.
537. May, J.C.; Knochenmuss, R.; Fjeldsted, J.C.; McLean, J.A. Resolution of Isomeric Mixtures in Ion Mobility Using a Combined Demultiplexing and Peak Deconvolution Technique. *Anal. Chem.* **2020**, *92*, 9482–9492, doi:10.1021/acs.analchem.9b05718.
538. Djambazova, K. V.; Dufresne, M.; Migas, L.G.; Kruse, A.R.S.; Van de Plas, R.; Caprioli, R.M.; Spraggins, J.M. MALDI TIMS IMS of Disialoganglioside Isomers─GD1a and GD1b in Murine Brain Tissue. *Anal. Chem.* **2023**, *95*, 1176–1183, doi:10.1021/acs.analchem.2c03939.
539. Xu, H.; Boucher, F.R.; Nguyen, T.T.; Taylor, G.P.; Tomlinson, J.J.; Ortega, R.A.; Simons, B.; Schlossmacher, M.G.; Saunders-Pullman, R.; Shaw, W.; et al. DMS as an orthogonal separation to LC/ESI/MS/MS for quantifying isomeric cerebrosides in plasma and cerebrospinal fluid. *J. Lipid Res.* **2019**, *60*, 200–211, doi:10.1194/jlr.D089797.
540. Domon, B.; Costello, C.E. A systematic nomenclature for carbohydrate fragmentations in FAB-MS/MS spectra of glycoconjugates. *Glycoconj. J.* **1988**, *5*, 397–409, doi:10.1007/BF01049915.
541. Ann, Q.; Adams, J. Structure determination of ceramides and neutral glycosphingolipids by collisional activation of [M + Li]+ ions. *J. Am. Soc. Mass Spectrom.* **1992**, *3*, 260–263, doi:10.1016/1044-0305(92)87010-V.
542. Domon, B.; Vath, J.E.; Costello, C.E. Analysis of derivatized ceramides and neutral glycosphingolipids by high-performance tandem mass spectrometry. *Anal. Biochem.* **1990**, *184*, 151–164, doi:10.1016/0003-2697(90)90028-8.
543. Zaia, J. Mass spectrometry of oligosaccharides. *Mass Spectrom. Rev.* **2004**, *23*, 161–227, doi:10.1002/mas.10073.
544. Kailemia, M.J.; Ruhaak, L.R.; Lebrilla, C.B.; Amster, I.J. Oligosaccharide Analysis By

Mass Spectrometry: A Review Of Recent Developments. *Anal. Chem.* **2014**, *86*, 196–212, doi:10.1021/ac403969n.
545. Schweppe, C.H.; Hoffmann, P.; Nofer, J.R.; Pohlentz, G.; Mormann, M.; Karch, H.; Friedrich, A.W.; Müthing, J. Neutral glycosphingolipids in human blood: A precise mass spectrometry analysis with special reference to lipoprotein-associated Shiga toxin receptors. *J. Lipid Res.* **2010**, *51*, 2282–2294, doi:10.1194/jlr.M006759.
546. Hunnam, V.; Harvey, D.J.; Priestman, D.A.; Bateman, R.H.; Bordoli, R.S.; Tyldesley, R. Ionization and fragmentation of neutral and acidic glycosphingolipids with a Q-TOF mass spectrometer fitted with a MALDI ion source. *J. Am. Soc. Mass Spectrom.* **2001**, *12*, 1220–1225, doi:10.1016/S1044-0305(01)00309-9.
547. Hsu, F.F.; Bohrer, A.; Turk, J. Electrospray ionization tandem mass spectrometric analysis of sulfatide. Determination of fragmentation patterns and characterization of molecular species expressed in brain and in pancreatic islets. *Biochim. Biophys. Acta - Lipids Lipid Metab.* **1998**, *1392*, 202–216, doi:10.1016/S0005-2760(98)00034-4.
548. Yuki, D.; Sugiura, Y.; Zaima, N.; Akatsu, H.; Hashizume, Y.; Yamamoto, T.; Fujiwara, M.; Sugiyama, K.; Setou, M. Hydroxylated and non-hydroxylated sulfatide are distinctly distributed in the human cerebral cortex. *Neuroscience* **2011**, *193*, 44–53, doi:10.1016/j.neuroscience.2011.07.045.
549. Hsu, F.F.; Turk, J. Studies on sulfatides by quadrupole ion-trap mass spectrometry with electrospray ionization: Structural characterization and the fragmentation processes that include an unusual internal galactose residue loss and the classical charge-remote fragmentation. *J. Am. Soc. Mass Spectrom.* **2004**, *15*, 536–546, doi:10.1016/j.jasms.2003.12.007.
550. Chai, W.; Piskarev, V.; Lawson, A.M. Negative-ion electrospray mass spectrometry of neutral underivatized oligosaccharides. *Anal. Chem.* **2001**, *73*, 651–657, doi:10.1021/ac0010126.
551. Chai, W.; Lawson, A.M.; Piskarev, V. Branching Pattern and Sequence Analysis of Underivatized Oligosaccharides by Combined MS/MS of Singly and Doubly Charged Molecular Ions in Negative-Ion Electrospray Mass Spectrometry. *J. Am. Soc. Mass. Spectrom.* **2002**, *13*, 670–679.
552. Chai, W.; Piskarev, V.E.; Mulloy, B.; Liu, V.; Evans, P.G.; Osborn, H.M.I.; Lawson, A.M. Analysis of chain and blood group type and branching pattern of sialylated oligosaccharides by negative ion electrospray tandem mass spectrometry. *Anal. Chem.* **2006**, *78*, 1581–1592, doi:10.1021/ac051606e.
553. Zhang, H.; Zhang, S.; Tao, G.; Zhang, Y.; Mulloy, B.; Zhan, X.; Chai, W. Typing of blood-group antigens on neutral oligosaccharides by negative-ion electrospray ionization tandem mass spectrometry. *Anal. Chem.* **2013**, *85*, 5940–5949, doi:10.1021/ac400700e.
554. Bayat, P.; Lesage, D.; Cole, R.B. Tutorial: Ion Activation in Tandem Mass Spectrometry Using Ultra-High Resolution Instrumentation. *Mass Spectrom. Rev.* **2020**, *39*, 680–702, doi:10.1002/mas.21623.
555. Li, Y.; Teneberg, S.; Thapa, P.; Bendelac, A.; Levery, S.B.; Zhou, D. Sensitive detection of isoglobo and globo series tetraglycosylceramides in human thymus by ion trap mass spectrometry. *Glycobiology* **2008**, *18*, 158–165, doi:10.1093/glycob/cwm129.
556. Heiles, S. Advanced tandem mass spectrometry in metabolomics and lipidomics—methods and applications. *Anal. Bioanal. Chem.* **2021**, *413*, 5927–5948, doi:10.1007/s00216-021-03425-1.
557. McFarland, M.A.; Marshall, A.G.; Hendrickson, C.L.; Nilsson, C.L.; Fredman, P.; Månsson, J.E. Structural characterization of the GM1 ganglioside by infrared

multiphoton dissociation, electron capture dissociation, and electron detachment dissociation electrospray ionization FT-ICR MS/MS. *J. Am. Soc. Mass Spectrom.* **2005**, *16*, 752–762, doi:10.1016/j.jasms.2005.02.001.

558. Jones, J.W.; Thompson, C.J.; Carter, C.L.; Kane, M.A. Electron-induced dissociation (EID) for structure characterization of glycerophosphatidylcholine: Determination of double-bond positions and localization of acyl chains. *J. Mass Spectrom.* **2015**, *50*, 1327–1339, doi:10.1002/jms.3698.
559. Fort, K.L.; Cramer, C.N.; Voinov, V.G.; Vasil'Ev, Y. V.; Lopez, N.I.; Beckman, J.S.; Heck, A.J.R. Exploring ECD on a Benchtop Q Exactive Orbitrap Mass Spectrometer. *J. Proteome Res.* **2018**, *17*, 926–933, doi:10.1021/acs.jproteome.7b00622.
560. Wolff, J.J.; Amster, I.J.; Chi, L.; Linhardt, R.J. Electron Detachment Dissociation of Glycosaminoglycan Tetrasaccharides. *J. Am. Soc. Mass Spectrom.* **2007**, *18*, 234–244, doi:10.1016/j.jasms.2006.09.020.
561. Wolff, J.J.; Laremore, T.N.; Aslam, H.; Linhardt, R.J.; Amster, I.J. Electron-Induced Dissociation of Glycosaminoglycan Tetrasaccharides. *J. Am. Soc. Mass Spectrom.* **2008**, *19*, 1449–1458, doi:10.1016/j.jasms.2008.06.024.
562. Kornacki, J.R.; Adamson, J.T.; Håkansson, K. Electron detachment dissociation of underivatized chloride-adducted oligosaccharides. *J. Am. Soc. Mass Spectrom.* **2012**, *23*, 2031–2042, doi:10.1007/s13361-012-0459-y.
563. Han, L.; Costello, C.E. Electron transfer dissociation of milk oligosaccharides. *J. Am. Soc. Mass Spectrom.* **2011**, *22*, 997–1013, doi:10.1007/s13361-011-0117-9.
564. O'Brien, J.P.; Brodbelt, J.S. Structural characterization of gangliosides and glycolipids via ultraviolet photodissociation mass spectrometry. *Anal. Chem.* **2013**, *85*, 10399–10407, doi:10.1021/ac402379y.
565. Kirschbaum, C.; Pagel, K. Lipid Analysis by Mass Spectrometry coupled with Laser Light. *Anal. Sens.* **2022**, *202200103*, doi:10.1002/anse.202200103.
566. Ryan, E.; Nguyen, C.Q.N.; Shiea, C.; Reid, G.E. Detailed Structural Characterization of Sphingolipids via 193 nm Ultraviolet Photodissociation and Ultra High Resolution Tandem Mass Spectrometry. *J. Am. Soc. Mass Spectrom.* **2017**, *28*, 1406–1419, doi:10.1007/s13361-017-1668-1.
567. Klein, D.R.; Brodbelt, J.S. Structural Characterization of Phosphatidylcholines Using 193 nm Ultraviolet Photodissociation Mass Spectrometry. *Anal. Chem.* **2017**, *89*, 1516–1522, doi:10.1021/acs.analchem.6b03353.
568. Williams, P.E.; Klein, D.R.; Greer, S.M.; Brodbelt, J.S. Pinpointing Double Bond and sn-Positions in Glycerophospholipids via Hybrid 193 nm Ultraviolet Photodissociation (UVPD) Mass Spectrometry. *J. Am. Chem. Soc.* **2017**, *139*, 15681–15690, doi:10.1021/jacs.7b06416.
569. Zhang, W.; Jian, R.; Zhao, J.; Liu, Y.; Xia, Y. Deep-lipidotyping by mass spectrometry: recent technical advances and applications. *J. Lipid Res.* **2022**, *63*, 100219, doi:10.1016/j.jlr.2022.100219.
570. Brodbelt, J.S.; Morrison, L.J.; Santos, I. Ultraviolet Photodissociation Mass Spectrometry for Analysis of Biological Molecules. *Chem. Rev.* **2020**, *120*, 3328–3380, doi:10.1021/acs.chemrev.9b00440.
571. Yoo, H.J.; Liu, H.; Håkansson, K. Infrared multiphoton dissociation and electron-induced dissociation as alternative MS/MS strategies for metabolite identification. *Anal. Chem.* **2007**, *79*, 7858–7866, doi:10.1021/ac071139w.
572. Lee, H.; An, H.J.; Lerno, L.A.; German, J.B.; Lebrilla, C.B. Rapid profiling of bovine and human milk gangliosides by matrix-assisted laser desorption/ionization Fourier transform ion cyclotron resonance mass spectrometry. *Int. J. Mass Spectrom.* **2011**, *305*, 138–150, doi:10.1016/j.ijms.2010.10.020.

573. Brodbelt, J.S. Photodissociation mass spectrometry: New tools for characterization of biological molecules. *Chem. Soc. Rev.* **2014**, *43*, 2757–2783, doi:10.1039/c3cs60444f.
574. Pham, H.T.; Ly, T.; Trevitt, A.J.; Mitchell, T.W.; Blanksby, S.J. Differentiation of complex lipid isomers by radical-directed dissociation mass spectrometry. *Anal. Chem.* **2012**, *84*, 7525–7532, doi:10.1021/ac301652a.
575. Pham, H.T.; Julian, R.R. Characterization of glycosphingolipid epimers by radical-directed dissociation mass spectrometry. *Analyst* **2016**, *141*, 1273–1278, doi:10.1039/c5an02383a.
576. Deimler, R.E.; Sander, M.; Jackson, G.P. Radical-induced fragmentation of phospholipid cations using metastable atom-activated dissociation mass spectrometry (MAD-MS). *Int. J. Mass Spectrom.* **2015**, *390*, 178–186, doi:10.1016/j.ijms.2015.08.009.
577. Campbell, J.L.; Baba, T. Near-complete structural characterization of phosphatidylcholines using electron impact excitation of ions from organics. *Anal. Chem.* **2015**, *87*, 5837–5845, doi:10.1021/acs.analchem.5b01460.
578. Baba, T.; Campbell, J.L.; Blanc, J.C.Y. Le; Baker, P.R.S. In-depth sphingomyelin characterization using electron impact excitation of ions from organics and mass spectrometry. *J. Lipid Res.* **2016**, *57*, 858–867, doi:10.1194/jlr.M067199.
579. Sleno, L.; Volmer, D.A. Ion activation methods for tandem mass spectrometry. *J. Mass Spectrom.* **2004**, *39*, 1091–1112, doi:10.1002/jms.703.
580. Lu, H.; Zhang, H.; Xu, S.; Li, L. Review of recent advances in lipid analysis of biological samples via ambient ionization mass spectrometry. *Metabolites* **2021**, *11*, 781, doi:10.3390/metabo11110781.
581. Zhao, X.E.; Zhu, S.; Liu, H. Recent progresses of derivatization approaches in the targeted lipidomics analysis by mass spectrometry. *J. Sep. Sci.* **2020**, *43*, 1838–1846, doi:10.1002/jssc.201901346.
582. Ma, X.; Xia, Y. Pinpointing double bonds in lipids by paternò-büchi reactions and mass spectrometry. *Angew. Chemie - Int. Ed.* **2014**, *53*, 2592–2596, doi:10.1002/anie.201310699.
583. Xia, F.; Wan, J.B. Chemical derivatization strategy for mass spectrometry-based lipidomics. *Mass Spectrom. Rev.* **2023**, *42*, 432–452, doi:10.1002/mas.21729.
584. Ma, X.; Chong, L.; Tian, R.; Shi, R.; Hu, T.Y.; Ouyang, Z.; Xia, Y. Identification and quantitation of lipid C=C location isomers: A shotgun lipidomics approach enabled by photochemical reaction. *Proc. Natl. Acad. Sci. U. S. A.* **2016**, *113*, 2573–2578, doi:10.1073/pnas.1523356113.
585. Ma, X.; Zhao, X.; Li, J.; Zhang, W.; Cheng, J.X.; Ouyang, Z.; Xia, Y. Photochemical Tagging for Quantitation of Unsaturated Fatty Acids by Mass Spectrometry. *Anal. Chem.* **2016**, *88*, 8931–8935, doi:10.1021/acs.analchem.6b02834.
586. Zhang, W.; Zhang, D.; Chen, Q.; Wu, J.; Ouyang, Z.; Xia, Y. Online photochemical derivatization enables comprehensive mass spectrometric analysis of unsaturated phospholipid isomers. *Nat. Commun.* **2019**, *10*, 1–9, doi:10.1038/s41467-018-07963-8.
587. Bednařík, A.; Bölsker, S.; Soltwisch, J.; Dreisewerd, K. An On-Tissue Paternò–Büchi Reaction for Localization of Carbon–Carbon Double Bonds in Phospholipids and Glycolipids by Matrix-Assisted Laser-Desorption–Ionization Mass-Spectrometry Imaging. *Angew. Chemie - Int. Ed.* **2018**, *57*, 12092–12096, doi:10.1002/anie.201806635.
588. Xu, T.; Pi, Z.; Song, F.; Liu, S.; Liu, Z. Benzophenone used as the photochemical reagent for pinpointing C=C locations in unsaturated lipids through shotgun and liquid chromatography-mass spectrometry approaches. *Anal. Chim. Acta* **2018**, *1028*, 32–44, doi:10.1016/j.aca.2018.04.046.

589. Deng, J.; Yang, Y.; Liu, Y.; Fang, L.; Lin, L.; Luan, T. Coupling Paternò-Büchi Reaction with Surface-Coated Probe Nanoelectrospray Ionization Mass Spectrometry for in Vivo and Microscale Profiling of Lipid C=C Location Isomers in Complex Biological Tissues. *Anal. Chem.* **2019**, *91*, 4592–4599, doi:10.1021/acs.analchem.8b05803.
590. Xie, X.; Zhao, J.; Lin, M.; Zhang, J.L.; Xia, Y. Profiling of Cholesteryl Esters by Coupling Charge-Tagging Paternò-Büchi Reaction and Liquid Chromatography-Mass Spectrometry. *Anal. Chem.* **2020**, *92*, 8487–8496, doi:10.1021/acs.analchem.0c01241.
591. Zhao, J.; Xie, X.; Lin, Q.; Ma, X.; Su, P.; Xia, Y. Next-Generation Paternò-Büchi Reagents for Lipid Analysis by Mass Spectrometry. *Anal. Chem.* **2020**, *92*, 13470–13477, doi:10.1021/acs.analchem.0c02896.
592. Thomas, M.C.; Mitchell, T.W.; Harman, D.G.; Deeley, J.M.; Nealon, J.R.; Blanksby, S.J. Ozone-induced dissociation: Elucidation of double bond position within mass-selected lipid ions. *Anal. Chem.* **2008**, *80*, 303–311, doi:10.1021/ac7017684.
593. Brown, S.H.J.; Mitchell, T.W.; Blanksby, S.J. Analysis of unsaturated lipids by ozone-induced dissociation. *Biochim. Biophys. Acta - Mol. Cell Biol. Lipids* **2011**, *1811*, 807–817, doi:10.1016/j.bbalip.2011.04.015.
594. Poad, B.L.J.; Green, M.R.; Kirk, J.M.; Tomczyk, N.; Mitchell, T.W.; Blanksby, S.J. High-Pressure Ozone-Induced Dissociation for Lipid Structure Elucidation on Fast Chromatographic Timescales. *Anal. Chem.* **2017**, *89*, 4223–4229, doi:10.1021/acs.analchem.7b00268.
595. Poad, B.L.J.; Zheng, X.; Mitchell, T.W.; Smith, R.D.; Baker, E.S.; Blanksby, S.J. Online Ozonolysis Combined with Ion Mobility-Mass Spectrometry Provides a New Platform for Lipid Isomer Analyses. *Anal. Chem.* **2018**, *90*, 1292–1300, doi:10.1021/acs.analchem.7b04091.
596. Vu, N.; Brown, J.; Giles, K.; Zhang, Q. Ozone-induced dissociation on a traveling wave high-resolution mass spectrometer for determination of double-bond position in lipids. *Rapid Commun. Mass Spectrom.* **2017**, *31*, 1415–1423, doi:10.1002/rcm.7920.
597. Barrientos, R.C.; Zhang, Q. Fragmentation Behavior and Gas-Phase Structures of Cationized Glycosphingolipids in Ozone-Induced Dissociation Mass Spectrometry. *J. Am. Soc. Mass Spectrom.* **2019**, *30*, 1609–1620, doi:10.1007/s13361-019-02267-7.
598. Marshall, D.L.; Criscuolo, A.; Young, R.S.E.; Poad, B.L.J.; Zeller, M.; Reid, G.E.; Mitchell, T.W.; Blanksby, S.J. Mapping Unsaturation in Human Plasma Lipids by Data-Independent Ozone-Induced Dissociation. *J. Am. Soc. Mass Spectrom.* **2019**, *30*, 1621–1630, doi:10.1007/s13361-019-02261-z.
599. Barrientos, R.C.; Vu, N.; Zhang, Q. Structural Analysis of Unsaturated Glycosphingolipids Using Shotgun Ozone-Induced Dissociation Mass Spectrometry. *J. Am. Soc. Mass Spectrom.* **2017**, *28*, 2330–2343, doi:10.1007/s13361-017-1772-2.
600. Feng, Y.; Chen, B.; Yu, Q.; Li, L. Identification of Double Bond Position Isomers in Unsaturated Lipids by m-CPBA Epoxidation and Mass Spectrometry Fragmentation. *Anal. Chem.* **2019**, *91*, 1791–1795, doi:10.1021/acs.analchem.8b04905.
601. Kuo, T.H.; Chung, H.H.; Chang, H.Y.; Lin, C.W.; Wang, M.Y.; Shen, T.L.; Hsu, C.C. Deep Lipidomics and Molecular Imaging of Unsaturated Lipid Isomers: A Universal Strategy Initiated by mCPBA Epoxidation. *Anal. Chem.* **2019**, *91*, 11905–11915, doi:10.1021/acs.analchem.9b02667.
602. Zhang, H.; Xu, M.; Shi, X.; Liu, Y.; Li, Z.; Jagodinsky, J.C.; Ma, M.; Welham, N. V.; Morris, Z.S.; Li, L. Quantification and molecular imaging of fatty acid isomers from complex biological samples by mass spectrometry. *Chem. Sci.* **2021**, *12*, 8115–8122, doi:10.1039/d1sc01614h.
603. Zhang, J.; Zhang, Z.; Jiang, T.; Zhang, Z.; Zhang, W.; Xu, W. Rapidly identifying and

quantifying of unsaturated lipids with carbon-carbon double bond isomers by photoepoxidation. *Talanta* **2023**, *260*, 124575, doi:10.1016/j.talanta.2023.124575.
604. Sawaki, Y.; Ogata, Y. Photoepoxidation of Olefin with Benzoins and Oxygen. Epoxidation with Acylperoxy Radical. *J. Am. Chem. Soc.* **1981**, *103*, 2049–2053, doi:10.1021/ja00398a029.
605. Tang, S.; Cheng, H.; Yan, X. On-Demand Electrochemical Epoxidation in Nano-Electrospray Ionization Mass Spectrometry to Locate Carbon–Carbon Double Bonds. *Angew. Chemie - Int. Ed.* **2020**, *59*, 209–214, doi:10.1002/anie.201911070.
606. Luo, K.; Chen, H.; Zare, R.N. Location of carbon-carbon double bonds in unsaturated lipids using microdroplet mass spectrometry. *Analyst* **2021**, *146*, 2550–2558, doi:10.1039/d0an02396e.
607. Zhao, Y.; Zhao, H.; Zhao, X.; Jia, J.; Ma, Q.; Zhang, S.; Zhang, X.; Chiba, H.; Hui, S.P.; Ma, X. Identification and Quantitation of C=C Location Isomers of Unsaturated Fatty Acids by Epoxidation Reaction and Tandem Mass Spectrometry. *Anal. Chem.* **2017**, *89*, 10270–10278, doi:10.1021/acs.analchem.7b01870.
608. Zhao, X.; Zhao, Y.; Zhang, L.; Ma, X.; Zhang, S.; Zhang, X. Rapid Analysis of Unsaturated Fatty Acids on Paper-Based Analytical Devices via Online Epoxidation and Ambient Mass Spectrometry. *Anal. Chem.* **2018**, *90*, 2070–2078, doi:10.1021/acs.analchem.7b04312.
609. Zhang, J.; Huo, X.; Guo, C.; Ma, X.; Huang, H.; He, J.; Wang, X.; Tang, F. Rapid Imaging of Unsaturated Lipids at an Isomeric Level Achieved by Controllable Oxidation. *Anal. Chem.* **2021**, *93*, 2114–2124, doi:10.1021/acs.analchem.0c03888.
610. Unsihuay, D.; Su, P.; Hu, H.; Qiu, J.; Kuang, S.; Li, Y.; Sun, X.; Dey, S.K.; Laskin, J. Imaging and Analysis of Isomeric Unsaturated Lipids through Online Photochemical Derivatization of Carbon–Carbon Double Bonds**. *Angew. Chemie - Int. Ed.* **2021**, *60*, 7559–7563, doi:10.1002/anie.202016734.
611. Lee, J.C.; Byeon, S.K.; Moon, M.H. Relative Quantification of Phospholipids Based on Isotope-Labeled Methylation by Nanoflow Ultrahigh Performance Liquid Chromatography-Tandem Mass Spectrometry: Enhancement in Cardiolipin Profiling. *Anal. Chem.* **2017**, *89*, 4969–4977, doi:10.1021/acs.analchem.7b00297.
612. Bollinger, J.G.; Rohan, G.; Sadilek, M.; Gelb, M.H. LC/ESI-MS/MS detection of FAs by charge reversal derivatization with more than four orders of magnitude improvement in sensitivity. *J. Lipid Res.* **2013**, *54*, 3523–3530, doi:10.1194/jlr.D040782.
613. Yang, K.; Dilthey, B.G.; Gross, R.W. Identification and quantitation of fatty acid double bond positional isomers: A shotgun lipidomics approach using charge-switch derivatization. *Anal. Chem.* **2013**, *85*, 9742–9750, doi:10.1021/ac402104u.
614. Wang, M.; Han, R.H.; Han, X. *Fatty acidomics: Global analysis of lipid species containing a carboxyl group with a charge-remote fragmentation-assisted approach*; 2013; Vol. 85; ISBN 4077452139.
615. Wang, S.S.; Wang, Y.J.; Zhang, J.; Sun, T.Q.; Guo, Y.L. Derivatization strategy for simultaneous molecular imaging of phospholipids and low-abundance free fatty acids in thyroid cancer tissue sections. *Anal. Chem.* **2019**, *91*, 4070–4076, doi:10.1021/acs.analchem.8b05680.
616. Cai, T.; Ting, H.; Xin-Xiang, Z.; Jiang, Z.; Jin-Lan, Z. HPLC-MRM relative quantification analysis of fatty acids based on a novel derivatization strategy. *Analyst* **2014**, *139*, 6154–6159, doi:10.1039/c4an01314j.
617. Narayana, V.K.; Tomatis, V.M.; Wang, T.; Kvaskoff, D.; Meunier, F.A. Profiling of Free Fatty Acids Using Stable Isotope Tagging Uncovers a Role for Saturated Fatty Acids in Neuroexocytosis. *Chem. Biol.* **2015**, *22*, 1552–1561,

doi:10.1016/j.chembiol.2015.09.010.
618. Canez, C.R.; Shields, S.W.J.; Bugno, M.; Wasslen, K. V.; Weinert, H.P.; Willmore, W.G.; Manthorpe, J.M.; Smith, J.C. Trimethylation Enhancement Using 13C-Diazomethane (13C-TrEnDi): Increased Sensitivity and Selectivity of Phosphatidylethanolamine, Phosphatidylcholine, and Phosphatidylserine Lipids Derived from Complex Biological Samples. *Anal. Chem.* **2016**, *88*, 6996–7004, doi:10.1021/acs.analchem.5b04524.
619. Wasslen, K. V; Canez, C.R.; Lee, H. Karl V. Wasslen, † , § Carlos R. Canez, † , § Hyunmin Lee, † Je ff rey M. Manthorpe, * , † , ‡ and Je ff rey C. Smith * , † , ‡ †. **2014**.
620. Wang, C.; Palavicini, J.P.; Wang, M.; Chen, L.; Yang, K.; Crawford, P.A.; Han, X. Comprehensive and quantitative analysis of polyphosphoinositide species by shotgun lipidomics revealed their alterations in db/db mouse brain. *Anal. Chem.* **2016**, *88*, 12137–12144, doi:10.1021/acs.analchem.6b02947.
621. Cai, T.; Niu, L.; Shu, Q.; Liu, P.; Niu, L.; Guo, X.; Ding, X.; Xue, P.; Xie, Z.; Wang, J.; et al. Characterization and relative quantification of phospholipids based on methylation and stable isotopic labeling. *J. Lipid Res.* **2016**, *57*, 388–398, doi:10.1194/jlr.M063024.
622. Zemski Berry, K.A.; Turner, W.W.; VanNieuwenhze, M.S.; Murphy, R.C. Stable isotope labeled 4-(dimethylamino)benzoic acid derivatives of glycerophosphoethanolamine lipids. *Anal. Chem.* **2009**, *81*, 6633–6640, doi:10.1021/ac900583a.
623. Han, X.; Yang, K.; Cheng, H.; Fikes, K.N.; Gross, R.W. Shotgun lipidomics of phosphoethanolamine-containing lipids in biological samples after one-step in situ derivatization. *J. Lipid Res.* **2005**, *46*, 1548–1560, doi:10.1194/jlr.D500007-JLR200.
624. Wang, M.; Hayakawa, J.; Yang, K.; Han, X. Characterization and quantification of diacylglycerol species in biological extracts after one-step derivatization: A shotgun lipidomics approach. *Anal. Chem.* **2014**, *86*, 2146–2155, doi:10.1021/ac403798q.
625. Liu, Y.D.; Liu, H.J.; Gong, G.W. Monitoring diacylglycerols in biofluids by non-isotopically paired charge derivatization combined with LC-MS/MS. *Front. Chem.* **2022**, *10*, 1–13, doi:10.3389/fchem.2022.1062118.
626. Yang, K.; Dilthey, B.G.; Gross, R.W. Shotgun Lipidomics Approach to Stabilize the Regiospecificity of Monoglycerides Using a Facile Low-Temperature Derivatization Enabling Their Definitive Identification and Quantitation. *Anal. Chem.* **2016**, *88*, 9459–9468, doi:10.1021/acs.analchem.6b01862.
627. Liebisch, G.; Binder, M.; Schifferer, R.; Langmann, T.; Schulz, B.; Schmitz, G. High throughput quantification of cholesterol and cholesteryl ester by electrospray ionization tandem mass spectrometry (ESI-MS/MS). *Biochim. Biophys. Acta - Mol. Cell Biol. Lipids* **2006**, *1761*, 121–128, doi:10.1016/j.bbalip.2005.12.007.
628. Adhikari, S.; Xia, Y. Thiyl Radical-Based Charge Tagging Enables Sterol Quantitation via Mass Spectrometry. *Anal. Chem.* **2017**, *89*, 12631–12635, doi:10.1021/acs.analchem.7b04080.
629. Mok, H.J.; Lee, J.W.; Bandu, R.; Kang, H.S.; Kim, K.H.; Kim, K.P. A rapid and sensitive profiling of free fatty acids using liquid chromatography electrospray ionization tandem mass spectrometry (LC/ESI-MS/MS) after chemical derivatization. *RSC Adv.* **2016**, *6*, 32130–32139, doi:10.1039/c6ra01344a.
630. Fhaner, C.J.; Liu, S.; Ji, H.; Simpson, R.J.; Reid, G.E. Comprehensive lipidome profiling of isogenic primary and metastatic colon adenocarcinoma cell lines. *Anal. Chem.* **2012**, *84*, 8917–8926, doi:10.1021/ac302154g.
631. Ryan, E.; Reid, G.E. Chemical Derivatization and Ultrahigh Resolution and Accurate

Mass Spectrometry Strategies for "shotgun" Lipidome Analysis. *Acc. Chem. Res.* **2016**, *49*, 1596–1604, doi:10.1021/acs.accounts.6b00030.
632. Aoki, K.; Heaps, A.D.; Strauss, K.A.; Tiemeyer, M. Mass spectrometric quantification of plasma glycosphingolipids in human GM3 ganglioside deficiency. *Clin. Mass Spectrom.* **2019**, *14*, 106–114, doi:10.1016/j.clinms.2019.03.001.
633. Ejsing, C.S.; Bilgin, M.; Fabregat, A. Quantitative profiling of long-chain bases by mass tagging and parallel reaction monitoring. *PLoS One* **2015**, *10*, 1–17, doi:10.1371/journal.pone.0144817.
634. Hanamatsu, H.; Nishikaze, T.; Miura, N.; Piao, J.; Okada, K.; Sekiya, S.; Iwamoto, S.; Sakamoto, N.; Tanaka, K.; Furukawa, J.I. Sialic Acid Linkage Specific Derivatization of Glycosphingolipid Glycans by Ring-Opening Aminolysis of Lactones. *Anal. Chem.* **2018**, *90*, 13193–13199, doi:10.1021/acs.analchem.8b02775.
635. Liu, Y.; Yang, L.; Li, H.; Liu, J.; Tian, R. Derivatization strategy for sensitive identification of neutral and acidic glycosphingolipids using RPLC-MS. *Int. J. Mass Spectrom.* **2022**, *482*, 116937, doi:10.1016/j.ijms.2022.116937.
636. Miura, Y.; Shinohara, Y.; Furukawa, J.I.; Nagahori, N.; Nishimura, S.I. Rapid and simple solid-phase esterification of sialic acid residues for quantitative glycomics by mass spectrometry. *Chem. - A Eur. J.* **2007**, *13*, 4797–4804, doi:10.1002/chem.200601872.
637. Sekiya, S.; Wada, Y.; Tanaka, K. Derivatization for Stabilizing Sialic Acids in MALDI-MS. *Anal. Chem.* **2005**, *77*, 4962–4968, doi:10.1021/ac050287o.
638. Kang, P.; Mechref, Y.; Klouckova, I.; Novotny, M. V. Solid-phase permethylation of glycans for mass spectrometric analysis. *Rapid Commun. Mass Spectrom.* **2005**, *19*, 3421–3428, doi:10.1002/rcm.2210.
639. Chen, P.; Werner-Zwansiger, U.; Wiesler, D.; Pagel, M.; Novotny, M. V. Mass spectrometric analysis of benzoylated sialooligosaccharides and differentiation of terminal α2→3 and α2→6 sialogalactosylated linkages at subpicomole levels. *Anal. Chem.* **1999**, *71*, 4969–4973, doi:10.1021/ac990674w.
640. Huang, Q.; Liu, D.; Xin, B.; Cechner, K.; Zhou, X.; Wang, H.; Zhou, A. Quantification of monosialogangliosides in human plasma through chemical derivatization for signal enhancement in LC-ESI-MS. *Anal. Chim. Acta* **2016**, *929*, 31–38, doi:10.1016/j.aca.2016.04.043.
641. Nabetani, T.; Makino, A.; Hullin-Matsuda, F.; Hirakawa, T.A.; Takeoka, S.; Okino, N.; Ito, M.; Kobayashi, T.; Hirabayashi, Y. Multiplex analysis of sphingolipids using amine-reactive tags (iTRAQ). *J. Lipid Res.* **2011**, *52*, 1294–1302, doi:10.1194/jlr.D014621.
642. Barrientos, R.C.; Zhang, Q. Isobaric Labeling of Intact Gangliosides toward Multiplexed LC-MS/MS-Based Quantitative Analysis. *Anal. Chem.* **2018**, *90*, 2578–2586, doi:10.1021/acs.analchem.7b04044.
643. Peterka, O.; Jirásko, R.; Vaňková, Z.; Chocholoušková, M.; Wolrab, D.; Kulhánek, J.; Bureš, F.; Holčapek, M. Simple and Reproducible Derivatization with Benzoyl Chloride: Improvement of Sensitivity for Multiple Lipid Classes in RP-UHPLC/MS. *Anal. Chem.* **2021**, *93*, 13835–13843, doi:10.1021/acs.analchem.1c02463.
644. Zheng, S.J.; Zheng, J.; Xiao, H.M.; Wu, D.M.; Feng, Y.Q. Simultaneous quantitative analysis of multiple sphingoid bases by stable isotope labeling assisted liquid chromatography-mass spectrometry. *Anal. Chim. Acta* **2019**, *1082*, 106–115, doi:10.1016/j.aca.2019.07.016.
645. He, X.; Dagan, A.; Gatt, S.; Schuchman, E.H. Simultaneous quantitative analysis of ceramide and sphingosine in mouse blood by naphthalene-2,3-dicarboxyaldehyde derivatization after hydrolysis with ceramidase. *Anal. Biochem.* **2005**, *340*, 113–122,

doi:10.1016/j.ab.2005.01.058.
646. Hermanson, G.R. *Bioconjugate Techniques*; 3rd ed.; Academic Press: San Diego, USA, 2013; ISBN 9780123822390.
647. Ghidoni, R.; Sonnino, S.; Masserini, M.; Orlando, P.; Tettamanti, G. Specific tritium labeling of gangliosides at the 3-position of sphingosines. *J. Lipid Res.* **1981**, *22*, 1286–1295, doi:10.1016/s0022-2275(20)37322-3.
648. Song, X.; Ju, H.; Lasanajak, Y.; Kudelka, M.R.; Smith, D.F.; Cummings, R.D. Oxidative release of natural glycans for functional glycomics. *Nat. Methods* **2016**, *13*, 528–534, doi:10.1038/nmeth.3861.
649. Zhang, T.Y.; Li, S.; Zhu, Q.F.; Wang, Q.; Hussain, D.; Feng, Y.Q. Derivatization for liquid chromatography-electrospray ionization-mass spectrometry analysis of small-molecular weight compounds. *TrAC - Trends Anal. Chem.* **2019**, *119*, 115608, doi:10.1016/j.trac.2019.07.019.
650. Chocholoušková, M.; Wolrab, D.; Jirásko, R.; Študentová, H.; Melichar, B.; Holčapek, M. Intra-laboratory comparison of four analytical platforms for lipidomic quantitation using hydrophilic interaction liquid chromatography or supercritical fluid chromatography coupled to quadrupole - time-of-flight mass spectrometry. *Talanta* **2021**, *231*, doi:10.1016/j.talanta.2021.122367.
651. Köfeler, H.C.; Ahrends, R.; Baker, E.S.; Ekroos, K.; Han, X.; Hoffmann, N.; Holcapek, M.; Wenk, M.R.; Liebisch, G. Recommendations for good practice in ms-based lipidomics. *J. Lipid Res.* **2021**, *62*, 1–13, doi:10.1016/j.jlr.2021.100138.
652. Rampler, E.; Abiead, Y. El; Schoeny, H.; Rusz, M.; Hildebrand, F.; Fitz, V.; Koellensperger, G. Recurrent Topics in Mass Spectrometry-Based Metabolomics and Lipidomics - Standardization, Coverage, and Throughput. *Anal. Chem.* **2021**, *93*, 519–545, doi:10.1021/acs.analchem.0c04698.
653. Ghorasaini, M.; Mohammed, Y.; Adamski, J.; Bettcher, L.; Bowden, J.A.; Cabruja, M.; Contrepois, K.; Ellenberger, M.; Gajera, B.; Haid, M.; et al. Cross-Laboratory Standardization of Preclinical Lipidomics Using Differential Mobility Spectrometry and Multiple Reaction Monitoring. *Anal. Chem.* **2021**, *93*, 16369–16378, doi:10.1021/acs.analchem.1c02826.
654. Lippa, K.A.; Aristizabal-Henao, J.J.; Beger, R.D.; Bowden, J.A.; Broeckling, C.; Beecher, C.; Clay Davis, W.; Dunn, W.B.; Flores, R.; Goodacre, R.; et al. Reference materials for MS-based untargeted metabolomics and lipidomics: a review by the metabolomics quality assurance and quality control consortium (mQACC). *Metabolomics* **2022**, *18*, 1–29, doi:10.1007/s11306-021-01848-6.
655. Reddy, N.R. "Stable Labeled Isotopes as Internal Standards: A Critical Review." *Mod. Appl. Pharm. Pharmacol.* **2017**, *1*, 1–4, doi:10.31031/mapp.2017.01.000508.
656. Triebl, A.; Wenk, M.R. Analytical considerations of stable isotope labelling in lipidomics. *Biomolecules* **2018**, *8*, doi:10.3390/biom8040151.
657. Shaner, R.L.; Allegood, J.C.; Park, H.; Wang, E.; Kelly, S.; Haynes, C.A.; Sullards, M.C.; Merrill, A.H. Quantitative analysis of sphingolipids for lipidomics using triple quadrupole and quadrupole linear ion trap mass spectrometers. *J. Lipid Res.* **2009**, *50*, 1692–1707, doi:10.1194/jlr.D800051-JLR200.
658. Wang, M.; Wang, C.; Han, X. Selection of internal standards for accurate quantification of complex lipid species in biological extracts by electrospray ionization mass spectrometry—What, how and why? *Mass Spectrom. Rev.* **2017**, *36*, 693–714, doi:10.1002/mas.21492.
659. Rohokale, R.S.; Li, Q.; Guo, Z. A Diversity-Oriented Strategy for Chemical Synthesis of Glycosphingolipids: Synthesis of Glycosphingolipid LcGg4 and Its Analogues and Derivatives. *J. Org. Chem.* **2021**, *86*, 1633–1648, doi:10.1021/acs.joc.0c02490.

660. Li, Q.; Guo, Z. Enzymatic Synthesis of Glycosphingolipids: A Review. *Synth.* **2021**, *53*, 2367–2380, doi:10.1055/a-1426-4451.
661. Chiang, Y.C.; Wu, C.Y.; Chiang, P.Y.; Adak, A.K.; Lin, C.C. A concise chemoenzymatic total synthesis of neutral Globo-series glycosphingolipids Globo A and Globo B, and Forssman and para-Forssman antigens. *Glycoconj. J.* **2023**, *40*, 551–563, doi:10.1007/s10719-023-10133-8.
662. Chiang, P.; Adak, A.K.; Liang, W.; Tsai, C.; Tseng, H.; Cheng, J.; Hwu, J.R.; Yu, A.L.; Hung, J.; Lin, C. Chemoenzymatic Synthesis of Globo-series Glycosphingolipids and Evaluation of Their Immunosuppressive Activities. *Chem. – An Asian J.* **2022**, *17*, doi:10.1002/asia.202200403.
663. Mills, K.; Eaton, S.; Ledger, V.; Young, E.; Winchester, B. The synthesis of internal standards for the quantitative determination of sphingolipids by tandem mass spectrometry. *Rapid Commun. Mass Spectrom.* **2005**, *19*, 1739–1748, doi:10.1002/rcm.1977.
664. Wu, L.; Mashego, M.R.; Van Dam, J.C.; Proell, A.M.; Vinke, J.L.; Ras, C.; Van Winden, W.A.; Van Gulik, W.M.; Heijnen, J.J. Quantitative analysis of the microbial metabolome by isotope dilution mass spectrometry using uniformly 13C-labeled cell extracts as internal standards. *Anal. Biochem.* **2005**, *336*, 164–171, doi:10.1016/j.ab.2004.09.001.
665. Rampler, E.; Coman, C.; Hermann, G.; Sickmann, A.; Ahrends, R.; Koellensperger, G. LILY-lipidome isotope labeling of yeast:: In vivo synthesis of 13C labeled reference lipids for quantification by mass spectrometry. *Analyst* **2017**, *142*, 1891–1899, doi:10.1039/c7an00107j.
666. Jaber, M.A.; de Falco, B.; Abdelrazig, S.; Ortori, C.A.; Barrett, D.A.; Kim, D.H. Advantages of using biologically generated 13C-labelled multiple internal standards for stable isotope-assisted LC-MS-based lipidomics. *Anal. Methods* **2023**, *15*, 2925–2934, doi:10.1039/d3ay00460k.
667. Visconti, G.; Boccard, J.; Feinberg, M.; Rudaz, S. From fundamentals in calibration to modern methodologies: A tutorial for small molecules quantification in liquid chromatography–mass spectrometry bioanalysis. *Anal. Chim. Acta* **2023**, *1240*, 340711, doi:10.1016/j.aca.2022.340711.
668. Vvedenskaya, O.; Wang, Y.; Ackerman, J.M.; Knittelfelder, O.; Shevchenko, A. Analytical challenges in human plasma lipidomics: A winding path towards the truth. *TrAC - Trends Anal. Chem.* **2019**, *120*, doi:10.1016/j.trac.2018.10.013.
669. Cajka, T.; Smilowitz, J.T.; Fiehn, O. Validating Quantitative Untargeted Lipidomics Across Nine Liquid Chromatography-High-Resolution Mass Spectrometry Platforms. *Anal. Chem.* **2017**, *89*, 12360–12368, doi:10.1021/acs.analchem.7b03404.
670. Ramaley, L.; Herrera, L.C. Software for the calculation of isotope patterns in tandem mass spectrometry. *Rapid Commun. Mass Spectrom.* **2008**, *22*, 2707–2714, doi:10.1002/rcm.3668.
671. Burla, B.; Arita, M.; Arita, M.; Bendt, A.K.; Cazenave-Gassiot, A.; Dennis, E.A.; Ekroos, K.; Han, X.; Ikeda, K.; Liebisch, G.; et al. MS-based lipidomics of human blood plasma: A community-initiated position paper to develop accepted guidelines. *J. Lipid Res.* **2018**, *59*, 2001–2017, doi:10.1194/jlr.S087163.
672. Lam, S.M.; Tian, H.; Shui, G. Lipidomics, en route to accurate quantitation. *Biochim. Biophys. Acta - Mol. Cell Biol. Lipids* **2017**, *1862*, 752–761, doi:10.1016/j.bbalip.2017.02.008.
673. Lange, M.; Fedorova, M. Evaluation of lipid quantification accuracy using HILIC and RPLC MS on the example of NIST® SRM® 1950 metabolites in human plasma. *Anal. Bioanal. Chem.* **2020**, *412*, 3573–3584, doi:10.1007/s00216-020-02576-x.

674. Zhang, N.R.; Hatcher, N.G.; Ekroos, K.; Kedia, K.; Kandebo, M.; Marcus, J.N.; Smith, S.M.; Bateman, K.P.; Spellman, D.S. Validation of a multiplexed and targeted lipidomics assay for accurate quantification of lipidomes. *J. Lipid Res.* **2022**, *63*, 100218, doi:10.1016/j.jlr.2022.100218.
675. Berkecz, R.; Lísa, M.; Holčapek, M. Analysis of oxylipins in human plasma: Comparison of ultrahigh-performance liquid chromatography and ultrahigh-performance supercritical fluid chromatography coupled to mass spectrometry. *J. Chromatogr. A* **2017**, *1511*, 107–121, doi:10.1016/j.chroma.2017.06.070.
676. Pataj, Z.; Liebisch, G.; Schmitz, G.; Matysik, S. Quantification of oxysterols in human plasma and red blood cells by liquid chromatography high-resolution tandem mass spectrometry. *J. Chromatogr. A* **2016**, *1439*, 82–88, doi:10.1016/j.chroma.2015.11.015.
677. Köfeler, H.C.; Eichmann, T.O.; Ahrends, R.; Bowden, J.A.; Danne-Rasche, N.; Dennis, E.A.; Fedorova, M.; Griffiths, W.J.; Han, X.; Hartler, J.; et al. Quality control requirements for the correct annotation of lipidomics data. *Nat. Commun.* **2021**, *12*, 19–22, doi:10.1038/s41467-021-24984-y.
678. Moein, M.M.; El Beqqali, A.; Abdel-Rehim, M. Bioanalytical method development and validation: Critical concepts and strategies. *J. Chromatogr. B Anal. Technol. Biomed. Life Sci.* **2017**, *1043*, 3–11, doi:10.1016/j.jchromb.2016.09.028.
679. González, O.; Blanco, M.E.; Iriarte, G.; Bartolomé, L.; Maguregui, M.I.; Alonso, R.M. Bioanalytical chromatographic method validation according to current regulations, with a special focus on the non-well defined parameters limit of quantification, robustness and matrix effect. *J. Chromatogr. A* **2014**, *1353*, 10–27, doi:10.1016/j.chroma.2014.03.077.
680. EMA, Committee for Medicinal Products for Human Use. Guideline on bioanalytical method validation (2011).
681. FDA, U.S. Department of Health and Human Services, Center for Drug evaluation and Research (CDER), Center of Veterinary Medicine (CVM). Bioanalytical Method Validation: Guidance for Industry (2018).
682. Kadian, N.; Raju, K.S.R.; Rashid, M.; Malik, M.Y.; Taneja, I.; Wahajuddin, M. Comparative assessment of bioanalytical method validation guidelines for pharmaceutical industry. *J. Pharm. Biomed. Anal.* **2016**, *126*, 83–97, doi:10.1016/j.jpba.2016.03.052.
683. Aristizabal-Henao, J.J.; Jones, C.M.; Lippa, K.A.; Bowden, J.A. Nontargeted lipidomics of novel human plasma reference materials: hypertriglyceridemic, diabetic, and African-American. *Anal. Bioanal. Chem.* **2020**, *412*, 7373–7380, doi:10.1007/s00216-020-02910-3.
684. Phinney, K.W.; Ballihaut, G.; Bedner, M.; Benford, B.S.; Camara, J.E.; Christopher, S.J.; Davis, W.C.; Dodder, N.G.; Eppe, G.; Lang, B.E.; et al. Development of a standard reference material for metabolomics research. *Anal. Chem.* **2013**, *85*, 11732–11738, doi:10.1021/ac402689t.
685. Triebl, A.; Burla, B.; Selvalatchmanan, J.; Oh, J.; Tan, S.H.; Chan, M.Y.; Mellet, N.A.; Meikle, P.J.; Torta, F.; Wenk, M.R. Shared reference materials harmonize lipidomics across MS-based detection platforms and laboratories. *J. Lipid Res.* **2020**, *61*, 105–115, doi:10.1194/jlr.D119000393.
686. Gouveia, G.J.; Shaver, A.O.; Garcia, B.M.; Morse, A.M.; Andersen, E.C.; Edison, A.S.; McIntyre, L.M. Long-Term Metabolomics Reference Material. *Anal. Chem.* **2021**, *93*, 9193–9199, doi:10.1021/acs.analchem.1c01294.
687. Bowden, J.A.; Heckert, A.; Ulmer, C.Z.; Jones, C.M.; Koelmel, J.P.; Abdullah, L.; Ahonen, L.; Alnouti, Y.; Armando, A.M.; Asara, J.M.; et al. Harmonizing lipidomics: NIST interlaboratory comparison exercise for lipidomics using SRM 1950-Metabolites

in frozen human plasma. *J. Lipid Res.* **2017**, *58*, 2275–2288, doi:10.1194/jlr.M079012.
688. Liu, K.H.; Nellis, M.; Uppal, K.; Ma, C.; Tran, V.L.; Liang, Y.; Walker, D.I.; Jones, D.P. Reference Standardization for Quantification and Harmonization of Large-Scale Metabolomics. *Anal. Chem.* **2020**, *92*, 8836–8844, doi:10.1021/acs.analchem.0c00338.
689. Quehenberger, O.; Armando, A.M.; Brown, A.H.; Milne, S.B.; Myers, D.S.; Merrill, A.H.; Bandyopadhyay, S.; Jones, K.N.; Kelly, S.; Shaner, R.L.; et al. Lipidomics reveals a remarkable diversity of lipids in human plasma1. *J. Lipid Res.* **2010**, *51*, 3299–3305, doi:10.1194/jlr.M009449.
690. Quehenberger, O.; Dennis, E.A. The Human Plasma Lipidome - Mechanisms of Disease, Diversity of Lipids in Human Plasma. *N. Engl. J. Med.* **2011**, *365 (19)*, 1812–23, doi:10.1056/NEJMra1104901.The.
691. Lin, W.J.; Shen, P.C.; Liu, H.C.; Cho, Y.C.; Hsu, M.K.; Lin, I.C.; Chen, F.H.; Yang, J.C.; Ma, W.L.; Cheng, W.C. LipidSig: A web-based tool for lipidomic data analysis. *Nucleic Acids Res.* **2021**, *49*, W336–W345, doi:10.1093/nar/gkab419.
692. Kyle, J.E.; Aimo, L.; Bridge, A.J.; Clair, G.; Fedorova, M.; Helms, J.B.; Molenaar, M.R.; Ni, Z.; Orešič, M.; Slenter, D.; et al. Interpreting the lipidome: bioinformatic approaches to embrace the complexity. *Metabolomics* **2021**, *17*, doi:10.1007/s11306-021-01802-6.
693. Hoffmann, N.; Mayer, G.; Has, C.; Kopczynski, D.; Machot, F. Al; Schwudke, D.; Ahrends, R.; Marcus, K.; Eisenacher, M.; Turewicz, M. A Current Encyclopedia of Bioinformatics Tools, Data Formats and Resources for Mass Spectrometry Lipidomics. *Metabolites* **2022**, *12*, doi:10.3390/metabo12070584.
694. Wolrab, D.; Cífková, E.; Cáň, P.; Lísa, M.; Peterka, O.; Chocholoušková, M.; Jirásko, R.; Holčapek, M. LipidQuant 1.0: Automated data processing in lipid class separation-mass spectrometry quantitative workflows. *Bioinformatics* **2021**, *37*, 4591–4592, doi:10.1093/bioinformatics/btab644.
695. Ni, Z.; Wölk, M.; Jukes, G.; Mendivelso Espinosa, K.; Ahrends, R.; Aimo, L.; Alvarez-Jarreta, J.; Andrews, S.; Andrews, R.; Bridge, A.; et al. Guiding the choice of informatics software and tools for lipidomics research applications. *Nat. Methods* **2023**, *20*, 193–204, doi:10.1038/s41592-022-01710-0.
696. Ross, D.H.; Guo, J.; Bilbao, A.; Huan, T.; Smith, R.D.; Zheng, X. Evaluating Software Tools for Lipid Identification from Ion Mobility Spectrometry–Mass Spectrometry Lipidomics Data. *Molecules* **2023**, *28*, 1–13, doi:10.3390/molecules28083483.
697. Zhou, Z.; Tu, J.; Xiong, X.; Shen, X.; Zhu, Z.J. LipidCCS: Prediction of Collision Cross-Section Values for Lipids with High Precision to Support Ion Mobility-Mass Spectrometry-Based Lipidomics. *Anal. Chem.* **2017**, *89*, 9559–9566, doi:10.1021/acs.analchem.7b02625.
698. Picache, J.A.; Rose, B.S.; Balinski, A.; Leaptrot, K.L.; Sherrod, S.D.; May, J.C.; McLean, J.A. Collision cross section compendium to annotate and predict multi-omic compound identities. *Chem. Sci.* **2019**, *10*, 983–993, doi:10.1039/c8sc04396e.
699. Ross, D.H.; Cho, J.H.; Zhang, R.; Hines, K.M.; Xu, L. LiPydomics: A Python Package for Comprehensive Prediction of Lipid Collision Cross Sections and Retention Times and Analysis of Ion Mobility-Mass Spectrometry-Based Lipidomics Data. *Anal. Chem.* **2020**, *92*, 14967–14975, doi:10.1021/acs.analchem.0c02560.
700. Zhou, Z.; Luo, M.; Chen, X.; Yin, Y.; Xiong, X.; Wang, R.; Zhu, Z.J. Ion mobility collision cross-section atlas for known and unknown metabolite annotation in untargeted metabolomics. *Nat. Commun.* **2020**, *11*, 1–13, doi:10.1038/s41467-020-18171-8.
701. Checa, A.; Bedia, C.; Jaumot, J. Lipidomic data analysis: Tutorial, practical guidelines and applications. *Anal. Chim. Acta* **2015**, *885*, 1–16, doi:10.1016/j.aca.2015.02.068.

702. Olshansky, G.; Giles, C.; Salim, A.; Meikle, P.J. Challenges and opportunities for prevention and removal of unwanted variation in lipidomic studies. *Prog. Lipid Res.* **2022**, *87*, 101177, doi:10.1016/j.plipres.2022.101177.
703. Tserng, K.Y.; Griffin, R. Studies of lipid turnover in cells with stable isotope and gas chromatograph-mass spectrometry. *Anal. Biochem.* **2004**, *325*, 344–353, doi:10.1016/j.ab.2003.10.037.
704. Bederman, I.R.; Kasumov, T.; Reszko, A.E.; David, F.; Brunengraber, H.; Kelleher, J.K. In vitro modeling of fatty acid synthesis under conditions simulating the zonation of lipogenic [13C]acetyl-CoA enrichment in the liver. *J. Biol. Chem.* **2004**, *279*, 43217–43226, doi:10.1074/jbc.M403837200.
705. Bowden, J.A.; Ulmer, C.Z.; Jones, C.M.; Heckert, A. Lipid Concentrations in Standard Reference Material (SRM) 1950 : Results from an Interlaboratory Comparison Exercise for Lipidomics Lipid Concentrations in Standard Reference Material (SRM) 1950 : Results from an Interlaboratory Comparison Exercise fo. *Nistir* **2017**, *8185*, 1–451.
706. Li, R.-H.; Zhang, L.; Wu, M.-Y. Tissue isoantigens A, B and H in primary carcinoma of the pancreas. *Wourld J. Gastroenterol.* **1996**, *2*, 241–242, doi:10.3748/wjg.v2.i4.241.
707. Hattori, H.; Uemura, K. ichi; Ishihara, H.; Ogata, H. Glycolipid of human pancreatic cancer; the appearance of neolacto-series (type 2 chain) glycolipid and the presence of incompatible blood group antigen in tumor tissues. *Biochim. Biophys. Acta (BBA)/Lipids Lipid Metab.* **1992**, *1125*, 21–27, doi:10.1016/0005-2760(92)90150-T.
708. de Mattos, L.C. Structural diversity and biological importance of ABO, H, Lewis and secretor histo-blood group carbohydrates. *Rev. Bras. Hematol. Hemoter.* **2016**, *38*, 331–340, doi:10.1016/j.bjhh.2016.07.005.
709. Wolpin, B.M.; Chan, A.T.; Hartge, P.; Chanock, S.J.; Kraft, P.; Hunter, D.J.; Giovannucci, E.L.; Fuchs, C.S. ABO blood group and the risk of pancreatic cancer. *J. Natl. Cancer Inst.* **2009**, *101*, 424–431, doi:10.1093/jnci/djp020.
710. Rahbari, N.N.; Bork, U.; Hinz, U.; Leo, A.; Kirchberg, J.; Koch, M.; Büchler, M.W.; Weitz, J. AB0 blood group and prognosis in patients with pancreatic cancer. *BMC Cancer* **2012**, *12*, 319, doi:10.1186/1471-2407-12-319.
711. Antwi, S.O.; Bamlet, W.R.; Pedersen, K.S.; Chaffee, K.G.; Risch, H.A.; Shivappa, N.; Steck, S.E.; Anderson, K.E.; Bracci, P.M.; Polesel, J.; et al. Pancreatic cancer risk is modulated by inflammatory potential of diet and ABO genotype: A consortia-based evaluation and replication study. *Carcinogenesis* **2018**, *39*, 1056–1067, doi:10.1093/carcin/bgy072.
712. Itzkowitz, S.H.; Yuan, M.; Ferrell, L.D.; Ratcliffe, R.M.; Chung, Y.S.; Satake, K.; Umeyama, K.; Jones, R.T.; Kim, Y.S. Cancer-associated alterations of blood group antigen expression in the human pancreas. *J. Natl. Cancer Inst.* **1987**, *79*, 425–434.
713. Pour, P.M.; Tempero, M.M.; Takasaki, H.; Uchida, E.; Takiyama, Y.; Burnett, D.A.; Steplewski, Z. Expression of blood group-related antigens ABH, Lewis A, Lewis B, Lewis X, Lewis Y, and CA 19-9 in pancreatic cancer cells in comparison with the patient's blood group type. *Cancer Res.* **1988**, *48*, 5422–5426.
714. Annese, V.; Minervini, M.; Gabbrielli, A.; Gambassi, G.; Manna, R. ABO blood groups and cancer of the stomach. *Int. J. Pancreatol.* **1990**, *6*, 81–88.
715. Aird, I.; Lee, D.R.; Roberts, J.A.F. ABO Blood Groups and Cancer of Oesophagus, Cancer of Pancreas, and Pituitary Adenoma. *Br. Med. J.* **1960**, *1*, 1163–1166, doi:10.1136/bmj.1.5180.1163.
716. Rizzato, C.; Campa, D.; Pezzilli, R.; Soucek, P.; Greenhalf, W.; Capurso, G.; Talar-Wojnarowska, R.; Heller, A.; Jamroziak, K.; Khaw, K.T.; et al. ABO blood groups and

pancreatic cancer risk and survival: Results from the PANcreatic Disease ReseArch (PANDoRA) consortium. *Oncol. Rep.* **2013**, *29*, 1637–1644, doi:10.3892/or.2013.2285.

717. Mahajan, U.M.; Alnatsha, A.; Li, Q.; Oehrle, B.; Weiss, F.U.; Sendler, M.; Distler, M.; Uhl, W.; Fahlbusch, T.; Goni, E.; et al. Plasma metabolome profiling identifies metabolic subtypes of pancreatic ductal adenocarcinoma. *Cells* **2021**, *10*, 1–16, doi:10.3390/cells10071821.